“The most exciting phrase to hear in science, the one that heralds the most discoveries, is not 'Eureka!' but 'That's funny...'”

Isaac Asimov

University of Alberta

Cellular mechanisms of ion and acid-base transport in aquatic animals

by

Scott Kenneth Parks

A thesis submitted to the Faculty of Graduate Studies and Research
in partial fulfillment of the requirements for the degree of

Doctor of Philosophy

in

Physiology, Cell and Developmental Biology

Biological Sciences

Fall 2009

Edmonton, Alberta

Examining Committee

Dr. Greg Goss, Biological Sciences

Dr. Declan Ali, Biological Sciences

Dr. Marek Duszyk, Physiology

Dr. Sally Leys, Biological Sciences

Dr. Stephen McCormick, Biology, University of Massachusetts Amherst.

This thesis is dedicated to Shawna, thanks for being the best part of my life!

Abstract

I investigated cellular mechanisms of ion and acid-base transport in rainbow trout (*Oncorhyncus mykiss*), crabs (*Neohelice granulata*), zebrafish (*Danio rerio*), Pacific hagfish (*Eptatretus stoutii*), and mosquito larvae (*Aedes aegypti*) with a primary focus on discerning the mechanisms governing ion transport and acid base regulation.

In rainbow trout I provide the first functional evidence for two physiologically distinct mitochondrion-rich (MR) cells at the gill and demonstrate a new model for transepithelial Na^+ uptake from freshwater involving apical Na^+ channels and basolateral Na^+/HCO_3^- co-transporters. These data are supported by extensive thermodynamic consideration of Na^+ uptake from freshwater. I also demonstrate functional Cl^-/HCO_3^- exchangers in both MR cell subtypes with roles for Cl^- uptake and intracellular pH (pH_i) regulation respectively and I present the first evidence for a Cl^- dependent Na^+/H^+ exchanger in gill MR cells. Finally I demonstrate a unique Na^+ dependent pH_i recovery mechanism that requires protein kinase C for activation. A major limiting factor in clarifying the mechanisms of Na^+ uptake in freshwater fish is the lack of a typical Na^+ channel in any of the fish molecular databases. My work on zebrafish, although preliminary, indicates that a member of the acid-sensing ion channel family could be responsible for Na^+ uptake from freshwater.

I then expanded my research outside the trout model using an isolated crab gill preparation. I provide a cellular model for H^+ secretion in crab gills

that supports the transepithelial Na^+ transport model that I described in rainbow trout.

In Pacific hagfish, I demonstrate that recovery from blood acidosis is dependent on a Na^+/H^+ exchanger in gill MR cells. This mechanism of regulation involves translocation from the cytoplasm to the apical membrane during acidotic stress. This data combines with other studies demonstrating the mechanisms of acid and base secretion from a single MR cell subtype.

Finally, I show that serotonin stimulation alkalinizes the pH_i of the anterior midgut cells in the larval mosquito to levels never before observed in cell biology. These data challenge the dogma of pH_i regulation in cell biology and demonstrate the power of using a comparative approach to systems physiology.

Acknowledgements

There are many people who I need to thank that contributed to making my thesis research so enjoyable. First off I need to thank my supervisor Greg Goss as I have thoroughly enjoyed my time spent in the Goss lab. Greg, your infectious enthusiasm for both science and life in general has always been inspiring. I have to thank you for all the opportunities to travel during the tenure of my PhD as these experiences mean a lot to me. We have had too many good memories to mention and for that I thank you. Your interest in my long term research goals has been greatly appreciated and I wish you many future successes in your lab.

My thesis experience would not have been the same without overlapping with Martin Tresguerres. Martin was the best lab mate to ever work with in my opinion. His sharp mind meant for great science conversation and research project development. A great sense of humour, lack of pretention, and laid back attitude helped me a great deal during my research. I will be forever grateful for the Argentina research trip that Martin initiated and organized. This will be a life-long memory. Thanks for making research fun and hopefully we will continue to collaborate in the future.

I would also like to acknowledge the whole Physiology RIG in particular the labs on the 5th floor of the Zoology wing. This is a fantastic group with great camaraderie and it has been nice to be a part of it. Members of the Goss lab including Fumi, James, Kim, Tyson, and Maria have helped me in various aspects throughout my PhD. I have had a nice relationship with Dr.

John Chang and his lab. Thank you for John for your efforts on my graduate committee. It is unfortunate that you could not make the final defence due to timing. I have enjoyed being able to contribute to your research program with the pH_i imaging experiments. Dr. Declan Ali and his PhD students Kessen and Chris have been helpful for any of my random zebrafish questions throughout the years. Their high quality of research has also been inspiring. Dr. James Stafford and his lab members Benjamin and Jacqueline have also been helpful in teaching me molecular techniques. I know I tested your patience at times but it has been great working in your lab. Also thanks for all the fun socializing times. I also want to thank previous students on the floor including Shawn, Sampson, Kee-Chan, and Wan-peng. These individuals were all very instrumental in the beginning of my research. Thanks to all!

The aquatics staff in the Biological Sciences building do an excellent job of maintaining our animals in good health so a big thanks to Tad and Clarence. Also the Bamfield Marine Sciences Centre Staff, in particular Dr. Bruce Cameron, were always a great help in ensuring that we could get our unrealistic number of experiments done in the limited time that we had. Jack Scott in the microscopy unit and Troy Locke in the molecular biology unit at the University of Alberta also provided valuable assistance during my research.

I appreciated the teaching component of my PhD that was enhanced by the teaching co-ordinator Maggie Hagg and Biology 107 lab co-ordinator Carla Starchuck. I would like to thank Dr. Reuben Kaufmann for the TA

experience in Zoology 241. Finally, I thank my supervisor Dr. Greg Goss for the TA and guest lecture experience in Zoology 340.

My generous funding sources were greatly appreciated. I wish to acknowledge the funding from an NSERC CGSD, the Honorary Izaak Walton Killam Memorial Scholarship, the Queen Elizabeth Doctoral Scholarship, the Donald M. Ross Memorial Scholarship, the Dick Peter Memorial Scholarship, and various conference travel grants.

Thanks to my Dad (Ken), Mom (Mary), and brother (Manson) for all of their support.

Thanks to my in-laws, Neil and Cheryl for putting up with Shawna and myself on a regular basis in Calgary and being the ideal travel companions. My PhD tenure was definitely enhanced by these experiences.

Lastly, Shawna, thanks for everything, you remain the reason why life is great!

Table of Contents

List of tables

List of figures

Chapter I

Chapter II

Chapter IV

Appendix II

List of abbreviations and symbols

[] (concentration of substance within the brackets)

‰ (Salinity abbreviation for parts per thousand)

a/b (acid-base)

AE (anion exchanger)

CA (carbonic anhydrase)

CBE (chloride-bicarbonate exchanger)

cDNA (complementary deoxyribonucleic acid)

Cl^- (chloride)

CO_2 (carbon dioxide)

DIDS (4,4′-Diisothiocyanatostilbene-2,2′-disulfonic acid disodium salt hydrate)

DNA (deoxyribonucleic acid)

FW (freshwater)

H^+ (hydrogen ion or proton)

HCO_3^- (bicarbonate)

hpf (hours post fertilization)

L-IR (like-immunoreactivity)

MR (mitochondrion-rich)

Na^+ (sodium)

NBC (sodium-bicarbonate co-transporter)

NHA (the prokaryote electrogenic Na^+/nH^+ exchanger)

NHE (sodium-proton exchanger)

NKA (sodium-potassium ATPase)

O_2 (oxygen)

PCO_2 (partial pressure of CO_2)

PCR (polymerase chain reaction)

Q-PCR (quantitative polymerase chain reaction)

rbc (red blood cell)

RNA (ribonucleic acid)

RNAi (RNA interference)

siRNA (small interference RNA)

SLC (solute carrier (human))

slc (solute carrier (non-human))

SW (seawater)

torr (partial pressure abbreviation for millimetres of mercury, mmHg)

VHA (vacuolar proton-ATPase)

V_{te} (transepithelial potential difference)

Chapter I: General Introduction

Maintenance of the internal milieu *via* the co-ordinated action of numerous bodily functions was first suggested by Claude Bernard (Bernard, 1878) and later expanded upon to be coined as homeostasis by Walter F. Cannon (Cannon, 1929). This concept of how different processes within the body of an animal interact to maintain a constant balance has been the driving force behind physiological research ever since these early descriptions.

The central theme of my thesis is the nature in which aquatic animals achieve salt and acid-base (a/b or pH) homeostasis in the face of a dynamic surrounding environment. From a general interest standpoint, there are numerous examples for the importance of regulating salt and a/b levels in the body. The most common example of salt balance is the link to high blood pressure (hypertension) in humans due to increased salt levels in the blood stream (for review see (Meneton et al., 2005)). It is important to note that the mechanism of mammalian salt balance ranges from individual cell shrinkage to whole body fluid retention. Therefore we get a clear indication that salt balance is an essential process of the co-ordinated physiological systems (cell to organ) within an animal.

The importance of maintaining pH within a narrow range is observed in assessing pH alterations on protein function. Proper protein performance determines cellular and whole animal survival. The amino acids that make up proteins are classified into acidic and basic categories with respect to the carboxyl or amine functional groups on their respective side chains (Roos and

Boron, 1981). pH alterations in the fluid surrounding a protein disrupt the ionization state of the amino acid-side groups thereby changing the three-dimensional structure of the protein (Roos and Boron, 1981). In the case of an enzyme, this alteration of protein structure can render it inactive directly, or indirectly by preventing proper substrate binding. Consequently, enzyme kinetic assays exhibit a tight relationship between pH and optimal performance. These optimal pH levels can range from very acidic (~pH 2 for stomach enzymes such as pepsin (Brier et al., 2007)) to the more neutral range (~pH 7 for phosphofructokinase, the rate limiting enzyme in glycolysis (Madshus, 1988)) and finally to the basic level (~pH 10 for the bacterial (*Bacillus*) amylase (Bezbaruah et al., 1991)). The important point to note is that an acidic or basic pH absolute value may not be detrimental to enzyme function but it is the maintenance of a narrow range near the enzyme optimal pH that ensures proper function.

Fish possess an amazing organ, the gill, which is capable of carrying out numerous physiological functions that are carried out by distinct organs in other animals. These functions include O_2 uptake, CO_2 removal, nitrogenous waste removal, ion regulation, and a/b regulation (Evans et al., 2005). A unique characteristic of freshwater gill function is that ion transport is intimately linked to a/b regulation with Na^+ and Cl^- uptake occurring concurrently with H^+ and HCO_3^- secretion respectively. This is the joy and the curse of working on fish gill physiology. We cannot study a/b regulation without gleaning information about ion regulation, however, we also cannot

isolate a/b separately from ion regulating properties in these experiments. This principle must remain paramount while performing our analysis to ensure that all potential data interpretations are realized.

In the following pages I will outline the 3 key themes of my thesis, which include intracellular pH (pH_i) regulation, extracellular pH (pH_e) regulation, and whole body ion regulation as dictated by membrane transport at the gill. I will outline key highlights from this vein of research leading up to my current set of hypotheses. This general introduction will be written in the context of comparative physiology and will draw examples from work done on a wide range of animals with fish as the predominant topic. By summarizing this diverse range of organisms we can gain an appreciation of the need for unique membrane transporting mechanisms in challenging environments. These comparative observations are necessary to develop further hypothesis-driven research.

Intracellular pH (pH_i) regulation

The concept of pH adheres to the following formula.

$$pH = -\log[H^+] \qquad \textbf{(Equation 1.1)}$$

From this equation, it is evident that $[H^+]$ is the most important component of determining pH and therefore the key molecule in a/b regulating systems. The definition of pH can be extended to the dissociation of a weak acid as described by the Henderson-Hasselbalch equation:

$$pH = pK' + \log\frac{[A^-]}{[HA]} \qquad \textbf{(Equation 1.2)}$$

Where pK' is the dissociation constant of the acid, $[A^-]$ refers to the H^+ acceptor or base, and [HA] refers to the H^+ donor or acid. This formula can be used to describe the relationship between HCO_3^- and CO_2 to pH by the following equation:

$$pH = pK' + \log \frac{[HCO_3^-]}{\alpha P_{CO2}} \textbf{ (Equation 1.3)}$$

Where P_{CO2} is the partial pressure of CO_2 and α is the solubility coefficient for CO_2.

Cellular Buffering

Disruption of pH_i occurs *via* a number of factors that include changes in PCO_2, temperature, metabolic end products, hydrolysis of ATP, and acidification of the extracellular fluid to name a few (for review see (Cardone et al., 2005; Pouyssegur et al., 2006; Roos and Boron, 1981)). The cellular buffering capacity is the first line of defence following a pH_i disturbance. Physiochemical buffering is defined as the ability of weak acids and bases to react with H^+ and minimize pH disturbances according to the following equation:

$$B^n + H^+ \leftrightarrow BH^{n+1} \textbf{ (Equation 1.4)}$$ modified from (Roos and Boron, 1981).

Where B^n is a weak base of valence *n* and BH^{n+1} is a weak acid of valence *n+1*.

The amino acid histidine is the most important cellular buffer and its role has been extensively investigated in the function of haemoglobin for

oxygen binding (for review see (Berenbrink, 2006)). Histidine is a key physiological buffer because its pK_a spans the physiological pH range of 6-8 (Berenbrink, 2006; Lukin and Ho, 2004). This is important for buffering because is means that any changes (even minor) within this pH range will have an immediate effect on the binding of H^+ to histidine's side group. Another buffering mechanism that can be utilized within the cell is the metabolic consumption or production of H^+ (reviewed by (Cohen and Iles, 1975)). For example, lactate can be converted into glucose in some cells thereby consuming H^+ to counteract an acidosis (Cohen et al., 1971). Conversely, H^+ production *via* the hydrolysis of ATP or oxidation of lactate to pyruvate (Cohen and Iles, 1975) can be utilized to buffer a cellular alkalosis. A final cellular buffering strategy is to transfer a/b units between the cytosol and cellular organelles such as mitochondria and lysosomes (see (Roos and Boron, 1981)). Despite the effectiveness of the buffering mechanisms listed above, they are all only temporary solutions for pH_i disturbances. It is vital that the cell extrudes a/b units from the cell to allow buffering proteins to return to their preferred protonation state and allow proper cell function. These membrane transporting mechanisms are the focus my thesis.

Membrane transport

A number of membrane transporters have been implicated as essential components in the maintenance of pH_i and are common to cells from a broad range of animals. These transporters either extrude H^+ from the cell, or transport HCO_3^- into or out the cell. There are no known physiological

mechanisms for H^+ import and it is not an established technique for pH_i regulation as the result is cell suicide (the exception to this is the prokaryote electrogenic Na^+/nH^+ exchanger (NHA) as will be discussed in chapter II). The primary proteins involved in regulating pH_i are Na^+/H^+ exchangers (NHE), Cl^-/ HCO_3^- exchangers (CBE), Na^+-HCO_3^- co-transporters (NBC), vacuolar-type H^+-ATPases (VHA), and carbonic anhydrase (CA). It is important to mention that not all cells possess all of these pH_i regulatory proteins, but they exist in some combination on the cell membrane to maintain pH_i as shown in figure 1.1. In epithelial tissues where directional movement of ions is required these proteins become specifically localized to either the apical or basolateral membrane and this functional relevance will be discussed throughout my thesis.

It is important to make a brief mention of ion transporting protein nomenclature before proceeding further. The standardized nomenclature of solute carrier (SLC) has been assigned to cell membrane exchangers, co-transporters, and passive transporters along with mitochondrial transporters and vesicular transporters (for review see (Hediger et al., 2004)). Ion channels, aquaporins, and ATP dependent pumps are not included in this classification. At least 43 different SLC families exist (termed SLC1-SLC43) with multiple isoforms found within each family (Hediger et al., 2004). Typically the nomenclature used follows the basic formula SLC#A# where the first # indicates the gene family and the second # indicates the isoform within that family (i.e. NHE1=SLC9A1). Capital letters are used for human genes

while lower case letters are typically used for non-human genes. With respect to this thesis, the HCO_3^- transporters (NBCs and AEs) are members of the SLC4 family, the NHEs belong to the SLC9 family, while the potential CBEs in fish belong to the SLC26 family. As most molecular identities for fish transporters remain unknown they will be referred to as their more traditional nomenclature throughout my thesis. Whenever possible the modern SLC nomenclature will be mentioned.

Although CA is not a direct a/b transporter *per se*, it is vital in the maintenance of pH_i. Its role is required to enhance the de/hydration of cellular CO_2 ($CO_2 + H_2O \leftrightarrow HCO_3^- + H^+$) and therefore provide the required a/b substrates necessary for membrane transporters to overcome a pH_i disturbance. CA's importance in regulating pH_i has been recently demonstrated in cancerous tumour cells (Chiche et al., 2009). Rapidly growing tumours require a complementary vasculature to provide the required oxygen and nutrients needed for survival (Cardone et al., 2005). However, some tumour masses develop faster than the blood supply, resulting in a hypoxic environment within the tumour mass. As a result, increased metabolic acids (e.g. lactic acid) are produced and excreted resulting in acidification of the microenvironment of the tumour (Brahimi-Horn et al., 2007; Brahimi-Horn and Pouyssegur, 2007; Chiche et al., 2009; Pouyssegur et al., 2006). This poses a stress on the cells in that the extracellular acidification can ultimately lead to a decrease in the pH_i. However, cancer cells are known to have a more alkaline intracellular pH_i compared to other non-cancerous cells despite

their more acidic surroundings and this is even more apparent in more aggressive tumours (Cardone et al., 2005). Chiche and colleagues (Chiche et al., 2009) used a gene silencing technique of CA isoforms IX and XII to demonstrate their absolute requirement in maintenance of pH_i along with cell survival. CA has also been shown to play a role in pH_i regulation across a wide range of cells including the stomach bacteria *Helicobacter pylori* (Essential for acid-acclimation and survival of this normally pH neutral growing stomach pathogen; (Marcus et al., 2005)), blowfly salivary gland cells (shown to be key for pH_i maintenance in direct cell studies; (Schewe et al., 2008)) lamprey red blood cells (classic pH_i regulatory observations; (Nikinmaa et al., 1986)), ion transporting skin cells of the FW frog (Harvey and Ehrenfeld, 1986),(they also showed the importance of H^+-ATPase in pH_i regulation), and mammalian neuronal cells (Deitmer and Rose, 1996) to name a few. Therefore, as is apparent from the range of animals studied, although CA is not a direct membrane transporter, its function in providing a/b substrates is vital to the maintenance of pH_i.

The most common pH_i regulatory protein is the Na^+/H^+ exchanger (NHE). The NHE family consists of nine different isoforms (termed NHE1-9) respectively (Orlowski and Grinstein, 2004; Slepkov et al., 2007). Credit is given to Harold and Papineau (Harold and Papineau, 1972) for providing the first direct evidence of NHE activity on the cellular membrane of the bacteria *Streptococcus faecalis.* An earlier report had also indicated NHE activity on the mitochondrial membrane (Mitchell and Moyle, 1969) however it had never

been shown on the cellular membrane until 1972. Almost 20 years later, a mammalian NHE1 was cloned for the first time (Sardet et al., 1989). NHE1 has since been termed the “housekeeping” isoform as it is ubiquitously expressed on the basolateral membrane of almost all cells (eukaryotic and prokaryotic) requiring pH_i regulation (for review see (Orlowski and Grinstein, 2004)). NHE1 is a simple electroneutral transporter driven by ion gradients alone that extrudes intracellular H^+ for extracellular Na^+ to counteract or prevent cellular acidification of the cell. As such, it is a fundamental element of most cells’ pH_i regulating machinery. The other NHE isoforms are implicated in a variety of processes and thermodynamic consideration of NHE as it pertains to ion uptake in FW fish is explored in great detail in chapter II.

HCO_3^- transporting proteins constitute the other main pH_i regulating strategy. Many of these proteins are grouped into the SLC4 gene family that includes Anion exchangers (AE or the classical CBEs), NBCs, and Na^+-dependent CBEs (NDCBE) (Romero et al., 2004). NBCs were first described to act in HCO_3^- reabsorption on the basolateral membrane of salamander kidney proximal tubule cells (Boron and Boulpaep, 1983). This kidney specific NBC (kNBC1 or SLC4A4) was shown to be electrogenic with a stoichiometry of 3 HCO_3^-: 1 Na^+ being transported each time (Romero et al., 1997; Soleimani et al., 1987; Yoshitomi and Fromter, 1985) and was finally cloned in 1997 (Romero et al., 1997). However, this NBC isoform was shown to be primarily responsible for the reabsorption of HCO_3^- from the lumen into the blood in co-ordination with apical NHEs and H^+-ATPases and not primarily for

pH_i regulation (for review see (Soleimani and Burnham, 2001)). Following the discovery of the kidney NBC, different NBC isoforms were revealed in other tissues such as the liver (Fitz et al., 1989; Gleeson et al., 1989) and heart (deHurtado et al., 1996; Lagadic-Gossmann et al., 1992) that acted to import Na^+ and HCO_3^- into the cell and thereby function primarily as pH_i regulators. Interestingly, these pH_i regulating NBCs had a different stoichiometry and were shown in heart tissue to have either a 2 HCO_3^-: 1 Na^+ transport (deHurtado et al., 1996) or to be electroneutral (Lagadic-Gossmann et al., 1992). Although various isoforms of NBC have been expressed throughout many mammalian tissues (Romero and Boron, 1999; Romero et al., 2004; Soleimani and Burnham, 2001), their role in other non-mammalian systems has not been extensively studied. Apart from mammalian tissues, NBCs have only been cloned and characterized from salamander kidney (Romero et al., 1997), fish gill (Hirata et al., 2003; Perry et al., 2003a), squid giant axons (Piermarini et al., 2007a), and *C. elegans* (unpublished paper NCBI accession number AF004926.1).

Another member of the Na^+ dependent HCO_3^- transporting family is the Na^+ dependent Cl^-/HCO_3^- exchanger (NDCBE). This transporter was actually the first protein functionally implicated in regulating pH_i from microelectrode recordings of pH_i in squid giant axons (Boron and Deweer, 1976a; Boron and Russell, 1983; Russell and Boron, 1976) and snail neurons (Thomas, 1977). The first NDCBE (termed NDAE1) was cloned from *Drosophila* (Romero et al., 2000) and has since also been characterized in squid (Virkki et al., 2003)

and humans (Grichtchenko et al., 2001). The NDCBE has not yet been characterized at a molecular level in fish although a study on cultured gill cells has suggested its presence (Wood and Part, 2000).

The other main HCO_3^- transporter involved in pH_i regulation is the CBE. The rbc anion exchanger (termed AE1 or the band 3 protein) was the first transporter ever characterized at a molecular level (Kopito and Lodish, 1985) and has been the most intensely studied CBE. AE1 plays a key role in O_2 and CO_2 delivery *via* the "Cl^-" or "Hamburger" shift where tissue derived CO_2 enters the rbc, is converted to H^+ and HCO_3^- by intracellular CA, and HCO_3^- is extruded from the cell via AE1 in exchange for Cl^-. This alters the affinity of haemoglobin for O_2 and aids in unloading of O_2 at the tissue and pick up of CO_2 while the opposite effect occurs at the lungs. This fundamental property of gas delivery is dependent on the pH_i regulatory ability of AE1. Two additional isoforms of AE have also been cloned and are activated by a rise in pH_i (for review see (Romero et al., 2004)).

Despite the importance of AE in other systems, it has not been implicated as a key component in fish gill ion-a/b regulation. The band 3 protein (AE1) was cloned from trout rbcs (Fievet et al., 1995) where it plays a role in gas transport and pH_i regulation (for review see (Nikinmaa, 1997)). Two AE isoforms, termed *ae*2.1 and *ae*2.2 respectively, have been characterized in zebrafish (Shmukler et al., 2008; Shmukler et al., 2005). However, expression of these AEs was restricted to the kidney, eye, tectum, and axial vasculature (Shmukler et al., 2008; Shmukler et al., 2005).

Furthermore, although a role for pH_i regulation was suggested, knock down of these genes using the morpholino technique did not significantly alter the development of the zebrafish embryo (Shmukler et al., 2008). These are the only molecular studies available for AE isoforms in fish and indicate that it is not an essential component of gill pH_i regulation.

Instead of the AE family, it is now believed that the molecular identity of CBE in fish belongs to the SLC26 gene family. The SLC26 family of anion exchangers are known to transport a variety of anions including HCO_3^- (Mount and Romero, 2004). So far none of these transporters have been fully characterized from fish gill tissue despite two independent laboratories suggesting their presence at conference proceedings (Bayaa and Perry, 2005; Goss et al., 2005). SLC26A1 has been cloned from trout kidney and is implicated in sulfate secretion (Katoh et al., 2006) and Slc26a6 has been cloned from mefugu intestine where it is proposed to play a role in the formation of calcium-carbonate precipitates (Kurita et al., 2008). However, these isoforms are not primarily linked to pH_i regulation. Pendrin (SLC26A4) has garnered the other attention for CBE in fish. Pendrin was discovered in studies on patients suffering from Pendred syndrome, a condition that can involve deafness and an enlarged thyroid (Reardon et al., 1999). Pendrin has been shown to perform Cl^-/I^- exchange (Scott et al., 1999) and can also carry out CBE (Soleimani et al., 2001). This is important for fish studies as Pendrin immunoreactivity was demonstrated on the apical membrane of dogfish gill MR cells and proposed to carry out HCO_3^- secretion in exchange for Cl^-

(Piermarini et al., 2002). Up to this point however, no known role for Pendrin exists at the FW fish gill. CBE has also been suggested as a mechanism for basolateral pH_i regulation in fish gill cells (Tang and Lee, 2007a; Tang and Lee, 2007b). Of the transporters involved in pH_i regulation, the CBEs remain the least described at the molecular level in fish. This information is required for directing future research efforts of fish gill pH_i regulation.

In fish gill cells, pH_i regulation has not received a great deal of attention in the published literature. Wood and Lemoigne (Wood and Lemoigne, 1991) provided estimates for resting pH_i values of ~7.40 based on whole gill homogenates. This study examined the global pH_i and pH_e regulation of various tissues and blood in response to environmental hyperoxia and found that pH_i regulation varied between tissues but generally occurred faster than pH_e regulation (Wood and Lemoigne, 1991). At a cell specific level, two studies performed on trout gill pavement cell (PVC) cultures suggest a role for NHE, NBC and/or NDCBE in basolateral pH_i regulation but not CBE or VHA (Part and Wood, 1996; Wood and Part, 2000). These same pH_i regulating transporters were also proposed in a different study on goldfish PVC cultures (Sandbichler and Pelster, 2004). This is in contrast with a study on cells from the pseudobranch (a gill-like hemibranch (additional structure) attached to the operculum in many teleost fish) which demonstrated the importance of both NHE and VHA in pH_i regulation (Kern et al., 2002). In addition, a molecular study suggested the use of NBC and VHA in branchial pH_i regulation and possibly whole body a/b regulation as well (Perry et al., 2003a). These few

studies provide the basis for our understanding of FW gill pH_i regulation leading into my thesis research and give an indication that most stereotypical pH_i regulating proteins are present in gill cells. A goal of my thesis was to improve on our understanding of this important homeostatic mechanism.

Extracellular/whole body pH regulation

Maintenance of blood pH (whole body) is also referred to as the regulation of extracellular pH (pH_e). Classically, there are two types of pH_e disturbances classified as respiratory or metabolic acidosis/alkalosis. Respiratory disruptions alter blood pH by changing the ratio of CO_2 found within the blood as described in equation 1.3. Increased CO_2 within the blood leads to an acidification while decreased levels of CO_2 result in an alkalinization. Metabolic disruptions of pH_e result from either a breakdown of the a/b regulating organ or in response to other physiological parameters that result in HCO_3^- or H^+ into the bloodstream. An example of metabolic acidosis is renal tubular acidosis (RTA) where either proximal tubule HCO_3^- reabsorption (into the blood) or distal tubule H^+ secretion (into the urine) become inhibited for a variety of reasons (for review see (Fry and Karet, 2007)). On the other hand, metabolic alkalosis can occur following the consumption of a meal. As part of collaborative studies during my PhD I studied the blood alkaline tide in the Pacific spiny dogfish (Tresguerres et al., 2006c; Tresguerres et al., 2007b). Following a meal, the dogfish secretes H^+ into the gut to aid in digestion while HCO_3^- is reabsorbed back into the bloodstream causing an alkaline tide (Wood et al., 2005) and for review see

(Wang et al., 2001)). This alkaline tide is common to a variety of animals including amphibians, reptiles, fish, and mammals (Wang et al., 2001).

Animals such as terrestrial mammals can simply manipulate ventilation rates to achieve blood a/b regulation by regulating the partial pressure of CO_2 (PCO_2) within the bloodstream. Increased pulmonary ventilation has been shown to compensate for a metabolic acidosis by decreasing the PCO_2 in the arterial blood (reviewed by (Swenson, 1998)). Although this is an effective strategy for a/b regulation, fish are prevented from utilizing this technique due to low levels of PCO_2 in their bloodstream (~2 torr in fish vs. ~40 torr in humans, see (Claiborne et al., 2002; Perry and Gilmour, 2006)). Blood PCO_2 levels in fish are low due to the large perfusion volume of water across the gill that is required for sufficient O_2 uptake. As CO_2 rapidly crosses the epithelium and enters the surrounding water to be converted into HCO_3^- and H^+, there exists a constant gradient for CO_2 excretion and therefore a low PCO_2 is found in the blood. Furthermore, lowering ventilation rates to retain CO_2 and therefore lower blood pH would prevent O_2 uptake and become an ineffective means to achieve a/b regulation as overall survival is compromised (reviewed by (Perry and Gilmour, 2006)).

FW fish regulate blood pH by adjusting the rates of HCO_3^- and H^+ secretion at gill mitochondrion-rich (MR) cells. The kidney plays a minor role in a/b balance as well with estimates of ~90% of a/b regulation occurring *via* the gill and the remaining ~10% *via* the kidney (Claiborne et al., 2002). Early studies in trout suggested that CBE is more important for net H^+ secretion

than NHE as there is a large net loss in blood Cl^- and only a small net gain of Na^+ in response to hyperoxia induced acidosis (Wood et al., 1984). During normoxic recovery (which induces blood alkalosis) a large net loss of blood Na^+ and large net gain of Cl^- was observed (Wood et al., 1984). Other studies examining hyperoxia or hypercapnia induced acidosis found similar changes in Na^+ and Cl^- fluxes (Goss and Wood, 1990a; Perry et al., 1987) clearly indicating that movement of a/b equivalents at the gill are rapidly altered depending on the a/b disturbance. Laurent and Perry (Laurent and Perry, 1990) demonstrated an increase in chloride cell (cc=MR cell type, see nomenclature discussion below) surface area on the trout gill epithelium that was coupled to increased rates of Na^+ and Cl^- influx. Goss and colleagues followed this by reporting that the covering/uncovering of ccs by pavement cells at the gill acts to alter levels of a/b secretion (Goss et al., 1992). Interestingly, they found that the cc fractional areas changes had a much greater effect on Cl^- uptake than Na^+ indicating a separation of these processes into two different cell types (Goss et al., 1992). Separation of MR cell subtypes will be discussed extensively later on in this introduction and throughout my thesis. Although the general concept of a/b regulation is well established in fish, the specific cellular mechanisms remain unknown.

In freshwater (FW) fish, molecular information specifically related to whole body a/b regulation is limited. VHA is strongly supported in acid recovery as has been shown by increases in gene expression (Sullivan et al., 1996; Yan et al., 2007), protein expression (Galvez et al., 2002; Sullivan et

al., 1995), and activity (Lin and Randall, 1993) at the gill. However, work on the Osorezan dace (*Tribolodon hakonensis*) that lives in an acidic lake (pH 3.5) in Japan did not show changes in VHA expression in response to acidosis (Hirata et al., 2003) however this could be a result of sufficient VHA existing at the gill in a basal condition. In this study gene expression increases were noted for CAII, NHE3, NBC1, aquaporin 3 (AQP3), and NKA (Hirata et al., 2003). NHE has received considerable attention for recovery from acidosis in FW fish. Although gene expression increases of NHE3 were found in the Osorezan dace (Hirata et al., 2003), acidosis in zebrafish resulted in a decrease in NHE3 mRNA (Yan et al., 2007). Use of mammalian antibodies (data of which must be interpreted with caution) revealed an increase in NHE2 protein expression but no change in NHE1 in the acidosis response of FW acclimated killifish (Edwards et al., 2005). These studies provide conflicting data and the use of NHE for FW recovery from acidosis requires further clarification.

Intracellular CA (CAII) was implicated in the acid recovery mechanism of trout *via* increased gene expression and an apparent mRNA cellular upregulation as observed by *in situ* analysis (Georgalis et al., 2006). However, in zebrafish, gene expression of CAII was unaffected by acidosis while another isoform (CA15) was increased (Lin et al., 2008). In this study, morpholino gene knockdown of both CAII and CA15 decreased H^+ secretion indicating that they may play a role in the overall a/b regulating machinery despite the lack of gene expression changes in CAII (Lin et al., 2008). These

few molecular reports of a/b regulation in FW fish indicate that a great deal of work is still required to clarify the specific cellular mechanisms responsible for a/b transport in gill cells.

Seawater (SW) fish are more predictable in terms of a/b regulation with the separation of acid and base secreting cells at the gill (Hawkings et al., 2004; Piermarini and Evans, 2001; Tresguerres et al., 2005). The generally accepted model is that acid-secreting cells utilize an apical NHE in concert with a basolateral NKA while base secreting cells have an apical CBE driven by basolateral VHA (reviewed by (Claiborne et al., 2002; Perry and Gilmour, 2006)). Pharmacological backing for the use of NHE in SW teleost acid secretion is limited to one study on longhorn sculpin (Claiborne et al., 1997) however this is likely related to the low solubility of NHE inhibitors in SW (personal observation). Recently, molecular evidence of NHE has been demonstrated at the gill of a SW teleost (Catches et al., 2006) and elasmobranch (Claiborne et al., 2008). This supports previous work using heterologous antibodies that had suggested NHE presence at the gill in a variety of SW fish including members of the agnathans, elasmobranchs, and teleosts (Choe et al., 1999; Choe et al., 2007; Choe et al., 2005; Choe et al., 2002; Claiborne et al., 1999; Edwards et al., 2001; Edwards et al., 2002; Edwards et al., 1999; Edwards et al., 2005; Tresguerres et al., 2005). In base secreting cells, apical CBE has been suggested by pendrin immunoreactivity (Piermarini et al., 2002). Basolateral VHA is also well supported in the HCO_3^- secretion model at the gill of the Pacific dogfish (Tresguerres et al., 2005;

Tresguerres et al., 2006c; Tresguerres et al., 2007b). These data from ancestral SW species have proven to be important for understanding mechanisms of FW whole body a/b regulation.

Some fish have unique strategies to tolerate severe a/b disturbances encountered in their dynamic environment. The armoured catfish (*Liposarcus pardalis*) from the Brazilian Amazon is reported to have the greatest respiratory acidosis ever observed when hypercapnia (elevated PCO_2) induced a fall in blood pH from 7.98 to 6.99 (Brauner et al., 2004). However, this fish only recovers its blood pH back by ~8% during the course of prolonged hypercapnia (Brauner et al., 2004). Instead, it focuses on pH_i regulation which is tightly regulated in the heart, liver, and muscle despite the severe external acidosis (Brauner et al., 2004). This tolerance of hypercapnia is suggested to be associated with the need to tolerate air exposure and is also found in the eel (*Anguilla anguilla*) (McKenzie et al., 2002) and white sturgeon (*Acipenser transmontanus*) (Crocker and Cech, 1998).

The above discussion introduces the general a/b regulating strategies used at both a cellular and whole animal level. By taking a snap shot of the literature pertaining to fish with regards to a/b regulation, it is clear that a number of areas require clarification. An aim of this thesis is to provide missing details of the gill a/b compensatory machinery.

Ion Regulation

Pioneering studies by Homer Smith, August Krogh, and Ancel Keys on ion and osmoregulation in the 1920s and 30s on both FW and SW fish

initiated the field of fish comparative physiology. These researchers recognized that FW fish would have the tendency to lose salts and gain water from their environmental conditions while SW fish would experience the opposite condition, both of which were regulated in teleost fish to maintain survival (Smith, 1932). In its simplest form, ion regulation in fish is achieved by excreting copious amounts of dilute urine and not drinking in a FW environment in comparison to drinking almost continuously (like a fish!) and limiting urine flow in the SW environment (this overall mechanism was discussed early on by (Smith, 1932)). This is complemented by active ion uptake at the gill in FW and ion excretion in SW.

Homer Smith developed his theories on fish ion regulation by working primarily on SW teleosts. Using the dye phenol red and by examining stomach and intestine contents of SW sculpin and eel, Smith documented the large drinking rate of SW teleosts (Smith et al., 1930). He went on further to measure the urine content of a variety of SW teleosts and found it to be mostly isosmotic with that of the blood (however this was hypoosmotic to the SW environment) (Smith et al., 1930). Therefore he proposed an extrarenal secretion of salts (suggested to be the gill) to achieve the low salt level maintained in SW fish compared to their environment (Smith et al., 1930). In this study Smith also described the extremely low drinking rate and large urine volume in FW fish (Smith et al., 1930). Smith's impressive body of work established many baseline physiological parameters of fish ion regulation to the point where David Evans revealed in a recent review that:

> “one reviewer of my first National Science Foundation proposal in 1970 wondered why they should fund my proposal, because "Homer Smith has told us what we need to know about fish osmoregulation."” (Evans, 2008).

However, components of the fish gill ion transporting mechanisms still elude us ~80 years later.

Ancel Keys took the work of Homer Smith a step further and developed an *in situ* heart-gill perfusion preparation from the eel that he could use to measure Cl^- content in the gill “blood” and surrounding environment (Keys, 1931b). Using this apparatus he definitively showed that Cl^- secretion occurred at the gills of eels into the surrounding SW (Keys, 1931a). Keys suggested that the gill Cl^- secretion mechanism was an active process and as a result he is credited with proposing one of the earliest descriptions of epithelial active transport in any system (Keys and Willmer, 1932).

August Krogh experimented on a variety of fish and found that when separating the head region from the rest of the body *via* a rubber membrane Cl^- uptake occurred in the head region only even in waters of micromolar Cl^- concentrations (Krogh, 1937). Krogh also demonstrated that the cation did not influence Cl^- uptake at the gills showing an important separation from Na^+ uptake and he suggested that Cl^- was exchanged for HCO_3^- (Krogh, 1937). Additional studies by Krogh suggested that Na^+ uptake occurs in exchange for NH_4^+ (Krogh, 1938) a mechanism that will be discussed further in chapter

II. The main principles derived from the studies of Krogh, Smith, and Keys still influence fish physiology research today.

Upon closer investigation (see chapter II), the ionic gradients found in FW would appear to prevent effective ion uptake into the body. Typically, FW teleosts maintain NaCl levels around 130 mM within the bloodstream (for review see (Evans et al., 2005)). This compares to environmental levels of NaCl that exist into the micromolar range (μM) (Wilson et al., 1999) which creates a ion gradient between the body and the environment of 1000 fold or greater. Although this would lead to the assumption of a major energetic cost for active transport at the gill, only ~2-4% of the resting oxygen consumption (MO_2) of the fish has been calculated to be required at the gill (Morgan and Iwama, 1999). Although this is not an insignificant component of the overall energy budget for the fish, it pales in comparison to that required for other functions such as gas exchange (10% of MO_2 in resting and upwards of 70% during exercise; reviewed by (Perry and McDonald, 1993)). These analyses allow us to infer that the fish gill possesses extremely efficient machinery to ensure ion uptake and prevent ion loss. An extensive thermodynamic consideration of ion uptake is provided in chapter II.

Mitochondria/on-rich (MR) cells

My thesis focuses primarily on MR cells which can be considered the "workhorse" at the gill due to their responsibility for carrying out a myriad of functions including a/b and ion regulation. The MR cell is one of at least 5 cell types at the fish gill (Laurent and Dunel, 1980). A brief history of studies on

MR cells and their nomenclature is required before we can appreciate the specific details of Na^+ and Cl^- transport in these cells.

Work on gill MR cell function was initiated by Keys and Wilmer where they first coined the term “chloride-secreting cells” in describing the morphology of the SW eel gill (Keys and Willmer, 1932). This nomenclature was assigned due to the known role for Cl^- secretion in marine teleost fish at the time. Keys and Wilmer also took initial steps to suggest that the Cl^- cells did not exist in FW species or marine elasmobranchs that do not require Cl^- secretion although they recognized limitations in this analysis (Keys and Willmer, 1932). Credit is given to Copeland (Copeland, 1948) for shortening the nomenclature to simply chloride cells (cc) and since then, the term became ubiquitous with both SW and FW gill ion transporting cells. These reports were not made without protest as Bevelander disputed the work of Keys and Wilmer claiming that there are no specialized “secretory cells” at the gill and these cells were simply mucous cells while the respiratory epithelium was likely more responsible for Cl^- secretion (Bevelander, 1935). The role of these cells in Cl^- secretion was finally confirmed over 40 years later in an elegant study by Foskett and Scheffey using a vibrating probe technique to localize Cl^- current specifically to the chloride cells (Foskett and Scheffey, 1982). Unfortunately, this blanket term was functionally misleading for the cells that it was being used to describe as the FW cells do not secrete Cl^-. A new term has slowly emerged, the mitochondrion-rich (MR) cell, based primarily on the high density of mitochondria found in these cells compared to

other gill cells. Although grammatical debate has existed over the use of mitochondria-rich versus mitochondrion-rich, MR cell is now the accepted terminology for gill ion transporting cells.

MR cells are now categorized into functional subtypes based on Cl^- or Na^+ transport. The potential for functionally distinct MR cells was established early on based on morphological differences in ultrastructure shown by transmission electron microscopy (TEM) (Doyle and Gorecki, 1961). Pisam and colleagues then described the MR cell subtypes in great detail based on a series of excellent microscopic studies (Pisam et al., 1993; Pisam et al., 1990; Pisam et al., 1987; Pisam et al., 1995; Pisam and Rambourg, 1991). α and β MR cells were classified based on various morphological features including their localization on the gill filament, light and dark staining, cell shape, basolateral tubular system, and mitochondria distribution. However, no physiological functional correlations were attempted in their studies. These studies also added a bit of confusion to nomenclature of gill MR cells as the α and β MR cells described by Pisam and colleagues actually correlated to the description of base secreting (β) and acid secreting (α) cells respectively at the mammalian kidney as will be described below.

Previous members of our lab were the first to biochemically separate two populations of MR cells from the FW trout gill (Goss et al., 2001a). Differential binding of peanut lectin agglutinin lead to the description of PNA^+ and PNA^- MR cells with implications for transepithelial Cl^- and Na^+ uptake respectively (Galvez et al., 2002; Goss et al., 2001a). Some confusion

occurred with regards to the previous nomenclature as the PNA^+ and PNA^- MR cells were compared to the base and acid secreting cells of the intercalated duct in the mammalian kidney (Galvez et al., 2002; Goss et al., 2001a). However, the PNA^+ cells were more similar to the α cells described by Pisam and colleagues than the β cells. Barring this however, the PNA^+ and PNA^- nomenclature has now become entrenched in the field of gill cell physiology.

In the last year, it has become apparent that the separation of MR cells into only two subtypes may be misleading. Although research on trout dominated the field of comparative physiology (with respect to ion and acid-base regulation) for many years, focus has shifted to the zebrafish model system since the turn of the millennium. This is due to its fully sequenced and annotated genome along with its ease of rearing and use in developmental studies. Consequently, zebrafish are now used for ion and a/b studies on both embryonic and adult zebrafish. Zebrafish do not have the same PNA^+ and PNA^- separation of MR cells as for trout, however, they have shown to be separated with binding of concanavalin A (conA) (Lin et al., 2006). Staining of conA in MR cells co-localised with VHA and not NKA (Lin et al., 2006). This was also matched with functional data as the vibrating probe technique was used to show H^+ secretion in the VHA rich cells that stained with conA (Lin et al., 2006). Although a different lectin was used in zebrafish compared to trout, a similar pattern was observed with two MR cell subtypes. However, a recent analysis of the MR cells in the euryhaline Mozambique tilapia (*Oreochromis*

mossambicus) gill reveals that the number of MR cell subtypes may be greater than originally thought (Hiroi et al., 2008). This impressive study included quintuple immonofluorescent analysis of various transporters and classified MR cells into four different subtypes (Hiroi et al., 2008). Therefore, although I will focus on two MR cell subtypes in this thesis, it will be important to remember the possibility of more subtypes in future studies and that this indeed may be a species specific phenomenon.

Chloride (Cl^-) Transport

The majority of my thesis focuses on Na^+ transporting mechanisms and I provide an extensive review of the literature pertaining to this topic in the following chapter. Here I will briefly outline the literature pertaining to Cl^- uptake as it forms the remaining component of my thesis.

Cl^- transport was originally the predominant mechanism studied in fish due to its relative ease of measurement compared to Na^+ (Evans, 2008). Despite this fact, the route of transepithelial Cl^- uptake at the FW gill has not been pursued as much as that for Na^+ and consequently less is still known about Cl^- movement at the gill. Krogh's work (see above), was extended during the 1960s by Maetz and Garcia-Romeu where they demonstrated that an increase in HCO_3^- in the water reduced Cl^- uptake rates in the goldfish (Maetz and Garcia-Romeu, 1964). In the same study, intraparitoneal injections of $NaHCO_3$ stimulated Cl^- uptake while inhibition of CA greatly reduced Cl^- uptake (Maetz and Garcia-Romeu, 1964). These results were later confirmed in trout using an isolated gill (fish out of water) preparation

however the importance of CA was not as evident (Kerstetter and Kirschner, 1972). Using a/b disturbance as a tool for studying ion transport, Goss and Wood stimulated Cl^- uptake by metabolic and respiratory alkalosis to definitively show a 1:1 linkage of HCO_3^- secretion and Cl^- uptake in trout (Goss and Wood, 1990a; Goss and Wood, 1990b; Goss and Wood, 1991). They showed that Cl^- uptake followed a two substrate model where both the external Cl^- and internal HCO_3^- could limit the flux of these substrates across the gill (Goss and Wood, 1991). Thermodynamic concerns have remained however regarding the energizing step for a non-energetic CBE acting for Cl^- uptake in FW. Our lab addressed this problem in a collaborative review that I was part of during my PhD (Tresguerres et al., 2006a). Briefly, we proposed a model in which a co-ordinated unit of apical and basolateral membrane transporters (a metabolon) could act together to overcome the unfavourable gradients that exist. The key to this model is the energizing step provided by basolateral VHA, a mechanism that was elegantly shown by Martin Tresguerres to exist in the SW Pacific dogfish and hagfish as well as FW trout (Tresguerres et al., 2005; Tresguerres et al., 2006a; Tresguerres et al., 2007a; Tresguerres et al., 2006c; Tresguerres et al., 2007b). Consideration of microenvironments and ion transporting metabolons will be a recurring theme in my thesis as they are thought to be necessary to overcome the unfavourable gradients for ion-transport that exist in various aquatic environments.

Perspectives and Objectives

Comparative physiology has been vital to our broad understanding of ion and a/b transport. Certain animals live in extreme environments that push their physiological systems to the limit. By studying these various animal model systems valuable information was provided for mammalian systems and consequently benefited the health care system. Conversely, the molecular era began predominantly in mammalian systems due to their importance to human health. This information is now being used to ask important questions in biology that will enable us to understand what environmental practices need to be followed to ensure proper maintenance of fragile ecosystems. Clearly, a comparative approach to physiological research is still relevant to society as a whole. In this dissertation, I aim to convey the importance of my research to both the field of fish physiology and to fundamental cell biology as well.

My thesis research began as a “simple” inquiry into the pH_i regulating proteins of trout gill MR cells. As I accumulated data a host of different projects sprung from my original hypotheses. Consequently, I do not pretend that the following goals were *a priori* hypotheses but they became the specific hypotheses in a serial manner throughout my PhD program. My underlying rationale was always to enhance our understanding of basic a/b and ion transport and the separation of function into specialized MR cell subtypes. My specific PhD thesis goals included:

1) functional separation of MR cell subtypes

2) Examining pH_i behaviour of MR cells in response to Na^+ substitution experiments
3) Providing a functionally supported model of transepithelial Na^+ uptake in one type of FW gill MR cell subtype
4) Examining the Na^+ uptake model in an isolated gill preparation from an estuarine crab
5) Providing support for my proposed transepithelial Na^+ uptake mechanism in a polarized crab gill epithelium from another animal phylum.
6) Attempting to elucidate the missing molecular identity of an apical Na^+ channel in FW fish
7) Demonstrating thermodynamic constraints on Na^+ uptake mechanisms in FW fish
8) Examining pH_i behaviour of MR cells in response to Cl^- substitution experiments
9) Providing the first direct functional evidence for Cl^-/HCO_3^- exchangers in trout gill MR cells
10) Demonstrating the first evidence for a Cl^- dependent Na^+/H^+ exchanger in fish
11) Observing pH_i recovery mechanisms from induced acidosis in trout gill MR cells
12) Providing a link of pH_i functional behaviours to identified PNA^+ and PNA^- MR cell subtypes

13) Demonstrating the use of a PKC activated Na^+/H^+ exchanger in trout gill cells for pH_i recovery from acidosis
14) Comparing FW Na^+ transport mechanisms to the strategies utilised by the marine Pacific Hagfish
15) Describing the importance of Na^+/H^+ exchanger in recovery from induced metabolic acidosis in hagfish
16) Examining the unique pH_i behaviour of mosquito anterior midgut cells that create an extremely alkaline lumen

General Themes

My thesis has three main underlying themes. The dominant theme is the maintenance of whole body Na^+ and Cl^- homeostasis that is achieved by membrane transport at gill MR cells. Supporting data for these mechanisms is presented in chapters II, IV, and V-VII. The second theme is the maintenance of systemic acid-base parameters. These data were obtained using a comparative approach with a South American estuarine crab and the Pacific hagfish (Chapters V and IX, appendix I and II). The third theme focuses on the regulation of intracellular pH (pH_i). For these questions I investigated the mechanisms of pH_i regulation in rainbow trout gill MR cells along with the midgut cells of the mosquito (*Aedes aegypti*) (Chapters VIII and X).

In this thesis I have worked on a variety of distantly related aquatic animals. Despite their distant relationship, specific characteristics of each animal were utilised to strengthen the overall conclusions of this thesis. The rainbow trout was used as the primary organism in my thesis as the functional

characterization of the trout gill MR cells was my primary objective. Zebrafish were utilized to take advantage of the wealth of molecular information available for this organism that enhances our ability to investigate molecular characterizations. The South American crab *Neohelice granulata* was studied based on our ability to successfully use a properly polarized and isolated gill preparation. These data were invaluable for comparisons to my isolated MR cell work. I studied Pacific hagfish for their unique status as an osmoconformer. Therefore, gill mechanisms utilized for compensating systemic pH disturbances could be studied in isolation without the interference of the linkage to ion-regulation as occurs in many other fishes. Lastly, larvae of the mosquito (*Aedes aegypti*) were used for the unique nature of the midgut alkalinization in these animals. This incredible ion transporting mechanism was studied for the influence on intracellular pH and to provide an important comparison for how challenging ion transport gradients can be overcome.

Figures

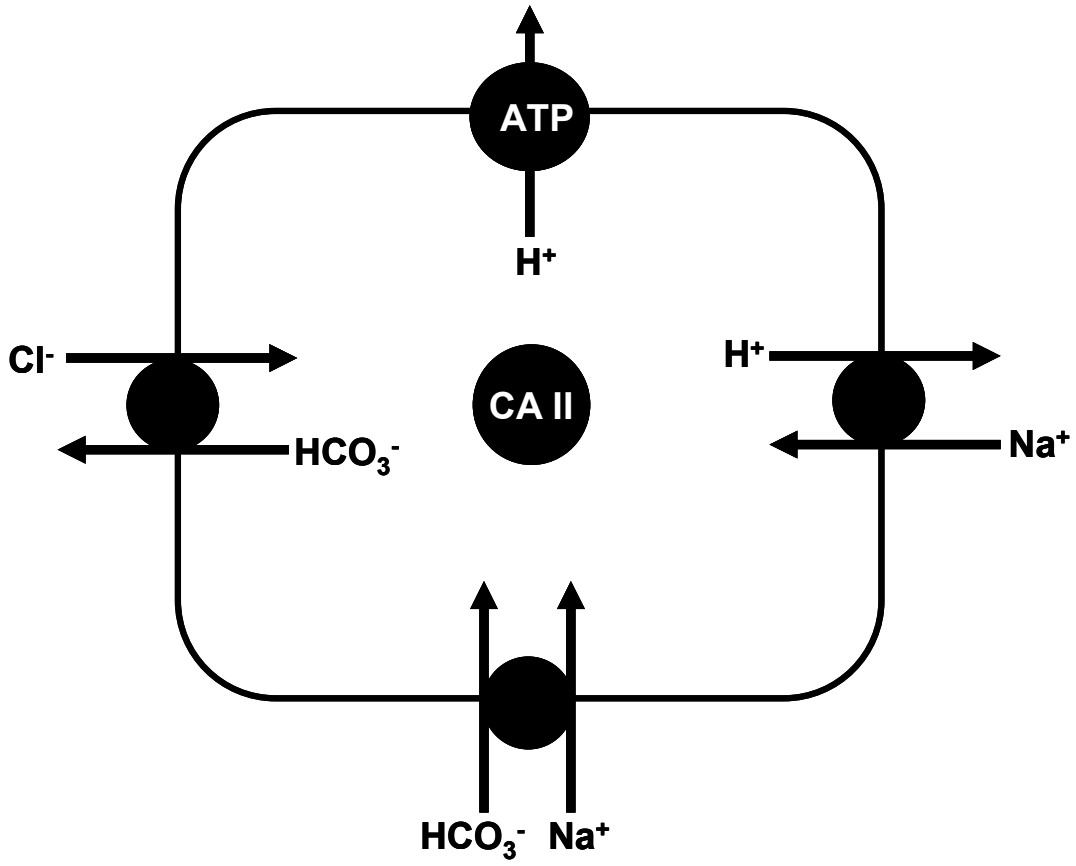

Figure 1.1 A generalized cell model for intracellular pH (pH_i) regulation. Cells possess these transporters in various combinations on the apical and basolateral membranes to achieve internal pH homeostasis. CA II represents the intracellular carbonic anhydrase that hydrates CO_2 to the HCO_3^- and H^+ units utilised by the various acid-base transporters.

Chapter II: Thermodynamic considerations underlying ion uptake mechanisms[1]

[1]A version of this section has been published previously (Parks et al., 2008):

Parks, S. K., Tresguerres, M. and Goss, G. G. (2008). Theoretical considerations underlying Na^+ uptake mechanisms in freshwater fishes. *Comparative Biochemistry and Physiology C-Toxicology & Pharmacology* **148**, 411-418.

Introduction

Despite extremely low ionic concentrations in many freshwater (FW) systems, fish are able to survive and maintain their plasma ion concentrations at stable levels up to 1000 fold higher than the external ion concentrations. This is accomplished by both a decrease in the relative permeability of the gill to ion loss and the development of elaborate mechanisms of active ion uptake at the gill. The rise of molecular biology in the field of comparative ion transport physiology, coupled with the use of the new zebrafish model system with its "fully annotated" genome, has resulted in significant advances over the past few years. My aim in this chapter is to provide a summary of recent data that have contributed to our understanding of the mechanisms of gill ion and acid–base regulation at a more detailed molecular level. Emphasis will be specifically focused on proposed mechanisms of Na^+ uptake, how these recent studies align with previous data demonstrating function, and thermodynamic parameters that must be considered when modeling fish ion transport in specific environments. This perspective is written in the light of new molecular advances to ensure that our understanding continues to grow in a clear, thermodynamically sound and logical manner.

Na^+ uptake mechanisms

As mentioned in chapter I, August Krogh (Krogh, 1938) pioneered the study of ion transport in fish by proposing that Na^+ is exchanged electroneutrally for NH_4^+ at the fish gill (Fig. 2.1 A). This was based on

concomitant and equimolar net reduction of Na^+ and net gain of NH_4^+ in the water that the fish were held in. Almost 30 years later Maetz and Garcia Romeu (Maetz and Garcia-Romeu, 1964) performed more advanced radioisotope experiments to analyze the unidirectional fluxes of Na^+ into the goldfish, *Carassius auratus*. Their studies supported the notion of Na^+ and Cl^- uptake to occur as independent mechanisms and they also supported Krogh's earlier assumptions (Krogh, 1938) that the mechanism of Na^+ uptake across the fish gill epithelium was via a Na^+/NH_4^+ exchanger. However, it was demonstrated soon after that Na^+ was in fact exchanged for H^+ rather than NH_4^+ (Kerstetter et al., 1970). Regardless, all studies concluded that the uptake of Na^+ was compensated by equimolar efflux of a cation (H^+ or NH_4^+) and it was thus proposed that the Na^+ transport mechanism across the fish gill was electroneutral. The energy required to drive the apical cation exchange was proposed to be provided by Na^+/K^+-ATPase (NKA), which is present in large amounts on the basolateral membrane of gill mitochondria-rich (MR) “chloride” cells (Fig. 2.1B). These early studies were supported pharmacologically when Kirschner and colleagues (Kirschner et al., 1973) were the first to report in FW fish, that amiloride, a general inhibitor of Na^+/H^+ exchangers (NHEs), greatly reduced Na^+ uptake.

Valuable information about cellular mechanisms for Na^+ uptake from very soft FW has been derived from studies with frog skin (reviewed by (Ehrenfeld, 1998; Ehrenfeld and Klein, 1997; Harvey, 1992). This epithelium has been extensively studied and is more amenable to direct measurements

of ion transport because it can be placed in Ussing chambers for electrophysiological and pharmacological analysis. Measurements under open- and short-circuit conditions clearly demonstrated that Na^+ enters the cell through an apical channel, driven by H^+ efflux from an apical H^+-ATPase (Ehrenfeld and Garcia-Romeu, 1977; Ehrenfeld et al., 1985).

The frog skin model also proved to be valid for other ion-transporting epithelia, like the turtle urinary bladder (Steinmetz et al., 1987). Not surprisingly, it also influenced research on fish ion uptake, since it was becoming clear that the NKA alone was insufficient to drive an electroneutral NHE in dilute FW and that an additional energizing step was required (reviewed in (Jensen et al., 2003; Kirschner, 2004). Using analogies to the frog skin and turtle bladder (Ehrenfeld and Garcia-Romeu, 1977; Ehrenfeld et al., 1985; Steinmetz et al., 1987), and consideration of both environmental and putative intracellular [Na^+] and [H^+], Avella and Bornancin (Avella and Bornancin, 1989) proposed that NHE could not function for Na^+ uptake in fish living in extremely dilute environments (e.g. μmol L^{-1} range). They proposed a new fish gill model whereby an apical vacuolar H^+-ATPase (VHA) electrochemically linked to a Na^+ channel drives Na^+ uptake from fresh water (Avella and Bornancin, 1989) Fig. 2.1C). Lin and Randall (Lin and Randall, 1993) then demonstrated VHA activity in crude homogenates of gill tissue from the rainbow trout and showed the activity was decreased during acclimation to seawater. Lin and colleagues (Lin et al., 1994) later also showed VHA immunoreactivity at the rainbow trout gill using a bovine VHA

antibody. Further supporting functional evidence for this model was provided when it was shown that bafilomycin, a selective inhibitor of VHA, dramatically reduced Na^+ uptake from FW during *in vivo* experiments on young tilapia and carp (Fenwick et al., 1999) and zebrafish (Boisen et al., 2003). In addition, both bafilomycin and phenamil (an amiloride derivative specific for inhibiting Na^+ channels; (Kleyman and Cragoe, 1988)) also reduced Na^+ uptake in rainbow trout (Bury and Wood, 1999; Grosell and Wood, 2002).

The last two decades has corresponded with a rapid advancement of understanding the molecular mechanisms of ion transport in a variety of species and a variety of transport epithelia, whose molecular and evolutionary characteristics have been recently reviewed (Alper, 2006; Alvarez de la Rosa et al., 2000; Orlowski and Grinstein, 2004; Romero et al., 2004; Slepkov et al., 2007; Wagner et al., 2004). In addition to the breakthroughs in molecular biology, there have been additional advances in understanding the physiology of ion transport in the fish gill. For example, the use of immunocytochemistry has significantly advanced our knowledge by demonstrating the presence and localization of particular transporters within the fish gill (Edwards et al., 1999; Lin et al., 1994; Lin et al., 2006; Parks et al., 2007b; Piermarini et al., 2002; Sullivan et al., 1995; Tresguerres et al., 2005; Tresguerres et al., 2006a; Tresguerres et al., 2006b; Tresguerres et al., 2007b; Wilson et al., 2000). However, a *caveat* that must be placed on some of these findings is the use of heterologous antibodies for detection which may give spurious results due to undetermined specificity of the antibody. More recently, the development of

homologous antibodies have significantly strengthened immunocytochemical studies in fish gills that are often complemented by mRNA *in situ* experiments using species–specific probes (Catches et al., 2006; Choe et al., 2007; Choe et al., 2005; Claiborne et al., 2008; Hirata et al., 2003; Katoh et al., 2003; Yan et al., 2007).

Early attempts at examining the functional physiology of the gill in isolation were performed primarily using isolated gill (Kerstetter and Keeler, 1976; Kerstetter et al., 1970) or perfused head preparations (Perry et al., 1985; Perry et al., 1984). These preparations provided substantial information on the overall gill mechanisms of transport. However, information at the cellular level was unattainable due to the complex nature of the gill. Our lab has identified two different cell types of mitochondria-rich (MR) cells at the trout gill, termed PNA^+ and PNA^- MR cells based on their binding of peanut lectin agglutinin (Galvez et al., 2002; Goss et al., 2001a). Members of our lab also demonstrated previously that VHA abundance increased in only the PNA^- MR cells during hypercapnic acidosis consistent with the role of H^+ secretion and Na^+ uptake occurring in this cell (Galvez et al., 2002). Moreover, members of our lab developed a protocol to isolate primary cultures of PNA^+ and PNA^- MR cells (Galvez et al., 2002; Goss et al., 2001a). This is a powerful technique since it allows for the direct examination of the functional physiology of the fish gill at the cellular level, albeit with certain limitations that are discussed further in chapter IV (Parks et al., 2007b). Members of our lab (Reid et al., 2003) performed radiotracer experiments

with isolated cells and reported that only the PNA^- MR cells exhibited a phenamil and bafilomycin sensitive Na^+ uptake mechanism implicating a Na^+ channel linkage to the VHA in these cells. More recently, using single cell pH imaging, I have confirmed the presence of at least two distinct MR cell populations in response to Na^+ substitution experiments (chapter IV (Parks et al., 2007b)). There I also demonstrated that only one population of MR cells performs phenamil sensitive Na^+ uptake. My results support the model of Na^+ uptake occurring apically via a phenamil sensitive Na^+ channel that is electrogenically linked to the VHA as suggested by others. Moreover, I was the first to functionally demonstrate that a basolateral membrane electrogenic Na^+/HCO_3^- co-transporter (NBC) moves Na^+ into the blood space, likely aided by NKA to maintain the required membrane potential ((Parks et al., 2007b), Fig. 2.1C). My results also suggest that this mechanism also exists at the gill in FW acclimated crabs, although it may only be involved in acid–base regulation (see chapter V, (Tresguerres et al., 2008)). My findings complement previous molecular work showing an upregulation of NBC mRNA in response to acidosis at the FW fish gill (Hirata et al., 2003; Perry et al., 2003a; Perry et al., 2003b).

Recent work elegantly demonstrated the presence of VHA-rich cells on the skin of zebrafish larvae, an epithelium responsible for ion uptake at the larval stage of development (Lin et al., 2006). Using the ion-selective vibrating probe technique, Hwang and colleagues (Lin et al., 2006) recorded apical bafilomycin sensitive H^+ flux from single cells of intact larvae. The authors

proposed a role for these VHA-rich cells in Na^+ uptake. Interestingly, these cells were not rich in NKA (Lin et al., 2006) which may indicate that NKA is not essential for Na^+ uptake, at least in zebrafish skin. These results were complemented by the first two studies from zebrafish on a/b and ion regulation taking advantage of the morpholino gene knockdown technique (Esaki et al., 2007; Horng et al., 2007). Knockdown of VHA reduced survival by ~50% in larvae placed in acidic water (Horng et al., 2007). Importantly, the knockdown of VHA also resulted in a reduced Na^+ content in mutants acclimated to low Na^+ environments (~0.01 mmol L^{-1}) compared to wild-type (WT) larvae (Horng et al., 2007). No differences were noted between mutant and WT larvae however in those animals acclimated to normal Na^+ environments of ~0.5 mmol L^{-1} (Horng et al., 2007). Fluorescent Na^+ dyes also demonstrated a bafilomycin sensitive Na^+ accumulation in skin cells of FW zebrafish embryos (Esaki et al., 2007). These studies clearly indicate that apical VHA is essential for Na^+ uptake in acidic or very soft water. This supports the requirement of an apical energizing step in bringing Na^+ into the body. However, the significant deficiency in confirming the model of Na^+ uptake via an apical Na^+ channel is that not a single member of the epithelial Na^+ channel family (ENaC homologs) has been found in any fish database (Hwang and Lee, 2007), including the fully sequenced and so called annotated genomes of both zebrafish and fugu. The inability to identify homologs of any ENaC subunits in any fish species is puzzling due to the fact that homologous members of the ENaC-Deg family exist in organisms across

a diverse range of organisms from *Caenorhabditis elegans* to *Homo sapiens* (for review see (Alvarez de la Rosa et al., 2000). While we have no explanation for this anomaly, we think it is possibly related to low homologies between species for the ENaC subunits and lack of complete and accurate annotations of the current fish genomes. Alternatively, it is possible that there was a genomic deletion that included the α ENaC gene after the divergence of the Sarcorpterygeans and Actinopterygeans resulting in all teleosts not having this ENaC gene. However, ENaC β and γ subunits also cannot be detected by current homology searching strategies. Importantly, the genes for the α (chromosome 12) and β and γ subunits (chromosome 16) are located in different chromosomes in mammals (Hummler et al., 2002). Therefore, this explanation would require the two genomic regions to be deleted by independent events.

Regardless, the presence of phenamil sensitive Na^+ transport in whole animals points to some type of Na^+ channel mechanism being present in fishes reared in low ionic strength water. Phenamil (at μmol L^{-1} concentrations) has been demonstrated to inhibit Na^+ uptake in FW fish as mentioned previously (Bury and Wood, 1999), 100 μmol L^{-1}); (Grosell and Wood, 2002),100 μmol L^{-1}); (Reid et al., 2003),10 μmol L^{-1}). In other studies, pharmacological inhibition by amiloride has been used to support the role of an NHE at the FW fish gill for Na^+ uptake (Esaki et al., 2007; Kirschner et al., 1973; Preest et al., 2005). However, amiloride also blocks Na^+ channels at even lower doses while phenamil has never been shown to inhibit NHEs at

either low (μmol L^{-1}) or even high (mmol L^{-1}) concentrations (Goss et al., 2001b; Kleyman and Cragoe, 1988). The logical conclusion from pharmacological studies is that the most specific inhibitor (phenamil and not amiloride) should determine the pharmacological identification of the Na^+ transport mechanism (Na^+ channel and not NHE).

Recently, there have been a number of papers demonstrating specific NHE isoforms in the gills of fish from a variety of environments. These studies have suggested a role of apical NHE in transepithelial Na^+ uptake in dilute FW and have revitalized the debate over the molecular identity of the apical transporter responsible for Na^+ uptake in the FW fish gill. Theoretically, either the ENaC-VHA model or the NHE-NKA model can function, but the NHE can only function under a very narrow range of environmental and cellular conditions compared to an ENaC-VHA mechanism. The primary purpose of this chapter is to clearly illustrate these theoretical limitations of an NHE in a range of freshwaters. Thermodynamic considerations will also be an underlying theme throughout the data chapters and final discussion of my thesis.

Na^+/H^+ exchanger (NHE)

The NHE is a bi-directional transporter that generally brings Na^+ into the cell in exchange for H^+. This can result in the regulation of intracellular pH (pH_i) or in transepithelial Na^+ uptake as in the mammalian proximal tubule (for review see (Orlowski and Grinstein, 2004; Slepkov et al., 2007)). However, it is important to note that NHE function is driven solely by environmental and

cellular concentration gradients of Na^+ and H^+ and it is not affected by membrane potential. For example, a larger [Na^+] in the environment compared to the cell favours H^+ secretion and consequently Na^+ uptake. This explains why NHEs are the prevalent mechanism for H^+ secretion in brackish water and seawater animals including crustaceans (Towle et al., 1997), hagfish (Edwards et al., 2001; McDonald et al., 1991; Parks et al., 2007a), elasmobranchs (Choe et al., 2005; Claiborne et al., 2008; Tresguerres et al., 2005), and teleost fish (Catches et al., 2006; Claiborne et al., 1999; Claiborne et al., 2008). However, one of the specific considerations for this electroneutral exchanger is that the transporter can work in the opposite direction if favourable conditions are present (i.e. a reversible transporter: Na^+ loss and H^+ gain). This is an important point to be considered in the section on thermodynamics since placing an NHE on the apical membrane of a fish under conditions which favour Na^+ loss and H^+ gain will be detrimental to the physiology of the organism.

NHE at the FW fish gill was originally implicated via immunological studies using various heterologous antibodies (see concerns with this technique above) against different NHE isoforms (Edwards et al., 1999; Wilson et al., 2000). The first molecular cloning and subsequent functional implication of a FW NHE was from the Japanese Osorezan dace (Hirata et al., 2003). This report of an NHE3 was remarkable in that the fish lives not only in FW (<1 mmol L^{-1} Na^+) but also at an acidic pH of 3.5 (Hirata et al., 2003). Each of these conditions (low Na^+ and low pH) would act to inhibit

NHE function according to thermodynamic principles (see below). The authors also noticed that the apical region of the ion-transporting cells presents an apical crypt, and suggested it provides a microenvironment that acts to increase [Na^+] outside the gill cells (Hirata et al., 2003). However, it is unclear how the "microenvironment hypothesis" would avoid a further proportional diminishing of pH in this area, which would eventually reverse the Na^+ flux. More recently, further molecular evidence has shown increased levels of NHE2 mRNA associated with FW acclimation in killifish (Scott et al., 2005) and zebrafish (Craig et al., 2007). At a first glance, the combination of these reports (Craig et al., 2007; Hirata et al., 2003; Scott et al., 2005) seem to unambiguously strengthen the role of NHE in Na^+ uptake in FW. However, every study, including these three, must be examined in detail before any solid conclusions are made. For example, the killifish is an estuarine animal that faces a range of salinities on a daily basis, and it is thus possible that NHE transcript upregulation is an initial response to water dilution that does not necessarily result in a functional apically inserted protein. Less subjective is the fact that the FW acclimation in the study by Scott and colleagues (Scott et al., 2005) was indeed to softwater, but with an NHE-favourable environmental pH of 8.0. Common to both the zebrafish and killifish studies are the facts that (1) NHE abundance and localization was not examined at the protein level, which is more functionally relevant than mRNA expression, and (2) upregulation of NHE does not rule out a concomitant, functionally

relevant upregulation of any relevant epithelial Na^+ channels (although this is currently impossible to test due to lack of molecular proof for its existence).

A recent study reports the impressive cloning and identification of eight different zebrafish NHE isoforms (termed *znhe1*, *-2*, *-3a*, *-3b*, *-5*, *-6*, *-7*, and *-8*, (Yan et al., 2007)). Of these eight different isoforms, only zNHE3b was expressed at the gill (Yan et al., 2007). This isoform was localized to the apical membrane of gill ionocytes and co-localised with VHA-rich cells only and not NKA-rich cells (Yan et al., 2007). This resulted in a model predicting the association of an apical NHE and VHA to function together for Na^+ uptake. Finally, I note that molecular sequences for rainbow trout NHE3 and NHE2 have recently been made available in studies focussing on both gill and kidney function (Ivanis et al., 2008a; Ivanis et al., 2008b). These authors also suggest a role for NHE function at the gill in ion uptake however the functional relevance is not confirmed (Ivanis et al., 2008b). These few references are the sum total of all the direct molecular evidence for NHEs in FW fishes. Undoubtedly, relative paucity of direct molecular information on fish NHE's is hampering our ability to clearly delineate its function in FW. However, given the strong evidence for the presence of various NHE isoforms in the gills of FW fish even from dilute environments, these isoforms likely play some role in Na^+ transport at the FW fish gill.

Thermodynamic consideration of Na^+ uptake from freshwater: NHE

The functionality of NHE as an apical mode of Na^+ uptake in FW is often dismissed as being “thermodynamically unfeasible” although firm

representations of these principles are lacking in the literature. This deficit is contributing to confusion in the literature whereby thermodynamic considerations are not being fully examined when interpreting data and proposing new models of transport for the fish gill. This section aims to illustrate how environmental and cellular conditions ultimately determine the direction of transport of an apical NHE in FW organisms.

If we simply consider an NHE antiport functioning in isolation, there are only 4 variables that can have an effect on its direction of transport. These include environmental pH (pH_o), intracellular pH (pH_i), environmental Na^+ ($[Na^+]_o$) and intracellular Na^+ ($[Na^+]_i$). It is important to restate that NHE function is unaffected by changes in transmembrane potential. Eq. (1) describes the transport equilibrium where there will be no net flow of Na^+ or H^+ in either direction in a NHE.

$$\frac{[Na^+]_i}{[Na^+]_o} = \frac{[H^+]_i}{[H^+]_o} \qquad \text{(Equation 2.1)}$$

However, for proper functioning, a driving gradient whereby higher $[Na^+]_o$ or higher $[H^+]_i$ is required to disturb the equilibrium and drive the transporter in the forward direction (Na^+ in and H^+ out) according to:

$$\frac{[Na^+]_i}{[Na^+]_o} < \frac{[H^+]_i}{[H^+]_o} \qquad \text{(Equation 2.2)}$$

Therefore we can re-arrange the above formula to demonstrate the influence of one variable on the functioning of NHE according to thermodynamic principles. An example whereby we are solving for $[H^+]_i$

required to drive NHE at fixed values of $[Na^+]_i$, $[H^+]_o$, and $[Na^+]_o$ is provided in Eq. (3).

$$\frac{[Na^+]_i[H^+]_o}{[Na^+]_o} < [H^+]_i \qquad \text{(Equation 2.3)}$$

Therefore to calculate this value we use Eq. (4) to define the transport equilibrium point, whereby any value below will result in forward transport of NHE. Any value above will then result in reverse transport mode of NHE.

$$\frac{[Na^+]_i[H^+]_o}{[Na^+]_o} = [H^+]_i \qquad \text{(Equation 2.4)}$$

By manipulating these variables, we can graphically represent (Fig. 2.2 and Fig. 2.3) the equilibrium point for NHE in relation to any set of environmental and cellular parameters. Moreover, it follows that we can similarly re-arrange the above formulae to illustrate the effect of any other parameters on NHE function.

Environmental $[Na^+]$ and pH are regularly reported in most publications allowing us to predict the potential functioning of NHE under those conditions. FW fish live in waters ranging from pH 3.5 (Hirata et al., 2003; Wilson et al., 1999; Wood et al., 1998) to as high as pH 10 (Randall et al., 1989). In addition, environmental Na^+ ranges from as low as 10 μmol L^{-1} and 20 μmol L^{-1} (Wilson et al., 1999) to full strength seawater of ~550 mmol L^{-1}. As mentioned above, the driving gradients for NHE in high Na^+ environments (>5 mmol L^{-1}) favour this transporter functioning as an acid–base regulator and are not of concern in our review. On the other hand, in dilute FW, pH and

environmental [Na^+] will be important in determining the direction of transport function of an NHE (it is reversible).

One variable that is key to these calculations is the $[Na^+]_i$: a low $[Na^+]_i$ would favour Na^+ uptake via an NHE while a high $[Na^+]_i$ would inhibit Na^+ uptake or result in Na^+ loss via an NHE. Unfortunately, obtaining reliable values for $[Na^+]_i$ has proven extremely difficult. At least three attempts have been made to describe the $[Na^+]_i$ in the cells of the fish gill (Eddy and Chang, 1993; Morgan et al., 1994; Wood and Lemoigne, 1991) (Table 2.1). It is important to note that each value reported for fish (62, 55, 80 mmol L^{-1}) is much higher than those described in other similar transporting epithelium (Table 2.1: ~2–20 mmol L^{-1}). If these values were indeed true, neither an NHE nor a Na^+ channel/VHA would be able to function under any FW condition. Therefore it is likely that $[Na^+]_i$ are severely overestimated in FW fish since high $[Na^+]_i$ would be inhibitory for Na^+ uptake by any mechanism. As discussed by Morgan and colleagues (Morgan et al., 1994) these values for fish must be interpreted with caution due to the technical difficulties associated with obtaining these data. However, if we observe a range of $[Na^+]_i$ reported from other systems we see values averaging 6−10 mmol L^{-1} (and as low as 2 mmol L^{-1} when the isolated epithelium was bathed in symmetrical 0.1 mmol L^{-1} Na^+ solutions (Harvey and Kernan, 1984), Table 2.1). Consequently to be as conservative as possible I will use and exceed the lowest measured $[Na^+]_i$ in all animals to demonstrate the range of feasibility of NHE function over a wide range of environmental parameters.

The second unknown in our calculations is the intracellular pH (pH_i) of the Na^+ transporting cell type. Similar to the influence of $[Na^+]_i$, low pH_i will favour Na^+ uptake via an NHE while a high pH_i would inhibit Na^+ uptake via an NHE. We must remember that pH_i is tightly regulated to ensure cell survival and in all cells is maintained at pH of ~6.9–7.6 dependent on temperature. Our work on isolated rainbow trout gill MR cells shows an apparent difference in resting pH_i in a mixed population of MR cells (chapter IV (Parks et al., 2007b)). Interestingly, resting pH_i in the putative Na^+ transporting cells was significantly lower than in the rest of the cells, which would favour NHE function as explained above. Based on our results, we will use resting pH_i values of 7.4 for the calculations, which is also similar to resting pH_i found in cultured rainbow trout and goldfish pavement cells (Sandbichler and Pelster, 2004; Wood and Part, 2000) and whole gill pH_i estimates (Wood and Lemoigne, 1991).

Influence of environmental pH and salinity: NHE

Using the above Eqs. (1), (2), (3) and (4), we have solved for a range of values the NHE transport equilibrium in relation to pH_o and $[Na^+]_i$ (Fig. 2.2A, dashed line). These values are obtained using an $[Na^+]_o$ of 0.5 mmol L^{-1} which was chosen to exceed environmental values reported in most of the literature (e.g. Ottawa Canada, 0.13 mmol L^{-1}, Vancouver Canada ~0.02 mmol L^{-1}, Taipei, Taiwan 0.3 mmol L^{-1} (they make zebrafish water artificially), Lake Osorezan, Japan ~0.9 mmol L^{-1}, Hamilton Canada ~0.5 mmol L^{-1}). Fig. 2.2A shows that Na^+ loss would dominate over a wide range of naturally

occurring environmental pH values (the NHE would function in reverse mode-red area). Na^+ uptake via an NHE in the pH_o ranges below 8.0 would technically be possible only if $[Na^+]_i$ is lower than any previously measured value in any cell type. Conversely, only when more alkaline pH_o are encountered (pH_o of ~8.4 and above) can we observe a reasonable $[Na^+]_i$ (i.e. 6 mmol L^{-1}) that would enable Na^+ uptake and H^+ excretion using an NHE (i.e. forward function of the NHE). We can clearly see from Fig. 2.2A that under a normal physiological range of environmental pH in FW systems, Na^+ loss would dominate over Na^+ gain if an NHE was utilised exclusively. To cement the contention that the range of environmental parameters where NHE can function effectively is limited, I have varied the $[Na^+]_o$ to higher and lower levels to demonstrate the range of function (Fig. 2.2B). If the $[Na^+]_o$ increases to 5 or 50 mmol L^{-1}, then the range of environmental pHs where NHE may function is shifted to environmentally realistic values (~pH 7.5 for 5 mmol L^{-1} $[Na^+]_o$ and ~pH 6.5 and above for 50 mmol L^{-1} $[Na^+]_o$) assuming a $[Na^+]_i$ of at least 6 mmol L^{-1}. Even so, at more acidic pHs, NHE will not function for Na^+ uptake. However, if the $[Na^+]_o$ decreases to 0.05 mmol L^{-1} (e.g. the level found in Vancouver tap water, Amazon basin, Canadian shield waters), then the range of environmental pHs where NHE may function is shifted to environmentally unrealistic values (> pH 9.5) for most fish bearing waters. This theoretical illustration is in direct concordance with our contention that NHEs can function at higher environmental salinities but simply cannot function at low environmental salinities. Moreover, it is

extremely important to note that if an NHE is present on the apical membrane at these low $[Na^+]_o$, then the NHE will actually function in reverse mode and Na^+ loss (and H^+ loading) would occur. These considerations likely allow the use of an apical NHE3 in the FW stingray that was tested living in relatively "hard" FW of ~4 mmol L^{-1} Na^+ (Choe et al., 2005) but call into question many studies placing the NHE on the apical membrane in fish acclimated to waters of very low $[Na^+]_o$. Clearly, the environmental pH and $[Na^+]$ play a major role in determining the potential function of an apical NHE. Finally, while boundary layers may be implicated in increasing $[Na^+]_o$ to a small extent, they would also concurrently result in acidification of the same boundary layer (Lin and Randall, 1990; Playle and Wood, 1989; Wright et al., 1986) which would act to simultaneously impair NHE function

Influence of cellular pH and salinity: NHE

If we re-arrange Eq. (1) and assume a typical FW $[Na^+]$ of 0.5 mmol L^{-1} (Fig. 2.3A), and an extracellular pH of 7.0 (a typical value for that environmental $[Na^+]$), we can plot the NHE transport equilibrium in relation to pH_i and $[Na^+]_i$. From this plot, we can see that Na^+ uptake would only occur via an NHE at pH_i values of ~5.9 and below when $[Na^+]_i$ is assumed to be equal to the lowest measured value from frog skin principle cells of 6 mmol L^{-1}. This is much lower than pH_i values reported previously of ~7.4 for fish gill (Parks et al., 2007b; Sandbichler and Pelster, 2004; Wood and Lemoigne, 1991; Wood and Part, 2000) or for any cell type for that matter. NHE could

function at normal pH_i only when environmental pH is higher than 9 (Fig. 2.3B).

Thermodynamic consideration of other modes of Na^+ uptake from freshwater:

Na^+ channel

An apical Na^+ channel with linkage to an energizing VHA is another potential mechanism for Na^+ uptake from freshwater as described above. As we envision a simple channel, it is reasonable to assume that problems could also arise with driving Na^+ into the cell and likewise in preventing Na^+ from leaving the cell to the water *via* this channel. The equilibrium point for a non-rectifying Na^+ channel adheres to the following equation:

$$\mu_m = zFV_m + RT \times \ln \frac{[Na^+]_i}{[Na^+]_o} \qquad \text{(Equation 2.5)}$$

An important point to notice about Eq. 2.5 for the Na^+ channel is that the equilibrium point is independent of environmental and cellular pH. In addition, movement through the channel is driven by the membrane potential (V_m) and environmental and intracellular [Na^+] only. Therefore movement can be driven by decreasing intracellular [Na^+] or increasing the V_m (to a greater negative value). If Eq. 2.5 is re-arranged the impact of Na^+ levels on the thermodynamic feasibility of movement *via* a Na^+ channel can be analysed according to the following equation:

$$Na^+{}_o = Na^+{}_i \times e^{(\frac{zFV_m}{RT})} \qquad \text{(Equation 2.6)}$$

Analysing Eq. 2.6 for the influence of $[Na^+]_i$ we can see that as you decrease $[Na^+]_i$ then Na^+ uptake can occur from very soft waters with a

reasonable V_m (Figure 2.4a). Furthermore, when the function is plotted to assess the impact of V_m we note some interesting effects as V_m becomes more negative (Figure 2.4b). For example, Na^+ uptake can occur from environmental Na^+ of 0.4mM if $[Na^+]_i$ is less than 4.2mM and V_m is less than -60mV. Furthermore, if V_m reaches levels around -90mV then Na^+ uptake can occur *via* a Na^+ channel from micro molar concentrations of environmental Na^+. However, as discussed throughout this thesis, an epithelial Na^+ channel has evaded molecular characterisation in any fish genome analysis and therefore can not yet be assigned as the primary mechanism for Na^+ uptake.

Electrogenic NHE

A possibility for a freshwater fish to enable thermodynamically feasible Na^+ uptake via an NHE would be to invoke the use of an electrogenic NHE. If we assume an NHE that transports $2Na^+$ for every H^+, the equilibrium point for an electrogenic NHE adheres to the following equation:

$$\mu_m = 2zFV_m + 2RT \times \ln\frac{[Na^+]_i}{[Na^+]_o} - zFV_m \times \ln\frac{[H^+]_i}{[H^+]_o} \quad \text{(Equation 2.7)}$$

The advantage of an electrogenic NHE would be similar to a Na^+ channel in that V_m can aid in driving ion movement across the membrane. Re-arranging Eq. 2.7 to solve for Na^+ levels that would allow uptake *via* an electrogenic NHE gives the following equation:

$$Na^+{}_o = Na^+{}_i \times \sqrt{\frac{[H^+]_i}{[H^+]_o}} \times e^{(\frac{zFV_m}{2RT})} \quad \text{(Equation 2.8)}$$

Using the same analysis of $[Na^+]_i$ and $[Na^+]_o$ in relation to changing V_m we can see how that an electrogenic NHE would enable Na^+ uptake from more dilute FW than the traditional electroneutral NHE (Figure 2.5). Currently I can not say if this is a possibility in gill MR cells as the stoichiometry of the cloned fish NHEs is not yet established. Evidence for electrogenic $2Na^+/H^+$ exchanger has been reported only in crustaceans (Ahearn and Clay, 1989; Ahearn and Franco, 1990; Ahearn et al., 1990; Shetlar and Towle, 1989) and echinoderms (Ahearn and Franco, 1991). Prokaryotes such as *Escherichia coli* possess an electrogenic Na^+/nH^+ transporter (NHA) that acts in the opposite direction of vertebrate NHE to allow survival in hyper saline and alkaline environments (Padan et al., 2005). Little is known about NHA activity in metazoans despite their presence in the genome of various vertebrate species (Brett et al., 2005). William Harvey and colleagues have recently cloned an NHA from the larval mosquito gut and implicated its role in a variety of physiological processes such as pH and volume regulation and Na^+ recycling (Rheault et al., 2007). However, as the NHA transports in the opposite direction, its importance in an electrogenic NHE for Na^+ uptake at the fish gill are likely slight. Further molecular and functional characterization of the NHA is required before we can understand its overall importance in a/b homeostasis.

Potential involvement of microenvironments and metabolon hypotheses

We can consider the possibility of the animal using local microenvironments (i.e. metabolons) to maximize the intracellular parameters

(low $[Na^+]_i$, low pH_i) that would favour NHE function in the forward direction (Na^+ uptake). There is an elaborate tubular system known to exist in the MR cells of the fish gill originating from multiple basolateral membrane infoldings ((Philpott, 1980), reviewed by (Tresguerres et al., 2006a)). In fact, our lab (Tresguerres et al., 2006a) have proposed that this distinct ultrastructural arrangement creates a cellular microenvironment that favours Cl^- uptake from FW. This could be possible by placing an apical anion exchanger (AE), cytosolic carbonic anhydrase (CA) and a basolateral VHA into close proximity. CA generates HCO_3^- and H^+ from CO_2 and H_2O, VHA removes the H^+ electrogenically from the area into the blood – and provides the driving force – while the AE is the apical facilitating transporter. The vital step in this mechanism is the energy input of a VHA to create a disequilibrium of the $[HCO_3^-]$ in the local environment. In principle, a similar microenvironment (but with reversed functional polarity) could be manipulated to create very acidic pH_i levels to help drive NHE-mediated Na^+ uptake. However, a significant requirement for this acidic compartment to exist is that the distinct environment must be supported by primary active transport of HCO_3^- out of the cell. This type of mechanism, (i.e. a HCO_3^- ATPase) has never been described in any physiological system and therefore the possibility of localized $[H^+]$ differences driven by HCO_3^- primary active transport is unlikely.

An alternate argument might be that a basolateral, electrogenic, Na^+/HCO_3^- co-transporter (demonstrated in chapter IV (Parks et al., 2007b) could deplete HCO_3^- sufficiently (and hence create a local H^+

microenvironment) to drive an apical NHE. However, in this situation, there would then be no direct energetic step (ATPase) in the transepithelial Na^+ transport mechanism. This would prevent Na^+ uptake due to the demonstrated energy barrier in place for transepithelial Na^+ transport (Jensen et al., 2003; Kirschner, 2004); explained below).

If pH_i cannot be reduced appreciably to allow NHE function, $[Na^+]_i$ could potentially be lowered to facilitate NHE function. This is not inconceivable considering the presence of massive numbers of Na^+/K^+-ATPase (NKA) on the basolateral membrane of all fish gills analyzed (Evans et al., 2005). However, even at the lowest $[Na^+]_i$ recorded (2 mmol L^{-1}, Table 2.1) pH_i would still be required to be extremely acidic (<pH 6.2) for Na^+ uptake via an NHE even at 0.5 mmol L^{-1} $[Na^+]_o$. In very soft waters (0.05 mmol L^{-1} $[Na^+]_o$, pH 6.0), and with a resting pH_i of ~7.0, $[Na^+]_i$ would need to be 0.005 mmol L^{-1} to function in the forward direction

Furthermore, Kirschner demonstrated elegantly that the energy barrier for Na^+ uptake could be overcome by the use of a NKA at external $[Na^+]$ of ~150 mmol L^{-1} (Kirschner, 2004). However, at µmol L^{-1} Na^+ levels, NKA alone cannot overcome the energy barrier imposed on Na^+ uptake unless it worked with 100% efficiency (Jensen et al., 2003; Kirschner, 2004). This is of course thermodynamically impossible, and thus another energizing step would be required. It is likely that NKA helps aid in Na^+ uptake by lowering $[Na^+]_i$ which would be necessary for both a Na^+ channel or a NHE model. However, it is quite clear that NKA alone cannot lower $[Na^+]_i$ to levels low

enough to drive NHE function under physiological pH_i and $[Na^+]_o$ ranges and a VHA (or another primary active transport mechanism) is required for Na^+ uptake from low Na^+ environments.

As mentioned above, a recent study has implicated the coordinated action of an apical NHE and VHA (facing outward to water) to be utilised for Na^+ uptake in the zebrafish (Yan et al., 2007). At first this may seem a reasonable assumption to make considering their recent advances in zebrafish NHE and the work of others on apical VHA in FW fish gill. However, if present at the same time, these transporters would be a detriment to overall Na^+ uptake via an exchanger (but would work for a Na^+ channel mechanisms). VHA would act to alkalinise the cellular compartment, and acidify the boundary layer, both actions of which would prevent Na^+ uptake via an NHE. We must therefore ensure that with recent advances in understanding FW gill membrane transport at the molecular level, that proper consideration is given to overall function with all parameters involved.

It is also well established that phosphorylation events can significantly alter the rate of NHE activity (reviewed by (Orlowski and Grinstein, 2004)). Additionally, the kinetic properties of an NHE can be altered somewhat by the presence of the intracellular H^+ modifier site which can allow for a shift in the activation profile of the NHE (Aronson, 1985; Aronson et al., 1982; Wakabayashi et al., 2003). However, activation of the NHE via any mechanism simply allows it to move towards its equilibrium point at a faster rate. We must be aware that under normal resting conditions, NHEs are

quiescent and in a disequilibrium state which favours normal forward function (Na^+ moving in/H^+ moving out). Activation cannot overcome or reverse unfavourable gradients and therefore cannot be invoked to "drive" NHE mediated transport where gradient do not favour its normal forward function.

Finally, ion transport at the MR cells of the gill depends on the action of carbonic anhydrase (CA) to hydrate CO_2 and provide the intracellular HCO_3^- and H^+ units required to counter Cl^- and Na^+ flux respectively (Perry and Gilmour, 2006). In a number of studies, inhibition of CA reduces the overall net transport rate of either net acid flux, net base flux or unidirectional rates of Na^+ or Cl^- transport (Boisen et al., 2003; Chang and Hwang, 2004; Kerstetter et al., 1970; Lin and Randall, 1991; Maetz and Garcia-Romeu, 1964; Parks et al., 2007b; Tresguerres et al., 2008; Tresguerres et al., 2007b; Yan et al., 2007). While CA provides the required H^+ and HCO_3^-, it is only equilibrative and cannot provide chemical energy to overcome energy barriers (Georgalis et al., 2006).

Summary

With the recent surge in reports linking NHEs to Na^+ uptake in the gills of FW fish it is important that we step back and consider their thermodynamic feasibility in the environment that the fish is living. The available data suggest that NHEs can function for Na^+ uptake, but within a very narrow range of environmental parameters that are either relatively high in Na^+, high in pH, or both. Importantly, it is clear that proper function of an apical NHE can indeed occur in certain FW environments explaining its presence in numerous FW

fish. However, placing an NHE on the apical membrane under unfavourable environmental conditions would actually cause an NHE to operate in reverse mode, with the concomitant Na^+ loss and H^+ gain. The major hurdle at this point is the direct physiological characterization of the fish NHEs. Our current knowledge of NHE function is only extrapolated from our understanding of mammalian pharmacology and this may be misleading for fish NHEs. While mammalian NHE function is being studied biochemically to the point of knowing the functional importance of each amino acid within the protein sequence ((Slepkov et al., 2007) review of NHE1, (Orlowski and Grinstein, 2004) review of NHE3), we are only now beginning to gain an appreciation of the evolutionary relationships of NHEs. Interestingly, the homology of NHEs is much higher between elasmobranchs and mammals than between teleosts and mammals (Claiborne et al., 2008). It is theoretically possible that the FW fishes possess NHEs with unique characteristics that allow them to function differently from mammalian exchangers but this remains to be demonstrated. Additionally, the potential role of microenvironments both outside and inside the gill MR cells needs to be addressed in the context of NHE function. Finally, it is possible that the presence of an NHE at the FW gill is simply a remnant from SW ancestry. Perhaps, the NHE protein in the gills of fish from very dilute FW is not functional either because it does not properly insert in the apical membrane or it does not undergo the necessary post-translational modifications to allow function under FW conditions. A non-functional protein would not evoke a selection pressure for its removal, and could remain as a

redundant mechanism that can contribute to Na^+ uptake when environmental conditions permit it to do so. We cannot deny the existence of NHEs in fish gill cells as there is strong evidence demonstrating expression of these exchangers in the MR cells of FW fish. The challenge is figuring out if or how they work under these conditions.

Thermodynamic constraints on membrane transport will be a recurring theme throughout this thesis. In addition to the mathematical analyses provided in this chapter, I will present further calculations for NBCs in freshwater trout gill MR cells (chapter IV) and the potential for a $Na^+/CO_3^{2-}/HCO_3^-$ co-transporter in the larval mosquito gut (chapter X).

Table

Table 2. 1 Intracellular Na^+ concentrations $[Na^+]_i$ in Na^+ transporting epithelia

Tissue Origin	$[Na^+]_i$ (mmol l^{-1})	Reference
Brown Trout Gill	62	(Morgan et al., 1994)
Rainbow Trout Gill	55	(Wood and Lemoigne, 1991)
Atlantic Salmon Gill	80	(Eddy and Chang, 1993)
Frog Skin	9	(Rick et al., 1978)
Frog Skin	14	(Nagel et al., 1981)
Frog Skin	7.9	(Nielsen, 1982)
Frog Skin	2.0-5.8	(Harvey and Kernan, 1984)
Frog Skin	3-9	(Garciadiaz et al., 1986)
Frog Skin (Principal cells)	6.2 ± 0.5	(Harvey and Ehrenfeld, 1986)
Frog Skin (MR Cells)	21.6 ± 16.8	(Rick, 1992)
Rabbit Urinary Bladder	7	(Wills and Lewis, 1980)
Rat Kidney (Proximal Tubule)	17.5 ± 2.8	(Yoshitomi and Fromter, 1985)
Rat Kidney (Cortical Collecting Tubule)	16.7 ± 5.4	(Natke and Stoner, 1982)
Rat Heart (Ventricular Myocytes)	14 ± 2	(Borzak et al., 1992)

Figures

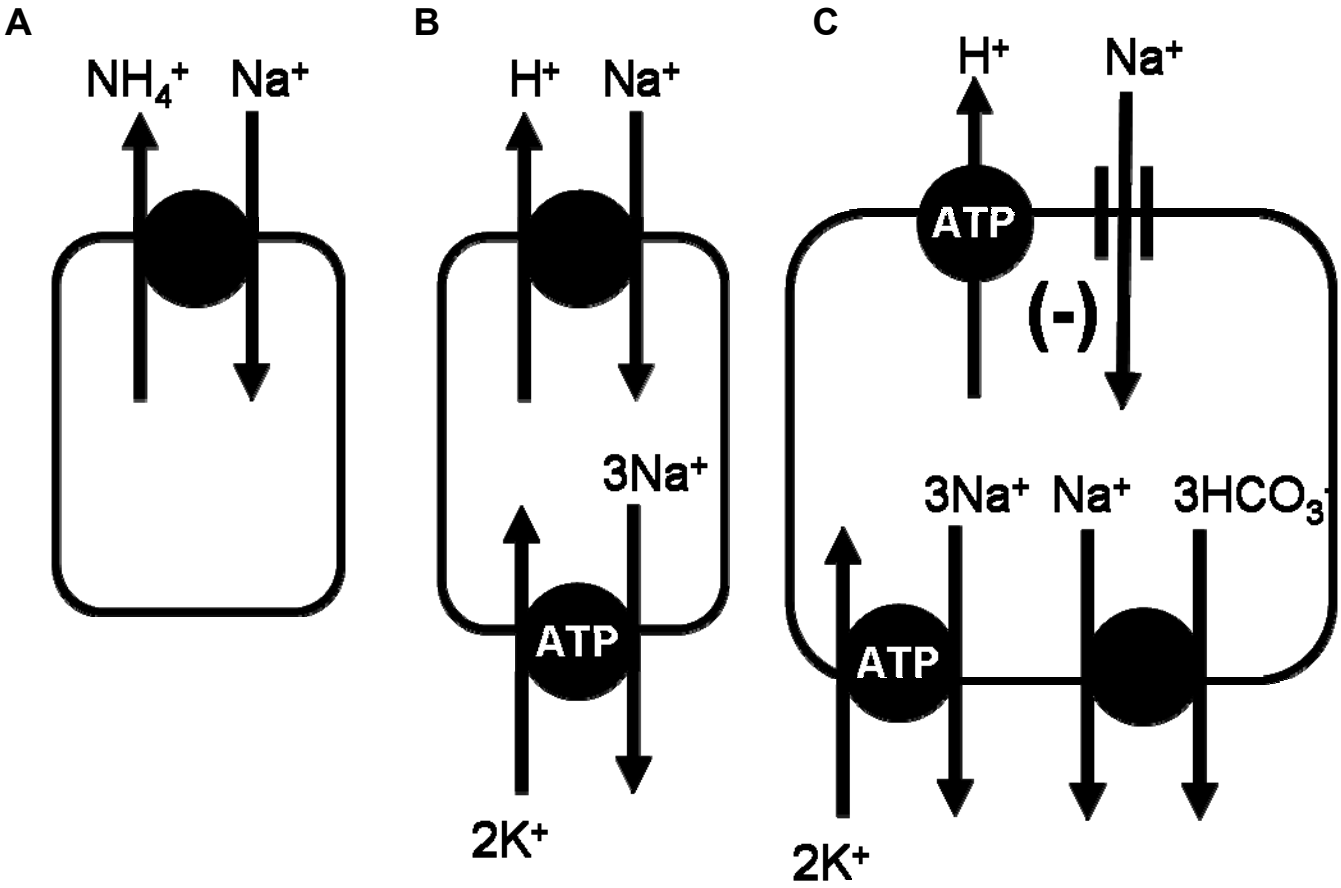

Figure 2. 1 A historical progression of the models for transepithelial Na^+ uptake at the freshwater fish gill

A. The original model proposed by Krogh (Krogh, 1938) of Na^+/NH_4^+ exchange. ***B.*** The model proposing apical Na^+/H^+ exchange driven by basolateral Na^+/K^+-ATPase. ***C.*** Most recent model that incorporates the coupling of an apical Na^+ channel and H^+-ATPase along with a basolateral Na^+/HCO_3^- co-transporter and Na^+/K^+-ATPase.

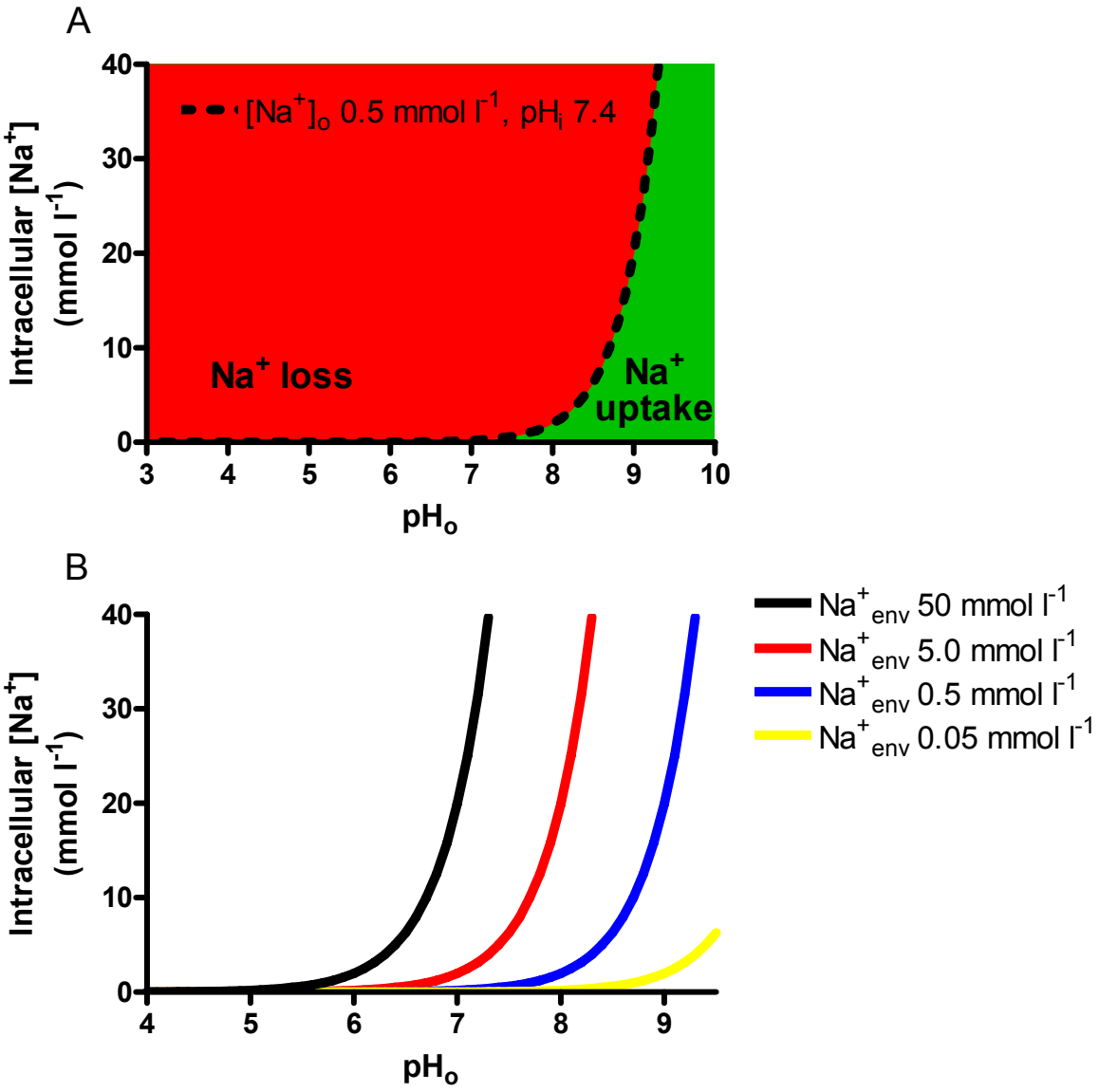

Figure 2. 2 Thermodynamic consideration of the influence of environmental Na^+ ($[Na^+]_o$) and pH (pH_o) on Na^+/H^+ exchanger (NHE) function.
A. The transport equilibrium is plotted as a function of $[Na^+]_i$ and pH_o at a pH_i of 7.4 and $[Na^+]_o$ of 0.5 mmol L^{-1}. The red shaded area represents the conditions where Na^+ loss would occur via an apical NHE while the green shaded area would allow Na^+ uptake. **B.** The influence of $[Na^+]_o$ on NHE function plotted assuming the same pH_i of 7.4. Each curve represents a different $[Na^+]_o$ as illustrated in the figure legend. The same red and green shading protocol from part A can be applied to each individual curve to illustrate the changes in pH_o dependence for an NHE. Note that elevating $[Na^+]_o$ greatly improves the chance of an NHE functioning under normal physiologically encountered environments.

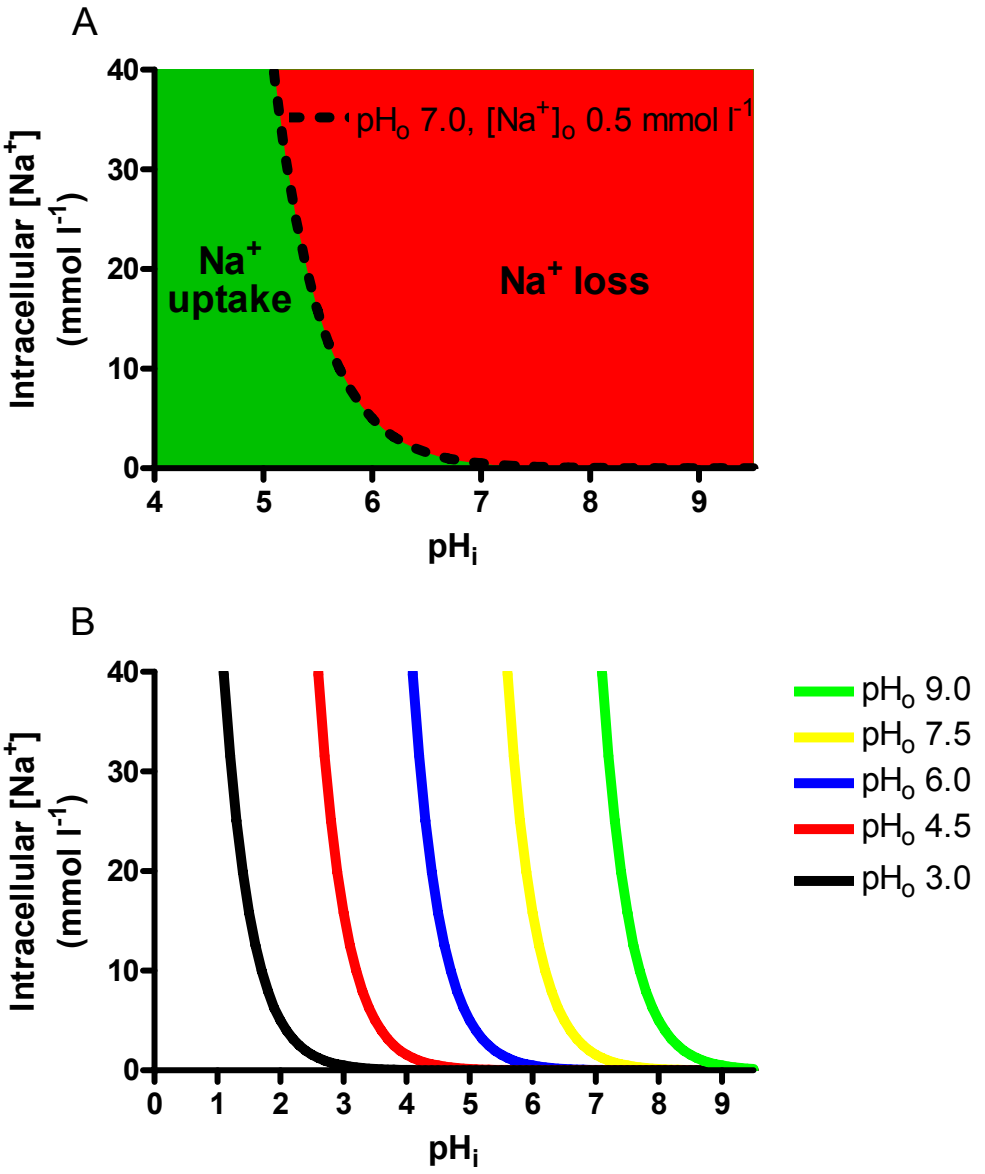

Figure 2. 3 Thermodynamic consideration of the influence of cellular pH (pH_i) and Na^+ ($[Na^+]_i$) on Na^+/H^+ exchanger (NHE) function.
A. The transport equilibrium is plotted as a function of $[Na^+]_i$ and pH_i at a pH_o of 7.0 and $[Na^+]_o$ of 0.5 mmol L^{-1}. The red shaded area represents the conditions where Na^+ loss would occur via an apical NHE while the green shaded area would allow Na^+ uptake. **B.** The influence of pH_o on NHE function plotted assuming the same $[Na^+]_o$ of 0.5 mmol L^{-1}. Each curve represents a different pH_o as illustrated in the figure legend. The same red and green shading protocol from part A can be applied to each individual curve to illustrate how the changes in pH_o require substantial changes in pH_i and/or $[Na^+]_i$ for an NHE to function properly. Note that for most ranges of pH_o, pH_i must be lower than values previously described. Reasonable values for pH_i and $[Na^+]_i$ that could enable the chance of an NHE functioning properly are found only at elevated pH_o (pH ≥ 9.0).

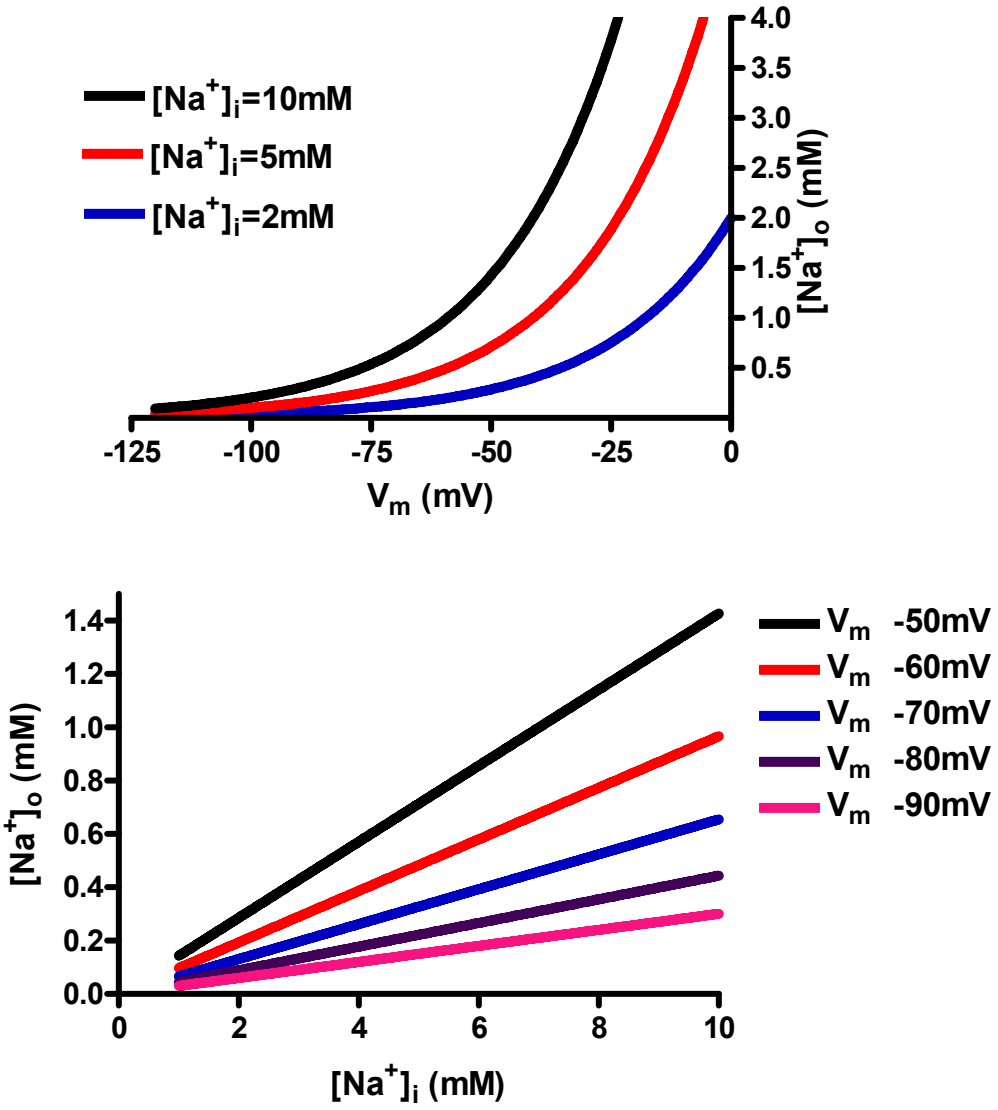

Figure 2. 4 Thermodynamic consideration of Na^+ concentrations and membrane potential on Na^+ uptake at the freshwater gill *via* a Na^+ channel. **A.** The transport function is plotted to illustrate the influence of $[Na^+]_i$ assuming a pH_i of 7.40. Na^+ uptake would occur in the environmental conditions below each curve. **B.** The influence of Vm on transport via a Na^+ channel. Na^+ transport would occur in the the environmental conditions below each curve and as Vm becomes more negative Na^+ can be brought into the animal from very low environmental concentrations.

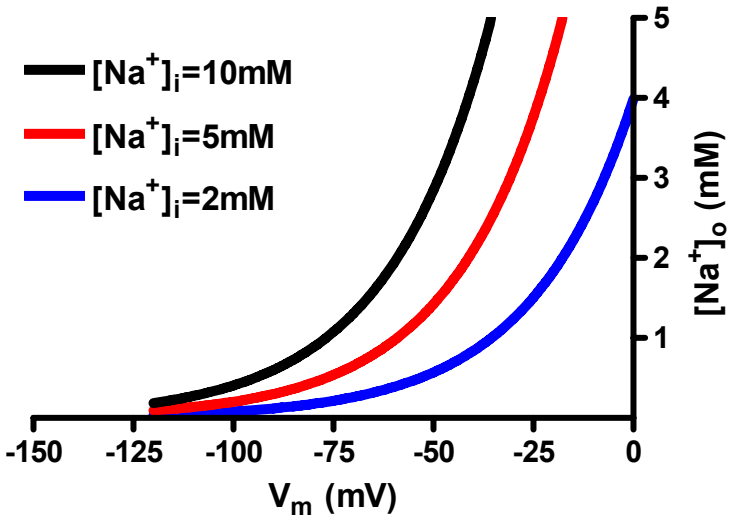

Figure 2. 5 Thermodynamic consideration of an electrogenic Na^+/H^+ exchanger functioning in apical Na^+ uptake at the freshwater gill.

The transport function is plotted to illustrate the influence of $[Na^+]_i$ assuming a pH_i of 7.40. Na^+ uptake would occur in the environmental conditions below each curve. This demonstrates that V_m can act to enhance Na^+ movement via the electrogenic NHE that is not possible with the electroneutral NHE (see Fig 2.2 and 2.3).

Chapter III: Methods and Materials

Experimental Animals

Adult rainbow trout (*Oncorhyncus mykiss*) were obtained from Alberta Trout Growers (Tofield, Alberta, Canada) and were maintained in flow through 450-liter fibreglass tanks filled with aerated and dechlorinated City of Edmonton tap water (hardness of 1.6 mmol/l as $CaCO_3$, total alkalinity of 120 mg/l, pH 8.2). Water temperature in the tanks was maintained permanently at 15°C, and the photoperiod mimicked the natural pattern found in Edmonton, Alberta, Canada. Fish were fed once per day with dry commercial trout pellets. Use of these animals followed Canadian Council on Animal Care and approved Biological Sciences Animal Care Committee protocol #215507.

Estuarine crabs (*Neohelice granulata*) were collected by hand from a muddy beach at San Antonio Oeste (Rio Negro, Argentina) during the Austral summer of 2006–2007 and spring of 2007. The animals were transported to the Laboratory of Aquatic Ecotoxicology Centro Internacional de Educación para el Desarrollo (CIEDE, San Martin de los Andes, Neuquén, Argentina), where the gill perfusion experiments were performed. Crabs were acclimated in plastic containers with aerated seawater of 2‰ salinity for at least 1 week. Water temperature was kept at 18 ± 2°C. The animals were fed twice a week with commercially available pellets of trout food. All procedures followed the Canadian Council for Animal care procedures. Stage C intermolt adult male crabs (Drach and Tchernig.C, 1967) were selected for the study.

Wild-type adult Zebrafsih (*Danio rerio*) were maintained in the Biological Sciences Building aquatic facility in flow through tanks at a temperature of 28.5°C and were fed once daily.

Pacific hagfish (*Eptatretus stoutii*) were caught with bait and a bottom-dwelling net from the Trevor Channel, Vancouver Island, British Columbia, Canada. Hagfish were transported to the Bamfield Marine Sciences Centre, where they were held in a 20 m^3 tank with flowing seawater (14°C). Fish were not fed while being held in this tank and were used for experimentation within the 2 weeks following capture.

Eggs of the yellow fever mosquito (*Aedes aegypti*) were obtained from Dr. Carl Lowenberger (Simon Fraser University, Burnaby, BC, Canada) and reared in covered plastic dishes in a temperature controlled chamber at 27^{o}C. The water was a 50:50 mixture of deionized water and City of Edmonton (Alberta; Canada) tap water. Larvae were fed daily with ground Tetramin (Tetrawerke, Melle, Germany). Larvae that were in day 1 or day 2 of the 4th instar were chosen for experiments. Isolation, mounting and perfusion of larval midguts was accomplished using previously described techniques (Onken et al., 2004; Onken et al., 2008) and resulted in removal of the peritrophic membrane from the preparation.

Trout experiments: Chapters III, VI, and VII

Isolation of MR cells.

Isolation of MR cells from the gill epithelium followed the techniques developed by Goss and colleagues (Goss et al., 2001a). Trout were removed from the holding tanks and anesthetized by an overdose of tricane methanesulfonate (1 g/l) solution. After the pericardial cavity was opened and the pericardium removed, gills were perfused through the bulbous arteriosus with 50 ml of ice-cold, heparinized (15 mg) PBS (in mM: 137 NaCl, 2.7 KCl,

4.3 Na_2PO_4, 1.4 NaH_2PO_4; pH 7.8, 290 mOsm). Gill arches were then immediately excised from the fish, rinsed with dechlorinated tap water, and blotted lightly on paper towels before being placed in ice-cold PBS. Next, gill filaments were removed from the gill rakers in ~2- to 5-mm-wide sections and incubated three times (each 20 min) at 18°C in 5 ml of trypsin-EDTA (0.05% trypsin, 0.53 mM EDTA; GIBCO, Burlington, ON, Canada). After each 20-min incubation, resultant cell suspensions were passed through a 96-μm nylon mesh filter into 5 ml of ice-cold FBS and rinsed through with PBS to inhibit trypsin activity. Final cell suspensions were washed twice with 50 ml of PBS and centrifuged (5 min, 1,500 g, 4°C). The resultant cellular pellets were resuspended in 3–5 ml of PBS and placed over a four-step Percoll gradient (2 ml, 1.09 g/ml; 2 ml, 1.06 g/ml; 2 ml, 1.05 g/ml; 3 ml, 1.03 g/ml) and centrifuged (45 min, 2,000 g, 4°C). The 1.09–1.06 g/ml Percoll interface has been found to contain a highly enriched population of MR cells, as demonstrated by positive staining for the vital mitochondrial dye 4-[4-(dimethylamino)styryl]-N-methylpyridinium iodide and transmission electron microscopy (Goss et al., 2001a). Therefore, cells from this interface were collected, washed in PBS, and used for all of the experiments in this study. The trypsin method of gill digestion was used because it improved adherence of MR cells to glass coverslips during perifusion experiments.

Inverted fluorescent microscopy.

Acid-washed coverslips (no. 1 thickness, 15 mm round; Warner Instrument, Hamden, CT) were coated with 0.1% poly-L-lysine overnight and

then rinsed with double-distilled water and 70% ethanol before each experiment. Aliquots of cell suspensions containing ~300,000 cells were added to 200 µl of 1% gentamicin sodium-containing buffer (in mM: 145 NaCl, 5 $CaCl_2$, 1 $MgCl_2$, 4 KCl, 15 HEPES; pH 7.8, 290 mOsm) with an additional 2 µl of both $CaCl_2$ (1 M) and $MgCl_2$ (1 M) to aid in cell attachment. Cellular suspensions were then placed on the prepared coverslips and kept undisturbed at 4°C for at least 1.5–2 h to allow for settlement and attachment of cells. I found that this length of time was sufficient to ensure cell attachment during perifusion experiments. Coverslips were then removed from the refrigerator, rinsed in Na^+-containing buffer, and immediately exposed to 200 µl of Na^+-containing buffer containing 2 µl of 5 mM, pH-sensitive BCECF-AM (50 µg in 16 µl DMSO and 20% pluronic acid). Incubation of the cells with BCECF-AM occurred for at least 45 min at a cooled room temperature of 18°C. Next, coverslips were placed into a 70-µl imaging chamber (RC-20H; Warner Instrument) for perifusion experiments. MR cells on the coverslips were subjected to differential interference contrast microscopy (Nikon Eclipse TM-300) and fluorescence imaging (TE-FM epifluorescence attachment) with the use of an inverted microscope. The microscope was fitted with a xenon arc lamp (Lambda LS; Sutter Instruments, Novato, CA) to enable excitation of the BCECF-AM-loaded cells at wavelengths of 495 and 440 nm. Exposure time and the gain were adjusted at each trial to elicit adequate fluorescence. Images at both 440 and 495 nm were captured digitally on a mono 12-bit charge-coupled device camera (Retiga EXi; Burnaby, BC, Canada) every 5 s

during the various perifusion experiments. Northern Eclipse version 6 software (Mississauga, ON, Canada) was used to compile the 495-to-440 nm ratios as an indication of the pH_i levels.

Perifusion protocol

Solutions were added to the perifusion chamber using a six-input manifold (Mp-6; Warner Instrument) attached to gravity-feed, 60-ml syringes in syringe holder blocks equipped with pinch valves (VE-6; Warner Instrument) and controlled by VC-6 valve controllers (Warner Instrument). The perifusion rate was adjusted to ~0.5 ml/min. Cells were alkalinized and acidified (chapter VIII) by a 3-min ammonium chloride (20 mM NH_4Cl) prepulse technique first described by Boron and De Weer (Boron and Deweer, 1976b). Cells were then allowed to recover from an acidification event under both Na^+-free (in mM: 142.5 *N*-methyl-D-glucamine-Cl, 2.5 $C_5H_{14}NO{\cdot}HCO_3^-$, 5 $CaCl_2$, 1 $MgCl_2$, 4 KCl, 2 glucose, 15 HEPES; pH 7.8, 290 mOsm) and Na^+-containing (in mM: 142.5 NaCl, 2.5 $NaHCO_3^-$, 5 $CaCl_2$, 1 $MgCl_2$, 4 KCl, 2 glucose, 15 HEPES; pH 7.8, 290 mOsm) conditions. Other experimental protocols involved observing changes in pH_i from the original resting state. This involved first cells to be exposed to Na^+-free medium and then switching to a Na^+-containing solution to cause a disturbance of pH_i (chapter IV). After the cells were observed under control parameters, the same perifusion procedure would occur but with the addition of various drug treatments including amiloride (500 μM), phenamil (50 μM), and 4,4′-Diisothiocyanatostilbene-2,2′-disulfonic acid disodium salt hydrate (DIDS 1

mM). All of the solutions used were bubbled continuously with a gas mixture of 0.3% CO_2 balanced with O_2 throughout the experiments.

In the Cl^- manipulating experiments (Chapter VII) cells were exposed to various experimental manipulations involving Na^+-free (composition listed above), Na^+-containing (composition listed above), and Cl^- free solutions (in mM: 125 D-Gluconic Acid-Sodium salt, 5 D-Gluconic Acid-Hemicalcium salt, 1 D-Gluconic Acid-Hemimagnesium salt, 4 D-Gluconic Acid-Potassium salt, 2.5 $NaHCO_3^-$, 2 glucose, 15 HEPES; pH 7.8, 290 mOsm). Subsequent pharmacological profiling occurred using amiloride, phenamil, DIDS, 5-(N-Ethyl-N-isopropyl)amiloride (EIPA), 5-Nitro-2-(3-phenylpropylamino)benzoic acid (NPPB), ouabain, and acetazolamide. All of the solutions used were bubbled continuously with a gas mixture of 0.3% CO_2 balanced with O_2 for most experiments. Experiments involving HCO_3^- free conditions had HCO_3^- removed from the solution composition, and the solutions were bubbled with 100% O_2.

High-K^+ solutions (in mM: 120 potassium gluconate, 20 KCl, 2 $MgCl_2$, 20 HEPES) were adjusted to four separate pH values (~8.40, 7.80, 7.20, 6.60) and used for calibration of pH_i at the end of each experiment. pH_i and extracellular pH were equilibrated by the addition of the ionophore nigericin (5 μM) (Boyarsky et al., 1988). The 495-to-440 nm ratios obtained at each calibration set point were then used to generate a regression equation for each cell. This equation was then extrapolated to the ratiometric data obtained

over the course of the whole experiment, resulting in an internally calibrated pH_i trace for each cell during the entire perifusion procedure.

Fluorescent imaging of identified MR cell subtypes

For identification of MR cell subtypes following Percoll separation, MR cells were incubated with 40 µg/ml PNA-biotin for 30 min, washed two times with PBS, then incubated for 30 minutes with Streptavidin-conjugated Alexa fluor 594 (Molecular Probes). Prior to pH_i imaging, cells were identified as either PNA^+ and PNA^- cells based on the presence of peripheral staining with Alexa fluor 594 using a Texas Red filter set (560 nm excitation, 630nm emission).

Calculation of Buffering Capacity (β)

Calculation of intracellular buffering capacity was estimated following the calculations described by Graber and colleagues (Graber et al., 1991). The buffering capacity (*β,* mM/pH unit) was calculated according to the following basic formula:

$\beta = \Delta {NH_4}^+_{in} / \Delta pH_i$

This estimate of the acid load assumes that all NH_4^+ exits the cell as NH_3 giving up an H^+ in the process as described previously (Graber et al., 1991). Calculations of NH_4^+ were done assuming a pK of 9.03 and equilibration of intra- and extracellular NH_3 at an extracellular pH of 7.80. Further details of the calculations followed the exact description by Graber and colleagues (Graber et al., 1991). I obtained values for buffering capacity in Na^+ free

experiments to limit the confounding variable of a Na^+ dependent acid extruding system interfering with my calculations.

Membrane potential experiments.

Membrane potential (V_m) behavior was monitored with the fluorescent anionic dye bis-oxonol (Molecular Probes, Eugene, OR). The dye is lipophilic and increases or decreases in fluorescence on depolarization or hyperpolarization, respectively. Importantly, the negative charge on bis-oxonol prevents accumulation in mitochondria; therefore, the dye distributes across cell membranes according to the V_m, giving a reliable measurement of relative changes in V_m (Mohr and Fewtrell, 1987). Bis-oxonol fluorescence was measured with the inverted microscope as explained previously. Briefly, cells were loaded with the 5 μM bis-oxonol for 1 h before each experiment. Cell fluorescence was then monitored at 495-nm excitation and 530-nm emission as changes in the extracellular medium were made. Bis-oxonol (5 μM) was also placed in the experimental perifusion solutions to enable the uptake or extrusion of the dye according to V_m changes. Perifusion experiments followed the above protocol with simple switching between Na^+-free condition and 145 mM Na^+ in the extracellular medium. Longer exposure times were required to capture fluorescence compared with the pH_i experiments. Consequently, images were captured once every 20 s to avoid excessive bleaching of the dye. Data are presented as change in fluorescence relative to initial fluorescent value for each individual cell.

Western blot analysis.

Western blot analysis was done according to the technique described by Tresguerres and colleagues (Tresguerres et al., 2006c). Briefly, gill samples were immersed in liquid nitrogen, pulverized in a porcelain grinder, resuspended in 1:10 wt/vol of ice-cold homogenization buffer (250 mmol/l sucrose, 1 mmol/l EDTA, 30 mmol/l Tris, 100 mg/ml PMSF, and 2 mg/ml pepstatin; pH 7.4), and sonicated on ice for 20 s. Debris was removed by low-speed centrifugation (3,000 *g*, 10 min, 4°C), and the supernatant was kept as the whole gill homogenate and combined with 2x Laemmli buffer (Laemmli, 1970). Twenty micrograms of total protein, as estimated by bicinchoninic acid protein determination analysis (Pierce, Rockford, IL), were separated in a 7.5% polyacrylamide mini-gel (45 min at 180 V) and transferred to a nitrocellulose (NC) membrane (1 h at 100 V) using a wet transfer cell (Bio-Rad Laboratories, Hercules, CA). After the blocking procedure (5% chicken ovalbumin in 0.5 mol/l Tris-buffered saline with 0.1% Triton X-100; pH 8.0, overnight at 4°C), the NC membranes were incubated with the rabbit anti-rat kidney Na^+-HCO_3^- cotransporter (rkNBC) antibody (Schmitt et al., 1999) with gentle agitation at 4°C overnight. After four washes of 15 min each with Tris-buffered saline-Triton X-100 (0.2%), the NC membrane was blocked for 15 min and then incubated with a fluorescent secondary goat anti-rabbit antibody at room temperature for 2 h. Bands were visualized by the Odyssey infrared imaging system and software (Li-Cor). NC membranes incubated without

primary antibody served as the control and never showed positive immunoreactivity.

Immunohistochemistry.

Immunohistochemistry with the anti-NBC (1:500 dilution) described above was carried out on the gill sections according to the procedure of Tresguerres and colleagues (Tresguerres et al., 2006c). Gills were fixed for immunohistochemistry in 3% paraformaldehyde, 0.1 mmol L^{-1} cacodylate buffer (pH 7.4) overnight at 4˚C. Samples were then transferred to 50% ethanol for 6 h and then immersed in 70% ethanol and preserved at 4°C until their final processing. Gills were then embedded into paraffin blocks and serial sections (4 μm) were cut. Paraffin was removed from the sections in toluene, then sections were hydrated in a decreasing ethanol series and double distilled water, incubated in 0.6% H_2O_2 for 30 min to devitalize endogenous peroxidase activity, and subsequently blocked with 2% normal goat serum (NGS) for 30 min. Sections were incubated overnight at 4°C with the anti-NBC antibody (1:500) diluted in 2% NGS, 0.1% bovine serum albumin, 0.02% keyhole limpet haemocyanin, 0.01% NaN_3 in 10 mmol L^{-1} PBS, pH 7.4. Secondary antibody incubation and signal developing were performed using the Vectastain ABC kit (Vector laboratories, CA, USA), according to the manufacture's directions.

A Leica LMRXA compound microscope (Leica Microsystems, Wetzlar, Germany) equipped with an Optronics MacroFire 1.0 digital camera and its associated software Picture Frame (Optronics, Goleta, California, USA) were

used to examine the sections and to capture and digitize the images. Micrographs were cropped and adjusted for brightness and contrast only using Adobe Photoshop version 7.0 (Adobe Systems Inc., San Jose, California, USA).

Scanning Electron Microscopy (SEM)

Isolated MR cells were prepared for SEM following the procedure laid out previously by Schafer and colleagues (Schafer et al., 1997). Briefly, MR cells were prepared as described above and plated down onto the acid-washed, poly-L-lysine coated coverslips to allow cell attachment. MR cells were fixed with 4% paraformaldehyde in 1X PBS for 1 h in the fridge. MR cells were then dehydrated in a series of increased ethanol solutions before being subject to chemical critical point drying using hexamethyldisilazane. Coverslips were mounted on stubs, coated with gold palladium and examined under a Philips/FEI LaB6 Environmental Scanning Electron Microscope (ESEM).

Analysis and statistics.

After an experimental manipulation, analysis was performed on initial rates of pH_i recovery. The initial change in pH_i over change in time ($\Delta pH_i/\Delta t$) was calculated for each cell under control and experimental conditions, and compiled results were compared by paired, two-tailed Student's *t*-test and one-way ANOVA with Bonferroni post hoc test for significance at the level of $P < 0.05$. $\Delta pH_i/\Delta t$ were analyzed over 30 or 60 s, following the invoked pH_i

change of interest. All summary data are presented as means ± SE. All experiments shown are representative of cells obtained from a minimum of two different fish. Total cell numbers and experimental trials are as presented. All statistical analysis was performed with GraphPad Prism version 3.0 software (San Diego, CA). Unless otherwise mentioned, the reagents used in this study were purchased from Sigma (St. Louis, MO).

Crab experiments: Chapter V, appendix I

Transepithelial potential difference (V_{te}) across isolated gills.

Crabs were killed by destroying the ventral ganglia using a pair of scissors. The carapace was then removed, and the posterior gills no. 6 and 7 were dissected and placed in a petri dish containing saline. Preliminary experiments had demonstrated that gills no. 6 and 7 responded in identical manner to the manipulations described in this chapter (also see (Luquet et al., 2002b). The afferent and efferent vessels were connected by polyethylene tubing (0.4 mm in diameter) to a peristaltic pump (afferent) and to a collecting tube (efferent). Tubing was held in place by a sponge-coated acrylic clamp. The preparation was placed into a glass beaker with the appropriate solution, which was constantly aerated. The perfusion rate was kept at 0.1 ml/min. The salt composition and pH of the perfusate and bath were identical at all times to avoid the passive movement of ions by diffusion. Therefore, the only asymmetries between the internal and external media were those created by the gill itself (V_{te}, pH).

Transepithelial potential difference (V_{te}) was measured via Ag^{+}/AgCl electrodes connected by agar bridges (3% agar in 3 mol/l KCl) to the bath (external side) and to the collecting tube (internal side). V_{te} was measured with two chart recorders equipped with mV-meters (Cole Palmer 8373–20, Chicago, IL; and Kipp & Zonen BD 40, Delft, Holland). V_{te} is given as the difference in electrical potential between the external and internal medium. For the statistical analyses, we considered the V_{te} values after stabilization for at least 30 min in each treatment and controls.

Apparent acid and base secretion across isolated gills.

Gills were perfused and bathed in the same saline as explained above. Apparent H^{+} (J_{H+}) and HCO_3^{-} ($J_{HCO3^{-}}$) secretion were calculated as explained by Siebers and colleagues (Siebers et al., 1994). Perfusate was collected after passing through the gills, and its pH was measured and compared against the pH of the preperfusion saline. To obtain enough volume for the measurement, perfusate was collected for 1 h under control and experimental (low pH, high [HCO_3^{-}]) conditions. The buffering capacity of the solutions was calculated by titration of 20 ml of perfusion saline with 0.1 N HCl. Immediately after the experiment, the gill was dried by gently pressing with a paper towel and its fresh weight (fw) was measured. J_{H+} and $J_{HCO3^{-}}$ were calculated using: $J\ (\mu mol \cdot g^{-1} \cdot h^{-1}) = [HCl] \cdot V_{HCl} \cdot \Delta pH_{gill} \cdot V_{collected} \cdot fw^{-1} \cdot Vol_{titr}^{-1} \Delta pH_{titr}^{-1}$, where [HCl] is 0.1 N, V_{HCl} is the volume of HCl needed to reach the final pH, ΔpH_{gill} is the change in the perfusate pH after passing through the gills, $V_{collected}$ is the volume of perfusate collected after passing through the gill during 1 h, Vol_{titr} is

the volume of saline used for titration (20 ml), fw is the fresh weight of the gill, and ΔpH_{titr} is the change in pH in the medium used for titration. A positive value represents J_{HCO3}^{-}, and a negative value is indicative of J_{H+}.

Solutions and reagents.

The composition of the control saline was (in mmol/l): 465 NaCl, 9.40 KCl, 7.50 $MgCl_2$, 12.40 $CaCl_2$, 2.50 $NaHCO_3$ and 5.00 HEPES; pH to 7.75 with Tris. In addition, the perfusate also contained 2.00 mmol/l glucose. This saline was used because it has been shown to induce a basal state in ion uptake estimated from V_{te}, I_{sc}, and $^{22}Na^{+}$ radiotracer experiments (Luquet et al., 2002b; Onken et al., 2003; Tresguerres et al., 2003). Combined with the available information on cellular ion transport mechanisms in gills from crabs acclimated to low salinity (Genovese et al., 2005; Luquet et al., 2002b; Luquet et al., 2005; Onken et al., 2003; Tresguerres et al., 2003), this facilitated the interpretation of the responses to high [HCO_3^{-}] and low pH.

The "high [HCO_3^{-}]" saline had 10 mmol/l NaCl substituted with $NaHCO_3$, which resulted in a final nominal [HCO_3^{-}] of 12.50 mmol/l, but with osmolarity similar to the control. The actual [HCO_3^{-}] was calculated from total CO_2 readings as described in (Tresguerres et al., 2006c) and was in the ranges of 2.3–2.5 mmol/l for control and 11.50–13.50 mmol/l for the high [HCO_3^{-}]. The extra HCO_3^{-} elevated the pH of the saline to 7.81. In some experiments, the pH was adjusted back to 7.75 with HEPES ("high [HCO_3^{-}] pH 7.75"). An additional saline contained control [HCO_3^{-}], but its pH was increased to 7.81 with Tris-base. The "low pH" saline was identical in

composition to the control saline, but pH was adjusted to 7.45 with HEPES. [HCO_3^-] in this saline was negligible. We changed the pH of the solutions by adding Tris and HEPES instead of using strong acid or base to avoid changing the strong ion concentrations. The strong ion difference has been reported to affect A/B regulation in crabs (Burnett and Mcmahon, 1987; Luquet and Ansaldo, 1997). The nominal Cl^- free solutions were prepared by substituting the Cl^- salts by the corresponding nitrates, while the nominal Na^+-free solution had choline chloride instead of NaCl.

Acetazolamide, amiloride, bafilomycin, ouabain, DIDS, SITS, and phenamil were purchased from Sigma (St. Louis, MO). Stock solutions of all of these inhibitors were prepared in DMSO and were added at a final dilution of 0.1% to the bath (SITS and phenamil) or perfusate (the rest), with the exception of oaubain, which was directly dissolved in the perfusion saline. The effects of the drugs were only tested on V_{te} because V_{te} measurements allow for real-time monitoring and therefore for an accurate estimation of the stable values. The addition of 0.1% DMSO alone to the control saline did not result in any significant effect on V_{te}. The effect of every drug during control [HCO_3^-] and pH conditions was also tested, and neither of them had any significant effect on the basal V_{te} (Genovese et al., 2005; Luquet et al., 2002a; Onken et al., 1991), with the exception of ouabain, which inhibits the basal ion transport activity.

Immunohistochemistry.

Posterior gill no. 6 was excised from crabs acclimated to 2‰ salinity and processed for immunohistochemistry as described previously (Tresguerres et al., 2006b) and above. The primary antibodies used included an anti-V-H^+-ATPase antibody designed against a synthetic peptide based on the highly conserved and hydrophilic region in the A-subunit (Katoh et al., 2003) and an anti-Na^+-K^+-ATPase antibody against a synthetic peptide corresponding to a part of a highly conserved region of the α-subunit (Katoh et al., 2000).

The specificity of the antibodies in crab tissues was analyzed by Western blotting (7.5% gels), using a donkey anti-rabbit fluorescent secondary antibody (Li-Cor, Lincoln, NE) as described above.

Statistics.

All data are given as means ± SE. Differences between groups were tested using one-way repeated measures ANOVA (1-way repeated-measures ANOVA), followed by Dunnet's post test or Tukey's multiple-comparisons test. Certain data sets were analyzed using paired Student's *t*-test. Statistical significance was set at $P < 0.05$. All statistical analyses were performed on GraphPad Prism v. 3.0 (GraphPad Software, San Diego CA).

Zebrafish experiments: Chapter 6

Total RNA Preparation and cDNA Synthesis

Total RNA was extracted using Trizol (Invitrogen) following the manufacturers procedures. The whole gill basket was removed from the zebrafish, placed in 1 mL of Trizol and homogenized with a 1 mL syringe and series of decresing needle diameters (18, 21, 22.5 gauge). Following extraction, RNA was dissolved in nuclease free water and quantified on a nanodrop spectrophotometer (ND-1000; Nanodrop Technologies Inc., Wilmington, DE, USA).

For cDNA synthesis, 2 µg of total RNA from each fish was reverse-transcribed in 20 µl reactions containing 10 µM oligo $(dT)_{18}$, 1mM dNTP mix, 5X Reaction buffer (50mM Tris-HCl (pH 8.3), 50mM KCl, 5mM $MgCl_2$, 10mM DTT), 10 u RiboLock^{TM} RNase inhibitor, 20u M-MuLV reverse transcriptase (Fermentas, #K1612). Reaction mixtures were incubated at 37˚C for 60 minutes and then the reaction was stopped by heating to 70˚C for 10 minutes. For quantitative PCR (Q-PCR), random hexamer primers (10 µM) were used and synthesis occurred with an additional pre-incubation at 25˚C for 10 minutes.

Cloning of Zebrafish ASIC 4.2

Fragments of DNA were amplified from gill cDNA with various primer sets designed against an unknown zebrafish kidney clone (GenBank: CK238032.1) sharing ~50% homology with mammalian αENaC. RT-PCR was

performed with 25 µl reactions according to manufacturer's recommended instructions (Fermentas). Reagents included Taq polymerase, 10X $(NH4)_2SO_4$ buffer, $MgCl_2$, dNTPs, gill cDNA, and FWD and RVS primers. Cycling parameters were typically as follows; 2.5 min at 95˚C, 35 cycles of 94˚C for 30 s, 55˚C for 30 s, 72˚C for 60 s, and a final extension step for 10 min at 72˚C. Annealing temperatures were adjusted accordingly to match the predicted melting temperatures of each primer set provided by IDT (Coralville, IA, USA). I found that the 10X $(NH4)_2SO_4$ buffer was much more effective for PCR in fish compared to the 10X $MgCl_2$ buffer.

PCR reactions were separated on a 1.5% TAE-agarose gel, and visualized by staining with ethidium bromide solution (50 mg/L). The ~500 bp PCR product was excised and gel purified using the Qiagen QIAquick Gel Extraction Kit (Cat. No 28704). Purified DNA was then cloned into the pJET1.2/blunt cloning vector using the blunted protocol (Fermentas) and transformed into competent NEB 10-beta *E. coli* cells (New England BioLabs #C2523H). Cells were plated on LB-ampicillin plates (100 mg/mL) and incubated overnight at 37˚C. Positive clones identified by performing colony PCR with the pJET1.2 Fwd and Rvs sequencing primers (Fermentas). Cycling parameters for colony PCR were as follows; 5 min at 95˚C, 25 cycles of 94˚C for 30 s, 50˚C for 30 s, 72˚C for 60 s, and a final extension step for 5 min at 72˚C. Randomly selected positive colonies were grown overnight in 6 mL of LB-ampicillin (100 mg/mL) at 37˚C. The plasmid was then isolated using the Qiagen QIAprep Spin Miniprep Kit (Cat. No. 27106) according to

manufacturer's instructions. Sequencing reactions were prepared using the Amersham DYEnamic ET kit and sequencing was performed at the molecular biology services unit in the Department of Biological Sciences, University of Alberta, on an ABI 3730 DNA sequencer.

Quantitative PCR (Q-PCR)

Q-PCR analyses were carried out using the Applied Biosystems 7500 fast real time PCR equipment using SYBR green dye. Relative changes in ASIC4.2 gene expression were compared to the endogenous control gene elongation factor 1α using primers generated with the Primer Express software (Applied Biosystems, see chapter VI). Thermocycling parameters were as follows: 95°C for 2 min, followed by 40 cycles of 95°C for 15 s and 60°C for 1 min. Analyses of the relative expression changes in response to low Na^+ (n = 4) were performed using the delta-delta ct method (Livak and Schmittgen, 2001) using microsoft excel.

In-situ Hybridization

Whole-mount *in situ* hybridization was performed on zebrafish embryos as described previously (Prince et al., 1998). DIG-labeled RNA probes (*ASIC4.2* sense or antisense) were constructed by linearizing plasmid DNA (Topo 2.1 TA) with the restriction enzyme Kpn1 (Fermentas), phenol/chloroform extracting, precipitating, and re-suspending linearized DNA after checking integrity on an agarose gel. ROCHE RNA polymerase and reagents were used for RNA probe synthesis and probes were purified using

SigmaSpin Columns. Embryos were fixed in 4% Paraformaldehyde/PBS overnight at 4°C. For RNA *in situ* hybridization, embryos were permeabilized for 12 min with protenase K and hybridized at 65°C overnight with the *ASIC4.2* sense and antisense probes. Hybridization of probes was detected with anti-digoxigenin (Roche) and NBT/BCIP (Roche). Embryos were mounted in glycerol and viewed on a Leica DMRXA upright microscope equipped with epifluorescence (10× and 20×). Image capture was done using an Optronics camera and the Picture frame software.

Hagfish Experiments (Chapter IX, appendix II)

Antibodies and reagents

We used a V-H^+-ATPase antibody designed against a synthetic peptide based on the highly conserved and hydrophilic region in the A-subunit (Katoh et al., 2003). The Na^+/K^+-ATPase antibody we used was raised against a synthetic peptide corresponding to a part of a highly conserved region of the α-subunit (Katoh and Kaneko, 2003; Katoh et al., 2000). Finally, we used a Na^+/H^+ exchanger 2 (NHE2) antibody designed against a fragment of the C-terminal region of mammalian NHE2 (Mark Donowitz, National Institutes of Health, Bethesda, Maryland, USA.). All of these antibodies were raised in rabbit, and immunoreactive cells and bands of the appropriate size were recognized by immunohistochemistry and Western blotting in gills of the Pacific hagfish (Tresguerres et al., 2006b). A donkey anti-rabbit fluorescent secondary antibody (LI-COR Inc., Lincoln, Nebraska, USA) was used for

Western-blot analysis. Unless otherwise mentioned, all the reagents used in this study were purchased from Sigma (St. Louis, Missouri, USA).

HCl infusions

Hagfish (body mass 89.00 ± 5.86 g (mean ± SE)) were anaesthetized in seawater containing 1:1000 tricaine methanesulfonate (TMS; AquaLife, Syndel Laboratories Ltd., Vancouver, British Columbia, Canada) and suspended by the head, which causes blood to accumulate in the caudal subcutaneous sinus. After taking a 200 µL blood sample (t = 0 h), acid (250 mmol·L^{-1} HCl, 250 mmol·L^{-1} NaCl) was injected using a heparinized 21 gauge syringe to achieve a HCl load of 6000 µmol·kg^{-1}. A similar infusion protocol has been used successfully with sulphuric acid by McDonald (McDonald et al., 1991), Edwards (Edwards et al., 2001), and colleagues. Hagfish were then inverted several times to facilitate mixing throughout the sinus and placed in individual seawater flow-through tanks (20 L) for the duration of the experiment. Subsequent blood samples were taken at t = 3, 6, 9, 12, 18, and 24 h, with acid infusions repeated at t = 6, 12, and 18 h. Control fish were subject to the same protocol with the exception of being infused with control saline (500 mmol·L^{-1} NaCl) to achieve the equivalent injection load as that of the acid-infused group.

Blood-sample analysis and terminal sampling

Blood samples (200 µL) were obtained as described above. Blood pH was measured immediately upon removal from the animal using a

thermojacketted Accumet micro-size pH electrode model 13-620-94 (Fisher Scientific, Pittsburgh, Pennsylvania, USA). Blood samples were then centrifuged (12 000*g* for 2 min) to obtain plasma. Plasma aliquots (40 µL) were used for immediate total CO_2 (TCO_2) determination in a Cameron chamber equipped with a CO_2 electrode (Radiometer, Copenhagen, Denmark). The remaining plasma was snap-frozen in liquid nitrogen for later [Na^+] measurements (atomic absorption spectrophotometer; model 3300; Perkin-Elmer, Norwalk, Connecticut, USA). At the end of each experiment, hagfish were anaesthetized in seawater containing TMS for 5 min and subsequently decapitated. Gill pouches were immediately snap-frozen in liquid N_2 for later Western-blot analyses or placed in fixative for immunohistochemistry.

Immunohistochemistry

Gill pouches were fixed and processed for immunohistochemistry as described above. Consecutive 4 µm sections were probed with the antibodies for Na^+/K^+-ATPase (1:3000), V-H^+-ATPase (1:500), and NHE2 (1:1000). Hagfish sections incubated with the secondary antibody alone did not show any immunoreactivity (refer to (Tresguerres et al., 2006b).

To detect potential changes in the cellular localization of NHE2-like proteins, I analyzed the staining pattern of NHE2 L-IR cells from three random fields of view (640×) of sections from three fish per treatment (nine fields of view per treatment). A total of 178 cells from NaCl-infused fish and 176 cells from HCl-infused fish were analyzed.

Western-blot analysis

Frozen gill samples were processed for western blotting as described above with a few modifications to obtain different fractions of the gill. Gill pouches were immersed in liquid nitrogen and pulverized in a porcelain grinder. The resultant powder was resuspended in 1:10 (*m*/*v*) of ice-cold homogenization buffer (250 mmol·L^{-1} sucrose, 1 mmol·L^{-1} EDTA, 30 mmol·L^{-1} Tris, 100 mg·mL^{-1} PMSF, and 2 mg·mL^{-1} pepstatin, pH 7.4) and sonicated on ice (3 × 5 s pulses). Debris was removed by low-speed centrifugation (3000*g*, 10 min, 4°C). An aliquot of the supernatant was stored at -80 C (whole-gill homogenate) and the remaining supernatant was centrifuged at high speed (100 000*g*, 60 min, 4 °C) to obtain the whole-membrane fraction of the gill. Aliquots of both the whole-gill and gill-membrane fractions were saved for protein determination (Pierce, Rockford, Illinois, USA).

Processed gill samples were separated in a 7.5% polyacrylamide mini-gel as described above. NC membranes were incubated with the primary antibodies (1:2500 in blocking buffer) with gentle rocking at 4°C overnight. The NC membranes were washed (4X 15min with 0.2% TBS–Triton X), blocked for 15 min, and incubated with the fluorescent secondary antibody (1:2500 in blocking buffer) at room temperature for 1 h. Bands were visualized and quantified using the Odyssey infrared imaging system and software (LI-COR Inc., Lincoln, Nebraska, USA). Differences in loading were corrected by quantifying the total protein concentration in each lane after staining with Coomassie Brilliant Blue R-250. For representative blots,

including controls without the addition of the primary antibodies, see (Tresguerres et al., 2006b). Values are given as arbitrary fluorometric units (a.f.u.).

Statistics

All data are given as means ± SE. Differences between groups were tested using one-way repeated-measures analysis of variance (one-way RM ANOVA), Student's *t* test, one-tailed Mann–Whitney test, or two-way repeated-measures analysis of variance (two-way RM ANOVA) followed by Bonferroni post hoc test when appropriate. Statistical significance was set at $p < 0.05$. All statistical analyses were performed on GraphPad Prism version 3.0 (GraphPad Software, San Diego California, USA).

Mosquito experiments: Chapter X

Solutions and Drugs

The hemolymph-side of the tissue was gravity-superfused (0.5 ml min^{-1}) with oxygenated saline with a composition based on larval *Aedes* hemolymph (Edwards, 1982a; Edwards, 1982b); (in mmol l^{-1}): NaCl, 42.5; KCl, 3.0; $MgCl_2$, 0.6; $CaCl_2$, 5.0; $NaHCO_3$, 5.0; succinic acid, 5.0, malic acid, 5.0; L-proline, 5.0; L-glutamine, 9.1; L-histidine, 8.7; L-arginine, 3.3; dextrose, 10.0; HEPES, 25. The pH was adjusted to 7.0 with NaOH. The gut lumen was perfused with NaCl (100 mmol l^{-1}) at a rate of 50 - 150 µl h^{-1}, using one or more Aladdin syringe pumps (World Precision Instruments, Sarasota, FL, USA). The components of the above solutions were purchased from Sigma

(St. Louis, MO, USA), Fisher Scientific (Pittsburgh, PA, USA) or Mallinckrodt (Hazelwood, MO, USA). Serotonin (Sigma) and $ZnCl_2$ (Baker Chemical, Phillipsburg, NJ, USA) were directly dissolved in the saline.

Fluorescence microscopy for measurement of intracellular pH (pH_i)

Measurements of intracellular pH (pH_i) were obtained following the protocol described in detail above for trout gill MR cells. The whole perfusion chamber was mounted on the stage of the Nikon Eclipse TM-300 inverted microscope (as opposed to cells attached to coverslips) where midguts were subjected to differential interference contrast microscopy for initial focusing and for photographic records of the appearance of the mounted tissue. Fluorescent images were taken at 10-sec intervals for all of the mosquito gut experiments.

After the tissue was attached to the perfusion pipette, it was loaded with the pH-sensitive intracellular dye BCECF-AM (InVitrogen; Carlsbad, CA, USA), as follows. Two µL of a 5mM solution of BCECF-AM dissolved in DMSO containing 20% pluronic acid were added to the chamber volume of 450 µL of standard saline to achieve a final BCECF-AM concentration of 0.5 µM. After 30 min of incubation in the dye solution, perfusion and superfusion were started, washing away all dye not taken up by the tissue. In 3 control experiments, 30-min exposure to the BCECF-DMSO-pluronic acid mixture with which the tissue was dye-loaded, was found to have no measurable effect on the transepithelial potential of unstimulated tissues, nor did it affect

the electrical response to serotonin or the ability of tissues to secrete alkali in response to serotonin.

At the beginning of each experiment, 3-8 areas of interest were established on the CCD image of the gut. Figure 10.1 shows an example of such areas in a typical experiment. Data presented represent the average of fluorescence collected from such areas, each of which is estimated to corresponds to approximately 3-7 of the large differentiated epithelial cells together with perhaps twice this number of the much smaller regenerative and epithelioendocrine cells.

At the end of each experiment, fluorescence ratios recorded during the experiment were calibrated by superfusing the tissue successively with high-K^+ solutions (in mM, 75 K^+ gluconate, 20 KCl, 2 $MgCl_2$, 20 HEPES) containing 5μM nigericin, adjusted to cover the range of pH values 6.6-8.4 (see Fig. 10.1). This calibration was used to convert the ratiometric data obtained over the course of the whole experiment into pH_i values as described above, resulting in an internally-calibrated pH_i trace that represents an average value for the several cells within that area. In several initial studies, the 40X objective of the microscope was used and individual cells were outlined as areas of interest. These studies failed to indicate heterogeneity among the large principal cells, either in initial pH_i or response to serotonin.

Analysis and Statistics

Data from the optical experiments were transferred to a Microsoft Excel spreadsheet, where fluorescence ratios were converted to pH_i values

by reference to linear fits of the corresponding calibration points. pH_i (or ΔpH_i) for the different regions of interest was then pooled (averaged) for each isolated midgut preparation. In the Results, the means ± S.E.M. of the independent preparations are given. Indicated N-values refer to the number of different preparations used. Differences between groups were tested with the pooled results from different preparations. Paired Student's t-test was used when comparing results obtained with each of the individual tissues, whereas unpaired student's t-test was used when results from different groups of preparations were compared. Significance was assumed at $P < 0.05$.

Chapter IV: Interactions between Na^+ channels and Na^+-HCO_3^- cotransporters in the freshwater fish gill MR cell: a model for transepithelial Na^+ uptake[1]

[1]A version of this chapter has been published previously.

Parks SK, Tresguerres M, and Goss GG. Interactions between Na^+ channels and Na^+-HCO_3^- cotransporters in the freshwater fish gill MR cell: a model for transepithelial Na^+ uptake. *American Journal of Physiology-Cell Physiology* 292: C935-C944, 2007.

Introduction

Fish living in a freshwater environment are faced with a considerable challenge to maintain a high internal osmolarity in relation to their external environment. Consequently, the fish must spend a great deal of energy to actively uptake salts at the gill while preventing their passive loss to the environment. The gill is a complex epithelium that is responsible for directional transport of both Na^+ and Cl^- as well as whole body acid-base regulation. It comprises at least five different cell types (Laurent and Dunel, 1980), with the bulk of ion transport and acid-base regulation attributed to the activity of the mitochondria-rich (MR) cell. Currently accepted models of ion transport link Cl^- uptake with HCO_3^- secretion, whereas Na^+ uptake is coupled to H^+ secretion via an apical Na^+ channel electrogenically coupled to a V-type H^+-ATPase (Fenwick et al., 1999; Goss et al., 1998; Perry, 1997; Perry et al., 2003b).

Goss and colleagues (Goss et al., 1992) first implicated direct MR cell involvement in whole body pH regulation. Because of the complex nature of the gill epithelium it is difficult to ascribe specific function to a particular cell type. Our laboratory (Galvez et al., 2002; Goss et al., 2001a; Reid et al., 2003) has developed a technique to isolate MR cells from the gill epithelium and subsequently has described two functionally distinct MR cell subtypes. These cells can be separated based on whether or not they bind peanut lectin agglutinin (PNA^+ and PNA^-, respectively) (Galvez et al., 2002). Further analysis has demonstrated an acid-activated phenamil and bafilomycin-

sensitive Na^+ influx in PNA^- cells but not in PNA^+ cells (Reid et al., 2003). However, the mechanisms involved in transepithelial Na^+ transport remain unresolved.

The regulation of intracellular pH (pH_i) is essential for the proper functioning of a number of cellular processes (Madshus, 1988). At the same time, Cl^- and Na^+ uptake across MR cells is directly linked to HCO_3^- and H^+ secretion, respectively, as noted above. Therefore, examining the pH_i regulatory characteristics of fish gill MR cells can provide information in four important areas: pH_i regulation, systemic pH regulation, and cellular and systemic ion regulation. In fish gills, pH_i regulation has been examined only in cultured epithelial pavement cells from rainbow trout (Part and Wood, 1996; Wood and Part, 2000) and goldfish (Sandbichler and Pelster, 2004). However, direct characterization of MR cell pH regulation has not been reported.

The goal of this study was to investigate pH_i regulation at the rainbow trout gill MR cells and to incorporate these findings into a working model for transepithelial ion and acid-base regulation. This study is the first to extensively investigate isolated and functionally identified gill MR cell pH_i regulation. I report evidence to support our lab's previous research indicating two functionally distinct MR cell populations. Differential pH_i recovery responses were noted in Na^+-free or Na^+-containing medium, which correspond to different cell types in a mixed MR cell fraction. These findings, coupled with membrane potential experiments in this study, are an important

step for the full characterization of MR cell subtypes and provide evidence for a new model for transepithelial Na^+ transport in freshwater fish.

Summary of methodological approach

To examine the mechanisms of ion transport, MR cells from rainbow trout gill were isolated and plated onto coverslips for intracellular pH (pH_i) imaging. Cells were exposed to Na^+-free and Na^+-containing medium and alkalinizing and acidifying behaviours were observed in two populations of MR cells. Various pharmacological agents were then tested on the Na^+ induced acidification event. These data were complemented by single-cell membrane potential imaging experiments. Finally, I used immunohistochemistry to demonstrate the presence of NBCs in gill cells of rainbow trout.

Results

i-Viability and responsiveness of isolated fish gill MR cells.

This was the first study involving pH_i imaging on isolated MR cells; therefore, I needed to establish that the MR cells were viable and able to respond similarly to repeated exposures to acid-base disturbances over the course of the experiment. Figure 4.1 shows a representative trace of the MR cell's ability to withstand multiple acidification events induced by 20 mM NH_4Cl exposure. Cells responded with consistent recovery patterns under repeated control experimental conditions. Viability of the cells over numerous pH_i disturbances provided a framework to structure the rest of my experimental protocols. For each ensuing experiment, a consistent control was established before pharmacological testing occurred.

ii-Effect of Na^+-free medium on pH_i recovery following an acid load: evidence for two distinct populations of MR cells at the gill.

In response to an intracellular acidification induced by 20 mM NH_4Cl exposure, the mixed population of MR cells separated into two distinct pH_i recovery patterns. One population of cells demonstrated a Na^+-independent pH_i recovery mechanism after acidification (Fig. 4.2*A*, *trace a*), whereas the other population of MR cells lacked pH_i recovery in the absence of Na^+ (Fig. 4.2*A*, *trace b*). During data analysis, I noticed that the ability to recover from an acid load in the absence of Na^+ correlated with the resting pH_i of the cells involved. Comprehensive analysis of all cells tested found that ~84% of cells

with a resting pH_i >7.80 displayed a Na^+-independent recovery behaviour compared with 16% that did not (*n* = 175; Fig. 4.2*B*). In contrast, 73% of cells with a resting pH_i <7.80 lacked a Na^+-independent recovery compared with 23% that could recover in Na^+-free conditions (*n* = 223; Fig. 4.2*B*). This suggested that there were at least two populations of cells with differential transport processes in the mixed MR cell population.

iii-Novel behaviour of one MR cell subtype: Na^+-induced acidification.

During experiments involving alteration of extracellular Na^+ concentration ($[Na^+]_e$), I noticed a peculiar Na^+-induced acidification event occurring in most of the MR cells. This occurred when the cells were switched from Na^+-free to Na^+-containing medium. All known transport mechanisms involving influx of Na^+ predict an intracellular alkalinization. Therefore, it was of interest to elucidate the mechanism underlying this peculiar pH_i acidification. Consequently, experiments were performed by exposing the cells to Na^+-free and Na^+-containing media in different combinations with no NH_4Cl disturbances. I found that initial perifusion of Na^+-free medium across the cells followed by a switch to Na^+-containing medium resulted in an intracellular acidification in one population of MR cells (Fig. 4.3*A*, black trace). This event could be repeated in the same cells with a tendency toward a slight but significant decrease in the rate of acidification on the second exposure to Na^+-containing medium after initial recovery in Na^+-free medium ($\Delta pH_i/\Delta t$ of –0.120 ± 0.008 and –0.095 ± 0.010 pH units/min, respectively; Fig. 4.3*B*). Within the same set of experiments, there were a smaller percentage of MR

cells that responded to this change with a Na^+-induced alkalinization of pH_i (Fig. 4.3*A*, gray trace). This event was also repeatable without a significant change in the pH_i alkalinization rates between the primary and secondary Na^+ exposure ($\Delta pH_i/\Delta t$ of 0.404 ± 0.072 and 0.374 ± 0.056 pH units/min, respectively; Fig. 4.3*C*). From this set of experiments and the ensuing pharmacology studies, I found that ~77% of cells from the mixed MR cell fraction demonstrated the Na^+-induced pH_i acidification behaviour vs. 23% that exhibited the Na^+-induced pH_i alkalinization behaviour (n = 227). These data support the finding of differential resting pH_i and functional behaviour as reported above as each subpopulation of MR cells segregates to either a low or high pH_i after exposure to Na^+.

iv-Na^+ induced acidification: involvement of Na^+ channels.

In this study, I specifically focused my attention on understanding the MR cell population exhibiting a Na^+-induced acidification because, to our knowledge, this had not been reported before in any system. Within this experimental protocol, I then began a series of pharmacological profiling experiments to determine the mechanism(s) of Na^+-induced acidification. In each experiment, cells were initially challenged with increased $[Na^+]_e$ to allow for identification of the specific cell type. The effect of subsequent pharmacological compounds was then examined in cells exhibiting a Na^+-induced acidification. Amiloride, an inhibitor of both Na^+/H^+ exchangers (NHEs) and epithelial Na^+ channels (eNaC) (Kleyman and Cragoe, 1988), effectively removed the acidification originally caused by Na^+ introduction and

replaced it with a slight alkalinizing trend (Fig. 4.4*A*). The effect of amiloride was statistically significant with a $\Delta pH_i/\Delta t$ of –0.145 ± 0.013 pH units/min induced on control exposure to Na^+-containing medium after Na^+-free exposure compared with a $\Delta pH_i/\Delta t$ of 0.062 ± 0.016 pH units/min when the same cells were exposed to Na^+ in the presence of amiloride (500 μM; Fig. 4.4*B*). Next, I tested phenamil, a 5'-substituted derivative of amiloride known to block eNaCs at micromolar concentrations (Kleyman and Cragoe, 1988) with no known effects on NHEs, even at much higher concentrations. After the same experimental protocol, Na^+-induced acidification was eradicated in the presence of 50 μM phenamil (Fig. 4.5*A*). I also observed that acidification would occur again in the presence of Na^+ when phenamil was removed, indicating effective and reversible washout of the drug (Fig. 4.5*A*). Both the control Na^+-induced acidification ($\Delta pH_i/\Delta t$ of –0.139 ± 0.009 pH units/min) and the washout Na^+-induced acidification ($\Delta pH_i/\Delta t$ of –0.138 ± 0.023 pH units/min) were significantly different from the pH_i change induced by Na^+ in the presence of 50 μM phenamil ($\Delta pH_i/\Delta t$ of 0.057 ± 0.010 pH units/min) but not significantly different from each other (Fig. 4.5*B*). Finally, application of amiloride under steady-state Na^+-free conditions did not result in a change in pH_i.

v-Na^+-induced acidification: involvement of NBC

One possibility for observing a pH_i acidification is via the extrusion of HCO_3^-. The NBC operating in export mode has been shown to function in this manner by transporting three HCO_3^- molecules for each Na^+ (Soleimani and

Burnham, 2001). Expression studies of the renal NBC exhibited a reduction in pH_i when extracellular Na^+ was removed from frog oocytes (Romero et al., 1997). This acidification of pH_i was attributed to Na^+ moving down the gradient created and an excess of HCO_3^- being carried with it. Therefore, I examined the effect of DIDS, a known inhibitor of NBCs (Boron et al., 1997; Romero et al., 2004; Romero et al., 1997), on the Na^+-induced acidification event. DIDS (1 mM) caused essentially the same effect as amiloride and phenamil by removing the Na^+-induced acidification (Fig. 4.6*A*). The control Na^+-induced acidification ($\Delta pH_i/\Delta t$ of –0.121 ± 0.007 pH units/min) was abolished in the presence of 1 mM DIDS ($\Delta pH_i/\Delta t$ of 0.038 ± 0.016 pH units/min) with a slight alkalinization noted (Fig. 4.6*B*). I was unable to wash out the DIDS because it tends to bind irreversibly. Instead, a continuation of the same trend with Na^+ washout was observed in comparison with Na^+ in the presence of DIDS (Fig. 4.6*A*). Application of DIDS under steady-state Na^+-free conditions did not result in a change in pH_i.

Next, I examined the role of carbonic anhydrase (CA) in providing the required HCO_3^- molecules for the electrogenic NBC activity. Experiments were performed as above with 500 μM acetazolamide, a level similar to that demonstrated to block gill CA activity (Georgalis et al., 2006). I observed that inhibition of CA acted to effectively replace the Na^+-induced acidification with an alkalinization, which was larger than that observed for either amiloride, phenamil, or DIDS treatment (Fig. 4.7*A*). The control Na^+-induced acidification ($\Delta pH_i/\Delta t$ of –0.192 ± 0.023 pH units/min) compared with the presence of 500

μM acetazolamide ($\Delta pH_i/\Delta t$ of 0.180 ± 0.037 pH units/min), as shown in Fig. 4.7*B*.

Changes in V_m: involvement of electrogenic NBC.

If an electrogenic NBC was involved in the Na^+-induced acidification event, it would be accompanied by distinct changes in V_m of the MR cells. A hallmark feature of an electrogenic NBC acting in efflux mode is the induction of a depolarization of V_m (Romero et al., 1997). By loading the MR cells with bis-oxonol and exposing them to single cell imaging, I again observed two distinct V_m behaviours. The large majority of cells (79%, n = 111) demonstrated a distinct and repeatable depolarization of V_m after introduction of 145 mM Na^+ following Na^+-free exposure (Fig. 4.8, black trace). Conversely, a smaller percentage of cells (21%, n = 29) demonstrated a hyperpolarization in response to the same experimental manipulation (Fig. 4.8, grey trace). The relative percentages of Na^+-induced depolarization (79%) match well with the relative proportion of cells demonstrating the Na^+-induced acidification (77%) (Fig. 4.3).

To further support our contention that an electrogenic NBC functions in export mode in our system, I tested the effect of DIDS on the Na^+-induced depolarization. DIDS was able to effectively remove the depolarizing effect of Na^+ or replace it with a hyperpolarizing trend in the majority of cells where depolarization occurred (75%, n = 28; Fig. 4.9).

NBC immunoreactivity

The anti-rkNBC antibody recognized a distinct band (~110 kDa) from gill homogenates as estimated from Western blot analysis (Fig. 4.10*A*). Immunohistochemistry in the trailing edge of the gill filament revealed distinct positive staining in cells located on the lamellae (Fig. 4.10*B*). The cellular staining pattern was concentrated in the basolateral region, and the apical region was mostly devoid of signal. Some cells exhibited a diffuse cytoplasmic staining pattern; however, this could be attributed to the extensive branching of the basolateral membrane.

Discussion

Freshwater fish gill MR cells perform transepithelial Na^+ uptake from an extremely dilute environment (<1 mM Na^+), which requires unique physiological solutions to overcome the unfavourable gradient. Here, I proposed a new model for transepithelial Na^+ uptake at the freshwater fish gill (Fig. 4.11) based on pH_i assessments and V_m imaging of isolated MR cells. My data clearly demonstrate two functionally distinct MR cell subtypes and support the previously reported findings from our laboratory (Galvez et al., 2002; Reid et al., 2003). There is a clear separation in resting pH_i between the two MR cell populations. Potentially, a lower resting pH_i would be advantageous for proton extrusion and a higher pH_i would be advantageous for base extrusion. However, to test this hypothesis, observation of the resting pH_i of MR cells in an intact gill filament is required.

Initially, I was investigating how changes in $[Na^+]_e$ would affect pH_i regulation. Surprisingly, the majority of MR cells exhibited a unique Na^+-induced acidification, a puzzling behaviour that to our knowledge had never been reported. Typically, in all other cells, switching from Na^+-free to Na^+-containing medium would activate either NHEs, which would drive Na^+ into the cell countered by H^+ extrusion (Orlowski and Grinstein, 2004), or activate inward-directed HCO_3^- cotransport via NBCs (Romero et al., 2004). Therefore, analyzing the data in terms of a single transport process could seemingly only result in a Na^+-induced pH_i alkalinization. To our knowledge, there is no specific Na^+-coupled H^+ import mechanism that could explain my

results. Therefore, I had to account for the behaviour by implicating an HCO_3^- export mechanism.

It is important to remember that a specific function of fish gill MR cells is transepithelial Na^+ uptake from dilute freshwater (Evans et al., 2005). Thus it is possible that the observed Na^+-induced acidification represents the coordinated response of transporters located at both the apical and basolateral membranes. I therefore proposed a model whereby Na^+ enters the cell via an apical transporter (phenamil-sensitive Na^+ channel) and subsequently leaves the cell via a basolateral transporter (DIDS-sensitive electrogenic NBC) (Fig. 4.11).

The present models for freshwater Na^+ uptake in MR cells involve Na^+ entry via apical eNaCs that are electrogenically coupled to a V-type H^+-ATPase (Evans et al., 2005; Goss et al., 1998; Perry, 1997; Perry et al., 2003b). In vivo application of the selective inhibitor of V-type H^+-ATPase bafilomycin to the water greatly reduced whole body Na^+ influx in both tilapia and carp (Fenwick et al., 1999). Similar experiments with phenamil, a selective inhibitor of eNaCs (Alvarez de la Rosa et al., 2000; Kleyman and Cragoe, 1988), resulted in comparable reductions of Na^+ influx in rainbow trout (Grosell and Wood, 2002). Although this is compelling evidence for Na^+ entry through an eNaC in the gill MR cells, cloning of an eNaC homologue from fish gill has been unsuccessful thus far. Consequently, Na^+ entry will only be attributed to a phenamil-sensitive Na^+ channel for the rest of this chapter discussion without regard to its molecular identity.

Phenamil sensitivity in our study supports an apical Na^+ channel as the route of entry for Na^+ into the gill. This complements a recent paper from our laboratory (Reid et al., 2003) demonstrating phenamil-sensitive Na^+ uptake in only the PNA^- MR cell fraction. This fraction is reported to be ~80% of the total mixed MR cell population (Goss et al., 2001a), and this is in agreement with the present study in which we found that ~77% of our cells displayed the phenamil-sensitive, Na^+-induced acidification. Together, this strongly suggests that a component of the Na^+-induced pH_i acidification observed in this study is via an apical Na^+ channel in PNA^- MR cells.

The mechanism for basolateral efflux of Na^+ has typically been attributed to the Na^+-K^+ ATPase, which is highly expressed in MR cells (Evans et al., 2005; McCormick, 1995; Perry et al., 2003b). However, exit of Na^+ via Na^+-K^+-ATPase would not result in any pH_i changes. This study is unique in that it provided functional evidence for an alternate route of Na^+ efflux. I proposed that a basolateral NBC is coupled with the apical Na^+ channel for transepithelial Na^+ movement. This is complemented by the action of the Na^+-K^+ ATPase to maintain a low $[Na^+]_i$, thereby allowing for uptake from the dilute medium. In my experiments, $[Na^+]_e$ is kept at 145 mM, which is much higher than normal environmental Na^+ concentration in freshwater (<1 mM). This would tend to drive the Na^+ influx via the apical Na^+ channel very strongly. It is not technically feasible for us to experimentally determine the relative importance of either NBC or Na^+-K^+-ATPase in the exit of Na^+ under physiological conditions where environmental Na^+ is very low (<1 mM).

However, my observed results suggest that NBC efflux is directly linked to Na^+ influx via a phenamil-sensitive Na^+ channel, which is the physiological mechanism of entry in intact freshwater fish (Evans et al., 2005; Grosell and Wood, 2002).

Perry and colleagues (Perry et al., 2003a) successfully cloned an NBC from rainbow trout that was homologous to the electrogenic NBC1. Furthermore, they observed a large increase in NBC1 mRNA at the gill in response to a hypercapnia-induced respiratory acidosis that was also associated with a transient increase in branchial V-type H^+-ATPase mRNA levels. In addition, acid infusions in rainbow trout were shown to cause an increase in Na^+ influx (Goss, 1995), whereas elevations of plasma HCO_3^- by infusion of $NaHCO_3$ is known to decrease Na^+ influx (Goss and Wood, 1990b). These data support my proposal that a basolateral electrogenic NBC could be utilized for transepithelial Na^+ uptake in vivo.

NBC activity was first described in 1983 to take place on the basolateral membrane of the proximal tubule in the salamander *Ambystoma tigrinum* (Boron and Boulpaep, 1983). However, it was not until recently (Romero et al., 1997) that this transporter (NBC1) was successfully cloned and subsequently localized to the basolateral membrane of the proximal tubule (Maunsbach et al., 2000; Schmitt et al., 1999). This breakthrough enabled further understanding of the NBC in a variety of other animals and tissues. An electrogenic NBC1 was recently cloned from the Japanese dace (*Tribolodon hakonensis*) gill and was localized to the basolateral membrane of

MR cells by immunohistochemistry (Hirata et al., 2003). Interestingly, NBC1 was only detected in a subset of MR cells from the Japanese dace gill, aligning with my findings of two functionally distinct MR cell subtypes. Similarly, I demonstrated specific immunoreactivity in a subset of cells on the gill lamellae. Cellular staining for rkNBC1 was basolateral or "cytosolic," similar to the pattern found previously (Hirata et al., 2003) and in accordance with a basolateral localization in the cell in our model.

Functional studies of the cloned proximal tubule NBC1 demonstrated a DIDS-sensitive pH_i acidification and V_m depolarization when acting in efflux mode (Romero et al., 1997). The stoichiometry of this transporter appears to be tissue specific, with one Na^+ being transferred for three HCO_3^- in the proximal tubule of the kidney vs. 1:2 in other parts of the body (Soleimani and Burnham, 2001). My V_m data strongly support the involvement of an electrogenic NBC as appropriate changes in response to our ion-substitution experiments were observed. The introduction of Na^+ induced a depolarization in virtually the same percentage of cells that exhibited an Na^+-induced intracellular acidification (79% vs. 77%). The sensitivity of both events to DIDS further implicates electrogenic NBC involvement in the transepithelial Na^+ movement in these MR cells.

For an NBC to function in export mode, a hyperpolarized V_m is absolutely required to have a net driving force for HCO_3^- export. Unfortunately, I was unable to directly calibrate the resting V_m of the cells due to technical difficulties with the dye. However, I can roughly calculate, based

on external and internal ion (Na^+ and HCO_3^-) levels, the reversal potential, which can give valid estimates of the required V_m to drive the transporter in export mode. Although measurements of $[Na^+]_i$ in gill MR cells are needed to complete transport models, they are difficult to obtain. The reported values for $[Na^+]_i$ of 55 mM (Wood and Lemoigne, 1991) and 62 mM (Morgan et al., 1994) must be interpreted with caution because of a number of confounding variables as discussed by Morgan and colleagues (Morgan et al., 1994). Comparatively, in cells from the frog skin epithelium, $[Na^+]_i$ levels have been measured at 6–17 mM (Harvey and Ehrenfeld, 1986; Rick, 1992). The fish gill is believed to mimic frog skin with respect to Na^+ uptake in MR cells; therefore, previous reports of gill MR cells $[Na^+]_i$ are likely overestimated.

The theoretical reversal potential (E_{rev}) is the point at which no flux would occur through the NBC in efflux mode and can be approximated by the following formula (Gross and Kurtz, 2002):

$$E_{rev} = \frac{RT}{F(n-1)} \times \ln \frac{[Na^+]_i [HCO_3^-]_i^n}{[Na^+]_o [HCO_3^-]_o^n} \qquad \text{(Equation 4.1)}$$

where R is the gas constant, T is the absolute temperature in kelvins, and F is the Faraday constant.

Therefore, a V_m slightly more hyperpolarized than the calculated reversal potential would be required to drive the transporter in export mode. In this formula, n refers to the transport ratio of HCO_3^- to Na^+ or simply the stoichiometry (either 1, 2, or 3). Using a conservative estimate of $[Na^+]_i$ of 10

mM, measured $[Na^+]_e$ of 145 mM, intracellular HCO_3^- concentration ($[HCO_3^-]_i$) of 2 mM (Goss and Wood, 1991), and extracellular HCO_3^- concentration ($[HCO_3^-]_e$) of 7 mM (Goss and Wood, 1990b) would result in a reversal potential of –82 mV when the NBC is operating with a stoichiometry of 1 Na^+ to 3 HCO_3^-. This means that the MR cells would only be required to maintain a V_m of less than –82 mV for the NBC to function in efflux mode, which is not beyond reasonable predictions. However, if the stoichiometry is 1 Na^+ to 2 HCO_3^-, the reversal potential then becomes –133 mV, a much more hyperpolarized value. If intracellular HCO_3^- concentration is raised, this will shift the reversal potential to a more depolarized value and therefore promote the transport in efflux mode. Furthermore, if we lower $[Na^+]_i$ to a very low value (2 mM) to help in apical entry from dilute freshwater, the reversal potential of the 1:3 NBC using these values is only –103 mV, again a feasible value. Therefore, the combination of NBC (1 Na^+ to 3 HCO_3^-) and a reasonably hyperpolarized V_m all support the transport mechanism in my proposed model. Interestingly, the only other place where the NBC functions in efflux mode is the mammalian proximal tubule (for review, see (Soleimani and Burnham, 2001), an epithelium also specialized for transepithelial Na^+ transport. The filtrate from which Na^+ reabsorption occurs contains much higher $[Na^+]_e$ than is found in freshwater, but the extrusion occurs at the basolateral membrane where the $[Na^+]_e$ is ~140 mM, supporting my findings that NBC activity can occur in export mode under these conditions.

Previous pH_i imaging experiments on trout hepatocytes have demonstrated electrogenic NBC activity (Furimsky et al., 2000). The putative NBC was proposed to act in influx mode, thus enabling pH_i recovery from acidosis. The stoichiometry, although not determined, was likely 1 Na^+ to 2 HCO_3^- because of its role in HCO_3^- influx (Boron et al., 1997). In my study, DIDS-sensitive acidification and depolarization indicate the presence of an NBC working in efflux mode, suggesting that trout express functionally different NBCs in a tissue-specific manner, as shown previously in mammalian systems (Soleimani and Burnham, 2001).

Structural analysis has revealed that there is extensive branching of the basolateral membrane of MR cells into an elaborate tubular system (Philpott, 1980) that is in very close contact with the apical membrane. This creates the potential for specialized microenvironments that can help to overcome otherwise energetically unfavourable processes. I proposed that one mechanism for transcellular Na^+ uptake from freshwater is facilitated via a close structural relationship of both apical Na^+ channels and basolateral NBCs acting in efflux mode. However, it is unknown whether ultrastructural characteristics such as the tubular system of the MR cell are maintained during cell isolation performed in this study. Yet, the data of this chapter imply that the MR cell ultrastructure is at least partially maintained during the isolation procedure to produce the cellular behaviours observed. Importantly, the tubular system has been known to become re-established with the

basolateral membrane in isolated MR cells that form aggregates (Philpott, 1980).

Overcoming the gradient for Na^+ extrusion via an NBC would be facilitated by the action of CA, which has been localized in MR cells in a variety of fish, including rainbow trout (Hirose et al., 2003). Abolishment of the Na^+-induced acidification with CA inhibition via acetazolamide in my study supports the involvement of CA in this process. Interestingly, the magnitude of the alkalinization after acetazolamide treatment was larger than that noticed using amiloride, phenamil, or DIDS. Because $[HCO_3^-]_i$ is the strongest determinant in the equation for the reversal potential of the NBC, lowering $[HCO_3^-]_i$ via acetazolamide will shift the reversal potential to more negative values, which would favour HCO_3^- influx and exacerbate the alkalinization.

The mammalian electrogenic NBC1 is known to bind CA II on its COOH-terminal domain (Gross et al., 2002; Romero et al., 2004), although this has not yet been demonstrated in fish. In my proposed model, CA would produce HCO_3^- within the proximity of the NBC to drive Na^+ efflux across the basolateral membrane despite the unfavourable Na^+ concentration gradient. This is supported in the mouse proximal convoluted tubule cell line mPCT1296(d) transfected with kidney NBC1 where inhibition of CA with acetazolamide leads to a 65% reduction in current in HCO_3^- efflux mode only (Gross et al., 2002). These points illustrate how multiple proteins can act as a functional unit for transepithelial Na^+ movement. My suggestion of a coordinated activity between an Na^+ channel, NBC, and CA follows the

concept of a metabolon described in biochemical context as a group of proteins acting together to accomplish one metabolic function (Srere, 1993). Therefore, I proposed to refer to this model as the freshwater Na^+ uptake metabolon.

In summary for this chapter, I have provided evidence for a new model of transepithelial Na^+ uptake in the freshwater fish gill. I support previous research that Na^+ influx into the trout is via an apical, phenamil-sensitive Na^+ channel. I proposed that one mode of Na^+ efflux from the MR cell is directly coupled to a basolateral NBC in contrast to the current models showing that the basolateral Na^+-K^+-ATPase is the only route for Na^+ efflux. Furthermore, I demonstrated that this transport occurs in one functionally distinct population of MR cells present on the gill. My novel findings open up new avenues for elucidating the cellular and molecular mechanism of transepithelial ion movement in this model epithelium.

Figures

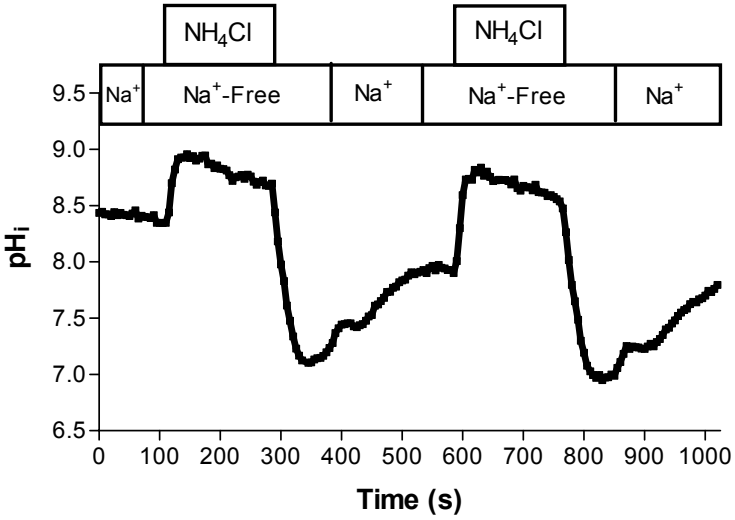

Figure 4. 1 Representative trace demonstrating the ability of the isolated mitochondrion-rich (MR) cells to withstand repeated acid-base disturbances Cells were subjected to 2 consecutive 20 mM NH_4Cl prepulse-induced acidifications and displayed the same behaviour after initial and secondary acidifications.

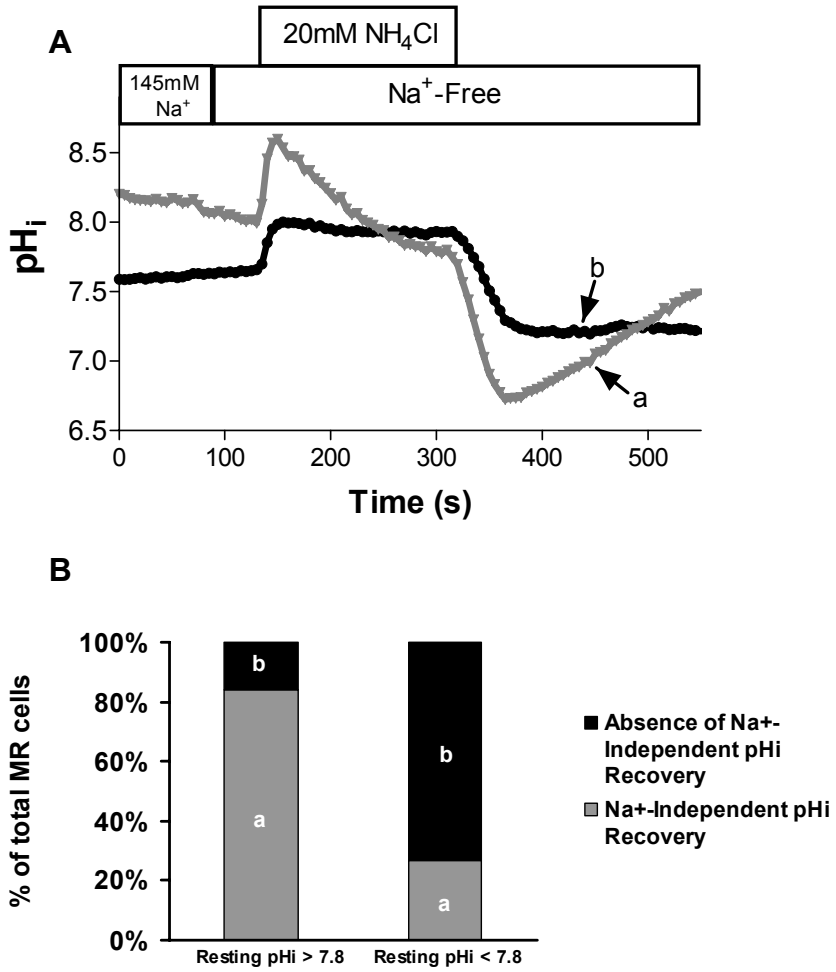

Figure 4. 2 Na^+-free recovery rates indicate 2 populations of MR cells. Cells were acidified with NH_4Cl prepulses and allowed to recover in the absence of Na^+.

A: representative traces of cells that demonstrated an ability to recover from an acidification in Na^+-free conditions (*trace a*) and those cells that were unable to recover pH_i in the absence of Na^+ (*trace b*). ***B:*** summary data demonstrating a link between Na^+-free pH_i recovery and the original resting pH_i of the cell. The majority (84%) of MR cells with a resting pH_i >7.8 (*n* = 175) displayed an Na^+-independent pH_i recovery mechanism compared with only a low percentage (23%) of cells with a resting pH_i <7.8 (*n* = 223) demonstrating this same ability. Letters *a* and *b* correspond to the representative traces in *A* in reference to Na^+-free recovery ability.

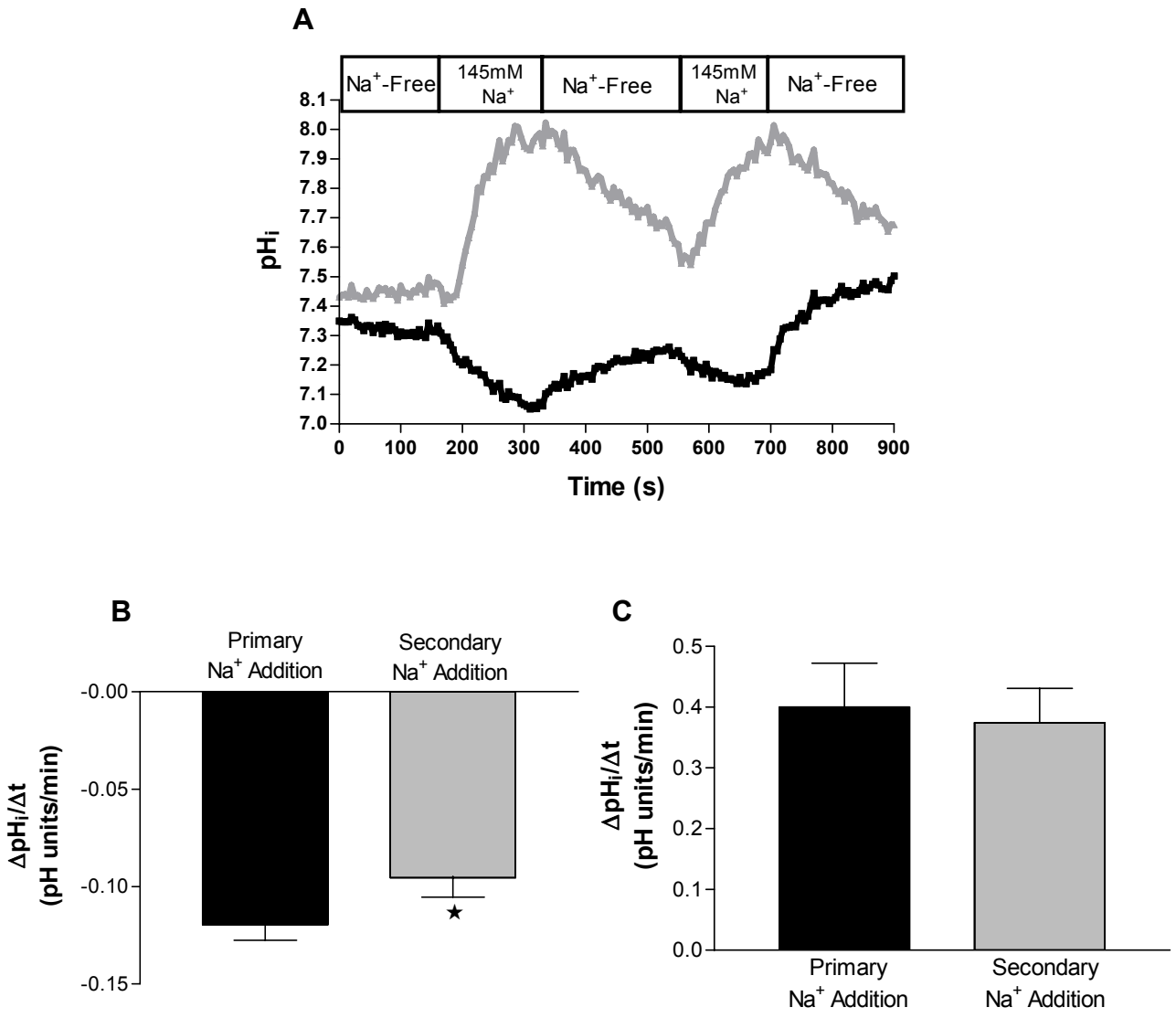

Figure 4. 3 Changes in pH_i of MR cells induced by extracellular Na^+. Cells were initially exposed to Na^+-free medium and then switched to 145 mM Na^+ solution.

A: sample traces demonstrating that 1 population of MR cells (black trace) responds to the change from Na^+-free to Na^+-containing medium with an acidification, whereas the other population (gray trace) exhibits an alkalinization in the same conditions. ***B:*** summary data showing the repeatability of the rate of Na^+-induced pH_i change ($\Delta pH_i/\Delta t$) in this population of MR cells. There was a slight but significant reduction in the rate of the second Na^+-induced acidification compared with the control (*$P < 0.05$, paired *t*-test, $n = 37$ cells, 6 separate experiments). ***C:*** summary data showing the repeatability of the rate of Na^+-induced alkalinization in this population of MR cells. There was no significant difference between the two rates of Na^+-induced alkalinization ($P > 0.05$, paired *t*-test, $n = 18$ cells, 6 separate experiments).

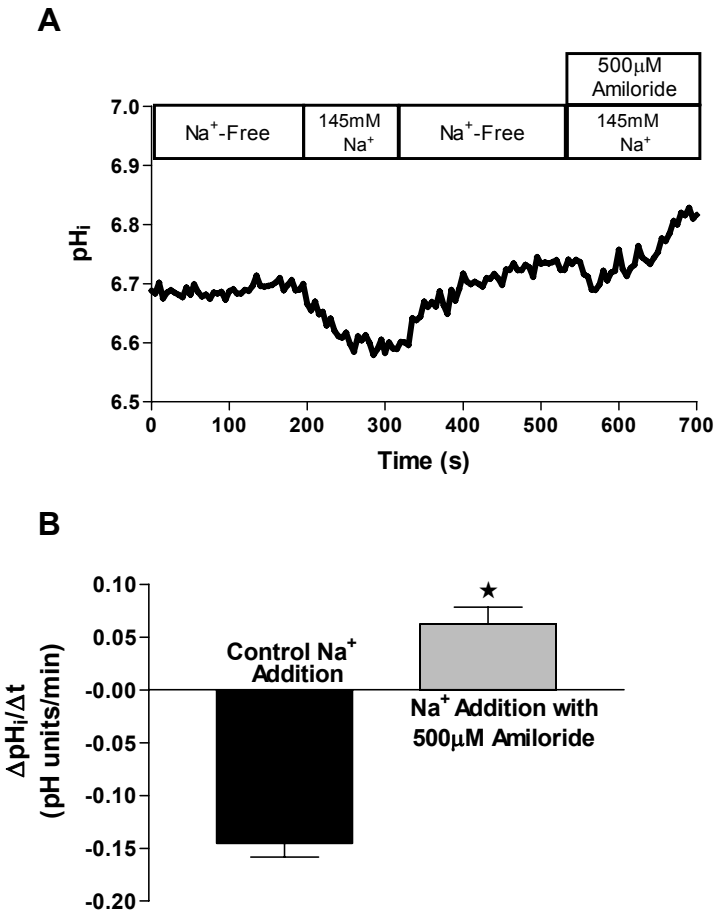

Figure 4. 4 Effect of 500 μM amiloride on the Na^+-induced acidification following Na^+-free exposure at resting pH_i.

A: representative trace showing the effective removal of Na^+-induced acidification in the presence of 500 μM amiloride. The acidification event was replaced with a trend toward alkalinization. ***B:*** summary data of the significant difference between the rates of pH_i change ($\Delta pH_i/\Delta t$) caused by the control Na^+ introduction and the Na^+ exposure in the presence of 500 μM amiloride (*$P < 0.05$, paired *t*-test, $n = 21$ cells, 2 separate experiments).

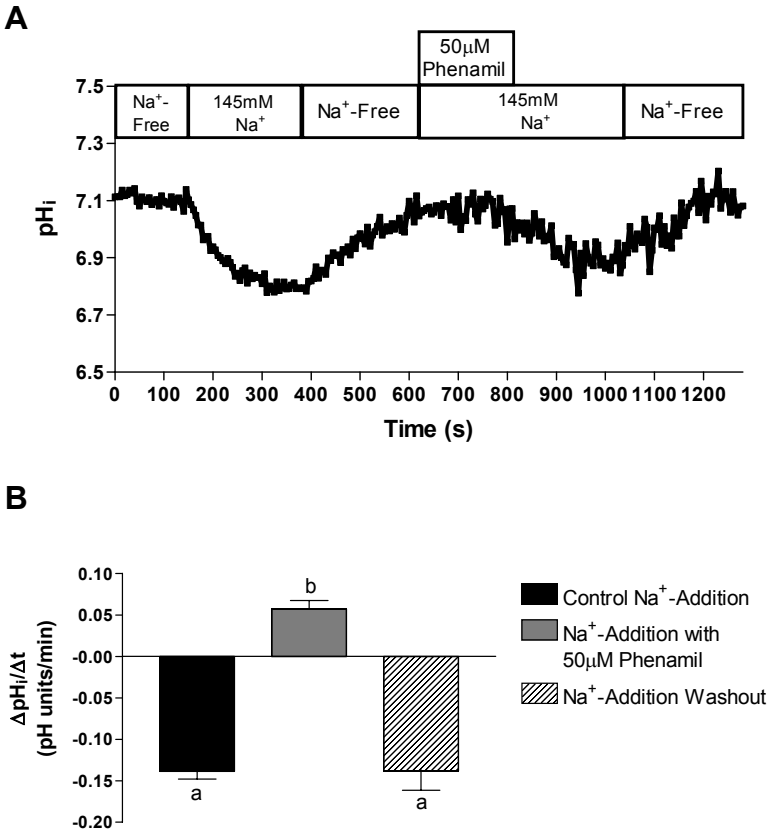

Figure 4. 5 Effect of 50 μM phenamil on the Na^+-induced acidification following Na^+-free exposure at resting pH_i.

A: representative trace showing the effective removal of Na^+-induced acidification in the presence of 50 μM phenamil. The effect of phenamil was reversed by washout with Na^+-containing solution. ***B:*** summary data showing that both the control Na^+ and washout Na^+ exposure caused the MR cells to acidify at a rate that was significantly different from the slight alkalinization rate caused by Na^+ exposure in the presence of 50 μM phenamil. No significant difference was noted between the acidification rate caused by the control Na^+ introduction and the washout Na^+ exposure ($P < 0.05$, repeated-measures one-way ANOVA, Bonferroni post hoc test, $n = 36$ cells, 4 separate experiments). Letters *a* and *b* indicate significant differences.

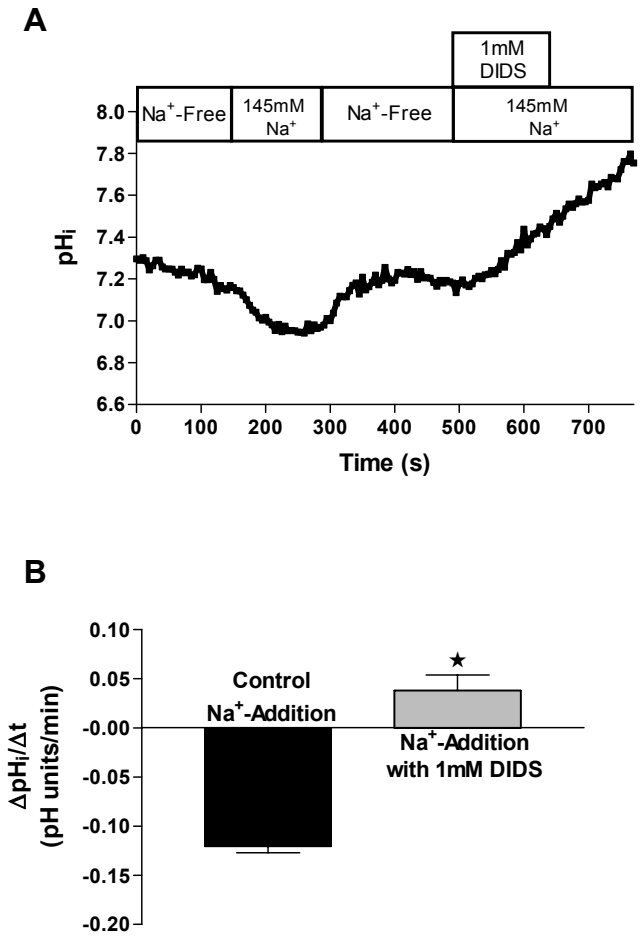

Figure 4. 6 Effect of 1 mM DIDS on the Na^+-induced acidification following Na^+-free exposure at resting pH_i.

A: representative trace showing the effective removal of Na^+-induced acidification in the presence of 1 mM DIDS. The effect of DIDS was not reversed by washout with Na^+-containing solution. ***B:*** summary data showing that the control Na^+ exposure caused the MR cells to acidify at a rate that was significantly different from the slight alkalinization rate caused by Na^+ exposure in the presence of 1 mM DIDS (*P < 0.05, paired t-test, n = 80 cells, 8 separate experiments).

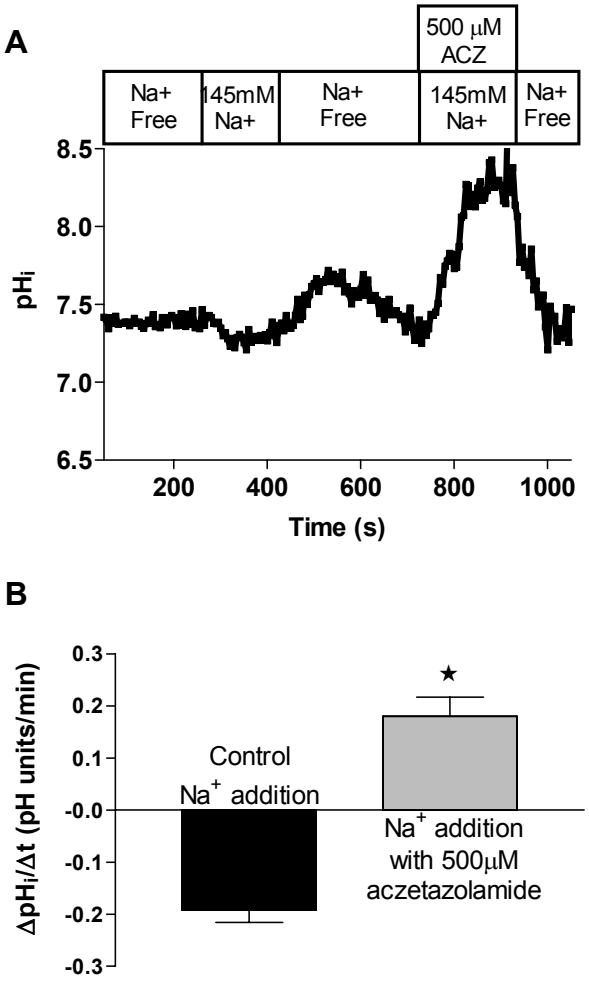

Figure 4. 7 Effect of 500 μM acetazolamide (ACZ) on the Na^+-induced acidification following Na^+-free exposure at resting pH_i.

A: representative trace showing the effective removal of Na^+-induced acidification in the presence of 500 μM acetazolamide. The effect of 500 μM acetazolamide was reversed by washout with Na^+-free solution. ***B:*** summary data showing that the control Na^+ exposure caused the MR cells to acidify at a rate that was significantly different from the effect of Na^+ exposure in the presence of 500 μM acetazolamide (*P < 0.05, paired t-test, n = 23 cells, 10 separate experiments).

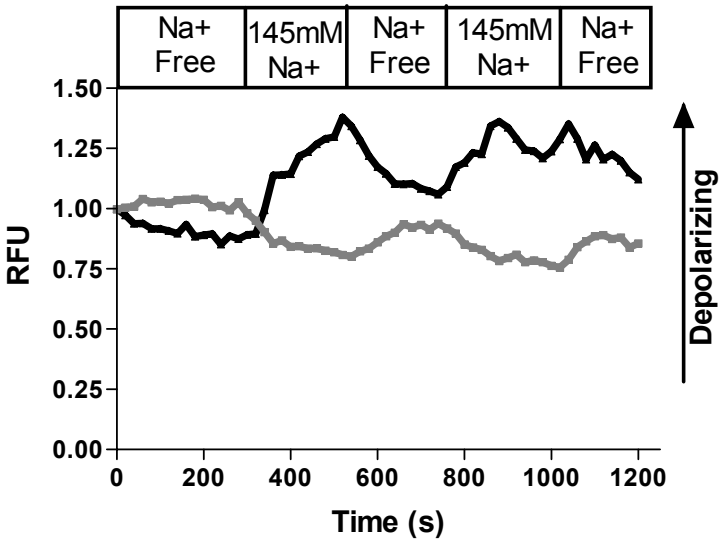

Figure 4. 8 Changes in membrane potential (V_m) of MR cells as indicated by the voltage sensitive dye bis-oxonol.

Changes in V_m are represented as changes in relative fluorescent units (RFU), with an increase in fluorescence being indicative of membrane depolarization. Black trace is representative of MR cells that demonstrated a repeatable Na^+-induced depolarization of V_m on switching from Na^+ free solution to 145 mM Na^+ (79%, n = 111/140, 14 separate experiments). Gray trace shows that the minority of MR cells demonstrated a repeatable Na^+-induced hyperpolarization of V_m under identical experimental conditions (21%, n = 29/140).

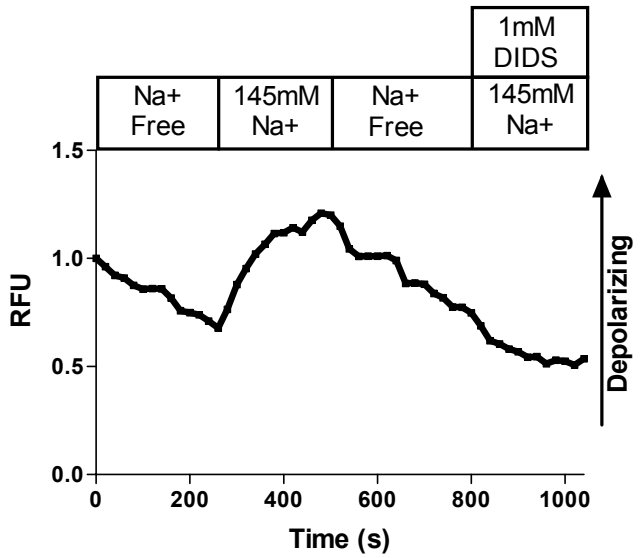

Figure 4. 9 Representative trace showing changes in membrane potential (V_m) of MR cells in the presence of Na^+ and 1 mM DIDS.

Changes in V_m are indicated by the voltage-sensitive dye bis-oxonol as indicated by RFU. DIDS (1 mM) was effective at removing the Na^+-induced depolarization in 75% of the MR cells that were demonstrated to originally show this behaviour (*n* = 21/28, 5 separate experiments).

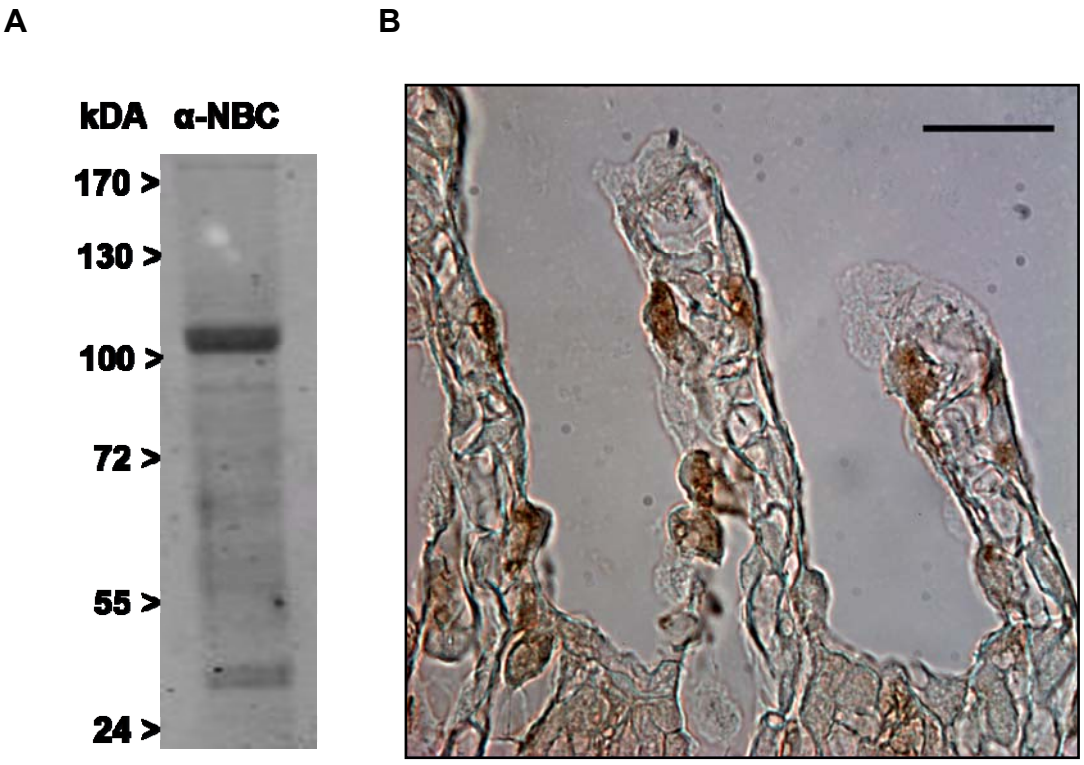

Figure 4. 10 Immunoreactivity of the anti-rat kidney Na^{+}-HCO_3^{-} cotransporter (rkNBC1) in the trout gill.

A: Western blot showing a distinct band of ~110 kDa from whole gill homogenates. ***B:*** immunohistochemistry of the trailing edge of the gill filament exhibiting specific cellular staining of NBC. Notice that positive cells are found mostly on the lamellae and that the cellular staining pattern is concentrated in the basolateral region with the apical area being devoid of signal in most cells. Cytoplasmic staining patterns are likely due to the extensive branching of the tubular system of the basolateral membrane in these cells. Scale bar = 10 µm.

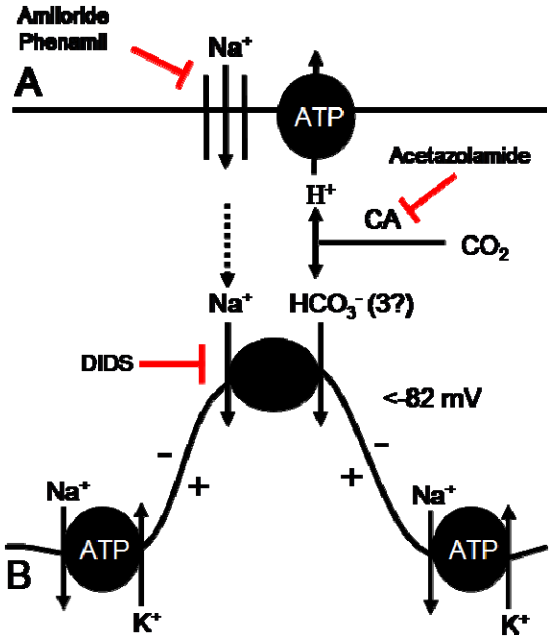

Figure 4. 11 Freshwater transepithelial Na^+ uptake metabolon in gill non-peanut lectin agglutinin binding (PNA^-) MR cells.

Note how the tubular system allows for the close proximity of the apical (*A*) Na^+ channel and H^+-ATPase with the basolateral (*B*) NBC. The electrogenic NBC transfer is represented as "3?" HCO_3^- transported with 1 Na^+ due to thermodynamic analysis but inability to directly ascribe the stoichiometry. Sites of pharmacological inhibition in my study are indicated by stop arrows. The proposed V_m is indicated, and +/ – signs are used to help demonstrate this point.

Chapter V: Regulation of ion transport by low pH in isolated gills of the crab *Neohelice* (*Chasmagnathus*) *granulata*[1]

[1]A version of this chapter has been published previously.

*****Tresguerres, M., ***Parks, S. K.**, Sabatini, S. E., Goss, G. G. and Luquet, C. Regulation of ion transport by pH and [HCO_3^-] in isolated gills of the crab *Neohelice (Chasmagnathus) granulata*. *American Journal of Physiology-Regulatory Integrative and Comparative Physiology* **294**, R1033-R1043, 2008. *** Both authors contributed equally to all aspects of this work.**

Introduction

In crustaceans, the gill is the main organ involved in acid/base (A/B) exchange with the environment, and thus it is probably the main A/B regulatory organ (Wheatly and Henry, 1992). The overall branchial mechanism for A/B regulation in crabs is similar to other aquatic animals: apical Na^+/H^+ and Cl^-/HCO_3^- exchanges (Dejours et al., 1982; Ehrenfel.J, 1974; Henry and Cameron, 1982; Henry and Cameron, 1983) energized by ATPases (Kimura et al., 1994). However, the only proteins involved in the gill A/B regulatory mechanism that have been identified so far in crabs are carbonic anhydrase (Henry, 1984; Henry, 1996; Siebers et al., 1994) and Na^+/K^+-ATPase (Siebers et al., 1994). Several other ion-transporting proteins have been molecularly and/or pharmacologically identified in crab gills, but to our knowledge, only their role in ion uptake and not A/B regulation has been directly tested (reviewed by (Freire et al., 2008).

A major advantage of the gills of certain crustaceans over other A/B regulatory organs (i.e., fish gill and mammalian kidney) is that they can be easily isolated from the animal and perfused with hemolymph-like saline using a peristaltic pump. This technique allows for the study of the ion transport physiology of the whole organ without the interference of hormonal or nervous factors. Isolated and perfused gills allow for accurate control of the composition of the perfusing and bathing salines, including the addition of specific inhibitors of ion-transporting proteins. These manipulations are impossible to perform in whole animal experiments. In addition, these

limitations were realized in the previous chapter as I was extrapolating transepithelial ion movement from work on isolated cells.

The cellular mechanisms for ion uptake across the posterior gills of *Neohelice granulata* (formerly named *Chasmagnathus granulatus*) are some of the better studied among aquatic animals. The basal (nonstimulated) ion transport mechanism in gills from crabs acclimated to low-salinity water (2 ‰) includes basolateral Na^+-K^+-ATPase, and Cl^- and K^+ channels (Luquet et al., 2002b; Luquet et al., 2005; Onken et al., 2003). In this condition, the apical routes of entry for Cl^- and Na^+ are apical Na^+-K^+-$2Cl^-$ (NKCC) cotransporters in parallel with K^+ channels (Luquet et al., 2005; Onken et al., 2003). This basal state of ion uptake can be activated by hormonal and nonhormonal factors. For example, dopamine can activate Na^+-K^+-ATPase via a D1-like receptor-G_s protein-cAMP-PKA pathway (Genovese et al., 2006; Halperin et al., 2004). A reduction in the osmolarity of the hemolymph-side of the isolated gill also stimulates ion uptake (Luquet et al., 2002b; Tresguerres et al., 2003), an effect that is partially mediated by cAMP and Na^+-K^+-ATPase (Tresguerres et al., 2003). In addition, CA and apical V-H^+-ATPases and Cl^-/HCO_3^- exchangers (CBEs) are also recruited during these stimulated conditions (Genovese et al., 2005). Apical V-H^+-ATPase and CBEs working in concert could facilitate Cl^- uptake from a dilute external medium (Genovese et al., 2005), but the combined effect of both transporters is neutral in terms of net A/B transport. Interestingly, the branchial cellular mechanisms for ion transport in *N. granulata* from different salinities resemble those from different

segments of the mammalian nephron. This is likely related to similar ionic gradients encountered at the apical membrane in each system.

In this chapter, I investigated the involvement of the gills of *N. granulata* in the acid recovery mechanism. I used the advantages of the isolated and properly polarized gill preparation to test the hypothesis that ion transport can be directly stimulated by low pH in the blood compartment of the gill. My results indicate that ion transport processes similar to those described in trout (chapter IV) are stimulated by low pH.

Summary of methodological approach

To study the role of the crab gill in recovery from an acidification of the hemolyph I used an isolated gill preparation to measure the transepithelial potential difference (V_{te}) as an index of ion transport. Stimulation of ion transport *via* low hemolymph pH was followed by a series of pharmacological blocking agents. Experiments were also performed to measure the acid secretion rate to the surrounding bath following low hemolymph pH exposure. These studies were complemented by immunohistochemistry of VHA and NKA at the crab gill.

Results

Stimulation of V_{te} by low pH in isolated perfused gills.

A reduction in the pH from 7.75 to 7.45 pH units in the perfusion conditions induced an immediate and significant stimulation of V_{te} from 3.68 ± 0.58 to 6.32 ± 0.72 mV (n = 13). The original V_{te} was restored upon reapplication of the saline with pH of 7.75. The low pH-stimulated V_{te} and subsequent wash-out was a repeatable event (Fig. 5.1*A*), and it was accompanied by an increase in net acid secretion from –79.1 ± 18.5 to –146.9 ± 19.2 μequiv·kg^{-1}·h^{-1} (net increase of –67.8 ± 18.4 μequiv·kg^{-1}·h^{-1}, $P < 0.05$; n = 5; Fig. 5.1*B*).

Pharmacological characaterization of low pH stimulation of V_{te}

To test whether CA is involved in the low pH-stimulating mechanism, 200 μmol/l acetazolamide was added into the 7.45 pH perfusate of isolated gills that had already been stimulated by low pH. Acetazolamide completely and reversibly abolished the stimulated V_{te} (Fig. 5.2). I also investigated the involvement of V-H$^+$-ATPase. Basolateral bafilomycin (100 nmol/l) inhibited the low pH-stimulated V_{te}, but, unlike acetazolamide, its effect was only slightly reversible (Fig. 5.3). However, the original resting V_{te} was restored upon reintroduction of the control pH 7.75 saline, indicating that the inhibitory effect of bafilomycin specifically acts on the mechanism stimulated by low pH. Next, I tested the involvement of apical Na^+ channels and basolateral Na^+/HCO_3^- cotransporters by adding apical phenamil (50 μmmol/l) and

basolateral DIDS (1 mmol/l), respectively, under low-pH stimulating conditions. An inhibitory effect of phenamil was seen in a 3 out of 5 preparations, but its magnitude was highly variable, and thus it is not shown or analyzed. On the other hand, basolateral DIDS totally inhibited the elevated V_{te}, although it first produced an important (~10 mV) hyperpolarization of V_{te} in most of the preparations (Fig. 5.4). The inhibitory effect of DIDS was not reversible. DIDS did not cause any significant changes when applied under control pH conditions (Fig. 5.4*C*), indicating that both the initial hyperpolarization and the inhibitory effect observed are related to the low pH-stimulating mechanism.

Lastly, I tested whether the low-pH stimulated V_{te} depends on the transepithelial movement of Na^+ and Cl^- by using solutions with reduced concentrations of these ions. As shown in Fig. 5.5, these conditions abolished and in some cases even reversed V_{te}. Introduction of Na^+-free pH 7.45 saline did not elicit an increase in V_{te}, demonstrating that the transepithelial movement of Na^+ (apical channel and basolateral NBC?) is essential for the low pH activation of V_{te} (Fig. 5.5, *A* and *B*). Conversely, a reduction in saline pH to 7.45 during Cl^--free conditions still induced a significant increase of V_{te} of a magnitude comparable to that in normal, Cl^--containing, saline. This effect was only partially reversible (Fig. 5.5, *C* and *D*).

V-H^+-ATPase and Na^+/K^+-ATPase immunolocalization.

The anti-V-H^+-ATPase and anti-Na^+-K^+-ATPase heterologous antibodies cross-reacted with crab gills and exhibited bands of the appropriate

size during Western blot analysis (~75 and 110 kDa, respectively, Fig. 5.6). No bands were detected when the primary antibodies were omitted (not shown).

The antibodies resulted in slightly different immunolabeling patterns on gill sections. Both V-H^+-ATPase and Na^+-K^+-ATPase immunoreactive cells were present throughout the pillar and principal cells, although Na^+-K^+-ATPase labeling was much stronger (Fig. 5.7, *A* and *B*). However, high-magnification micrographs revealed that V-H^+-ATPase is also present in the apical region of some cells (Fig. 5.7*C*). No signal was found when the primary antibodies were omitted (Fig 5.7*D*). A schematic diagram of the crab gill morphology modified from previous publications (Freire et al., 2008; Onken and Riestenpatt, 1998) is presented in Fig 5.7 along with the immunohistochemistry to assist in identification of the cellular regions within the gill.

Discussion

My results in this chapter demonstrate that ion transport across posterior gills of *N. granulata* is stimulated by a decrease in pH. This suggests that the posterior gills are important in detecting and correcting A/B disturbances in the hemolymph of the whole animal.

Gills from crabs acclimated to 2 ‰ salinity maintain a basal ion uptake activity when perfused with the control saline used in the current study, as estimated from V_{te}, short-circuit current and $^{22}Na^{+}$ uptake (Luquet et al., 2002b; Onken et al., 2003; Tresguerres et al., 2003). These V_{te} measurements are not without certain limitations. In particular, V_{te} is a reflection of both current (I) and transcellular and paracellular resistance (R). Therefore, it is possible that the changes observed were produced by changes in R. However, our saline manipulations were always performed at constant osmotic pressure, and thus it is unlikely that 'paracellular R' changes in the dramatic fashion that is required to justify the observed changes in V_{te}. Similarly, transcellular R would have to increase substantially, which could only happen by a reduction in the conductance of the ion-transporting proteins involved (most likely at the apical membrane). However, this hypothesis would make it difficult to explain the pharmacological inhibition of the stimulated V_{te} by low pH (and HCO_3^- see appendix I). Therefore, I am confident that the V_{te} measurements are indeed a reasonable estimation of net transepithelial ion transport (I) under these experimental conditions. In addition, V_{te} measurements in open-circuit conditions have certain advantages over short-

circuit conditions (i.e., inactivation of V-H^+-ATPase, see (Freire et al., 2008; Kirschner, 2004)).

Carbonic anhydrase.

My results indicate that CA is essential for the gill responses to low pH. Intracellular CA would likely hydrate CO_2 into H^+ and HCO_3^- (Fig. 5.8), the main intracellular substrate in the mechanism stimulated by low pH (and high HCO_3^-, see appendix I). I cannot discount the possible involvement of both extra- and intracellular CA in this mechanism as they are both present at the crab gill (Genovese et al., 2005). Unfortunately, the drug used in this study does not differentiate between extracellular and intracellular CA, and further studies are necessary to confirm the involvement and specific roles of both CA isoforms. On the other hand, saline [HCO_3^-] was negligible in the low pH experiments. Therefore, the source of CO_2 for the acid secretion mechanism is unclear. One possibility is that the HCO_3^- that is reabsorbed into the hemolymph combines with H^+, generating CO_2 (*via* extracellular CA) that diffuses back into the cell. Yet another interesting option is derived from studies on fish intestinal epithelium, where mitochondria-produced CO_2 is an important substrate for ion transport (reviewed in (Grosell, 2006)). The gill ionocytes of *N. granulata* possess large numbers of mitochondria (Luquet et al., 2002a; Luquet et al., 2000), which supports this model. Furthermore, low pH did not produce any change in gill V_{te} when the same protocol was attempted during the winter months (Dr. Carlos Luquet personal communication). Although preliminary, these results may indicate that gills

from winter crabs are metabolically less active than in summer crabs. Whether winter crabs conform to acidotic conditions or use different mechanisms for recovery is a fascinating topic that is currently being investigated in Dr. Luquet's laboratory.

Low pH-stimulating mechanism.

The inhibition of the low pH-stimulated V_{te} by bafilomycin is a good indicator of the importance of V-H^+-ATPase in this response. On the basis of the outside positive V_{te}, I propose that V-H^+-ATPase is located in the apical membrane and acts to secrete the excess H^+ into the water covering the gills. Although bafilomycin was applied to the basolateral space, it is a membrane-permeable compound (Drose and Altendorf, 1997) and thus it can inhibit V-H^+-ATPase located at the apical membrane even if applied at the basolateral space.

Apical V-H^+-ATPase has been proposed to energize apical Cl^- absorption in some strong hyperregulating freshwater crabs (Onken et al., 1991; Onken and McNamara, 2002; Onken and Putzenlechner, 1995; Riestenpatt et al., 1995; Weihrauch et al., 2004a), and also in *C. granulatus* (Genovese et al., 2005; Luquet et al., 2002b). However, the Cl^- independence demonstrated in this chapter suggests that the low-pH stimulating mechanism is different from the Cl^- uptake mechanism. On the basis of Na^+-uptake models from certain aquatic organisms (for a review, see (Kirschner, 2004) and chapters 1, 2), and following up on the hypothesis developed in chapter IV, I tested for the putative involvement of apical Na^+ channels by applying

apical phenamil on gills with stimulated V_{te}. Although phenamil did inhibit the stimulated V_{te} in certain preparations, the effect was not consistent, probably because of permeability issues at the apical cuticle (Onken and Riestenpatt, 2002). The preliminary model presented here includes apical Na^+ channels (Fig. 5.8), although further investigation is required to confirm this component.

My previous data chapter reports the involvement of a basolateral electrogenic Na^+/HCO_3^- cotransporter (NBC) as the way of exit of HCO_3^- and Na^+ in isolated fish gill cells (Parks et al., 2007b). In the current study, basolateral application of DIDS produced an initial further stimulation of the V_{te} already stimulated by low pH, followed by a rapid, complete, and irreversible inhibition. I tentatively propose that DIDS indeed inhibits basolateral NBCs and that the initial V_{te} stimulation is due to the pumping of protons by apical V-H^+-ATPases, which is not totally compensated due to the reduction in the transcellular flux of Na^+ as a result of the inhibition of its basolateral transport. Additionally, a transient increment in Cl^- uptake through Cl^-/ HCO_3^- exchange, favored by the activation of the V-H^+-ATPases and by the intracellular accumulation of HCO_3^-, could be an alternative cause of this peak in V_{te}. In the longer term, the apical V-H^+-ATPase probably shuts down because the HCO_3^- accumulation inside the cells reduces the availability of H^+, and then V_{te} is inhibited. Lastly, DIDS penetrating into the cell and affecting transporters located at the apical membrane cannot be ruled out. In addition, the results from the Na^+ and Cl^- substitutions indicate that the low pH-induced increase in V_{te} depends on transepithelial Na^+ transport. This

leaves only the possibility of an NBC and/or Na^+-K^+-ATPase on the basolateral side. The NBC would be more likely as the HCO_3^- produced via CA hydration of CO_2 would need to be transported across the basolateral surface to maintain the charge distribution, as the H^+ is pumped out apically.

V-H^+-ATPase and Na^+-K^+-ATPase immunolocalization.

Although V-H^+-ATPase and Na^+/K^+-ATPase have been previously detected in *C. granulatus* by pharmacological, biochemical (Genovese et al., 2006; Halperin et al., 2004; Luquet et al., 2002b; Tresguerres et al., 2003), and molecular biology techniques (Luquet et al., 2005), this is the first immunolocalization report of these transporters in this crab. Na^+-K^+-ATPase is present in both principal and pillar cells, being restricted to the basolateral area in both cell types. A basolateral localization is consistent with the literature (reviewed in (Lucu and Towle, 2003)) and with the role of Na^+-K^+-ATPase in energizing ion uptake in basal and stimulated conditions (Genovese et al., 2005; Genovese et al., 2006; Luquet et al., 2002b; Luquet et al., 2005; Onken et al., 2003; Tresguerres et al., 2003). A basolateral Na^+-K^+-ATPase is also important for the low pH stimulatory mechanism reported in this study (Fig. 5.8).

The apical V-H^+-ATPase localization in some pillar and principal cells is consistent with its role in acid secretion derived from our perfusion experiments. The V-H^+-ATPase labeling found throughout the majority of cells could be due to V-H^+-ATPase stored in vesicles. These vesicles might insert into the apical membrane for enhanced acid or ammonia secretion (reviewed

in (Weihrauch et al., 2004b)) or when ion uptake is stimulated by hypo-osmotic shock. Similar V-H^+-ATPase immunolabeling patterns have been recently reported in 13 other species of crabs (Tsai and Lin, 2007).

Na^+-K^+-ATPase and V-H^+-ATPase are present both in pillar and principal cells. Therefore, it is possible that the gill epithelium of *N. granulata* has only one cell type for A/B regulation, which could alternatively perform acid or base secretion depending on the physiological status of the animal. This would match hagfish gills, in which Na^+-K^+-ATPase, V-H^+-ATPase, and NHE are all located in the same cells ((Parks et al., 2007a; Tresguerres et al., 2006b; Tresguerres et al., 2007a) and see chapter 10, appendix II). However, it is also possible that the cytoplasmic pool of V-H^+-ATPase from the principal and pillar cells differentially insert into the apical membrane during acidosis. Alternatively, it is possible that V-H^+-ATPase is present in the basolateral membrane of certain gill cells, but the labeling looks cytoplasmic due to the deep infoldings of the basolateral membrane (Luquet et al., 2002a; Luquet et al., 2000) (see (Tresguerres et al., 2006a) for a similar situation in teleost fish).

Perspectives and Significance

The low-pH and HCO_3^- stimulation of V_{te} reported in this study raise the following interesting questions: *1*) Do these two mechanisms take place in the same gill cell type or are there specific cell subtypes for each of them? *2*) Is ion regulation linked to A/B regulation in the gills of crustaceans? *3)* What is the identity of the pH sensor that regulates the activation of one mechanism

over the other? Finally, given that the key ion-transporting proteins (e.g., Na^+-K^+-ATPase, V-H^+-ATPase, CA) involved in our proposed A/B regulatory mechanisms in crab gills are also present in ion-transporting epithelia from vertebrates, it is possible that they all share a similar direct activation by blood A/B variables. There are many exciting areas of gill acid-base physiology that can be exploited in this preparation in the future. These data strengthen the conclusions of chapter 4 for the proposal of an apical Na^+ channel linkage to a basolateral, electrogenic NBC for transepithelial Na^+ uptake. I have used a properly polarized electrophysiological preparation to enhance the pH_i imaging work from trout gill MR cells in chapter 4. It will be interesting to see the future years unfold in terms of the universal use of this mechanism in animals inhabiting ion poor environments.

Figures

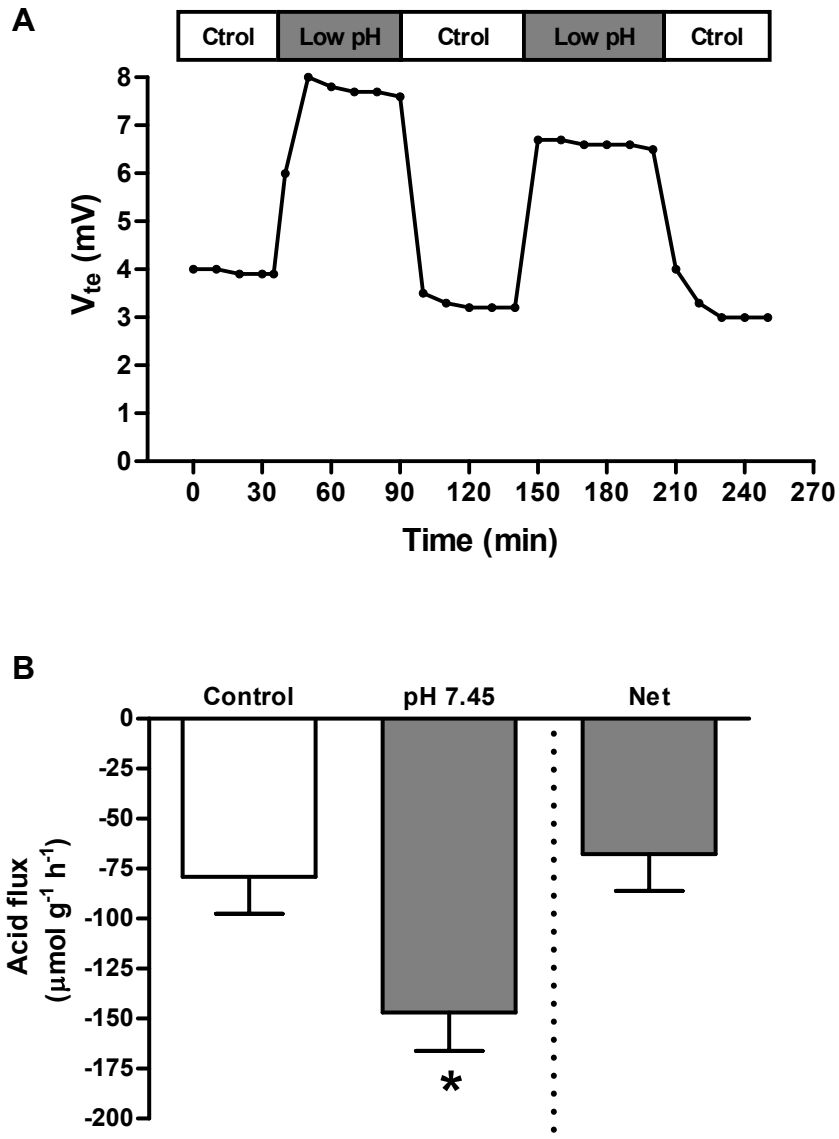

Figure 5. 1 Acid-induced activation of V_{te} and acid secretion.

A: representative V_{te} trace showing repeatability of the event. ***B***: acid secretion. Control saline, pH = 7.75. *Statistically significant difference (P < 0.05, n = 5; paired Student's t-test).

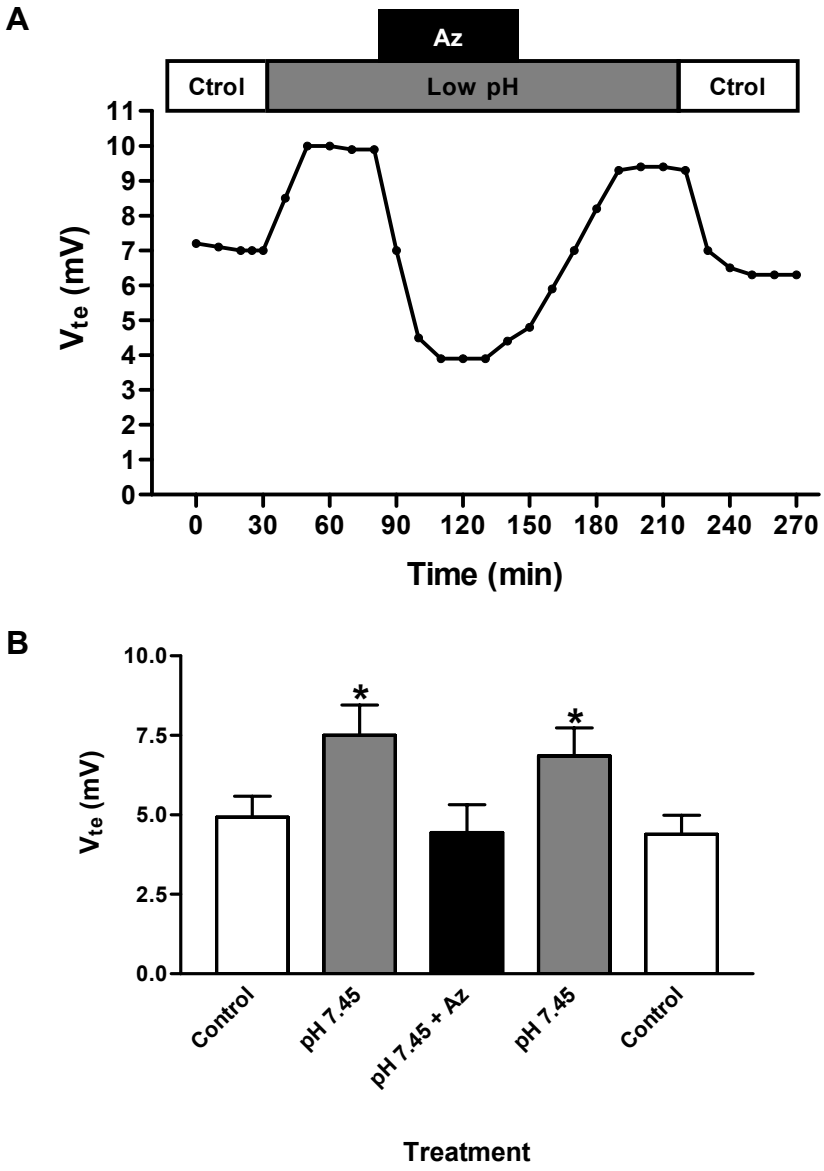

Figure 5. 2 Inhibition of the acid-induced V_{te} stimulation by basolateral acetazolamide**.**

A**:** representative trace. ***B*****:** summary statistics. Control saline, pH 7.75. Az, 200 µmol/l acetazolamide added in the basolateral perfustate. *Statistically significant differences with the control ($P < 0.05$; $n = 7$; one-way repeated-measures ANOVA, Dunnett's multiple-comparison posttest).

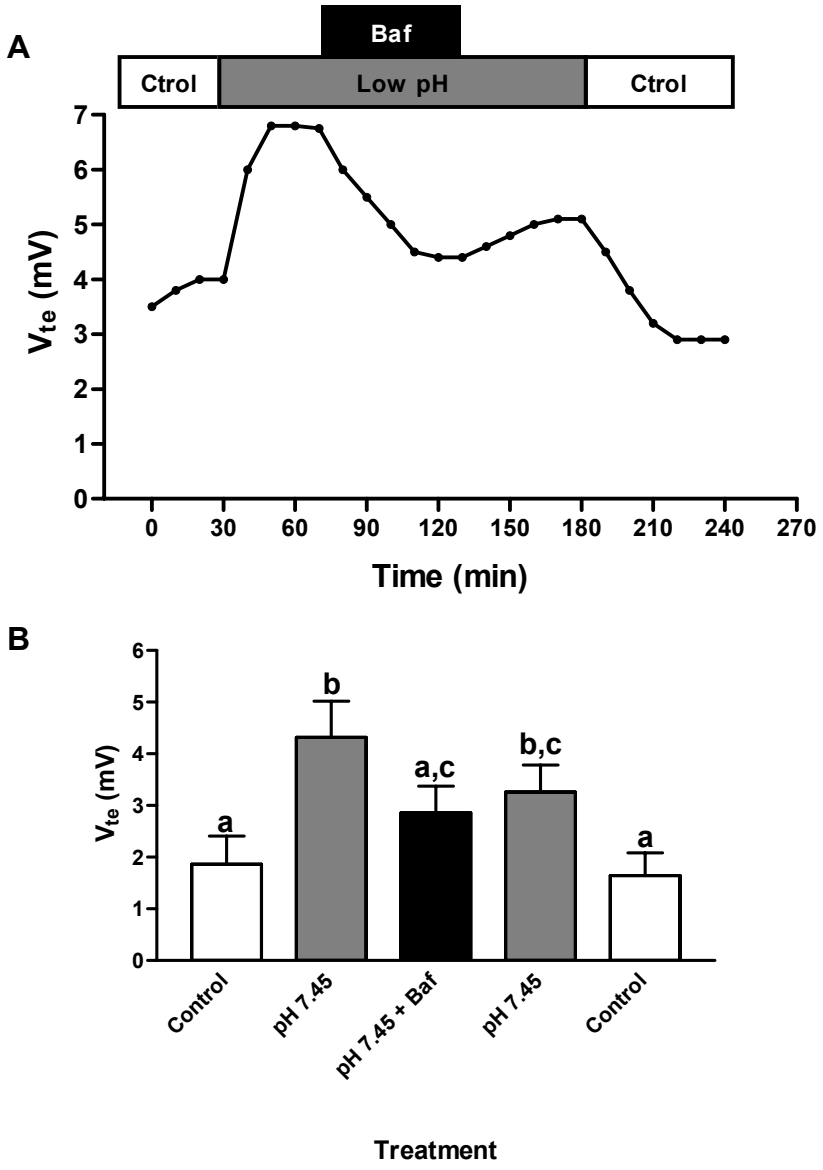

Figure 5. 3 Inhibition of the acid-induced V_{te} stimulation by basolateral bafilomycin.

***A*:** representative trace. ***B*:** summary statistics. Control saline, pH 7.75. Baf, 100 nmol/l bafilomycin added in the basolateral perfusate. ^{a,b,c} Differing letters indicate different levels of statistical significance ($P < 0.05$; $n = 5$; one-way repeated-measures ANOVA, Tukey's multiple-comparison post test).

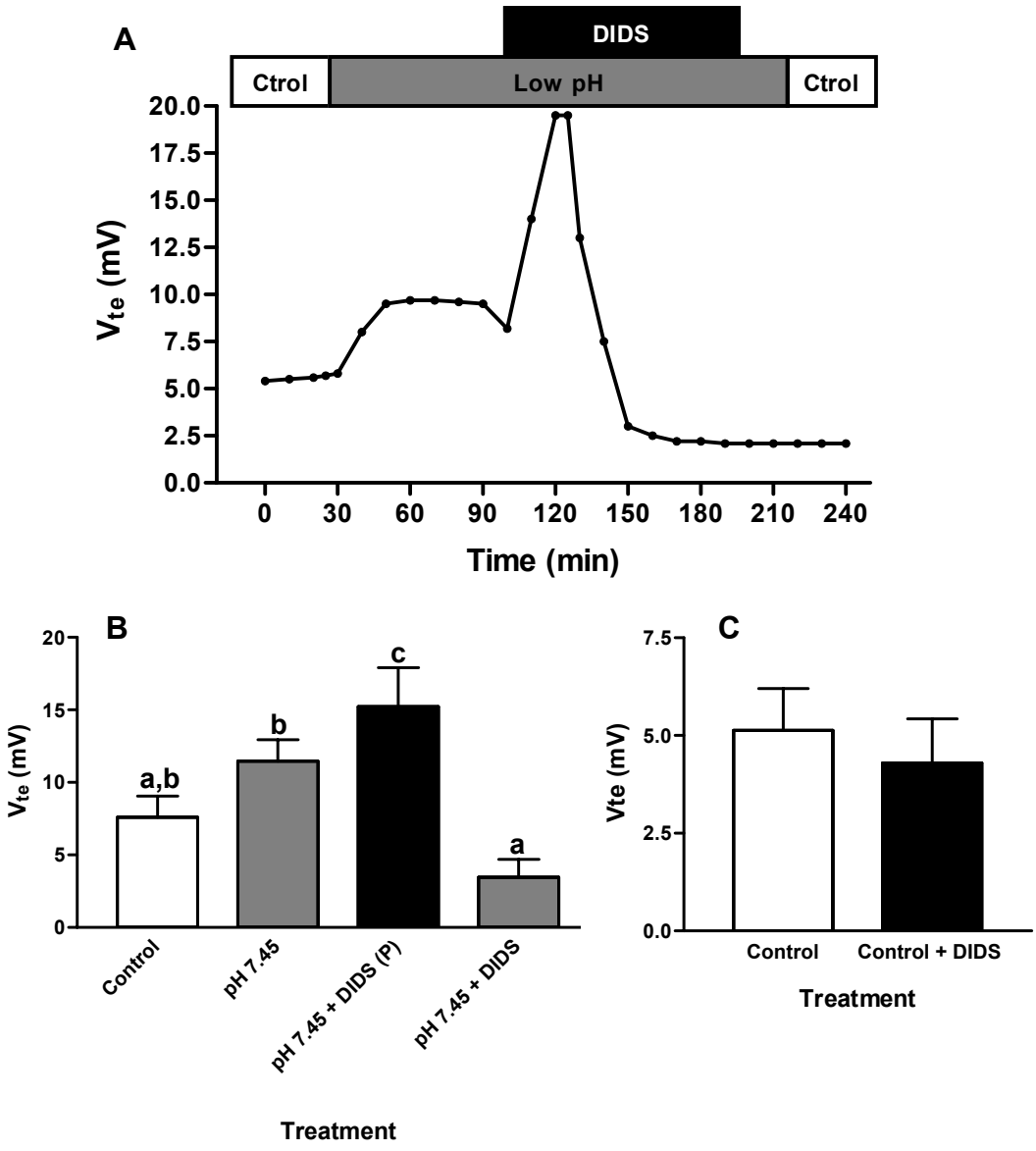

Figure 5. 4 Inhibition of the acid-induced V_{te} stimulation by basolateral DIDS. ***A*****:** representative trace. ***B*****:** summary statistics in pH 7.45 saline (*n* = 5). ***C*****:** summary statistics in control pH 7.75 saline (*n* = 3). Control saline, pH 7.75. DIDS, 1.00 mmol/l DIDS added in the basolateral perfusate. (P), V_{te} peak. ^{a,b,c} Differing letters indicate different levels of statistical significance ($P < 0.05$; one-way repeated-measures ANOVA, Tukey's multiple-comparison posttest).

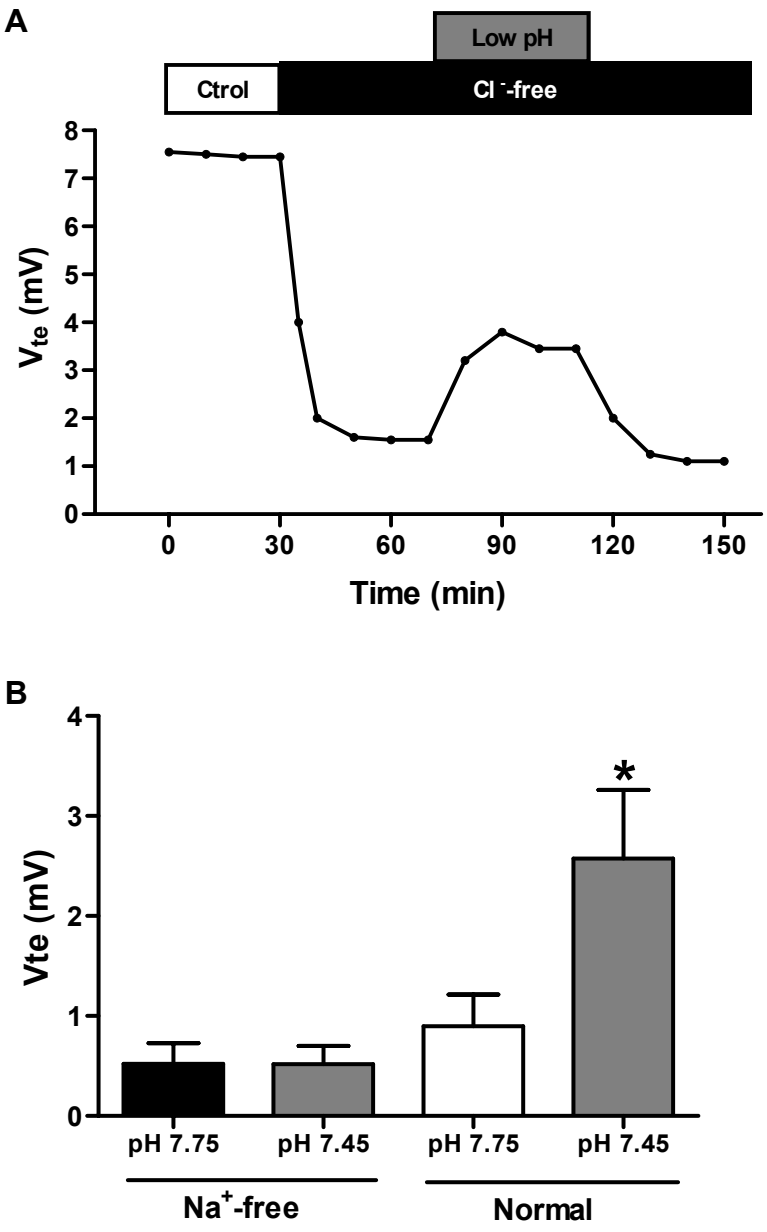

Figure 5. 5 Acid-induced V_{te} stimulation in Cl^--free conditions and lack thereof in Na^+-free conditions.

***A*:** representative trace of a Na^+-free experiment. ***B*:** summary statistics of the Na^+-free experiments.

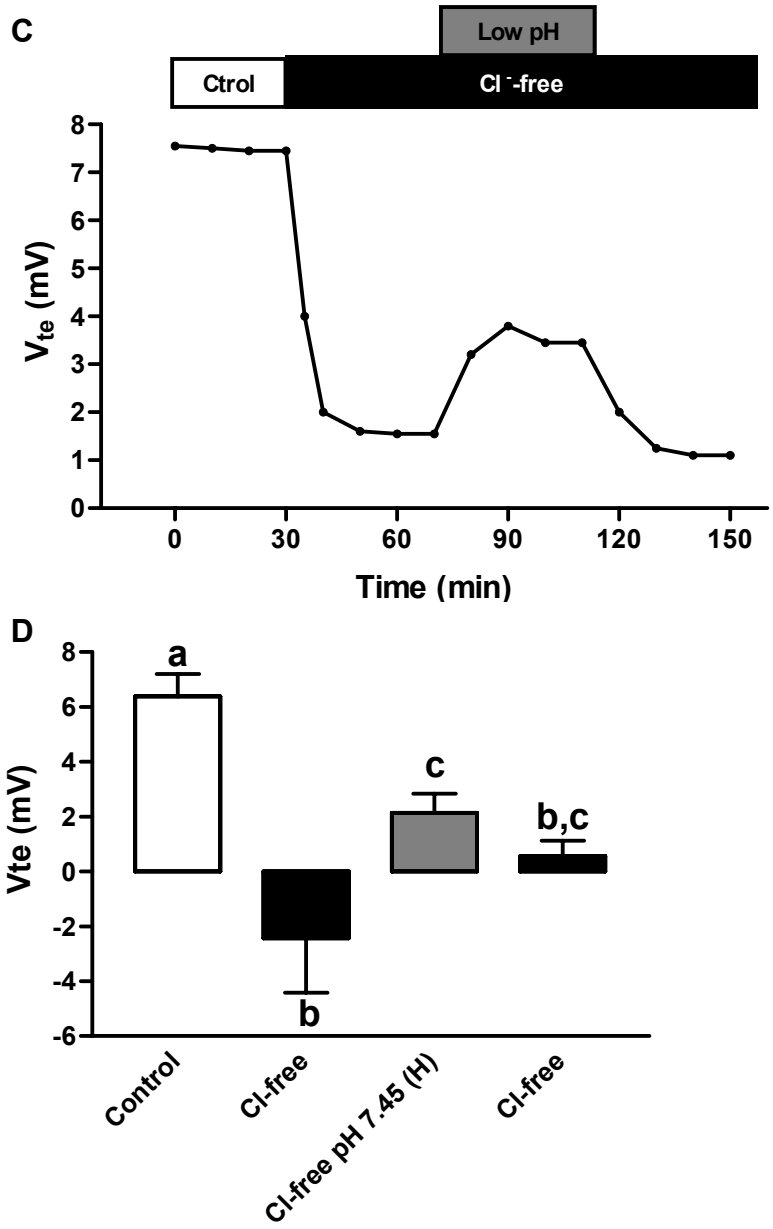

Figure 5.5 Continued. *C*: representative trace of a Cl^--free experiment. ***D*:** summary statistics of the Cl^--free experiments. Control saline, pH 7.75. [a,b,c]Differing letters and asterisk (*) indicate statistical significance ($P < 0.05$; $n = 5$; one-way repeated-measures ANOVA, Tukey's multiple-comparison posttest).

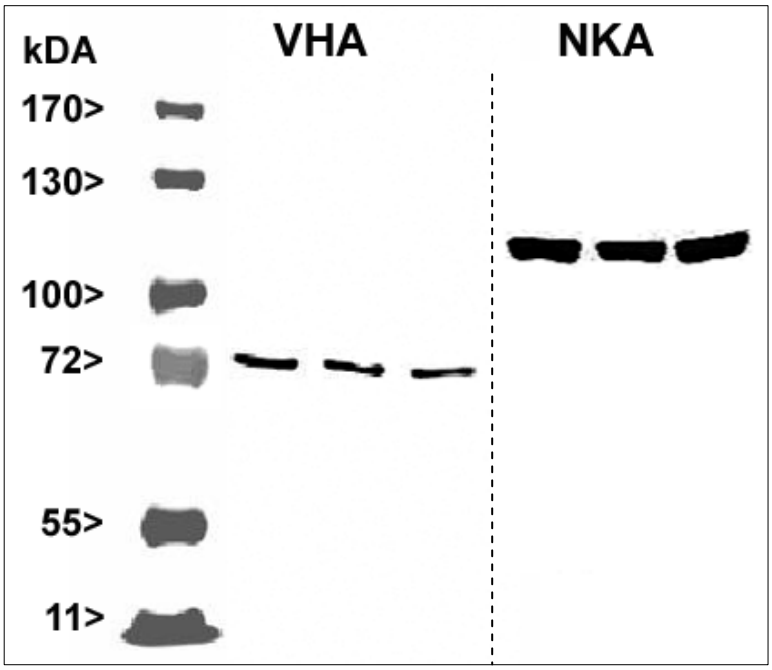

Figure 5. 6 Western blot analysis in gill homogenates from *C. granulatus* using antibodies against V-H^+-ATPase (VHA) and Na^+-K^+-ATPase (NKA). Three independent gill samples are shown for each antibody. Blots incubated with secondary antibody alone did not show any signal. The dotted line indicates that VHA and NKA antibodies were tested in different blots, and the images were merged for this figure.

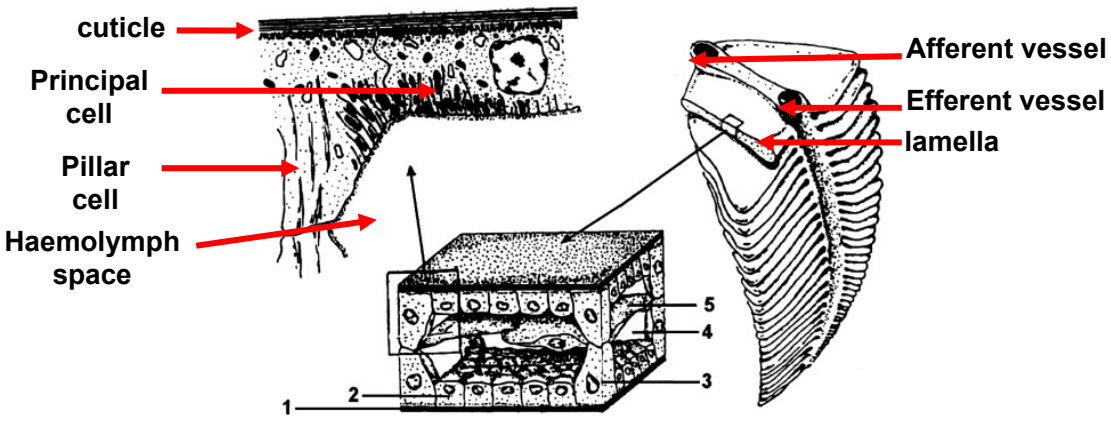

Figure 5.7 Diagram of the gill morphology of *N. granulata*.

Both principal and pillar cells are indicated to assist in the interpretation of the following figure immunohistochemistry. This figure is modified from previous publications (Freire et al., 2008; Onken and Riestenpatt, 1998).

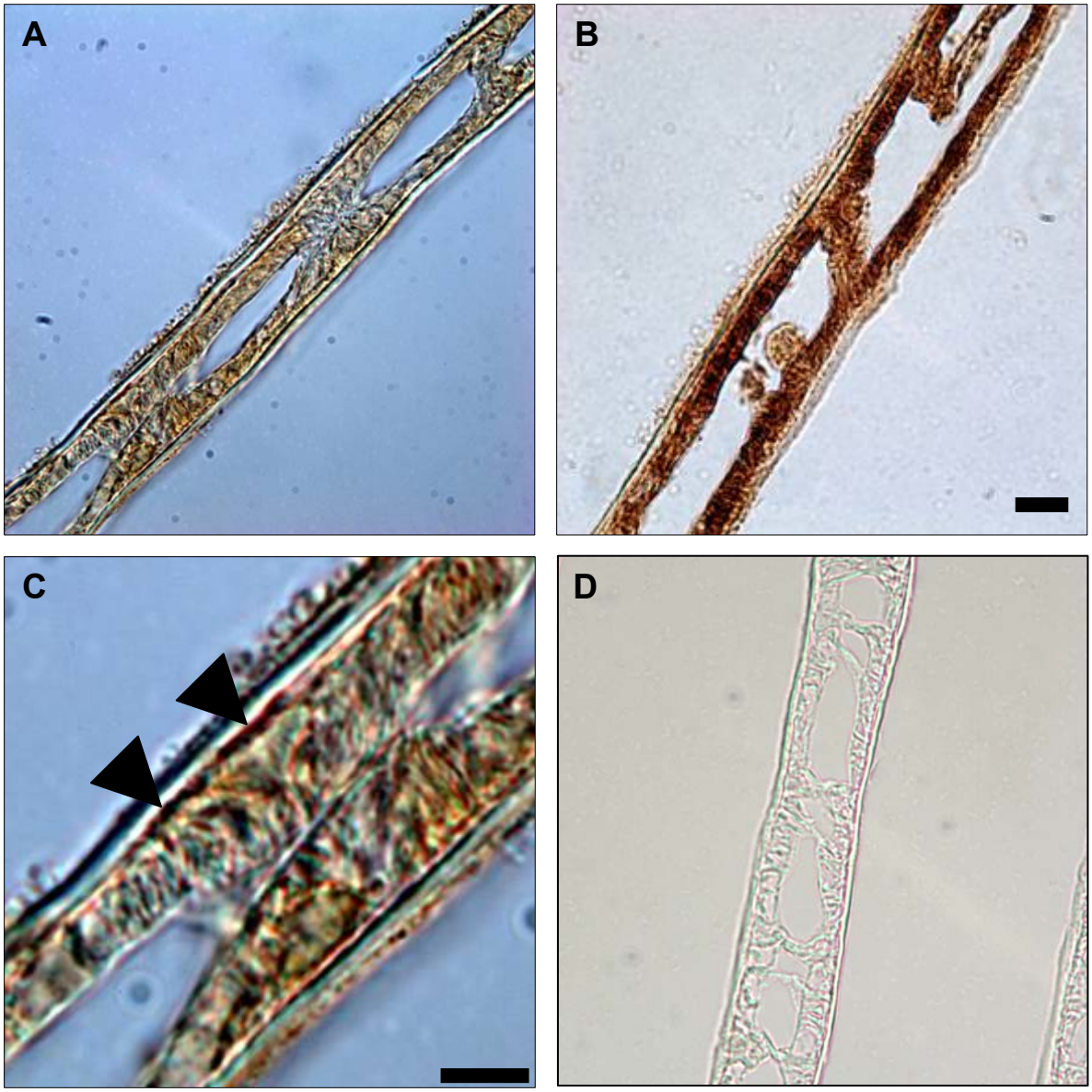

Figure 5. 7 Immunohistochemistry of VHA and NKA in the gills of C. granulatus.

VHA (***A*** and ***C***) and Na^+-K^+-ATPase (***B***) immunolocalization in gills of *C. granulatus*. Apical V-H^+-ATPase labeling is indicated with arrowheads in ***C***. Control image lacking primary Ab is shown in ***D***. Scale bars = 10 µm (***A***, ***B, and D***) and 5 µm (***C***).

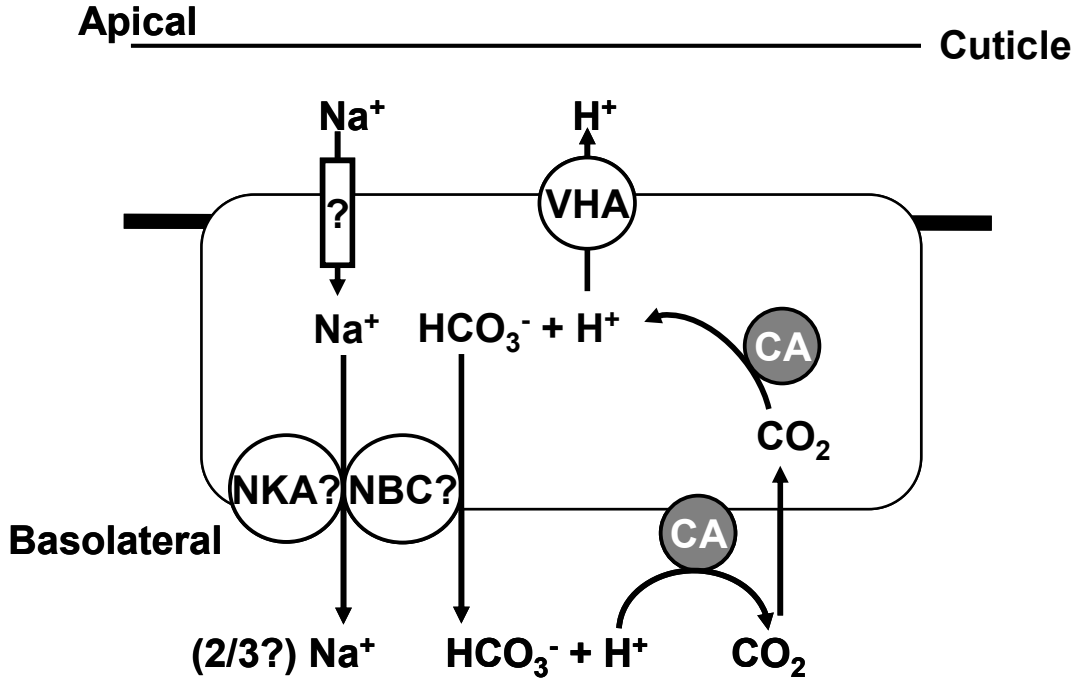

Figure 5. 8 Proposed model for acid secretion in the gill epithelium of *Neohelice granulata* in response to low pH stimulation of V_{te}.
Mitochondria-produced CO_2 might be an additional source of substrate for CA (see text). The molecular identity and exact stoichiometry of the transporters is unknown, and a question mark (?) indicates that no direct evidence exists for the involvement of the transporter. This model is based on the results from the current data chapter complemented by previous studies in this crab (Luquet and Ansaldo, 1997; Luquet et al., 2002b; Onken et al., 2003; Towle and Weihrauch, 2001), other aquatic organisms (chapter 4 and (Parks et al., 2007b), and appendix I. CA, carbonic anhydrase; NBC, Na^+/HCO_3^- cotransporter; NKA, Na^+-K^+-ATPase; VHA, V-type H^+-ATPase.

Chapter VI: Cloning of ASIC4.2 in zebrafish and trout: implications for a role in gill Na^+ transport

Introduction

As discussed in the introduction and chapters II and IV, the molecular identity of an apical Na^+ channel in FW fish is lacking despite a great deal of effort in this regard. The epithelial Na^+ channel (ENaC) has been a target for cloning of the purported method of Na^+ transport in FW fish based on the well-established role of ENaC in transepithelial Na^+ uptake in the FW frog skin MR cell (Ehrenfeld and Garcia-Romeu, 1977; Ehrenfeld et al., 1985). In frog skin, Na^+ transport *via* an ENaC occurs in conjunction with an apical VHA and the same mechanism has been hypothesized for FW fish gill MR cells (Avella and Bornancin, 1989; Boisen et al., 2003; Bury and Wood, 1999; Fenwick et al., 1999; Grosell and Wood, 2002; Lin et al., 1994; Lin and Randall, 1993; Reid et al., 2003). While ENaC has been cloned from a diverse range of animals spanning single cell organisms to mammals (Alvarez de la Rosa et al., 2000) there do not appear to be any homologous ENaC sequences (in any of the 3 subunits) in the genomes of fish species sequenced and published to date.

Regardless, we know that some fish possess distinct Na^+ transport mechanisms that are amiloride and phenamil sensitive and are, in some way, linked to the activity of a V^+- ATPase (Boisen et al., 2003; Bury and Wood, 1999; Fenwick et al., 1999; Grosell and Wood, 2002). Therefore, in this chapter I will provide preliminary experimental evidence resulting from my attempts at identifying the molecular identity of an apical Na^+ channel in FW fishes.

It was hypothesized that one potential explanation for the lack of ENaC expression in fish is that FW fish express a Na^+ channel of different molecular identity than that of other typical Na^+ transporting epithelia. A candidate gene of interest is the family of acid-sensing ion channels (ASICs). ASICs are members of the ENaC/Deg family of ion channels and consist of Na^+ conducting channels that are for the most part activated in response to an extracellular acidosis (Alvarez de la Rosa et al., 2000; Paukert et al., 2004). ASICs are primarily expressed in neuronal tissues and are a major research topic for their role in pain sensation (for review see (Wemmie et al., 2006)). In zebrafish, six different isoforms of ASICs have been cloned with differential expression patterns throughout the fish (Paukert et al., 2004). Interestingly, it has been reported that ASIC expression patterns were apparently investigated at the gill via RNA *in-situ* analysis (Hwang and Lee, 2007). Although the search appeared to be unsuccessful, it is only mentioned as a single sentence in a review article and a detailed analysis of ASIC function at the gill is lacking.

ASIC4.2 was a favourable target for a number of reasons. Although it belongs to the ASIC family, it is actually insensitive to extracellular H^+ yet displays amiloride sensitivity (Chen et al., 2007). Moreover, it shares a reasonable homology with ENaC subunits (i.e. 47% positive identity with human ENaC alpha subunit) and it is the earliest ASIC isoform expressed during development (Paukert et al., 2004). Based on the fact that I cloned ASIC 4.2 from the gills of zebrafish and trout (and not neuronal tissue) I

decided to further investigate the potential role of the ASIC 4.2 isoform as the potential Na^+ channel in fish gill.

Summary of methodological approach

To investigate the molecular identity of a Na^+ channel for use in ion uptake I performed various blast searches of ENaC subunits to the zebrafish database. Primers designed against an unknown clone in the database from kidney revealed a match to ASIC4.2 in zebrafish gill. I proceeded to demonstrate the presence of this channel in trout gill tissue and isolated MR and PV cells. Initial attempts to assess the role of this channel in ion uptake were performed with low Na^+ exposures in zebrafish followed by semi-quantitative and quantitative PCR. Localization of ASIC4.2 in larval zebrafish was also attempted via in-situ hybridization.

Results

Cloning of Zebrafish (zf) ASIC 4.2

Using the protein sequence of the alpha subunit of mammalian ENaC, I performed a blast search of the zebrafish EST database. A candidate protein of unknown identity was found from kidney tissue that exhibited a 49% positive identity with αENaC (GenBank: CK238032.1). Various primers were designed against this unknown clone from kidney and PCR was performed on zebrafish gill cDNA. A band of ~500 bp was amplified using the primer set FWD (TTC CGC CCA AGA GCC GTA AAG) and RVS (GGA TGA AGC CCG ACA GTT) in agreement with the predicted size of 477 bp for this primer set (Fig. 6.1a).

The band was excised from the gel and purified, cloned into pJET 1.2 cloning vector, checked by colony PCR and sequenced as described in the methods section. Translation of the open reading frame revealed a nearly 100% sequence homology with the previously cloned zf ASIC 4.2 (Chen et al., 2007; Paukert et al., 2004) (See Fig. 6.2 for alignment of zf contig, trout contig, and ZF known ASIC 4.2 sequence). RT PCR demonstrated expression of this gene in adult gill, spleen, kidney, liver, heart, and brain along with 12, 24, and 48 hour post fertilization embryos.

Semi-quantitative PCR

To investigate whether this gene was important in gill ion uptake, I first performed a preliminary semi-quantitative PCR experiment. Wild type adult

zebrafish were removed from a high Na^+ environment (~12mM) and placed in a low Na^+ environment (~500 μM) to follow acclimation over a seven-day period. Fish were removed at 6h, 24h, 4d, and 7d following transfer to low Na^+ and total RNA was extracted from gill tissue. All of the gills were required from each fish to achieve sufficient RNA extraction, which decreased my expected number of replicates from each time point. Semi-quantitative PCR was performed on cDNA from the various time points with samples being removed at 22, 24, 26, 28, and 30 cycles and equal amounts of PCR product were separated out on an agarose gel (Fig 6.3a). These preliminary results indicated a time dependent increase in gene expression of ASIC4.2 following exposure to low environmental Na^+ conditions. Low expression was noted at 6h and a steady increase occurred with an apparent peak of expression at 4d and 7d post exposure. However, the control sample was obtained by taking fish reared in chronic high Na^+ control water, and this sample also had a high level of expression. These results were compared to the same semi-quantitative PCR analysis of β-actin gene expression, which did not indicate any noticeable changes in expression between treatments (Fig 6.3b). These results indicated that ASIC4.2 expression is altered during an ion challenge which prompted the use of more quantitatively reliable techniques.

Real Time Quantitative PCR (Q-PCR)

A new protocol was set up to obtain gill cDNA for Q-PCR analysis. Zebrafish were placed into two separate black tanks (42 fish in each tank) in "high" Na^+ water (~12mM). The water was not in a flow through system but

was continuously aerated and replaced each day as fish were acclimated to these conditions for 7 days. Fish were fed daily during the acclimation period up to 1 day before the start of the experiment and then starved for the course of the low Na^+ exposure. Gill samples were removed at t=0h to serve as a control. One tank was then changed over to City of Edmonton tapwater (~500 μM Na^+) while the other tank was replaced again as before with the "high" Na^+ water. Water Na^+ levels were confirmed *via* atomic absorption spectrometry. Samples were removed from both tanks at 6h, 24h, and 4d. One sample or "n" consisted of all the gills from 3 different fish and 12 fish were removed at each time point for an n=4. It is important to note that unfortunately, the "high" Na^+ water was ~pH 7.10 while the low Na^+ tapwater was ~pH 8.30. I was unable to alter this as the pH difference was noticed at t=6h when the experiment was already underway.

Primers for Q-PCR were designed with software linked to the ABI Q-PCR machine. 4 different primer sets were designed for ASIC4.2, 2 for elongation factor 1 α, and 2 for ribosomal L8. Regular RT-PCR was performed for each primer set and a predicted product of 75 bp was present for all but one of the primer sets (Fig 6.4). Q-PCR primer validation indicated that primers for ASIC4.2 (**FWD**: ACC AAA TCA TCA CAA TGC ACA AC **RVS**: AAT GAA CAG ACA GAG GTC GTC CTT) and elongation factor 1 α (**FWD**: TCC CAA CCT CTT GGA ATT TCT C **RVS**: CCG ATG GGT TTT AAT CAG CAT T) were valid for ddCt analysis.

Q-PCR revealed a steady increase in gene expression in response to low Na^+ acclimation over the 4 days of exposure (Fig. 6.5). Interestingly, there was also a rapid increase zf ASIC4.2 gene expression in the High Na^+ group by 24h that was maintained at 4 days. No statistical differences were noted between groups.

In-situ hybridization of ASIC4.2

The 477 bp ASIC4.2 fragment was re-amplified from gill tissue and inserted into the Topo TA 2.1 vector. After sequencing, selected clones exhibited the inserted fragment in the opposite orientations and two were selected to make the *in-situ* antisense and sense probes. These probes were first applied to 24, 48, and 72 hpf (hours post fertilization) embryos however the coloration reaction was not successful. The technique was re-applied to 72 hpf embryos only. Positive signal appeared in the zebrafish where embryonic ion transport occurs, however, this was also found in the sense strand indicating that the probe was not effective (Fig. 6.6).

Cloning of ASIC4.2 From Trout Gill

My thesis focuses primarily on trout and the mechanisms of Na^+ uptake, therefore I was interested in investigating ASIC4.2 in trout gill. Using the same primer set that was successful in zfASIC4.2, I was able to amplify the same fragment from trout gill tissue, and more importantly, from both isolated MR and PV cells (Fig 6.1b). Sequencing revealed 100% homology to the zfASIC4.2 for this 477bp fragment of the gene (Fig 6.2). This is the first

molecular evidence for ASIC4.2 in trout but time constraints prevented me from pursuing this avenue of research further.

Discussion

The lack of molecular information for an epithelial Na^+ channel in any fish has prevented the confirmation of the apical VHA Na^+ channel model for Na^+ uptake and given credibility to a role for NHEs even in the face of adverse thermodynamic constraints. In this chapter, I pursued the cloning of what was originally thought to be an ENaC homolog in fish. However, this turned out to be a match to the previously described zfASIC4.2 (Chen et al., 2007; Paukert et al., 2004). Regardless, a number of points regarding this Na^+ channel caused me to continue to explore whether there might be a role for ASIC4.2 in apical Na^+ uptake at the FW fish gill. These included a lack of pH sensitivity, amiloride sensitivity, robust expression on the cell surface, and the fact that it is the earliest ASIC to occur during development (Chen et al., 2007; Paukert et al., 2004). These unique properties of ASIC4.2 compared to other members of the ASIC family indicated a potential for utilization as the apical Na^+ conductance in FW fish gill cells.

Admittedly, this data chapter requires significant further experimentation and refinement (discussed below) to confirm the ASIC4.2 as the apical Na^+ conductance, however, some promising results were discovered. Both semi-quantitative and quantitative PCR demonstrated a change in gene expression in response to a low Na^+ challenge. Q-PCR results were not statistically significant but this was possibly due to confounding variables mentioned below. Regardless, if ASIC4.2 is only a neuronal channel as has been postulated in the early analysis of this family of

transporters, it should be unaffected by changes in environmental ion concentrations. Therefore, the low Na^+ exposures and apparent changes in gene expression of ASIC4.2 indicate a possible biological significance in apical Na^+ uptake and should be pursued further.

Interestingly, the control high Na^+ fish also had a rapid increase in ASIC4.2 gene expression by 24h that remained high at 4 days compared to time zero. This increase actually occurred quicker than the low Na^+ group. A possible explanation for the low Na^+ group having a delay is that the freshwater was of a higher pH. From thermodynamic considerations in chapter II this would favour the use of an NHE instead of a Na^+ channel and therefore reduce the necessity for use of a Na^+ channel. Eventual upregulation by day 4 of ASIC4.2 indicate that it is actually required to ensure Na^+ uptake in low Na^+ environments. For the high Na^+ group, the only change during the experiment was the removal of feeding. A possible explanation for the increase ASIC4.2 expression in this group is that the fish food used (Trout chow) is high in salt content. When this food is ingested on a regular basis by the zebrafish, they absorb enough NaCl through the intestine to maintain the levels required in their plasma (while being maintained in a relatively hard FW of ~12 mM Na^+). This intake of NaCl from the food, coupled with a tight gill epithelium, would not require a great deal of active transport of NaCl at the gill and an NHE could function under these conditions. However, when the food is removed, the zebrafish is then required to obtain the essential salts from the water, leading to an elevation of the Na^+ channel gene expression. If this

hypothesis holds true, it would be rather powerful as it is showing that a Na^+ channel (ASIC4.2) is required for uptake in a freshwater environment even of ~12 mM NaCl. A caution in this diet related prediction and ASIC4.2 expression is that the low Na^+ group also experienced a cessation of feeding and yet their gene expression alteration was delayed compared to the high Na^+ group. This cannot be explained with the limited data set thus far and will need to be explored in the future.

Dietary salt has been shown to influence gill function in previous studies. A high salt diet in rainbow trout caused the conversion of the FW trout gill morphology to a more typical SW morphology (Perry et al., 2006). In addition, a study on the natural diet of salmonids estimated that NaCl uptake from food may potentially exceed uptake from the water across the gills (Smith et al., 1989). It was even suggested that under certain seasonal conditions, dietary salt uptake may temporarily exceed the Na^+ requirements to maintain homeostasis and excretion of excess Na^+ may need to occur. Na^+ loss at the gills was then shown to be responsible for maintaining Na^+ homeostasis in response to high dietary Na^+ (Smith et al., 1995). It was also demonstrated that Na^+ is rapidly absorbed across the gut of rainbow trout (Smith et al., 1995) and that faecal material is low in Na^+ content even in fish fed a high Na^+ diet (Salman and Eddy, 1988). Dietary salt has also been shown to be essential in maintaining ion homeostasis during exposure to chronic acidic environments, a situation that decreases Na^+ and Cl^- uptake at the gill (D'Cruz et al., 1998; D'Cruz and Wood, 1998; Dockray et al., 1996).

Recently, a net absorption of Cl^- and K^+ but not Na^+ was shown following a meal in rainbow trout however the authors speculate that the lack of Na^+ absorption in their study may be due to confounding external and internal ion and pH levels (Bucking and Wood, 2006). The influence of diet on ion homeostasis needs to be carefully considered and controlled for in future studies on ion transport in freshwater fishes, a fact that is not generally discussed in the literature.

(a) Future Directions

These Na^+ challenge experiments need to be repeated with the high Na^+ and low Na^+ water having matching pH values. This will help discount any effect of pH on gene expression for an ASIC compared to an NHE. The best way to perform this would be to acidify a large volume of tap water and set up a re-circulation system. It would also be best to perform these experiments with fed and unfed (and also pre-starved) fish. This suite of experiments should clearly establish the gene expression pattern in response to low environmental Na^+.

Preliminary radiotracer Na^+ uptake experiments were performed on zebrafish with minimal success. The main obstacle was thought to be a lack of access to a gamma counter. However, we have indications that perhaps the zebrafish take up very little Na^+ as we were unable to match the Na^+ uptake results described previously (Boisen et al., 2003). To ensure our experimental set up was functioning properly we performed the same experiments on juvenile rainbow trout and found Na^+ uptake rates that

matched previously reported values. To my understanding, no other publications have reported values to match with the Boisen paper and apparently further experimentation is required in this area. These radio-tracer experiments could be repeated (assuming establishment of proper control Na^+ uptake rates) to compare rates of branchial Na^+ uptake (from the water) in fed and unfed fish. I predict that fed fish will have sufficient levels of NaCl and not require as much Na^+ uptake compared to unfed fish. I also propose to perform these experiments in the presence and absence of phenamil to solidify the pharmacology of the Na^+ channel hypothesis. Zebrafish ASIC4.2 has been expressed in Xenopus oocytes and amiloride was demonstrated to abolish the electrophysiological properties of the channel (Paukert et al., 2004). It is important to repeat these experiments with phenamil to match the importance of ASIC4.2 in whole animal Na^+ uptake experiments. Currently no pharmacological data is available for any of the ASIC family members with respect to phenamil sensitivity.

Localization of ASIC4.2 to the gill epithelium

My preliminary RNA *in-situ* hybridization experiments were unsuccessful for ASIC4.2 in zebrafish. New probes need to be designed of larger size and with attention to exon-intron boundaries to increase the specificity of the probe. It will also be important to determine when maximum gene expression is achieved (see above) and then use fish from those conditions for *in situ* analysis. If these results are promising, I would propose

to perform *in situs* on adult gill sections and develop an antibody to look at protein expression patterns as well.

Interaction with other ion transporting proteins

Pung-Pung Hwang's group have shown molecular evidence for the use of NHE3b and CA15 In response to low environmental Na^+ (Lin et al., 2008; Yan et al., 2007). It would be important to perform Q-PCR on these proteins in addition to ASIC4.2 on the Na^+ experiments described above to get an indication of the relative importance of each under low Na^+ stress. If the molecular information for FW fish CBE becomes available (from the proposed slc26 family) then these genes would be analysed as well for an overall index at the gill.

Kidney Expression of ASIC4.2

This series of experiments was initiated by kidney sequence for ASIC4.2. Therefore, it is possible that it is utilised in kidney for Na^+ re-absorption. Gene expression data in kidney in response to ion stresses would be a more long term goal of this project.

Developmental studies

Gene knockdown of ASIC4.2 in zebrafish using morpholinos combined with the above experiments would solidify if this channel acts as the apical Na^+ conductance in FW fish embryos. In these experiments, survival and Na^+ uptake would be observed in response to gene knockdown. In addition, compensatory changes in NHE3b expression would also be observed. These

experiments could also be done in the low Na^+ experiments to observe importance under stressed and control conditions.

Perspectives

Although this study is still in the preliminary stages, it provides the framework for uncovering the molecular information for the Na^+ conducting channel in FW fish. Confirmation of this channel's role *via* the above mentioned experiments will be a major advance in the comparative physiology field of research.

Figures

A

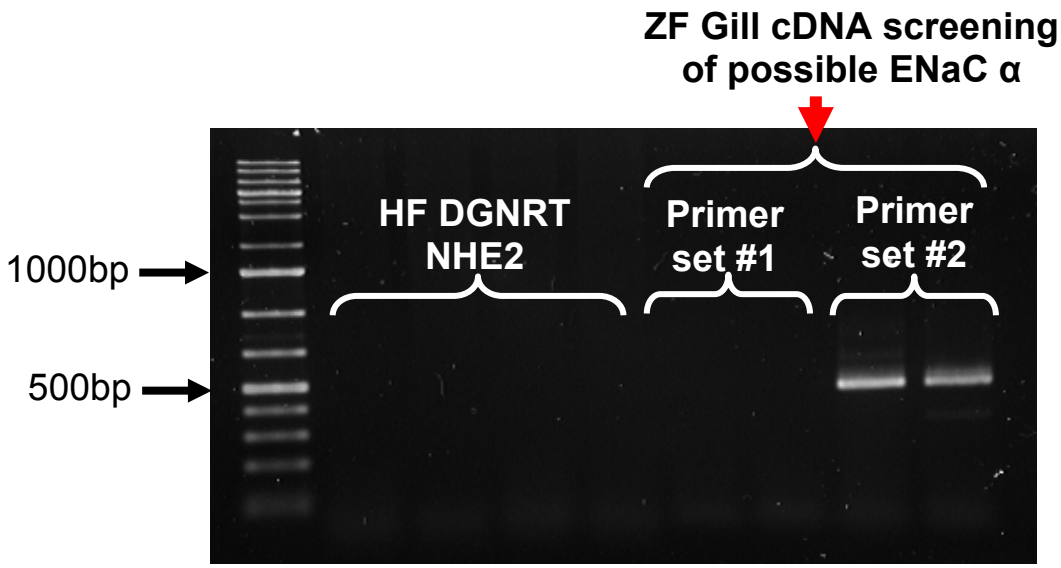

B

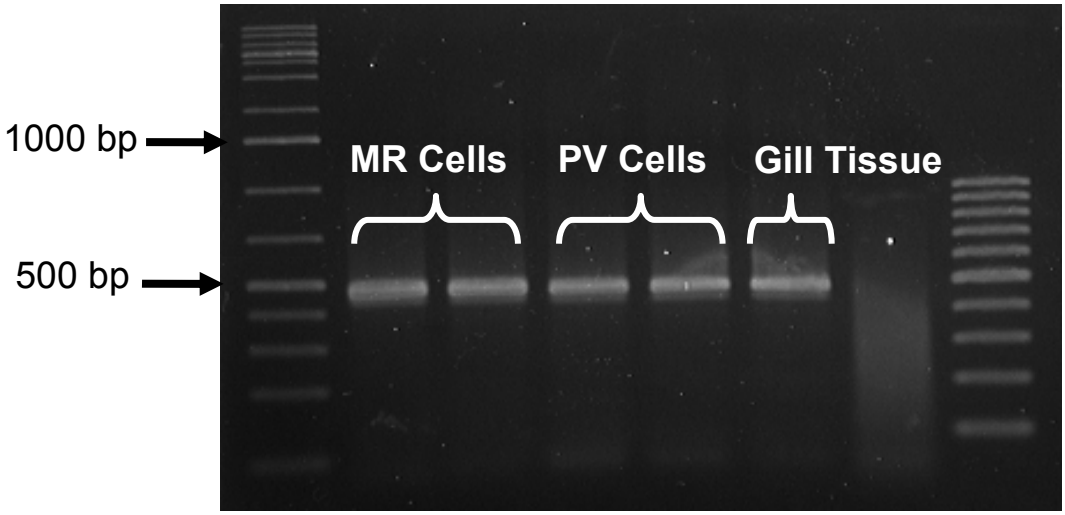

Figure 6. 1 ASIC4.2 RT-PCR results from zebrafish and trout. Representative RT-PCR results from zebrafish (***A***) and trout (***B***). A product of ~500 bp was identified in zebrafish and trout gill and specifically in trout PV and MR cells.

```
                                         110       120       130       140       150
Trout ASIC 4.2 translate#23AC44   -------------------------------------------FPPKSRK    7
ZF ASIC 4 b protein               LAALREETRRELTFPAITLCNVNRFRFSALTDADIYHLANLTGLPPKSRK  150
ZF Contig 1 Protein               --------------------------------------------PPKSRK    6

Majority                          GHRPSELQYPPPNMLDIFQRTGHQLEDMLKSCNFSGQNCSSEDFSVVYTR
                                         160       170       180       190       200
Trout ASIC 4.2 translate#23AC44   GHRPSELQYPPPNMLDIFQRTGHQLEDMLKSCNFSGQNCSSEDFSVVYTR   57
ZF ASIC 4 b protein               GHRPSELQYPPPNMLDIFQRTGHQLEDMLKSCNFSGQNCSSEDFSVVYTR  200
ZF Contig 1 Protein               GHRPSELQYPPPNMLDIFQRTGHQLEDMLKSCNFSGQNCSSEDFSVVYTR   56

Majority                          YGKCYTFNGNKTSPKRVRQGGTGNGLEMMLDIQQDEYLPIWRETNETTLE
                                         210       220       230       240       250
Trout ASIC 4.2 translate#23AC44   YGKCYTFNGNKTSPKRVRQGGTGNGLEMMLDIQQDEYLPIWRETNETTLE  107
ZF ASIC 4 b protein               YGKCYTFNGNKTSPKRVRQGGTGNGLEMMLDIQQDEYLPIWRETNETTLE  250
ZF Contig 1 Protein               YGKCYTFNGNKTSPKRVRQGGTGNGLEMMLDIQQDEYLPIWRETNETTLE  106

Majority                          AGIRVQIHTQNEPPYIHQLGFGVSPGFQTFVSCQEQRLTYLPQPWGNCRA
                                         260       270       280       290       300
Trout ASIC 4.2 translate#23AC44   AGIRVQIHTQNEPPYIHQLGFGVSPGFQTFVSCQEQRLTYLPQPWGNCRA  157
ZF ASIC 4 b protein               AGIRVQIHSQNEPPYIHQLGFGVSPGFQTFVSCQEQRLTYLPQPWGNCRA  300
ZF Contig 1 Protein               AGIRVQIHTQNEPPYIHQLGFGVSPGFQTFVSCQEQRLTYLPQPWGNCRA  156

Majority                          SS------------------------------------------------
                                         310       320       330       340       350
Trout ASIC 4.2 translate#23AC44   SS                                                  159
ZF ASIC 4 b protein               SSEPVIPGYDTYSVSACRLHCESTQVQRECNCRMVHMPGDADICAPSKIK  350
ZF Contig 1 Protein               SS                                                  158
```

Figure 6. 2 ASIC4.2 sequence

Amino-acid sequence alignment for the open reading frame of the cloned trout (top line) and zebrafish (bottom line) ASIC from this study compared to the published ASIC4.2 zebrafish sequence (middle line: Reference sequence NP_999951.1). Yellow shaded regions indicate identical amino acids between all three sequences.

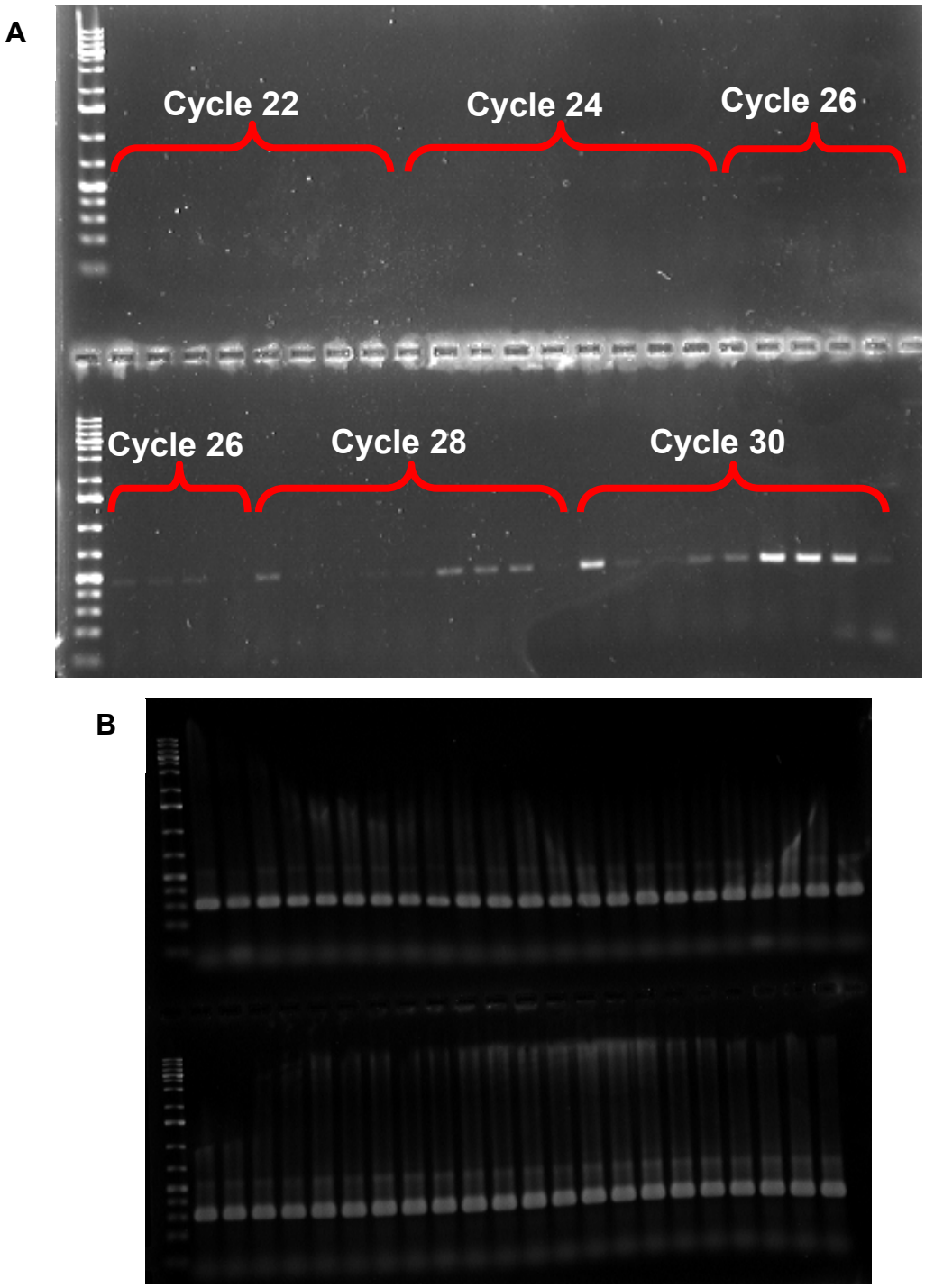

Figure 6. 3 Semi-quantitative PCR results for the time course exposure of zebrafish to low environmental Na^+.
Samples were loaded in the following order: 1 Control chronic high Na^+, 2 6h low Na^+, 2 24h low Na^+, 1 4d low Na^+, 2 7d low Na^+, 1 chronic low Na^+. PCR cycle numbers are indicated above respective bands on the gel. Changes in gene expression were indicated for ASIC4.2 (**A**) but not for β-actin (**B**).

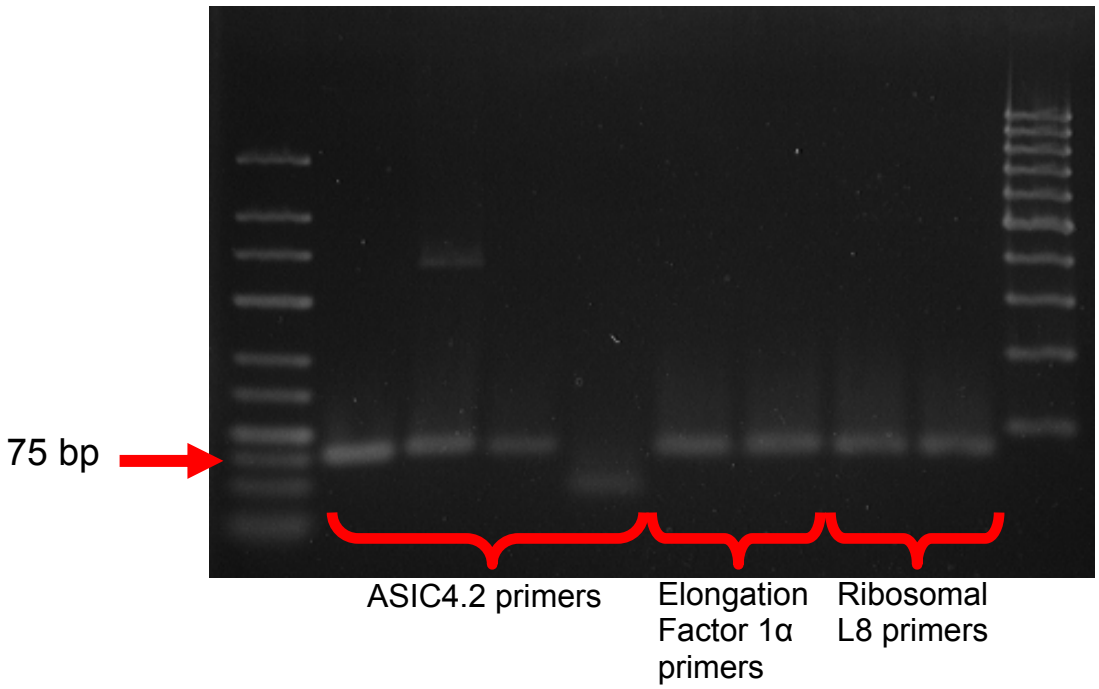

Figure 6. 4 Primer validation for Q-PCR analysis

RT-PCR revealed a predicted product size of ~75bp in zebrafish gill tissue for the designed primer sets.

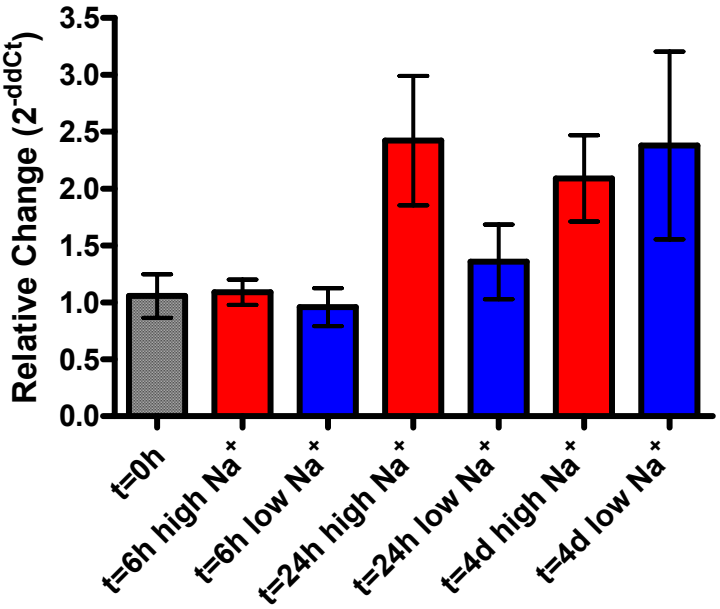

Figure 6. 5 Quantitative PCR analysis of ASIC4.2

Q-PCR results for ASIC4.2 expression in zebrafish gill tissue following exposure to low environmental Na^+. Red bars represent fish left in high Na^+ water (~12mM) while blue bars represent fish exposed to low Na^+ water (~500μM).

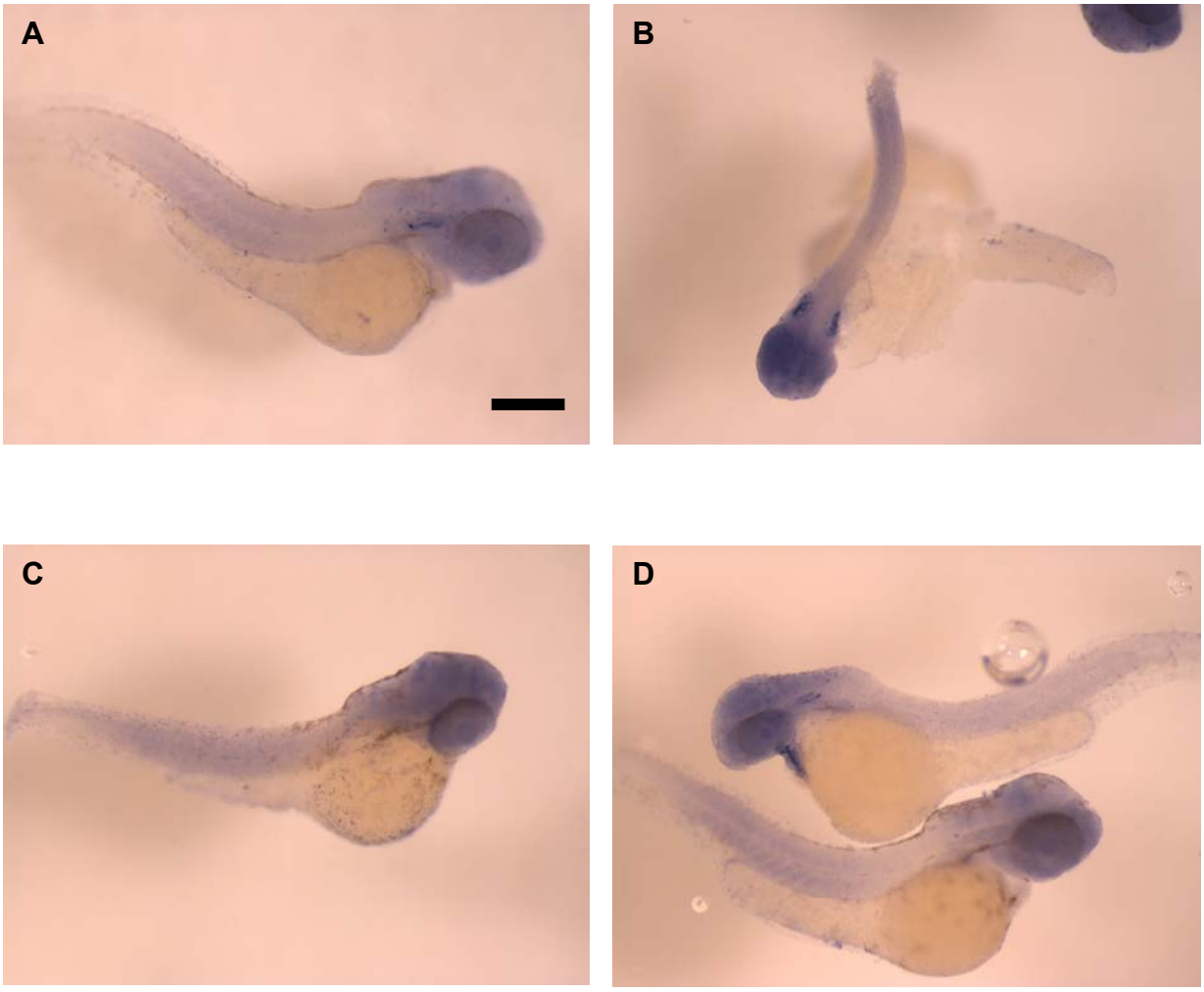

Figure 6. 6 RNA *in-situ* analysis of ASIC4.2 in zebrafish embryos.
Representative images demonstrating that both antisense (***A, B***) and sense (***C, D***) probes displayed similar patterns of staining indicating that this probe was ineffective. Scale bar is equivalent to 20 μm.

Chapter VII: Cellular mechanisms of Cl^- transport in trout gill mitochondrion-rich (MR) cells[1]

[1]A version of this chapter has been published previously.

Parks, S. K., Tresguerres, and Goss, G. G. (2009) Cellular mechanisms of Cl^- transport in trout gill mitochondrion-rich (MR) cells. *American Journal of Physiology-Regulatory Integrative and Comparative Physiology*. 296: R1161 - R1169.

Introduction

Freshwater fish continually face an ionic stress due to large volumes of dilute water that pass over their gill epithelium. This is compounded by an acid-base disturbance as the mechanisms of ion and acid-base transport are linked at the gill. The fish maintains homeostasis by active transport at specialized mitochondrion-rich (MR) cells on the gill surface. Consequently, the freshwater gill has been an important model system in understanding the transport mechanisms that enable overcoming of unfavorable ion gradients. In the past decade numerous studies have utilized a variety of techniques to elucidate the mechanisms of ion and acid-base transport in freshwater fishes (Chang and Hwang, 2004; Evans, 2008; Galvez et al., 2002; Georgalis et al., 2006; Goss et al., 2001a; Hiroi et al., 2008; Horng et al., 2007; Hwang and Lee, 2007; Ivanis et al., 2008b; Katoh et al., 2008; Lin et al., 2006; Lin and Hwang, 2004; Lin et al., 2008; Parks et al., 2007b; Perry, 1997; Perry et al., 2003a; Perry and Gilmour, 2006; Reid et al., 2003; Tresguerres et al., 2006a; Yan et al., 2007), which we have reviewed recently in our lab (Parks et al., 2008; Tresguerres et al., 2006a). However, both general traits and specific details about the cellular and molecular mechanisms remain largely unknown.

Two distinct subpopulations of MR cells have been characterized at the trout gill based on their ability to bind peanut lectin agglutinin (PNA) and termed PNA^- and PNA^+ MR cells (Galvez et al., 2002; Goss et al., 2001a; Reid et al., 2003). PNA^+ cells were proposed to carry Cl^-/HCO_3^- exchange (Galvez et al., 2002) and PNA^- cells have been implicated in Na^+ uptake and

H^+ secretion (Parks et al., 2007b; Reid et al., 2003). However, a recent study has suggested that the division of functions between trout MR cell subtypes may not be that clear cut (Ivanis et al., 2008b). In addition, a detailed immuncytochemical study on Mozambique tilapia has proposed that as many as four MR cell subtypes may exist at the gill (Hiroi et al., 2008) and it suggested that apical Na^+/Cl^- cotransporters (NCC) may constitute a previously unappreciated way of ion uptake in freshwater fish (Hiroi et al., 2008). In most freshwater fishes examined, the bulk of apical chloride uptake supposedly occurs via a Cl^-/HCO_3^- exchanger (CBE) (Goss and Wood, 1991; Kerstetter and Kirschner, 1972; Krogh, 1939; Maetz and Garcia-Romeu, 1964) which has been demonstrated to be SITS and DIDS sensitive in whole animal experiments (Chang and Hwang, 2004; Perry and Randall, 1981). Based on immunoreactivity in the Atlantic stingray (***Dasyatis sabina***) gill, the CBE appears to be a member of the SLC26 family (Piermarini et al., 2002), but direct evidence is lacking for the teleost gill.

At the basolateral membrane, part of the Na^+ exits to the blood via the Na^+/K^+-ATPase (for review see (Evans et al., 2005)). Using intracellular pH (pH_i) imaging in isolated gill cells, I have experimentally determined that a basolateral electrogenic Na^+/HCO_3^- cotransporter (NBC) is also involved in transepithelial Na^+ transport (chapter 4; (Parks et al., 2007b)). However, basolateral Cl^- transport in the MR cells from freshwater fish has received much less attention. The prevailing hypothesis is that Cl^- moves through basolateral channels driven by the blood-positive electrochemical potential.

Support for this model is found in immunostaining at the basolateral membrane of MR and pavement cells in the opercular epithelium of freshwater killifish (Marshall et al., 2002). In addition, a current consistent with a maxi-Cl^- channel was described in cultured gill cells of rainbow trout and postulated to transport Cl^- across the basolateral membrane (O'Donnell et al., 2001). Finally, expression of a CLC-3-like protein (a member of the CLC chloride channel family) has been shown to be greater in the gills of freshwater acclimated pufferfish compared to seawater acclimated animals (Tang and Lee, 2007a). The CLC-3-like protein was proposed to be located at the basolateral membrane and involved in transepithelial Cl^- uptake while a CBE on the basolateral membrane would be involved in intracellular acid/base regulation (Tang and Lee, 2007a; Tang and Lee, 2007b).

The goal of this chapter was to examine potentials routes for Cl^- movement in isolated freshwater trout gill MR cells. I have monitored their intracellular pH (pH_i) behavior in real time in response to Cl^- substitution and present evidence directly demonstrating the presence of a Cl^-/HCO_3^- exchangers in two functionally distinct MR cell subtypes. I have also found a peculiar acidification event following Cl^- removal which is attributed to a Cl^- dependent Na^+/H^+ exchanger mechanism. These results are discussed in the context of an overall mechanism for transepithelial Cl^- uptake at the freshwater fish gill along with regulation of pH.

Summary of methodological approach

To investigate the mechanisms of Cl^- transport in trout gill MR cells, I used the intracellular pH (pH_i) imaging technique of isolated cells as described for chapter IV. Functional separation of MR cell subtypes was performed via Na^+ substitution experiments followed by exposure to Cl^--free conditions. Further experiments were performed with Cl^- manipulations alone along with pharmacological blocking agents and removal of HCO_3^- from the solutions to investigate the presence of Cl^-/HCO_3^- exchangers. Cl^- induced acidification was investigated with pharmacological blocking agents for the Cl^- dependent NHE. The Na^+ induced alkalinization was also exposed to a variety of pharmacological blocking agents. Lastly, I addressed the issue of a loss in cellular polarity following isolation by examining the morphology of isolated cells via scanning electron microscopy.

Results

SEM of isolated MR cells

A main criticism associated with studying ion transport mechanisms in isolated cells is the potential loss of polarity, mainly because epithelial cells are specialized for vectorial transport. Results from a previous study suggest that cell polarity was maintained after isolation (chapter 4 (Parks et al., 2007b)) since coupling between apical and basolateral processes following isolation was demonstrated. However, maintenance of cell polarity following isolation has not been directly established. In Figure 7.1, I demonstrate that the morphology of isolated trout gill MR cells clearly maintain an apparent polarity as seen under SEM. Some isolated cells demonstrated a clear polarity where one surface displayed fingerlike projections while the opposite pole displayed a wavy, fold-like appearance suggesting apical and basolateral membranes respectively (Figures 7.1 a, b). In the same preparation, I also include a picture of a contaminating pavement cell (PVC) in my MR cell population indicating that the distinct microridges characteristic of PVCs can be maintained in isolation as well (Figure 7.1 c). Previously published SEM images (Greco et al., 1996) of intact trout gill epithelia are provided (Figure 7.1 d and e) to assist the reader in comparing the isolated cell SEM to that found in an intact gill.

Pharmacological profile of Na^+ induced alkalinization event

A functional separation of trout gill MR cell subtypes based on their response to Na^+ substitution experiments was demonstrated previously in chapter IV (Parks et al., 2007b). Cells responded either with an acidification or alkalinization when switched from Na^+ containing medium to Na^+ free medium (Parks et al., 2007b). In that chapter, it was shown that the Na^+ induced acidification was due to the interaction of transporters in the apical and basolateral membrane where Na^+ enters the cell through apical channels and exits via basolateral NBCs; with the exit of HCO_3^- resulting in acidification of the cell. In the current chapter I sought to resolve the transporter involved in the other noted cellular behavior, the Na^+ induced alkalinization. Switching the perifusion solutions from Na^+-free to Na^+-containing resulted in an alkalinization in a subpopulation of cells (as demonstrated previously in chapter IV (Parks et al., 2007b)). Since this manipulation is repeatable, it allowed me to apply various pharmacological inhibitors in specifically identified cells (see Figure 7.2a for a sample trace). The general inhibitors of NHEs (amiloride, 500 μM), Na^+ channels (phenamil, 50 μM), and Na^+/HCO_3^- co-transporter (DIDS, 1mM) had no inhibitory effect on the alkalinization (Figure 7.2c). Similar concentrations of these inhibitors were effective in inhibiting other pH_i regulatory processes in isolated MR cells as shown in chapter IV (Parks et al., 2007b). Furthermore, no effects were observed with inhibitors of either carbonic anhydrase (500 μM acetazolamide) or Na^+/K^+-ATPase (500 μM ouabain, data not shown). However, EIPA (500 μM), which

is a more selective inhibitor of mammalian NHE1 than other NHE isoforms (Masereel et al., 2003) and the Cl^--dependent NHE (Sangan et al., 2002), did have an effect and replaced the alkalinizing behavior by an acidification (Figures 7.2 b, c). The insensitivity to amiloride and other results shown below advocates for a Cl^--dependent NHE.

Cl^- induced alkalinization in two functionally identified MR cell populations

In this series of experiments cells were exposed to Cl^- free medium following identification by Na^+ removal (Figure 7.3) to examine the Cl^- dependent mechanisms in each of the cell types. Both functionally identified MR cell subtypes responded to Cl^- free conditions with an alkalinization of pH_i indicating that a Cl^-/HCO_3^- exchanger was being driven in the reverse direction as Cl^- exited the cell to achieve equilibrium (Figures 7.3 a, c). Summary statistics of the Cl^- free exposure demonstrated a significant alkalinization event in the Na^+ acidified cells (-0.10 ± 0.01 pH units/min in Na^+ compared to 0.18 ± 0.03 pH units/min in Cl^- free) and a greater alkalinization rate (0.27 ± 0.04 pH units/min in Na^+ compared to 0.51 ± 0.07 pH units/min in Cl^- free) in the Na^+ alkalinizing cells (Figures 7.3 b, d).

Inhibition of Cl^- induced alkalinization

Since both functionally (Na^+ substitution) identified MR cell subtypes responded to Cl^- removal with an alkalinization of pH_i, I eliminated the initial Na^+ substitution to focus on the Cl^- dependent mechanisms. However, in this protocol, while some cells still responded to Cl^- free conditions with an

alkalinization, others acidified instead. I first focused on the alkalinization behavior. The Cl^- free induced alkalinization was a repeatable event, enabling comparisons of pH_i recovery rates between controls and treatments within the same cells (Figure 7.4a). In cells demonstrating a Cl^- free induced alkalinization (0.13 ± 0.02 pH units/min), the presence of DIDS, a general inhibitor of Cl^-/HCO_3^- exchangers prevented the Cl^- free induced alkalinization (-0.08 ± 0.02 pH units/min; Figures 7.4b, c).

Since most Cl^- dependent pH regulated transport processes are linked to HCO_3^- transport, I conducted experiments in HCO_3^- free solutions that were continuously aerated with 100% O_2 during the experiments. Equilibration with HCO_3^- free medium was established before testing the effect on Cl^- free pH_i alterations. Similar to the results found with DIDS, removal of HCO_3^- from the extracellular fluid effectively eliminated the Cl^- free induced alkalinization (0.12 ± 0.02 pH units/min) which was replaced with an acidification (-0.21 ± 0.04 pH units/min) (Figure 7.4c). A lack of alkalinization in Cl^- free/HCO_3^- free conditions coupled with DIDS inhibition supports the hypothesis of a Cl^-/HCO_3^- exchange mechanism present in both MR cell populations.

Further support for the presence of a CBE was obtained when cells recovering in Na^+ free media from a Na^+-induced acidosis were then compared to the same manipulation in the presence of 1 mM DIDS (Figure 7.5). Cells showed a consistent pH_i recovery from Na^+-induced acidosis in Na^+ free conditions (0.44 ± 0.06 pH units/min, Figure 7.5a) which was

significantly inhibited by the presence of DIDS (0.15 ± 0.02 pH units/min; Figures 7.5b, c).

Cl^- free conditions induce an acidification of pH_i

As mentioned above, switching from NaCl to Cl^- free solution resulted in a peculiar Cl^- free induced acidification of pH_i in the majority of cells (Figure 7.6a). This event was repeatable and was found to be greater in the absence of extracellular HCO_3^- (Figures 7.6a, b). Moreover, when experiments were performed in the absence of HCO_3^-, I observed the Cl^- free induced acidification in all cells. One possible explanation for this behavior is activation of a Cl^- dependent Na^+/H^+ exchange. This transporter has been cloned from mammalian colon and is suggested to play an important role in both movement of Na^+ across the epithelium and pH_i regulation (Rajendran et al., 1995; Rajendran et al., 1999; Rajendran et al., 2001; Sangan et al., 2002). It has been demonstrated that the Cl^- dependence of the NHE activity is not the result of interactions with a Cl^-/HCO_3^- exchanger but presumed to be due to an association with a Cl^- channel (Rajendran et al., 1999; Rajendran et al., 2001; Sangan et al., 2002). A hallmark feature of the Cl^- dependent NHE is a much greater sensitivity to the NHE inhibitor EIPA than amiloride along with inhibition by the Cl^- channel blocker NPPB. I hypothesized that when subjecting the MR cells to Cl^- free conditions, Cl^- exit from the cell via a Cl^- channel would result in the activation of a Cl^- dependent NHE where Na^+ is brought out of the cell in exchange for external H^+. To test this hypothesis, I tested the effects of NPPB and EIPA in the absence of extracellular HCO_3^-. I

found that NPPB (500 μM), a general inhibitor of Cl^- channels, replaced the Cl^- free induced acidification with an alkalinization (Figures 7.7a, b). I then tested inhibition of the NHE portion of the system. Amiloride (500 μM) or EIPA (100 μM) did not affect the acidification of pH_i caused by Cl^- free conditions (data not shown). However, at higher concentrations of EIPA (500 μM), the acidifying effect of Cl^- free medium was effectively inhibited (Figure 7.7b). These results, together with the EIPA sensitivity of the Na^+-induced alkalinization described earlier, support the presence of a Cl^- dependent NHE in gill MR cells.

Discussion

In this chapter I provide the first direct physiological evidence for Cl^-/HCO_3^- exchange at the fish gill MR cells. My results also indicate a unique intracellular acidification associated to Cl^- exit from the cell and potential linkage with a NHE. These data provide an important step in understanding the complexity of overall transport mechanisms in fish gill MR cells.

A criticism of working with isolated cells from a transporting epithelium is that there is a perceived loss of membrane polarity. I fully recognize this limitation and the difficulty in attributing results from isolated cells to *in vivo* conditions (as also discussed above in chapter IV). My SEM results help to alleviate those concerns, as trout isolated MR cells maintain external morphological polarity similar to that demonstrated for isolated MR cells from mammalian kidney (Schafer et al., 1997) and Japanese eel gill (Wong and Chan, 1999b). However, I am still aware that external morphology does not necessarily correspond to ultrastructure or functional polarity. That the internal ultrastructure, in particular the elaborate tubular system, of gill MR cells can be maintained following isolation has been established early on (Philpott, 1980). More recently (as described in chapter IV), functional apical-basolateral coupling of ion transport processes was demonstrated which suggest the maintenance of functional cell polarity in isolated MR cell populations (Parks et al., 2007b). While a definitive confirmation of polarity in isolated cells awaits more advanced electrophysiological and/or imaging methods, I believe that primary cultures of isolated gill MR cells combined

with real-time pH_i imaging is a robust technique to study ion transport processes.

Cl^-/HCO_3^- exchange in both MR cell populations

Using Na^+ substitution to originally separate MR cell populations, my hypothesis was that by using Cl^- substitution I would uncover Cl^- uptake mechanisms in the Na^+ alkalinizing MR cells. This MR cell population, the PNA^+ MR cells, is proposed to be responsible for transepithelial Cl^- uptake (Galvez et al., 2002; Goss et al., 2001a; Parks et al., 2007b; Tresguerres et al., 2006a). Interestingly I discovered that both functionally identified MR cell populations responded to Cl^- free conditions with an alkalinization of pH_i. Under Cl^- free conditions, the gradients would favor a CBE working in the reverse direction thus bringing HCO_3^- into the cell and resulting in an increase of pH_i. This cellular behavior has been used to demonstrate the presence of a CBE in colonic crypt cells (Ikuma et al., 2003). In my experiments, DIDS and the removal of extracellular HCO_3^- was effective in abolishing the Cl^- free induced alkalinization. Furthermore, DIDS effectively inhibited the Na^+ free pH_i recovery from Na^+ induced acidification. Combined, these results present the first direct cellular evidence for a CBE in freshwater gill MR cells. Given the models that exist for freshwater fish gill, I tentatively propose that this Cl^-/HCO_3^- exchange activity would function on the apical membrane for apical Cl^- uptake in one MR cell (PNA^+) population while performing pH_i regulation at the basolateral membrane in the other MR cell (PNA^-) subtype. Based on previous analysis of the proportion of cells in a mixed MR cell population

responding in a functionally distinct manner (Parks et al., 2007b), these mechanisms would be ascribed to the PNA^+ and PNA^- MR cells respectively. Although I can not definitely assign polarity to these mechanisms, the above discussion is in line with currently accepted models for overall Cl^- transport at the freshwater fish gill (Evans et al., 2005; Hwang and Lee, 2007; Tresguerres et al., 2006a).

The need for consideration of thermodynamic constraints on ion transport in freshwater fishes has been discussed already in this thesis (see Chapter II and IV above and (Parks et al., 2008; Tresguerres et al., 2006a)). Unfavorable gradients exist for the action of an electroneutral CBE. However, consideration of the microenvironments within the cell coupled with the driving force provided by basolateral V-type H^+-ATPase (VHA) provide theoretical support for a CBE functioning in freshwater (Tresguerres et al., 2006a). The results in this chapter further contribute to the presence of a CBE in freshwater gill MR cells.

In fish, CBE was originally proposed almost 80 years ago as a means for Cl^- uptake from the water (Krogh, 1939). While a role for members of the AE family of transporters (SLC4) was extensively researched, no conclusive evidence could be obtained for a role in the fish MR cell. Focus has shifted to investigating members of the Slc26 gene family of anion exchangers which are known to transport a variety of counter-ions including HCO_3^- (Mount and Romero, 2004). Recent work on the euryhaline pufferfish (*Takifugu obscurus,* mefugu) demonstrated the role of Slc26a6A and Slc26a6B for HCO_3^-

secretion in the intestine and the formation of carbonate precipitates (Kurita et al., 2008). Slc26A1 has been cloned from rainbow trout trunk kidney, where it facilitates sulfate secretion (and likely base absorption as well) (Katoh et al., 2006). Although a few abstracts have reported the presence of Slc26a6 based on molecular studies in trout (Goss et al., 2005) and zebrafish gills (Bayaa and Perry, 2005), these results have not been published in the primary literature.

Cl^- free induced acidification

When the initial Na^+ substitution portion of my experiments was removed to focus on the Cl^- free induced alkalinization, I observed an acidification of pH_i in the majority of cells. This had not been observed in my original experiments of Cl^- free exposure following initial Na^+ substitution. This behavior was peculiar in that no obvious predicted mechanisms for an outward flow of Cl^- from the cell would cause an acidification of pH_i. I noted that the rate of acidification in the absence of HCO_3^- was greater than in the presence of HCO_3^- suggesting the contribution of a HCO_3^- import mechanism. Alternatively, the noted increased rate of acidification could result from a reduced cellular buffering capacity as a result of HCO_3^- depletion.

A candidate for the Cl^- free induced acidification is a linkage to a H^+ importing Na^+/H^+ exchanger (NHE). A transporter with this characteristic is the Cl^- dependent Na^+/H^+ exchanger (Cl-NHE) that has been sequenced and characterized in mammalian colonic crypts, where it is responsible for pH_i recovery and overall fluid absorption (Rajendran et al., 1995; Rajendran et al.,

1999; Rajendran et al., 2001; Sangan et al., 2002). Cl-NHE is also expressed in a wide range of epithelial tissues suggesting a role in several transport processes (Sangan et al., 2002) including cellular volume regulation (Goss et al., 2001b). Cl-NHE activity was first described in red blood cells from dogs (Parker, 1983) and has since been also shown in trout red blood cells (Guizouarn and Motais, 1999), barnacle muscle fibers (Davis et al., 1994), and cultured rat mesangial cells (Miyata et al., 2000). The pharmacological profiling from our studies on the Cl^- free induced acidification match that of the Cl-NHE profile (Sangan et al., 2002). Although the mechanism of Cl^- activation for NHE in this protein remains unclear I predict from my data that the extrusion of Cl^- *via* a Cl^- channel results in an activation of a Cl-NHE in reverse mode to import H^+ from solution in exchange for cellular Na^+. Normally, the Cl-NHE acts for H^+ removal from the cell and this is what I would predict would occur in the fish gill MR cells *in vivo* as well. I postulate that both MR cell populations possess a type of Cl-NHE on the basolateral surface since all cells exhibited the Cl^- free acidification when extracellular HCO_3^- was absent. This protein could be utilized for both pH_i and cell volume regulation. The importance in cell volume regulation is particularly attractive for future studies as these MR cells face changing freshwater environments. This is the first suggestion for a Cl-NHE in the gills of any fish species and although I ascribe the Cl^- free acidification to a Cl-NHE based only on pharmacology at this time, it will be the focus of future studies in our lab.

It is peculiar that I only observed the Cl^- free induced acidification when the initial Na^+ free to Na^+ containing substitution was eliminated from the experimental design. I speculate that Na^+ substitution primed both MR cell types to uncover the alkalinizing activity of a CBE. A likely explanation is that the initial Na^+ treatment resulted in cellular Cl^- loading. In the Na^+ alkalinizing cells, a CBE would counteract the alkalinization by exporting HCO_3^- in exchange for Cl^-. When extracellular Cl^- is subsequently removed, Cl^-/HCO_3^- exchange is reversed alkalinizing the cells. In chapter IV I demonstrated that in the other MR cell (PNA^-) population the Na^+ acidification was due to HCO_3^- export *via* a basolateral NBC (Parks et al., 2007b). In this scenario, the cell would be depleted of HCO_3^- and then removal of extracellular Cl^- would create a gradient for a CBE working in reverse mode. The above behaviors would both result in activation of a CBE in reverse mode and account for the observation of Cl^- free pH_i alkalinization.

Na^+ induced alkalinization

My earlier work demonstrated a functional separation of trout gill MR cell subtypes based on Na^+ substitution (Chapter IV). Although the Na^+ induced alkalinization was insensitive to high concentrations of amiloride, it was inhibited by the more specific NHE blocker EIPA suggesting a commonality to the Cl^- free acidification mechanism mentioned above. In light of the recent NHE characterization in ion transporting cells from trout (Ivanis et al., 2008b) and zebrafish (Yan et al., 2007) coupled with the implications

for a Cl-NHE in this study, the in vitro functional and pharmacological characterization of fish NHEs is imperative.

Perspectives and Significance

Here I have presented direct functional evidence for CBE in two populations of MR cells at the freshwater fish gill. The CBE is proposed to play important roles in transepithelial Cl^- uptake and pH_i regulation in the PNA^+ and PNA^- MR cells, respectively. I also describe an interesting Cl^- free acidification of pH_i which leads me to propose the involvement of a Cl-NHE in pH_i regulation in these cells. These results suggest the requirement for an expanded repertoire of membrane transporters at the gill than are realized in the current body of data. Finally, I demonstrate that isolated MR cells can be used as a model system for studying gill transport since cellular polarity is maintained following isolation. These newly described transport mechanisms will form interesting components of future working models for the molecular mechanisms of Cl^- and Na^+ transport at the freshwater fish gill.

Figures

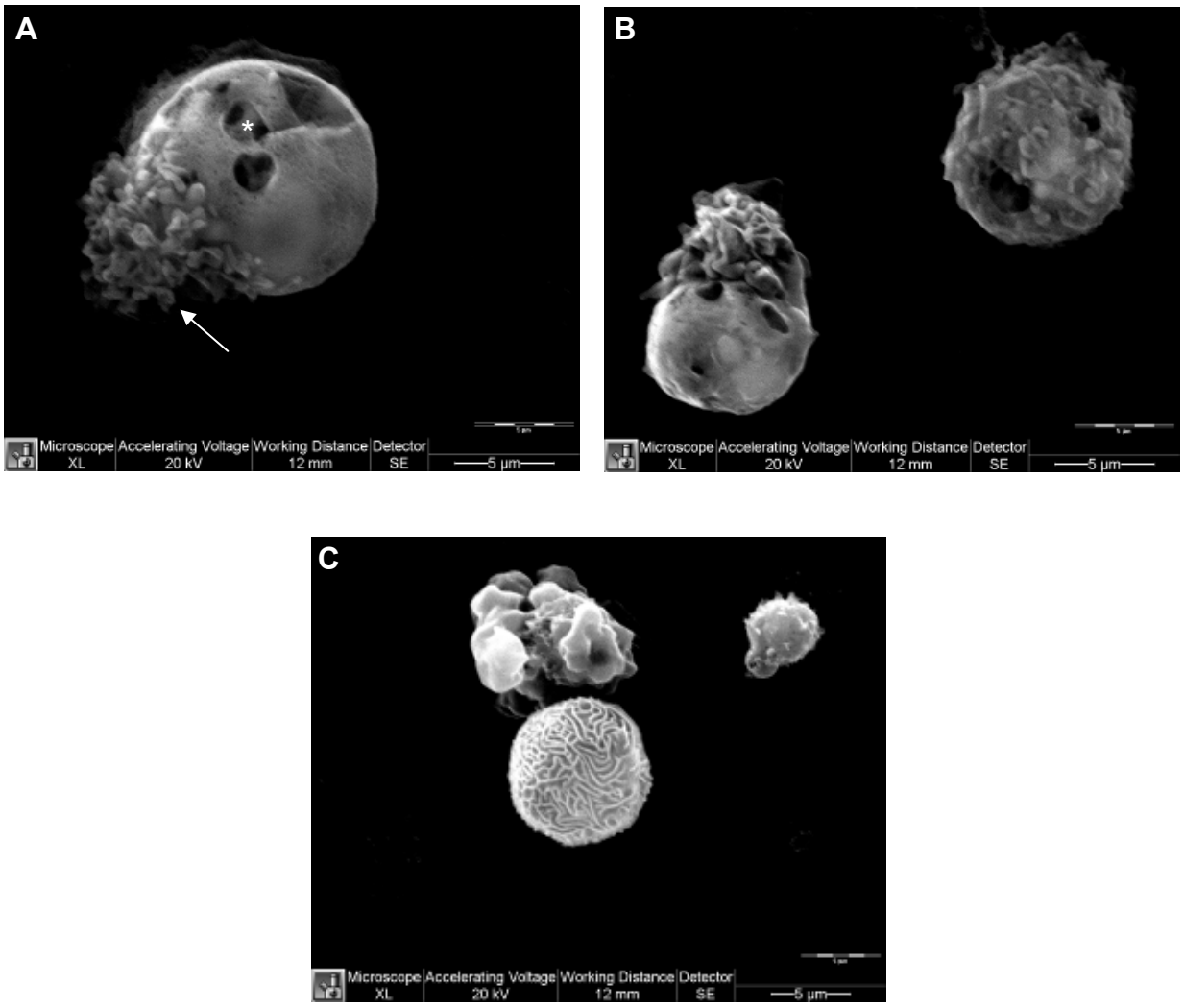

Figure 7. 1 Scanning electron micrographs of isolated MR cells.

A+B Isolated MR cells maintain polarized morphology with fingerlike projections on one pole (see arrow in ***A***) and wavy infoldings on the other pole (see asterisk in ***A***). The top right cell in ***B*** represents a more generalized wavelike appearance over the whole cell perhaps with the opposite pole region being hidden from view as the point of attachment to the coverslip ***C*** A contaminating pavement cell demonstrating that the distinct microridges can be maintained in isolation as well.

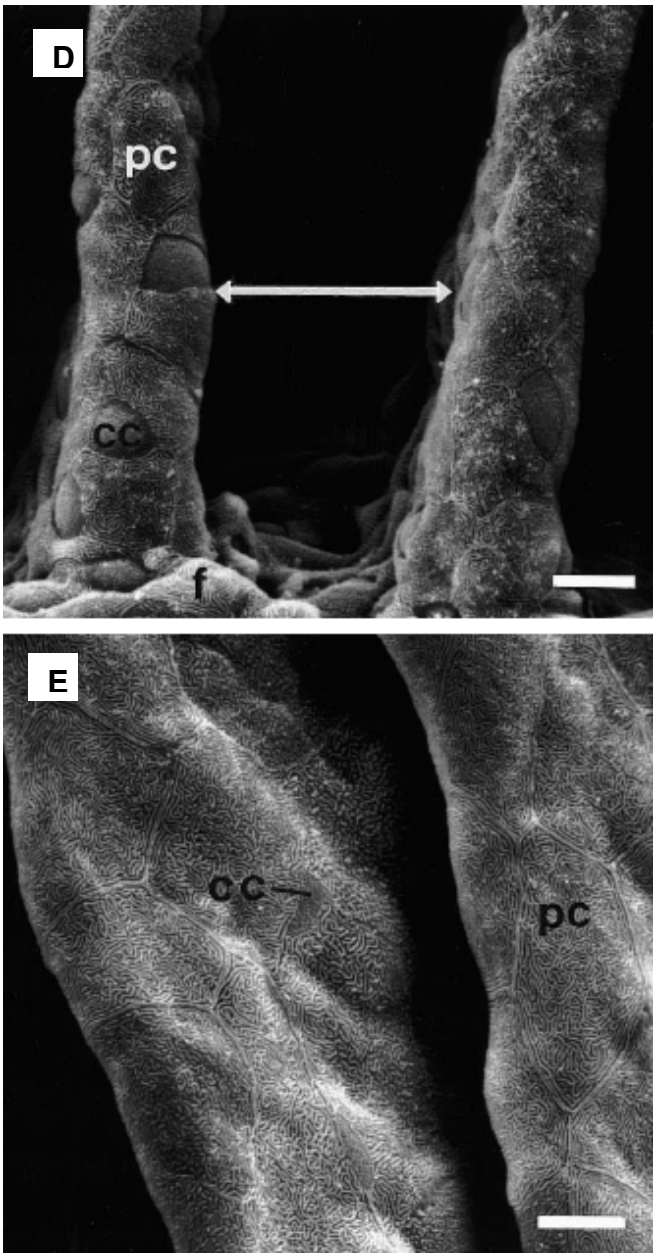

Figure 7.1 continued: Previously published scanning electron micrographs of rainbow trout gill lamellar epithelium (Greco et al., 1996). CC represents mitochondrion-rich cells, pc represents pavement cells, and f refers to the gill filament that the lamellae extend from. Images are provided to assist the reader in identifying the morphology of the isolated cells in Fig 7.1 A-C. Scale bars are 10 μm.

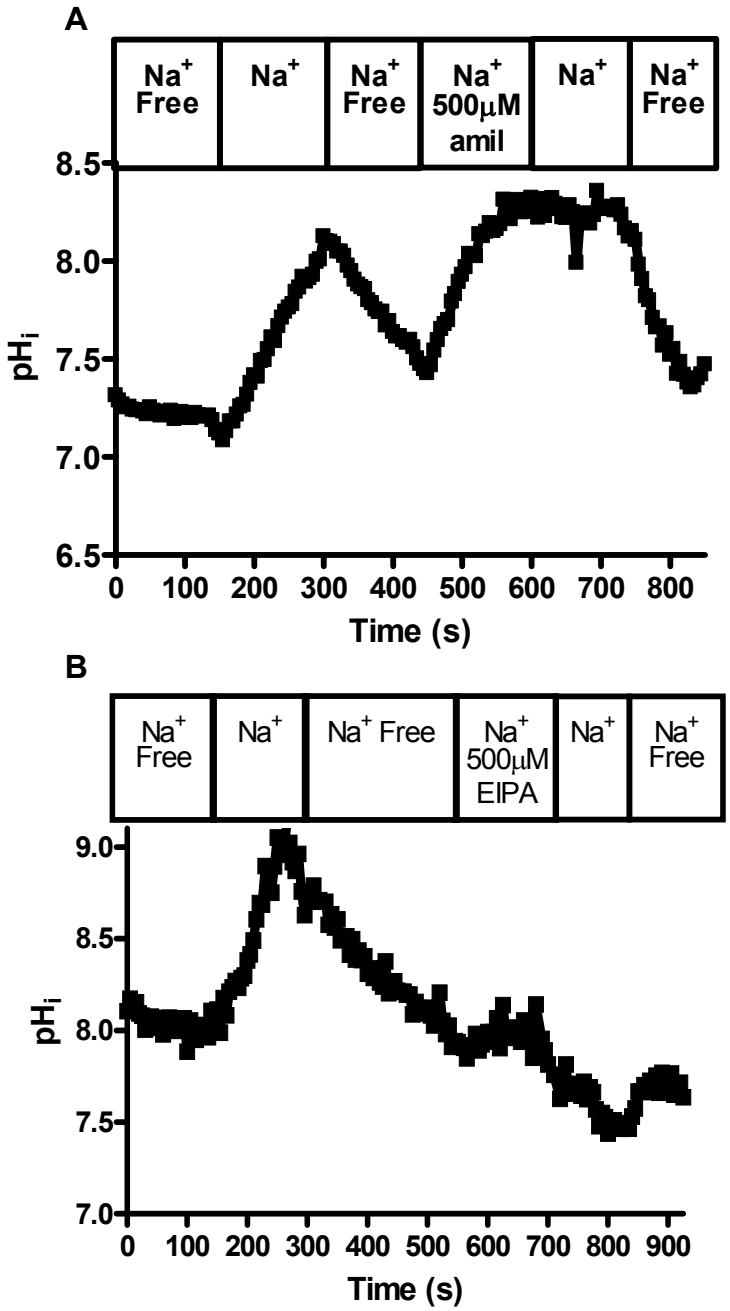

Figure 7. 2 NHE-dependent Na^+ induced alkalinization in one separated population of MR cells as determined via Na^+ substitution.

A Sample trace demonstrating unsuccessful removal of the Na^+ induced alkalinization in the presence of the general NHE inhibitor amiloride. Similar results were observed for the application of phenamil and DIDS (data not shown). ***B*** Sample trace demonstrating effective inhibition of the Na^+ induced alkalinization in the presence of the more selective NHE1 inhibitor EIPA.

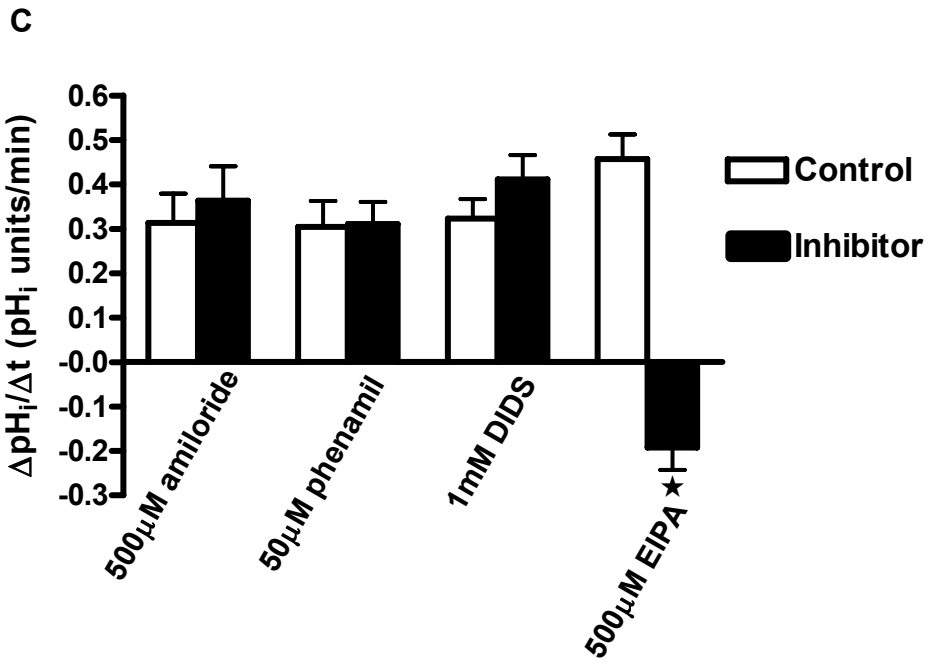

Figure 7.2 continued. ***C*** Summary statistics showing no significant differences between the rates of control Na^+ alkalinization and the rate in the presence of amiloride ($p>0.05$, paired t-test n=22), phenamil ($p>0.05$, paired t-test n=16), or DIDS ($p>0.05$, paired t-test n=17) but removal in the presence of EIPA ($p<0.05$, paired t-test n=32).

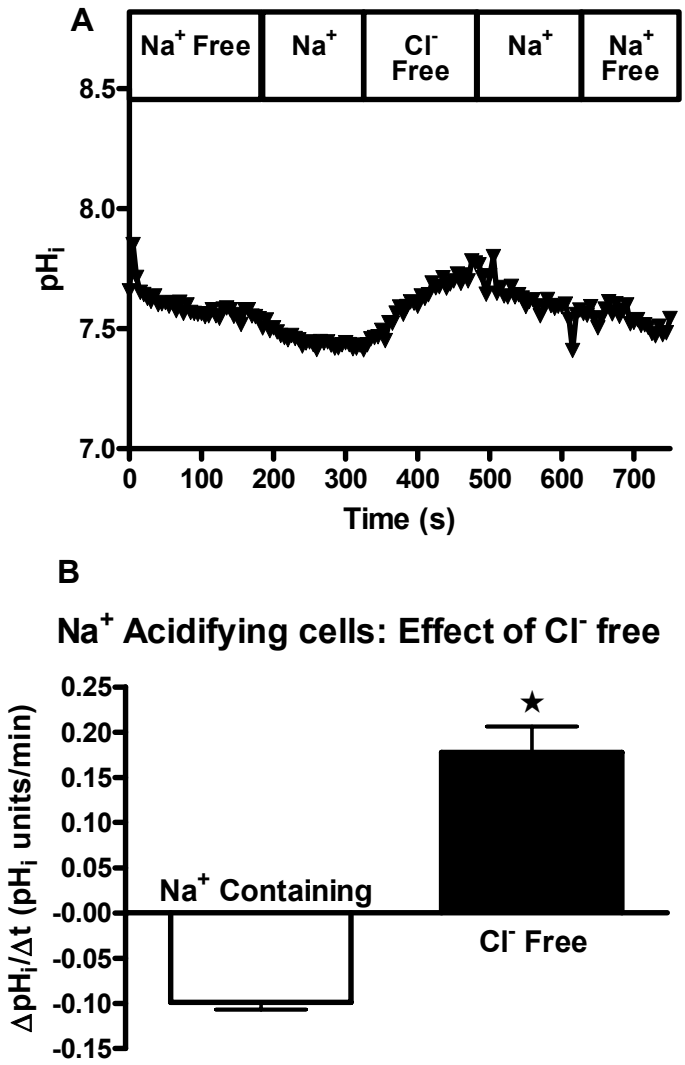

Figure 7. 3 Cl^- free exposure results in an alkalinization of pH_i in both functionally identified MR cells as separated via Na^+ substitution.

A Sample trace representing cells that acidified upon exposure to Na^+-containing medium following initial Na^+ free perifusion and were subjected to Cl^- free perifusion which resulted in an alkalinization of pH_i. ***B*** Summary statistics showing that a significant difference between the acidification caused by Na^+ exposure and the alkalinization caused by Cl^- free conditions ($p<0.05$, paired t-test n=60).

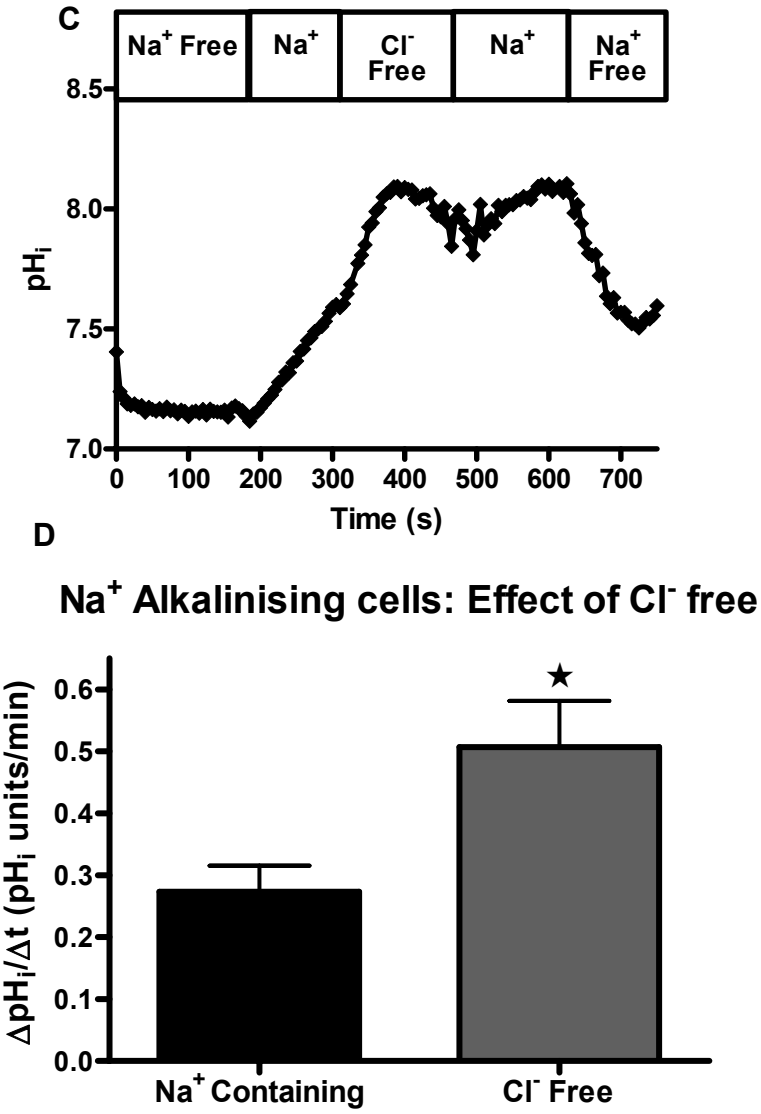

Figure 7.3 continued. ***C*** Sample trace representing cells that alkalinized upon exposure to Na^+-containing medium following initial Na^+ free perifusion and were then subjected to Cl^- free perifusion which resulted in an increased alkalinization of pH_i. ***D*** Summary statistics showing a significant increase in the rate of pH_i alkalinization upon exposure to Cl^- free conditions compared to that caused by Na^+ exposure ($p<0.05$, paired t-test n=32).

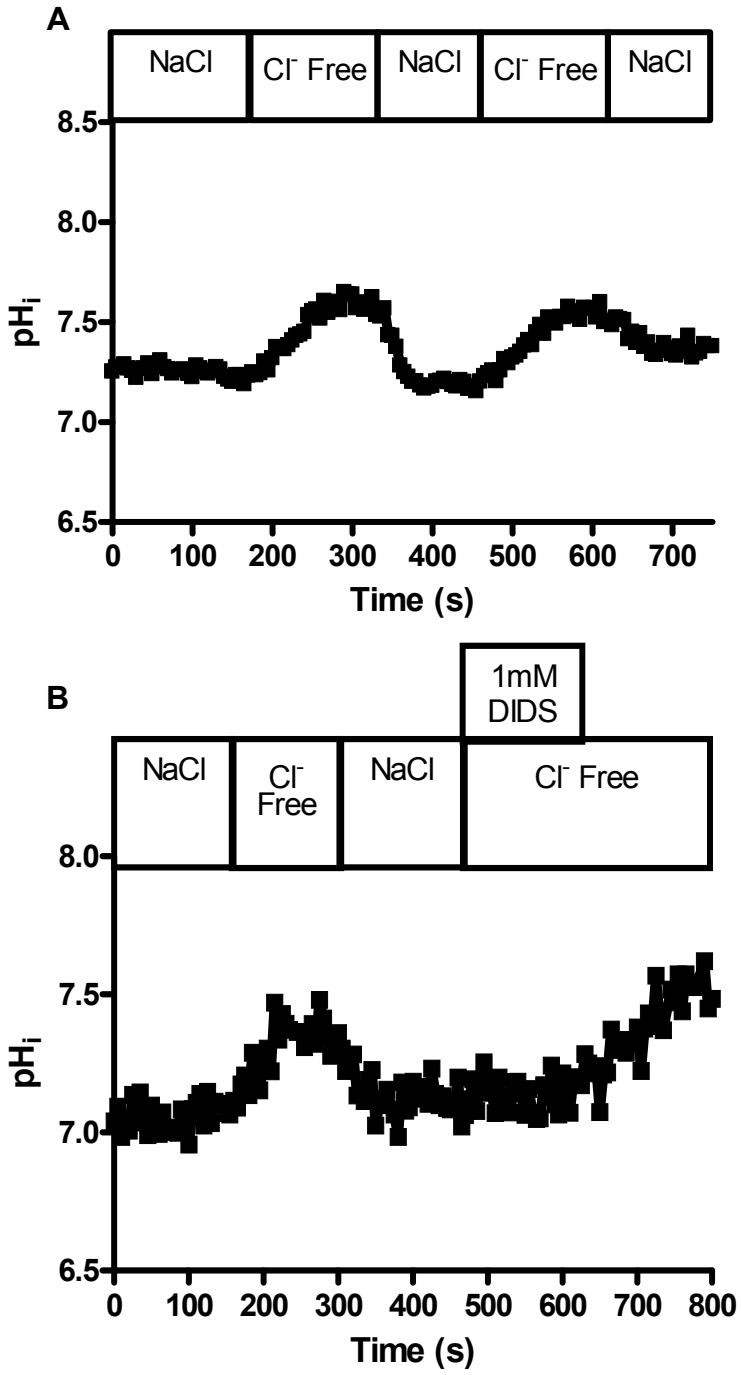

Figure 7. 4 Repeatable Cl^- free induced alkalinization protocol for inhibitor profiling.

A A representative trace demonstrating the ability to repeatedly expose cells to Cl^- free conditions with the same alkalinization effect. ***B*** Sample trace showing that the original Cl^- free alkalinization is inhibited when Cl^- free re-exposure occurs in the presence of 1mM DIDS.

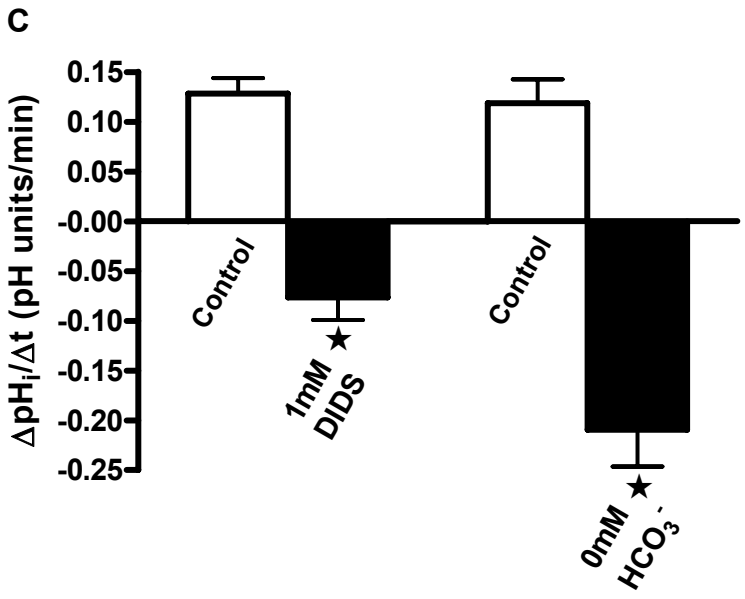

Figure 7.4 continued. ***C*** Summary statistics showing a significant removal of the Cl^- free induced alkalinization of pH_i in the presence of DIDS compared to control conditions ($p<0.05$, paired t-test, n=24). In the other group of experiments cells were acclimated to HCO_3^- free conditions following initial Cl^- free alkalinization and upon and Cl^- free re-exposure no alkalinization was observed in the absence of HCO_3^- ($p<0.05$, paired t-test, n=32).

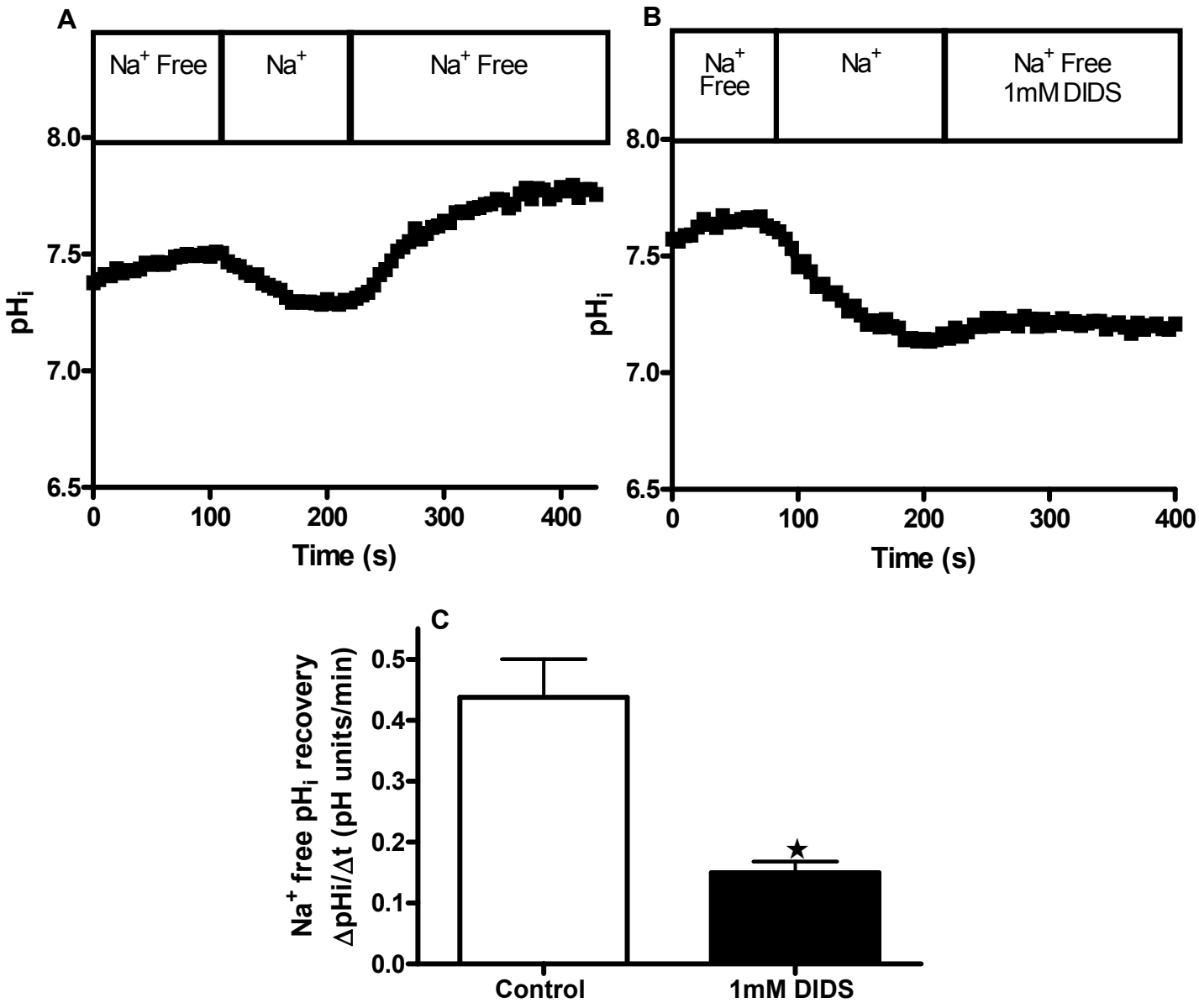

Figure 7. 5 Na^+ free pH_i recovery from Na^+ induced acidosis is removed in the presence of 1mM DIDS

A Representative trace demonstrating a control Na^+ free recovery of pH_i following acidification by Na^+. ***B*** Representative trace demonstrating Na^+ free recovery of pH_i following acidification by Na^+ in the presence of 1mM DIDS. ***C*** Summary statistics showing significant inhibition of Na^+ free pH_i recovery rates in the presence of DIDS compared to control ($p<0.05$, unpaired, non-parametric t-test, n=18 for control and 53 for DIDS).

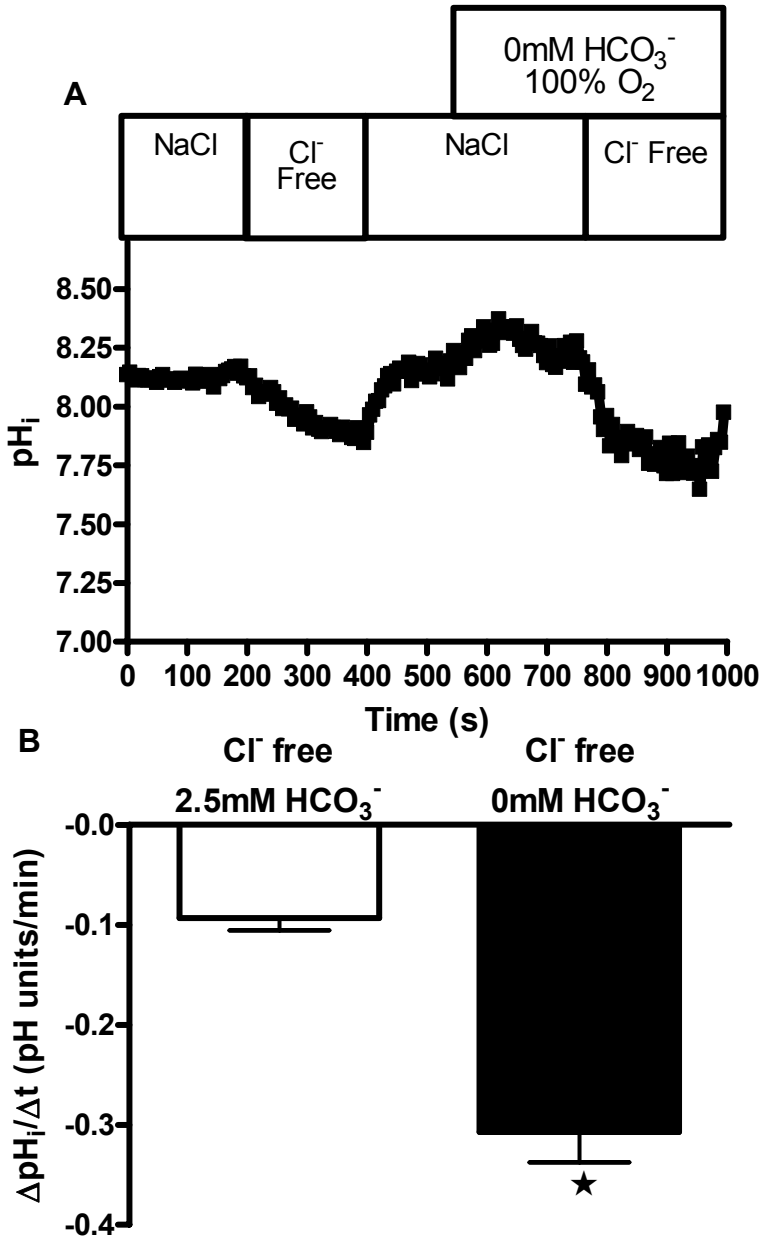

Figure 7. 6 Cl^- free exposure causes an acidification of pH_i that is enhanced in HCO_3^- free conditions.

A Representative trace demonstrating an acidification of pH_i following Cl^- free introduction. Upon recovery, pHi was equilibrated with HCO_3^- free medium aerated with 100% O_2 and Cl^- free introduction was repeated resulting in a greater acidification of pH_i. ***B*** Summary statistics showing a significantly greater acidification of pH_i in the absence of HCO_3^- compared to control conditions ($p<0.05$, paired t-test, n=46).

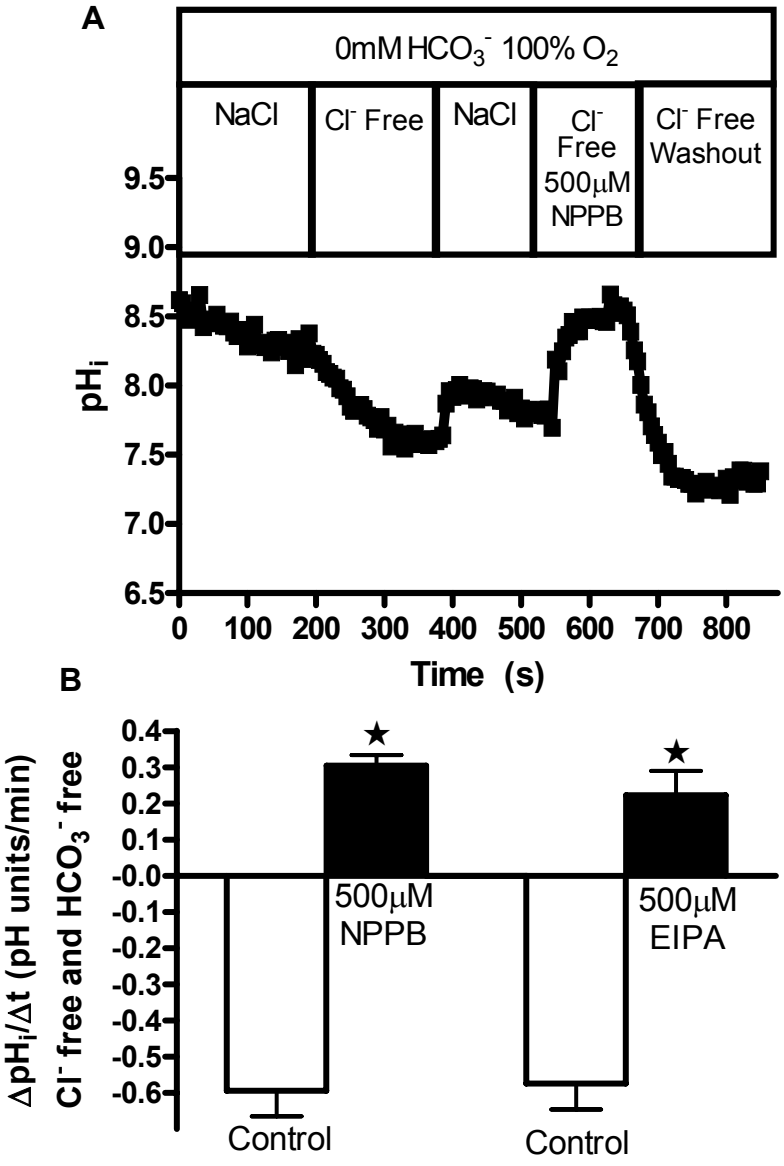

Figure 7. 7 NPPB and EIPA-sensitive Cl^- free induced acidification

A Representative trace demonstrating a removal of the acidification caused by Cl^- and HCO_3^- free conditions in the presence of 500μM NPPB. The same protocol was followed for EIPA. ***B*** Summary statistics showing a significant removal of Cl^- induced pH_i acidification in the presence of 500μM NPPB ($p<0.05$, paired t-test, n=86) or 500μM EIPA ($p<0.05$, paired t-test, n=60) compared to control conditions.

Chapter VIII: Na^+/H^+ exchange activity in isolated rainbow trout gill PNA^+ and PNA^- mitochondrion-rich (MR) cells following intracellular acidosis[1]

[1]A version of this manuscript is currently under review for publication

Parks SK, Tresguerres M, Galvez F, and Goss GG. Na^+/H^+ exchange activity in isolated rainbow trout gill PNA^+ and PNA^- mitochondrion-rich (MR) cells following intracellular acidosis. Submitted to the Journal of Comparative Physiology B on March 12, 2009 (Currently under revision for re-submission following editors suggestions). Manuscript # JCPB-09-0781.

Introduction

Maintenance of constant intracellular pH (pH_i) is essential for proper cell function and survival (Roos and Boron, 1981). Not surprisingly, efficient transporters exist on cellular membranes to ensure regulation of pH_i within narrow limits. The ubiquitous "housekeeping" Na^+/H^+ exchanger (NHE1) is the primary protein responsible for maintaining pH_i across a broad range of cell types (for review see (Orlowski and Grinstein, 2004).

Mitochondrion-rich (MR) cells at the fish gill have been extensively studied due to their importance in maintaining blood acid-base and ion levels. Consequently, information for pH_i regulation has so far only been extrapolated from studies focusing on systemic regulation. MR cells are endowed with a variety of acid-base relevant proteins including carbonic anhydrase (CA), V-type H^+-ATPase (VHA), Na^+/HCO_3^- co-transporters (NBC), Cl^-/HCO_3^- exchangers (CBE), and the aforementioned NHE (for review see chapter II and (Evans, 2008; Evans et al., 2005; Hwang and Lee, 2007; Perry and Gilmour, 2006; Tresguerres et al., 2006a). In gills from seawater (SW) fish, current models predict that some of these proteins are differentially expressed in at least two distinct cell subtypes, each of them achieving acid or base secretion (Hawkings et al., 2004; Perry and Gilmour, 2006; Piermarini and Evans, 2001; Tresguerres et al., 2005). This is similar to the gills of FW trout where two distinct MR cell subtypes were identified based on their ability to bind peanut lectin agluttinin. The terms PNA^+ and PNA^- MR cells (Goss et al., 2001a) were coined to coincide with the mammalian literature where

functionally and morphologically analogous cell types in the cortical collecting duct of the kidney were found with differential PNA staining (Lehir et al., 1982). Further studies demonstrated the importance of VHA (Galvez et al., 2002), Na^+ channels (see chapter IV: (Parks et al., 2007b)), and NBCs (see chapter IV: (Parks et al., 2007b)) in the PNA^- MR cell fraction while CBEs and Cl^--dependent NHEs were shown to be present in both MR cell subtypes (see chapter VII: (Parks et al., 2009)). The combined evidence suggests that PNA^- MR cells are responsible for Na^+ uptake and H^+ secretion using apical sodium channels coupled to VHA and coordinated with basolateral NBC and Na^+/K^+-ATPase (NKA), while PNA^+ MR cells perform Cl^- uptake and HCO_3^- secretion through transporters of unknown molecular identity (Hwang and Lee, 2007; Parks et al., 2008; Parks et al., 2009; Perry and Gilmour, 2006; Tresguerres et al., 2006a).

Only a few studies have directly monitored the pH_i of gill cells and found functional evidence for NHE exchanger activity in cultured gill pavement (PV) cells of goldfish (Sandbichler and Pelster, 2004) and trout (Part and Wood, 1996; Wood and Part, 2000). However, functional evidence for NHE activity and pH_i regulation in gill MR cells is absent. The red blood cell β-NHE was the first transporter to be cloned from trout (Borgese et al., 1992). That seminal paper demonstrated that the β-NHE could be activated by cAMP *via* PKA or PKC pathways independent from each other (Borgese et al., 1992). Studies on sculpin and killifish lead to the hypothesis that β-NHE performed the function of NHE1 at the gill (Claiborne et al., 1999). Hwang's

laboratory (Yan et al., 2007) have recently cloned all of the known NHE isoforms from zebrafish. Phylogenetic analysis grouped zNHE1 closely with trout β-NHE and zNHE1 was strongly expressed in erythrocytes contrary to mammalian expression patterns (Yan et al., 2007). Although zNHE1 was detectable in the gill *via* RT-PCR, no expression was noted in gill cells *via in situ* hybridization. Recently, NHE2 and NHE3 genes have been cloned from rainbow trout and found to be expressed in gill and kidney (Ivanis et al., 2008a; Ivanis et al., 2008b), however a trout homolog to NHE1 has not yet been established. Direct evidence for NHE1-like activity in gill MR cells along with characterizations of the cellular signaling mechanisms controlling ion and acid-base transport are lacking and remain an area of future research. The goal of this chapter was to establish the mechanisms responsible for acid recovery in trout gill MR cells and use this information to aid as physiological markers for identifying PNA^+ and PNA^- MR cell subtypes.

Summary of methodological approach

Intracellular pH imaging was performed on isolated trout gill MR cells as described in chapter IV, and VII. Cells from mixed MR populations were acid loaded using NH_4Cl pre-pulse and recovery was monitored in the presence and absence of Na^+. This was correlated to experiments on magnetically isolated PNA^+ and PNA^- MR cells. A temporary Na^+-dependent recovery mechanism was then tested with various pharmacological agents to elucidate the membrane-transporter and cellular signaling mechanism responsible for the behaviour.

Results

Na^+ free recovery following NH_4Cl induced acidification and buffering capacity

Following intracellular acidification by NH_4Cl only one sub-set of MR cells were able to restore pH_i in Na^+ free conditions (Figure 8.1a). The ability to recover pH_i in Na^+ free conditions establishes a functional separation of MR cells as described previously (see chapter IV). These behaviours corresponded to a difference in buffering capacity (β) between the two MR cell subtypes (Figure 8.1b) with the Na^+ free recovering cells having a significantly higher buffering capacity (β = 18.71 ± 5.19 mM/pH unit) than the non-Na^+ free recovering cells (β = 2.07 ± 0.46 mM/pH unit).

PNA^+ and PNA^- MR cells correspond to functional behaviours

The rate of pH_i recovery following NH_4Cl-induced acidification was also measured in identified PNA^+ and PNA^- MR cells. Recovery from acidosis in Na^+ free conditions occurred in the PNA^+ MR cell fraction only (Figure 8.2a). PNA^+ cells also had a higher resting pH_i and higher buffering capacity (β ~2X higher, Figure 8.2b) than PNA^- cells. This matches the characteristics of the Na^+ free recovering cells described above and previously (see chapter IV). Therefore, recovery from NH_4Cl induced acidification in the absence of Na^+ can be used as a marker for PNA^+ MR cells.

Effect of Na^+-addition on pH_i recovery following an acid load

Introduction of Na^+-containing buffer following NH_4Cl pre-pulse induced acidification resulted in a cellular behaviour where both cell types would exhibit a robust surge in pH_i recovery that was quickly followed by a rapid re-acidification (Figure 8.3). This transient recovery-acidification event was also observed following a second acidification of the same cells (compare dashed boxes in Figure 8.3). The repeatability of this event allowed me to examine the effect of pharmacological agents on this transient Na^+ dependent pH_i recovery.

Effect of amiloride on Na^+ dependent pH_i recovery

Amiloride is commonly used as a general inhibitor of Na^+/H^+ exchangers as well as Na^+-channels (Kleyman and Cragoe, 1988). The transient pH_i recovery induced by Na^+ addition ($\Delta pH_i/\Delta t$ of 0.66 ± 0.08 pH units/minute) was effectively removed by 500 μM amiloride ($\Delta pH_i/\Delta t$ of 0.07 ± 0.04 pH units/minute, Figure 8.4a, b). However, phenamil (50 μM) a known pharmacological blocking agent specific for Na^+ channels but with no known inhibition of NHEs did not inhibit the Na^+ induced recovery (Figure 8.4c). These results indicate that the transient intracellular alkalinization is due to an NHE.

Effect of the phorbol ester PMA on Na^+ induced pH_i recovery

Protein kinase C (PKC) has been linked to NHE activation in the trout red blood cell β-NHE (Borgese et al., 1992; Malapert et al., 1997; Motais et

al., 1992) and this led me to test the involvement of PKC on the Na^+ dependent pH_i recovery mechanisms found in trout MR cells. Following a control acidification/recovery, cells were then exposed to a second acidification and recovery but with the addition of 1 μM PMA. This resulted in a sustained pH_i recovery (no re-acidification event) in both the Na^+-dependent and independent recovering cell populations (Figure 8.5a, 8.6a). In PNA^- MR cells (those displaying no recovery in Na^+ free conditions-Fig 8.2), PMA resulted in a sustained Na^+-induced pH_i recovery ($\Delta pH_i/\Delta t$ of 0.38 ± 0.06 pH units/minute) that was not significantly different from the initial transient Na^+-induced alkalinization ($\Delta pH_i/\Delta t$ of 0.42 ± 0.06 pH units/minute, Figure 8.5a, b). Cells demonstrating Na^+-independent pH_i recovery (PNA^+ MR cells-Fig 2) had an initial pH_i recovery rate of 0.49 ± 0.11 pH units/minute in Na^+ free medium. Addition of Na^+ temporarily increased the rate significantly ($\Delta pH_i/\Delta t$ = 0.80 ± 0.05 pH units/minute) but the rate later returned to a value that was not significantly different from the original Na^+-free conditions ($\Delta pH_i/\Delta t$ 0.36 ± 0.04 pH units/minute) (Figures 8.6a, b). PMA did not affect the Na^+ independent recovery ($\Delta pH_i/\Delta t$ 0.46 ± 0.05 pH units/minute), but it maintained the elevated rate of pH_i recovery observed during the early phase of recovery upon Na^+ addition (0.90 ± 0.12 pH units/minute) (Figures 8.6a, b).

Discussion

Functional separation of gill MR cell subtypes

Pisam and colleagues first described two types of MR cells (termed chloride cells at the time) based on morphological characteristics (Pisam et al., 1993; Pisam et al., 1987) however a functional separation was lacking. To pursue functional differences, a Percoll separation technique was used to isolate pure MR cell populations from Japanese eel and separate subtypes based on flow cytometry (Wong and Chan, 1999a; Wong and Chan, 1999b). Goss and colleagues then reported the identification of MR cells subtypes at the freshwater trout gill based on peanut lectin agglutinin binding (Galvez et al., 2002; Goss et al., 2001a) eventually leading to a method to functionally separate and characterize the isolated MR cell subtypes (Galvez et al., 2002; Hawkings et al., 2004; Reid et al., 2003). Work on zebrafish has also suggested at least 2 MR cell subtypes based on co-localization of concanavalin A (Con A) with VHA and not NKA (Esaki et al., 2007; Lin et al., 2006). These studies in zebrafish have also demonstrated the functional importance of VHA and NHE3 in acid secretion and Na^+ uptake from freshwater in identified ionocytes (a more generic term for MR cells in fish) (Esaki et al., 2007; Horng et al., 2007; Lin et al., 2006; Yan et al., 2007). Interestingly however, Con A co-localizes with NKA in MR cells from tilapia yolk sac membrane which is the exact opposite of the trend in zebrafish (Lin and Hwang, 2004). Moreover, an excellent immunohistochemical analysis suggests as many as four different MR cell subtypes exist at the gill of tilapia

(Hiroi et al., 2008). These recent results suggest that potential species specific differences should always be considered when interpreting functional physiology of the fish gill. My data showing differential pH_i recovery following acidification in PNA^- cells and PNA^+ MR cells provide additional evidence for functional differences in isolated trout gill MR cell subtypes.

In the previous chapter, I provided evidence for the presence of a Cl^-/HCO_3^- exchanger (CBE) in both functionally identified MR cell subtypes. Consequently, it is reasonable to assume that both MR cell subtypes would be capable of demonstrating a Na^+ free recovery pattern. However, my data from this chapter and chapter IV indicate that only one MR cell subtype (PNA^+ cells) uses the CBE for recovery from acidosis. One possibility is that the CBE in the Na^+ free recovering cells (PNA^+ cells) is more active under my experimental conditions and/or present in greater levels on the membrane due to their attributed *in vivo* role for transepithelial Cl^- uptake (Evans, 2008; Evans et al., 2005; Parks et al., 2009; Tresguerres et al., 2006a) whereas the CBE present in PNA^- MR cells (non Na^+-free recovering cells) is not activated sufficiently by acidosis to achieve pH_i recovery.

Correlation of MR cell subtypes with cellular buffering capacity

Previous estimates of buffering capacity (β) in HEPES buffered medium for the trout gill epithelia were 13.4 and 13.7 Slykes (mM/pH unit) in cultured PV cells and gill homogenates respectively (Part and Wood, 1996; Wood and Lemoigne, 1991; Wood and Part, 2000). These fall within the values found in this study for Na^+ free recovering cells (18.71 ± 5.19 mM/pH

unit**)** but are much greater than that found in the non-Na^+ free recovering cells (2.07 ± 0.46 mM/pH unit). This analysis was consistent with that observed in experiments involving identified PNA^+ and PNA^- MR cells where PNA^+ cells exhibited a significantly higher buffering capacity compared to PNA^- cells. Relative differences in buffering capacity may be related to higher levels of intracellular HCO_3^- present in PNA^+ cells versus PNA^- cells. Higher intracellular HCO_3^- in PNA^+ cells may well be utilized to enhance Cl^- uptake, whereas lower HCO_3^- in PNA^- cells could result from the extrusion of HCO_3^- across the basolateral membrane as suggested previously (chapter IV). Higher HCO_3^- levels in these cells would also explain the higher resting pH_i noted in chapter IV in Na^+ free recovering cells compared to non-Na^+ free recovering cells.

NHE1-like activity in MR cells pH_i recovery: a role for PKC

Amiloride sensitivity and lack of inhibition by phenamil establish that the alkalinizing effect of Na^+ introduction is dependent on an NHE and not a Na^+ channel linked to a V-H^+-ATPase. In chapter VII, I demonstrated the presence of a Cl^- dependent NHE (Cl-NHE) in both trout MR cell subtypes. However, the Cl-NHE mechanism in chapter VII was insensitive to amiloride unlike this chapter's results that were fully abolished by amiloride. Furthermore, the continuous Na^+/H^+ exchange is dependent on activation by PKC. Activation by PKC matches with the established role for PKC in stimulating trout RBC β-NHE (Borgese et al., 1992; Malapert et al., 1997) and it also aligns with the role of PKC in maintaining the activity of mammalian

non RBC NHE1 isoforms (Magro et al., 2005). In contrast, the Na^+ absorbing mammalian isoform NHE3 is inhibited by PKC (Donowitz et al., 2000). Considering all of these factors, I propose that the Na^+ dependent, PMA potentiated pH_i recovery noted in this chapter is mediated by an NHE-1 like protein. However, a definitive conclusion depends on the cloning and pharmacological profiling of trout NHE isoforms.

One alternative explanation is that under control conditions, Na^+ introduction first activates an NHE to alkalinize the cell and subsequently activates a net acid transport (H^+ import or HCO_3^- export) that masks the NHE mediated alkalinization. When PMA is present, this masking mechanism would be inhibited resulting in the sustained alkalinization noted. However, the primary candidate for this would be the NBC mediated HCO_3^- extrusion mechanism as observed previously for PNA^- cells only (see chapter IV). In other systems, PKC activation has been shown to increase both the kidney and intestinal NBC activity (Bachmann et al., 2006; Ruiz et al., 1997). This response is the exact opposite to that required for my noted responses in this chapter. Furthermore, PMA activation of recovery is found in both MR cell types suggesting that these results demonstrate direct PMA mediated stimulation of NHE and not inhibition of NBC.

One of the problems associated with working on isolated gill MR cells is the existence of distinct PNA^+ and PNA^- MR cells. While it is possible to physically separate the MR cell subtypes (Galvez et al., 2002), this procedure substantially extends the time required for cell isolation and it results in a

lower cell yield, thus limiting the number and type of pH_i experiments that can be performed. The results from this chapter suggest that we can directly identify MR cell subtypes within a mixed population of MR cells simply by their ability to recover from an NH_4Cl induced acidosis in Na^+ free medium. This correlates directly to the behaviours found in separated PNA^+ and PNA^- MR cells respectively. Therefore the ability to recover pH_i in Na^+ free media is a direct functional marker correlated with identified trout gill MR cell subtypes. This mechanism can now be used as a distinguishing characteristic of the subtypes allowing for future functional studies on mixed PNA^+ and PNA^- MR cell populations.

In summary I present a direct single cell functional marker (Na^+ free recovery from acidosis) for use in the study of individual MR cell subtypes at the fish gill. I also report differences in buffering capacities between the two MR cell subtypes and these differences should be explored for their functional relevance to the basic membrane transport properties of these cells. Finally, I observed a transient Na^+ dependent pH_i recovery event that was stimulated by PKC providing the first step in understanding the signaling pathways that control of membrane ion transport in gill MR cells.

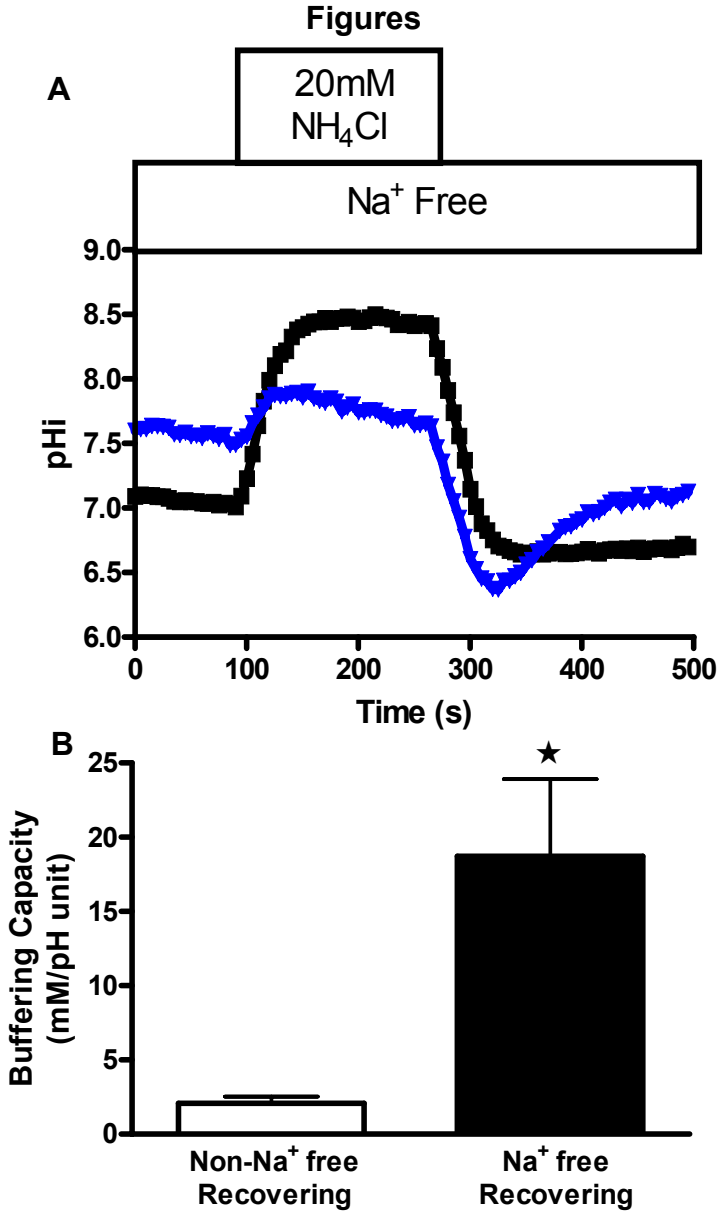

Figure 8. 1 Na^+ free recovery from acidosis correlates to higher cellular buffering capacity.

A Sample trace showing a cell that recovers from NH_4Cl induced acidosis in Na^+ free medium (blue trace) compared to one that does not (black trace). ***B*** Na^+ free recovering cells have a significantly higher buffering capacity (18.71 ± 5.19 mM/pH unit, n=33) compared to non Na^+ free recovering cells (2.07 ± 0.46 mM/pH unit, n=37). $p<0.05$ unpaired non-parametric Mann Whitney t-test.

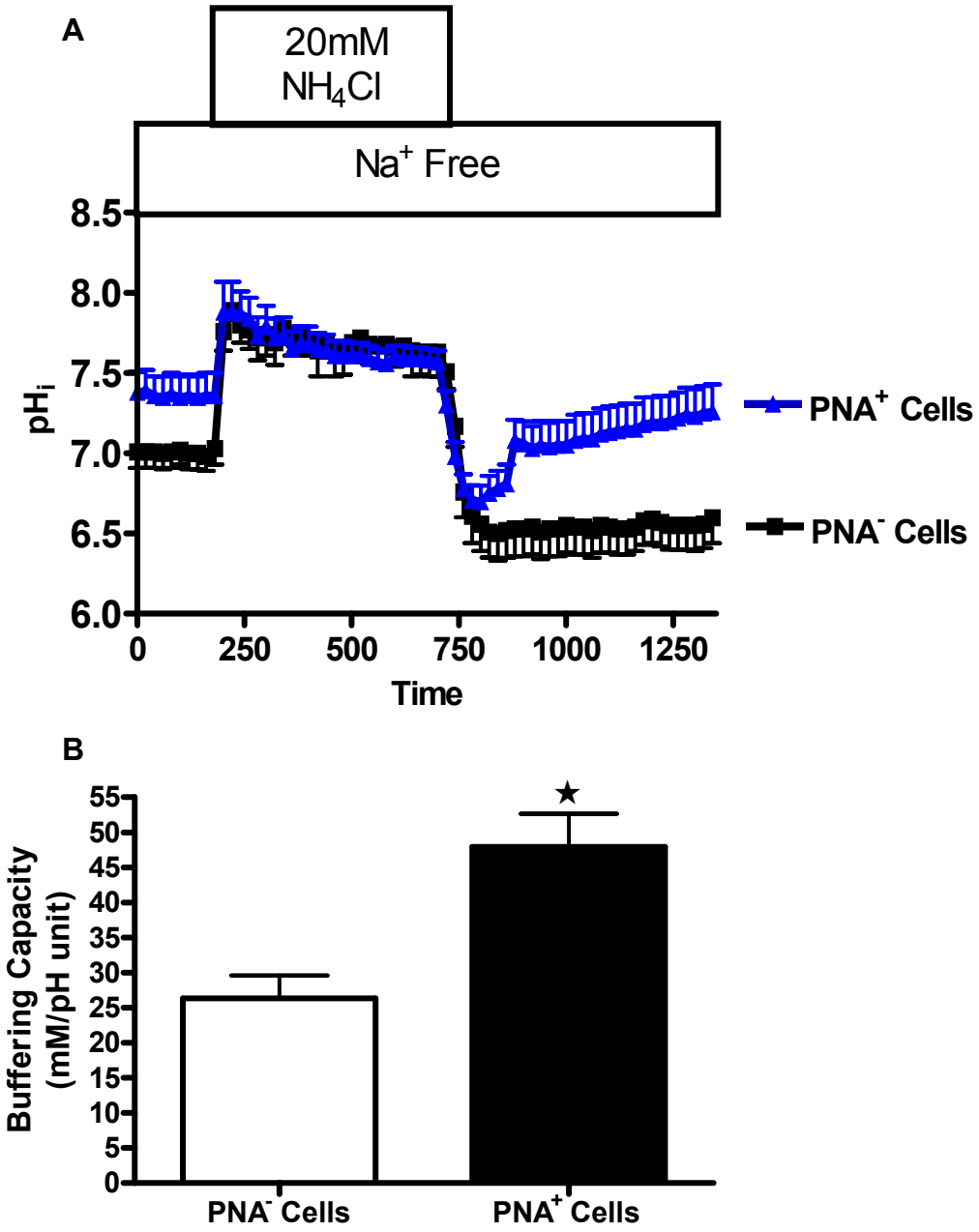

Figure 8. 2 PNA^+ and PNA^- MR cell responses to NH_4Cl induced acidosis. ***A*** PNA^+ MR cells (blue trace n=16) demonstrate Na^+ free recovery following NH_4Cl induced acidosis, while PNA^- MR cells do not (black trace n=6). ***B*** Buffering capacity of PNA^+ and PNA^- MR cells. $p<0.05$ unpaired non-parametric Mann Whitney t-test.

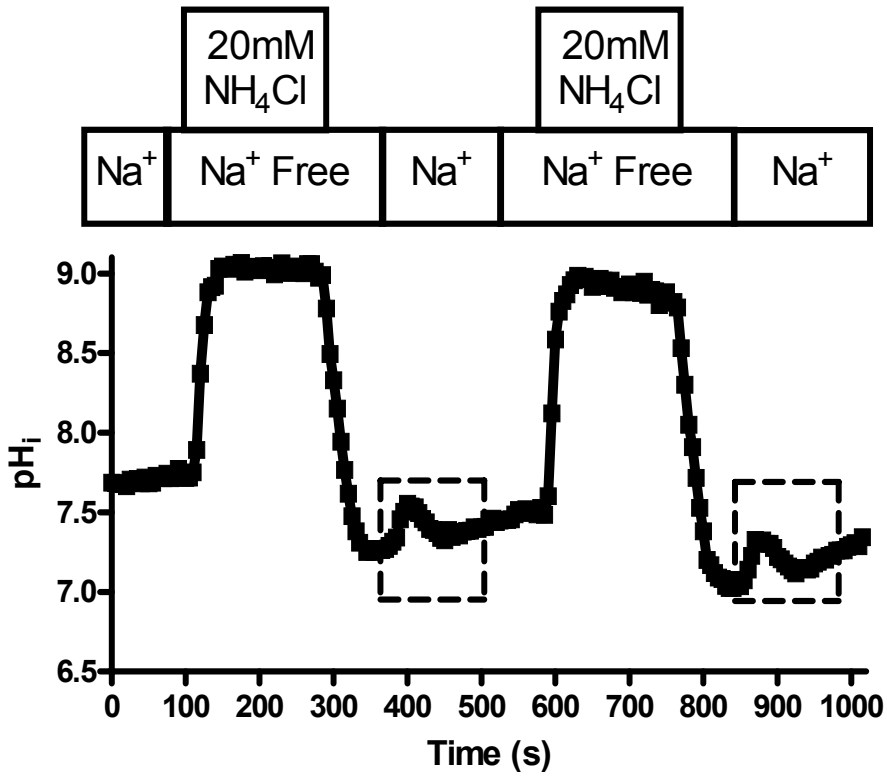

Figure 8. 3 Na^+ induced recovery from NH_4Cl induced acidosis

Representative trace demonstrating the effect of Na^+ addition following a 20mM NH_4Cl pre-pulse induced acidification. Dashed box highlights a transient Na+ dependent alkalinization and re-acidification. Cells were subjected to two consecutive acidification events and displayed the same behavior following initial and secondary acidifications (compare the two dashed boxes, n=7).

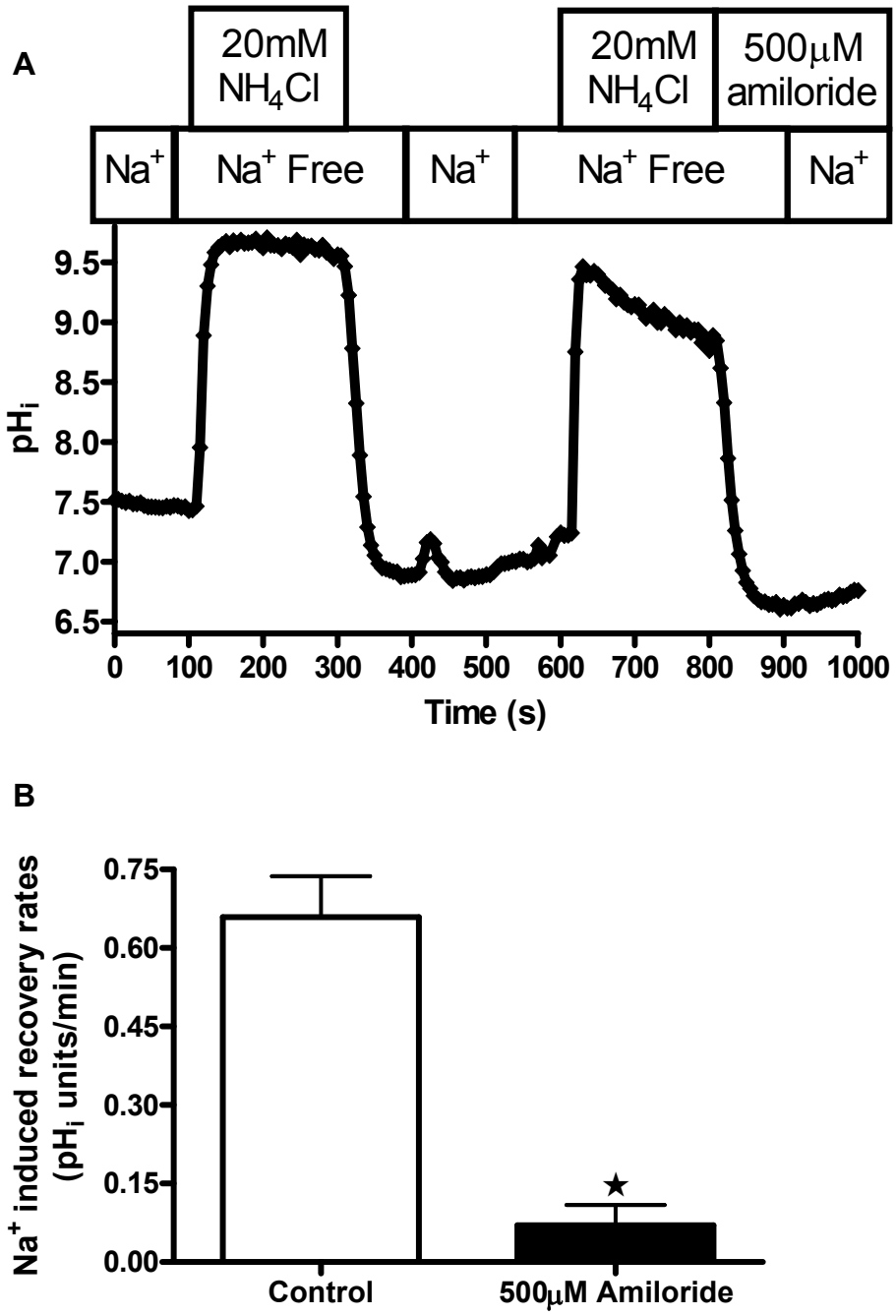

Figure 8. 4 Amiloride and phenamil effects on the transient Na^+ dependent pH_i recovery

A representative trace demonstrating abolishment of the transient Na^+-dependent pH_i recovery with the addition of amiloride (500 μM). ***B*** summary statistics for part **A** ($p<0.05$, paired t-test, n=30 cells).

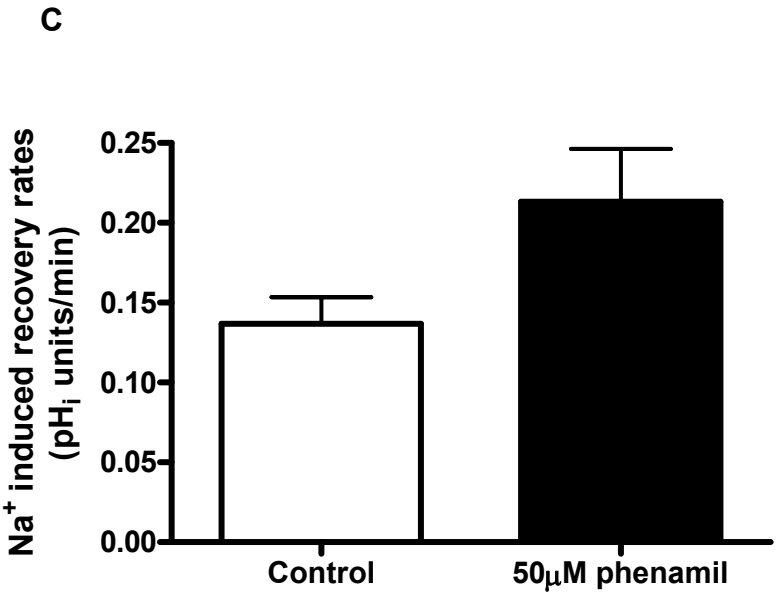

Figure 8.4. continued. ***C*** summary statistics for the effect of 50 μM phenamil on the transient Na^+ dependent pH_i recovery ($p>0.05$, paired t-test, n=23 cells).

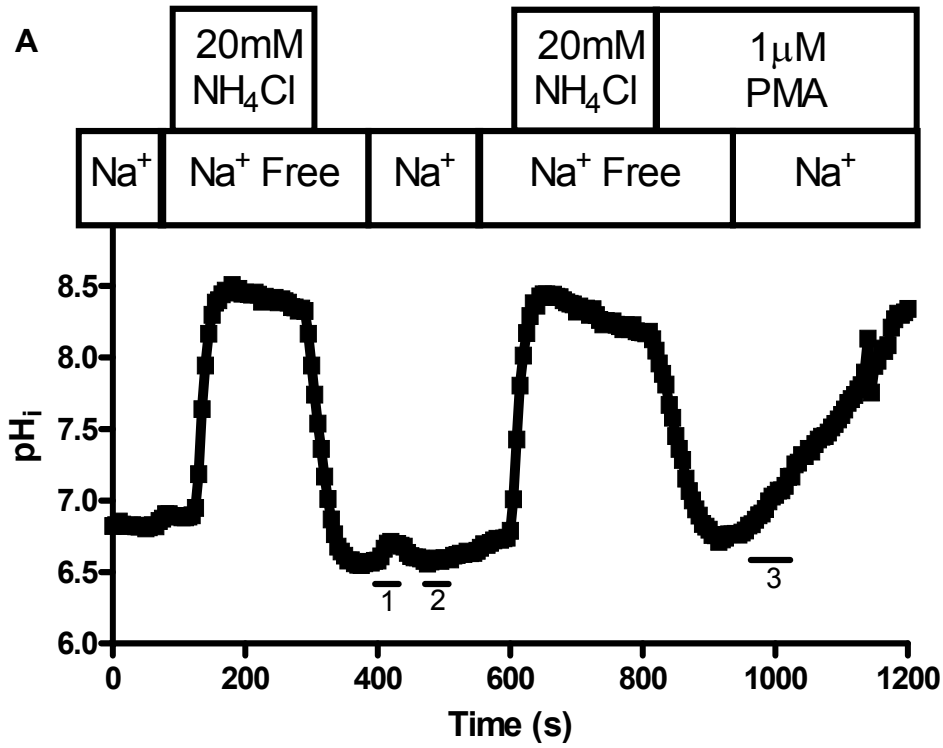

Figure 8. 5 The effect of 1μM PMA on Na^+-induced pH_i recovery from acidification following exposure to 20mM NH_4Cl in PNA^- cells.

A Na^+-dependent pH_i recovery is sustained in the presence of 1μM PMA. Lines and corresponding numbers under the sample trace correspond to regions of pH_i recovery analysed in summary statistics.

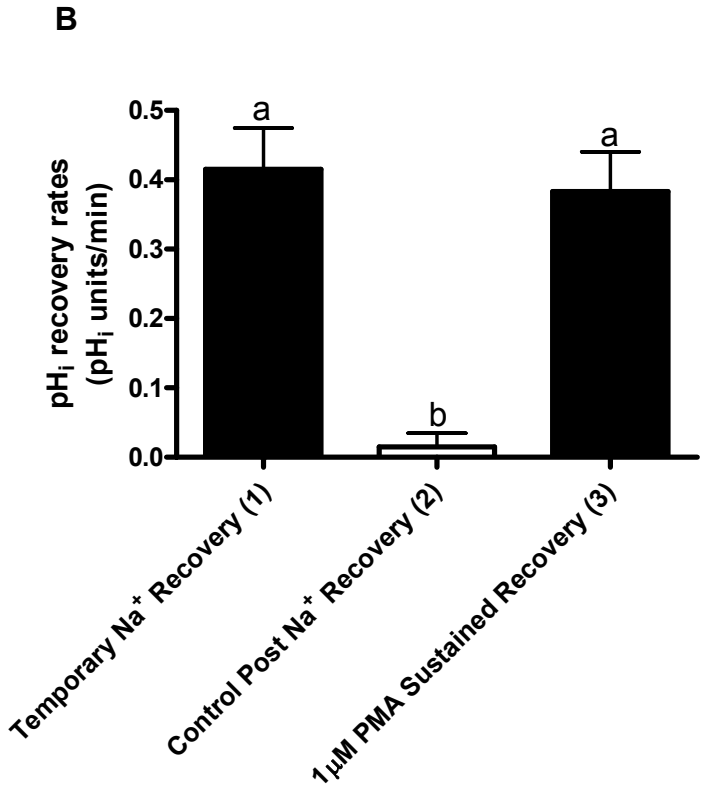

Figure 8.5 continued. ***B*** summary statistics for specific regions (1-3) of the traces demonstrated in part **A** Significant differences between groups are indicated by letters . $p<0.05$, repeated measures one-way ANOVA, Tukey post-hoc test, n=16.

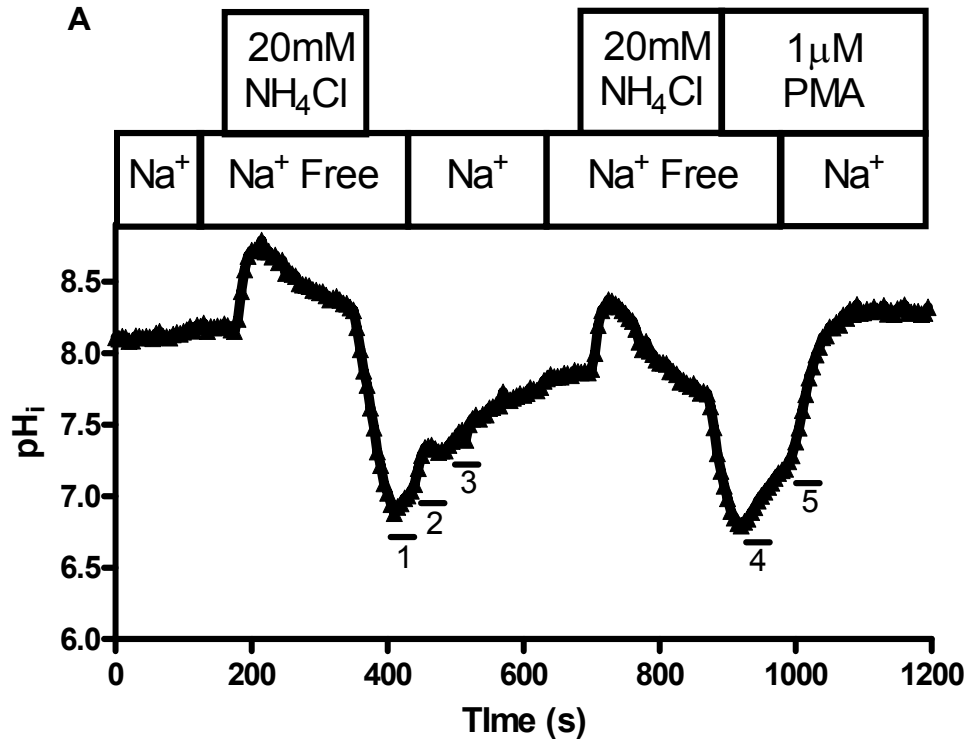

Figure 8. 6 The effect of 1μM PMA on Na^+-induced pH_i recovery from acidification following exposure to 20mM NH_4Cl in PNA^+ cells.

A Na^+ addition resulted in an additive pH_i recovery which required PMA to be sustained. Lines and corresponding numbers under the sample trace correspond to regions of pH_i recovery analysed in summary statistics. ***b*** summary statistics for specific regions (1-5) of the traces demonstrated in part **a**. Significant differences between groups are indicated by letters. $p<0.05$, repeated measures one-way ANOVA, Tukey post-hoc test, n=10.

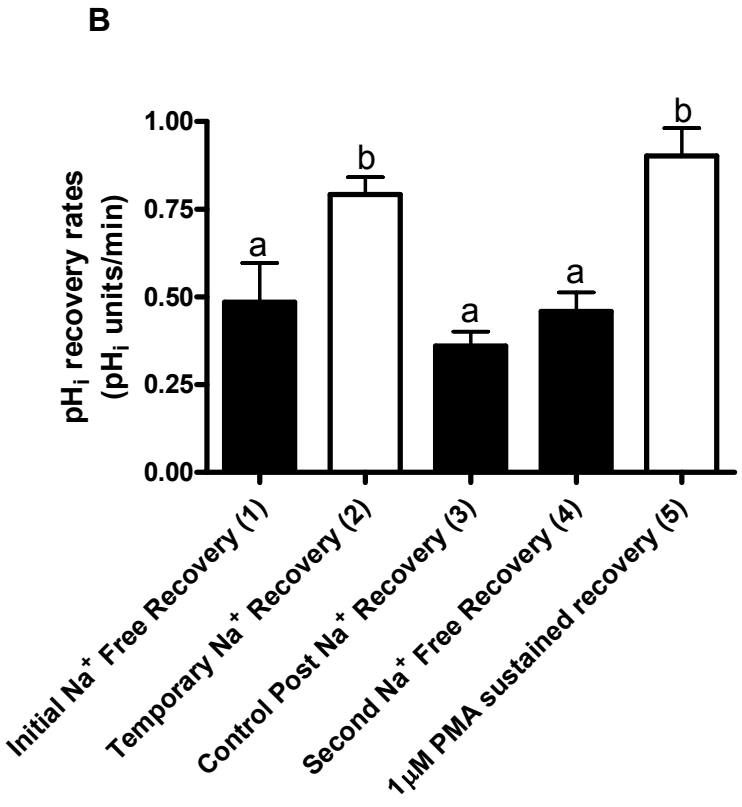

Figure 8.6 continued. ***B*** summary statistics for specific regions (1-5) of the traces demonstrated in part **A**. Significant differences between groups are indicated by letters. $p<0.05$, repeated measures one-way ANOVA, Tukey post-hoc test, n=10.

Chapter IX: Mechanisms of acid-recovery in the Pacific hagfish (*Eptatretus stoutii*)[1]

[1]A version of this chapter has been published previously.

Parks, S. K., Tresguerres, M. and Goss, G. G. (2007). Blood and gill responses to HCl infusions in the Pacific hagfish (*Eptatretus stoutii*). *Canadian Journal of Zoology* **85**, 855-862.

Introduction

The hagfish is the only craniate with an internal ionic composition similar to that of the surrounding seawater (Alt et al., 1981; Morris, 1965). Although hagfish do not osmoregulate their internal fluids to any appreciable extent, their gill epithelium possess great numbers of mitochondria-rich (MR) cells, which are morphologically similar to the typical “chloride” cells used for osmoregulation and acid–base regulation in other marine fishes (Mallatt et al., 1987). In Atlantic (*Myxine glutinosa*) and Pacific (*Eptatretus stoutii*) hagfish, MR cells on the trailing region of the gill express Na^+/K^+-ATPase , Na^+/H^+ exchangers (NHE), carbonic anhydrase (CA), and vacuolar proton ATPase (VHA) (Choe et al., 1999; Choe et al., 2002; Edwards et al., 2001; Mallatt et al., 1987; Tresguerres et al., 2006b). Since these transporters are implicated in both ionic and pH regulatory mechanisms in a variety of fishes (Evans et al., 2005), it has been proposed that their role in hagfish MR cells is primarily for acid–base regulation (Mallatt et al., 1987).

All animals periodically face the challenge of adjusting blood pH owing to respiratory or metabolic acidosis. Hagfish are under a continual challenge to maintain plasma pH at appropriate levels. They live in oxygen-poor conditions in the deep sea, which at least in the Atlantic hagfish is compensated by using anaerobic metabolism (Hansen and Sidell, 1983). Furthermore, they utilize sudden bursts of swimming in search of food, which have been shown to cause severe lactic acidosis in the blood of Pacific hagfish (Ruben and Bennett, 1980). Hagfish are also known to slightly hyper-

regulate Na^+ but not Cl^- in the plasma; Mallat and colleagues (Mallatt et al., 1987) proposed that this is likely due to a net branchial excretion of H^+ required for the acidosis produced by the animal in the conditions listed above.

Evans (Evans, 1984) proposed that hagfish use the orthodox mechanism of acid–base regulation consisting of exchanging Na^+ for H^+ and Cl^- for HCO_3^- at the apical side of the gill. More recent studies have focused on the specific cellular mechanism for the pH-compensating mechanism. Based on an increase in mRNA expression in response to metabolic acidosis (Edwards et al., 2001), the primary candidate for apical Na^+/H^+ exchange is a NHE-like protein. In addition, NHE2-like immunoreactivity (NHE2 L-IR) was shown in MR cells at the gill of Pacific hagfish (Tresguerres et al., 2006b). Although the immunolabelling pattern was described as predominantly cytoplasmic, a minority of cells showed concentrated signal in apical regions, and a role of NHE-cycling from cytoplasmic vesicles to the apical plasma membrane was proposed to occur in response to acidosis. This corresponds with the known role of NHE isoforms for acid–base regulation, where NHE1 is known to act as a housekeeper of intracellular pH, while NHE2 and NHE3 have been linked specifically to acid secretion and transepithelial Na^+ uptake in a number of systems. More complete information on the role and functions of different NHE isoforms, are found in several excellent recent reviews (Evans et al., 2005; Hirose et al., 2003; Orlowski and Grinstein, 2004).

Summary of methodological approach

In this chapter I induced a metabolic acidosis via serial acid infusions (HCl 6000 μmol·kg^{-1}) every 6h over a 24h period and investigated subsequent changes in abundance and cellular localization of an NHE-like protein found in Pacific hagfish. My results suggest the role of an apical NHE in the mechanism for acid recovery at the hagfish gill.

Results

Twenty-four hour HCl infusions: blood and plasma variables

No notable changes in blood pH were found in NaCl-infused controls, but a marked blood acidosis was induced upon injection of HCl. Blood pH was reduced from 7.93 ± 0.02 at t = 0 h to 6.21 ± 0.07 at t = 3 h (Fig. 9.1A). Remarkably, blood pH was restored to 7.31 ± 0.09 by 6 h without any mortality. Subsequent HCl infusions also resulted in blood acidification, but they were significantly less severe compared with the initial stress (6.21 ± 0.07 at t = 3 h vs. 6.73 ± 0.06 at t = 9 h, $p < 0.05$, N = 5). The fact that the fish were infused at this point with an already depressed blood pH and did not experience an increased acidification compared with the original HCl infusion indicates that acid-recovery mechanisms had been initiated. Following this, blood pH was measured at 6 h time periods to prevent anemia. Blood pH remained stable at t = 12, 18, and 24 h despite the repeated acid infusions. Although this new steady state represented a significant recovery from the induced acidosis, it remained significantly lower than those of the NaCl-infused controls (Fig. 9.1A).

Total CO_2 levels followed a pattern similar to the pH changes induced by HCl infusion. Starting at a similar level to that of the control, TCO_2 was titrated essentially to 0 mmol·L^{-1} at t = 3 h (0.08 ± 0.08 mmol·L^{-1}), rebounded slightly at t = 6 h (1.82 ± 1.38 mmol·L^{-1}), and returned close to 0 mmol·L^{-1} at t = 9 h (0.52 ± 0.52 mmol·L^{-1}) before returning to control levels at t = 12, 18, and 24 h in HCl-infused fish (Fig. 9.1B). Although there were noticeable

differences in TCO_2 between NaCl- and HCl-infused fish, no statistical significance was recorded at any point likely because of the large variability in the samples.

Plasma [Na^+] in NaCl- and HCl-infused fish were similar at all time points except for t = 3 h, where HCl-infused fish had significantly reduced levels compared with the control fish (Table 9.1). Both NaCl- and HCl-infused fish had an elevation of plasma [Na^+] from t = 9–24 h (Table 9.1).

Na^+/K^+-ATPase, V-H^+-ATPase, and Na^+/H^+ exchanger 2 (NHE2) gill abundance

There were no significant differences in Na^+/K^+-ATPase abundance in whole-gill (1.63 ± 0.10 vs. 1.89 ± 0.27 a.f.u., $p > 0.05$) and whole-membrane (0.75 ± 0.11 vs. 0.74 ± 0.16 a.f.u., $p > 0.05$) homogenates from NaCl- and HCl-infused fish, respectively. V-H^+-ATPase demonstrated no significant changes in abundance in both whole-gill (1.56 ± 0.15 vs. 2.30 ± 0.30 a.f.u., $p > 0.05$, N = 5) and whole-membrane (0.25 ± 0.04 vs. 0.40 ± 0.09 a.f.u., $p > 0.05$, N = 5) fractions from NaCl-infused fish compared with HCl-infused fish. HCl-infused fish exhibited a significant increase in NHE2-like abundance in whole gill compared with NaCl-infused fish (2.30 ± 0.43 vs. 0.99 ± 0.14 a.f.u., $p < 0.05$, N = 5; Fig. 9.2A), indicating increased synthesis of a NHE-like protein in acidotic hagfish. The whole-membrane fraction of HCl-infused fish also showed a significant increase in NHE2-like abundance compared with NaCl-infused fish (2.10 ± 0.23 vs. 1.14 ± 0.29 a.f.u., $p < 0.05$, N = 5; Fig. 9.2B).

Na^+/K^+-ATPase, V-H^+-ATPase, and NHE2 gill immunohistochemistry

Serial sections of control fish demonstrated that Na^+/K^+-ATPase, V-H^+-ATPase, and NHE2 like-immunoreactivity (L-IR) were generally located in the same gill cells, as was noted previously (Tresguerres et al., 2006b) (Figs. 9.3A, 9.3C, 9.3E). Na^+/K^+-ATPase, V-H^+-ATPase, and NHE2 L-IR displayed an almost exclusive cytoplasmic distribution, but a minority of cells labelled slightly apically for NHE2 L-IR (Fig. 9.3E). Na^+/K^+-ATPase and V-H^+-ATPase staining remained unchanged in HCl-infused fish compared with control fish (Figs. 9.3B, 9.3D). However, NHE2 L-IR was unique in that there was a clear increase in the intensity of labelling at the apical region in a large number of cells (Fig. 9.3F).

Quantification of cytoplasmic, intermediate, and apical NHE2 L-IR localization

High-magnification (1600×) images representing the three distinct cellular immunolabling patterns for NHE2 L-IR are shown in Fig. 9.4. Many cells labelled strictly in the cytoplasm (Fig. 9.4A). Other cells had a more concentrated labelling in the apical region but were not as distinctly apical and were categorized as intermediate (Fig. 9.4B), whereas the remaining cells had a distinctly apical labelling pattern (Fig. 9.4C). Quantification of cells revealed that in control fish, ~73% exhibited NHE2 L-IR in a cytoplasmic manner, 20% labelled intermediate, and only 7% labelled apically (Table 9.2). In contrast, cells of HCl-infused fish had 54% labelled cytoplasmically, 19% labelled intermediate, and 27% labelled apically (Table 9.2). Apical localization in HCl-infused fish was significantly higher than in control fish,

whereas cytoplasmic staining was significantly higher in control fish ($p < 0.05$, Table 9.2). Intermediate staining did not vary between treatments.

Discussion

In this chapter I have demonstrated that the Pacific hagfish can readily recover from metabolic blood acidosis. To my knowledge this is the greatest acidification of blood pH ever reported in the fish literature. As a comparison, when a similar HCl load was attempted in experiments on the Pacific spiny dogfish (*Squalus acanthias*), mortality was 100% within a few hours (Tresguerres et al., 2005). This degree of acidosis, while large, is not unreasonable for the Pacific hagfish. It was demonstrated previously that only 5 min of exercise resulted in a drop in blood pH by 0.7 units (1.5 h following exercise) as a result of lactic acid build-up (Ruben and Bennett, 1980). Additionally, hagfish are known to live in extremely hypoxic, even anoxic, conditions and utilize anaerobic metabolism that necessitates a strong H^+ excretion mechanism.

My results suggest that activation of a branchial H^+ secretory mechanism is at least partially responsible for the strong pH recovery in hagfish. After the pronounced blood acidosis induced by the initial HCl load, subsequent acidification events are less pronounced. This suggests that activation of H^+ secretion was initiated within 6 h of the initial HCl load. Specific aspects of the branchial mechanism include increased synthesis of a NHE-like protein of currently unknown molecular identity. In addition, the density of this protein increases at the apical region of the gill MR cells.

I must point out that the HCl-infusion method is not without certain flaws, most of which are explained in detail by McDonald and colleagues

(McDonald et al., 1991). The greatest limitation is that the blood from the caudal sinus and that of systemic vessels might be slow to equilibrate with each other (Forster et al., 1989). However, equilibration required ~8 h (Forster et al., 1989), which would give plenty of time for the diffusion of H^+ from the subcutaneous sinus into the systemic blood in my 24 h infusion experiments. Supporting this assumption, the observed changes at the gill suggest that the systemic blood was indeed affected by the HCl infusions into the subcutaneous sinus, albeit the pH disturbance might have been of a smaller magnitude compared with that in the sinus blood. Similarly, injections of HCl, NH_4Cl, and even urea into the peritoneal space (another compartment with presumably slow equilibration with the systemic blood) have been traditionally used in fish to induce acid–base disturbances of the systemic blood and to look for branchial ion fluxes and (or) changes in the abundance and expression of ion-transporting proteins (for recent works see (Catches et al., 2006; Claiborne et al., 1999; Claiborne et al., 1997; Ip et al., 2005; Lim et al., 2004)). Therefore, I consider that the infusion protocol was suitable for the goal of inducing blood acidosis.

Secretion of H^+ using NHEs would result in a Na^+ load in the blood. Although there were changes in plasma [Na^+] during the experiments, they occurred in both NaCl- and HCl-infused fish. Therefore, I cannot relate them to activation of a NHE system in HCl-infused fish. Given the high [Na^+] of hagfish plasma, detection of the putative Na^+ fluxes require the use of radiotracer techniques.

My results suggest a relocation of NHE within hagfish gill MR cells in response to acidosis, which is an event previously unreported in the fish literature. The role of membrane transporter translocation from cytoplasmic vesicles to the plasma membrane with respect to ion transport and acid–base regulation has been well illustrated in a number of systems (Breton and Brown, 2007; Dames et al., 2006; Pastor-Soler et al., 2003; Tresguerres et al., 2005; Tresguerres et al., 2006c; Tresguerres et al., 2007b). It is now evident from this study that membrane transporter translocation from cytoplasmic vesicles to the apical plasma membrane may be important also in the hagfish.

NHE involvement in acid–base regulation has been traditionally proposed for seawater animals (Claiborne et al., 2002; Claiborne et al., 1997; Edwards et al., 2001; Edwards et al., 2002; Evans et al., 2005). However, determining the subcellular localization of both NHE2 L-IR and NHE3 L-IR has been difficult because of granular cytoplasmic staining in several marine elasmobranchs and teleosts (Catches, 2004; Edwards et al., 2002), thereby hindering conclusions about its specific function. More recently, species-specific antibodies were used to demonstrate NHE2 localization in the apical region of certain gill cells of the longhorn sculpin (*Myoxocephalus octodecemspinosus* (Catches et al., 2006). However, confocal microscopy showed that NHE was not located directly on the membrane and that the NHE signal was punctuated and in the cytoplasm in most immunoreactive cells. In addition, the abundance of this NHE did not change in response to

four sequential intraperitoneal HCl infusions over an 8 h period. Nonetheless, the authors proposed that NHE2-containing vesicles move to the apical membrane during blood acidosis to secrete the excess H^+. Finally, apical, cytoplasmic, and (or) basolateral NHE localization have been seen in the gill of the Pacific spiny dogfish (Weakley, 2003), as well as in a variety of mammalian tissues (Wakabayashi et al., 1997). My observation of an increased NHE2 L-IR at the apical plasma membrane region under acid-stressed conditions and increased abundance in gill membranes suggests a role for NHE relocation and involvement in acid secretion for the hagfish.

In this study an antibody raised against rabbit NHE2 was used and there is the potential for cross-reactivity with other NHE isoforms. The amino acid identity of available fish NHE2 sequences compared with the rabbit NHE2 ranges from 37% (zebrafish) to 63% (Pacific spiny dogfish). Comparing the C-terminal 87 amino acid region of rabbit NHE2 where the antibody was raised with the C-terminal region of the Pacific spiny dogfish NHE2, there is a stretch of 25 amino acids that are 50% identical (excluding gaps) and 68% similar when conserved substitutions are taken into account. I believe that this could be a region of potential cross-reactivity, which allows the polyclonal antibody to bind the NHE proteins in both mammals and fish. The sequence homology of the hagfish NHE2 with the rabbit antibody used is unknown and this molecular information needs to be pursued in further studies. To date, only a partial NHE clone has been obtained from the Atlantic hagfish (Edwards et al., 2001). The hagfish NHE was not closely related to any other

vertebrate isoforms but was seen to group closest to the mammalian NHE3 and the invertebrate NHE (Edwards et al., 2001). This putative NHE was implicated in acid recovery though, as there was a significant increase in NHE mRNA expression at 2 h post acid infusion. Conversely, NHE2 (Tresguerres et al., 2006b) and NHE1 and NHE3 (Choe et al., 2002) immunoreactivity have been shown previously in hagfish using mammalian antibodies. This coupled with the apical localization of NHE3 seen in Atlantic stingray, *Dasyatis Sabina* (Choe et al., 2005), and Pacific spiny dogfish (Choe et al., 2007) using an elesmobranch-specific antibody make it possible that my results represent an increase and translocation of a NHE similar to NHE3. However, it is also conceivable that the observed changes in expression are due to multiple NHE isoforms of an identical molecular weight being detected and differentially regulated during acidosis. Unfortunately, I cannot determine using the techniques of this study if this has occurred.

Recent research into acid–base regulatory mechanisms in both elasmobranchs (Piermarini and Evans, 2001; Tresguerres et al., 2005) and teleosts (Catches et al., 2006; Choe et al., 2005; Galvez et al., 2002; Goss et al., 2001a; Parks et al., 2007b; Reid et al., 2003) suggest that independent cell types exist for net acid and net base secretions. However, based on the data presented in this chapter and previous research from our laboratory (Tresguerres et al., 2006b), it appears that hagfish possess only a single MR cell type. This cell must perform either net H^+ or net HCO_3^- secretion as required, creating unique demands for subcellular control over surface

expression of transporters. The data from this chapter leads me to hypothesize that the H^+-transporting NHEs are normally sequestered into vesicles. During acidosis, the response of increasing synthesis of NHE (genomic response) must be coupled with the insertion of new and existing NHEs into the apical membrane (post-translational response), and together this would ensure that acid secretion dominates over base secretion under these conditions. This complements well with our study demonstrating differential insertion of Na^+/K^+-ATPase and H^+-ATPase in response to blood alkalosis at the hagfish gill to allow net base secretion (see appendix II and (Tresguerres et al., 2007a)).

In summary, I have demonstrated that Pacific hagfish can restore blood pH following an induced metabolic acidosis. This ability is likely enabled *via* the increased synthesis of a NHE-like protein in the gill coupled with an apparent translocation of this transporter to the apical region of the gill cells.

Tables

Table 9. 1 Plasma [Na^+] ($mmol \cdot L^{-1}$) of the experimental Pacific hagfish (*Eptatretus stoutii*) at the sampling times.

Time (h)	(NaCl Infused)	(HCl Infused)
0	473.67 ± 11.59	468.03 ± 5.42
3	473.78 ± 8.63	436.19 ± 16.61#
6	470.88 ± 7.81	458.05 ± 10.67
9	517.89 ± 9.34*	505.90 ± 9.43*
12	529.64 ± 5.62*	520.73 ± 4.05*
18	522.35 ± 9.29*	506.14 ± 3.38*
24	531.02 ± 8.89*	534.29 ± 9.18*

Note: Values are means ± s.e.m (*N*=5) from both NaCl and HCl infused treatments. # indicates significant differences between treatments for the given time point (2-way-RM-ANOVA, Boneferroni post test, $p<0.05$). * indicate significant differences from $t=0$ h within each treatment (1-way-RM-ANOVA, Dunnett's post test, $p<0.05$).

Table 9. 2 NHE2 L-IR staining patterns from NaCl-infused (control) and HCl-infused Pacific hagfish following 24 h experiments.

	Cytoplasmic (%)	Intermediate (%)	Apical (%)
NaCl	73 ± 2*	20 ± 2	7 ± 3
HCl	54 ± 5	19 ± 2	27 ± 5*

Note: Descriptions of the staining patterns are found in results and figure 4. * indicate values that are significantly higher between treatment groups (p<0.05, Man Whitney one-tailed test) (N=3).

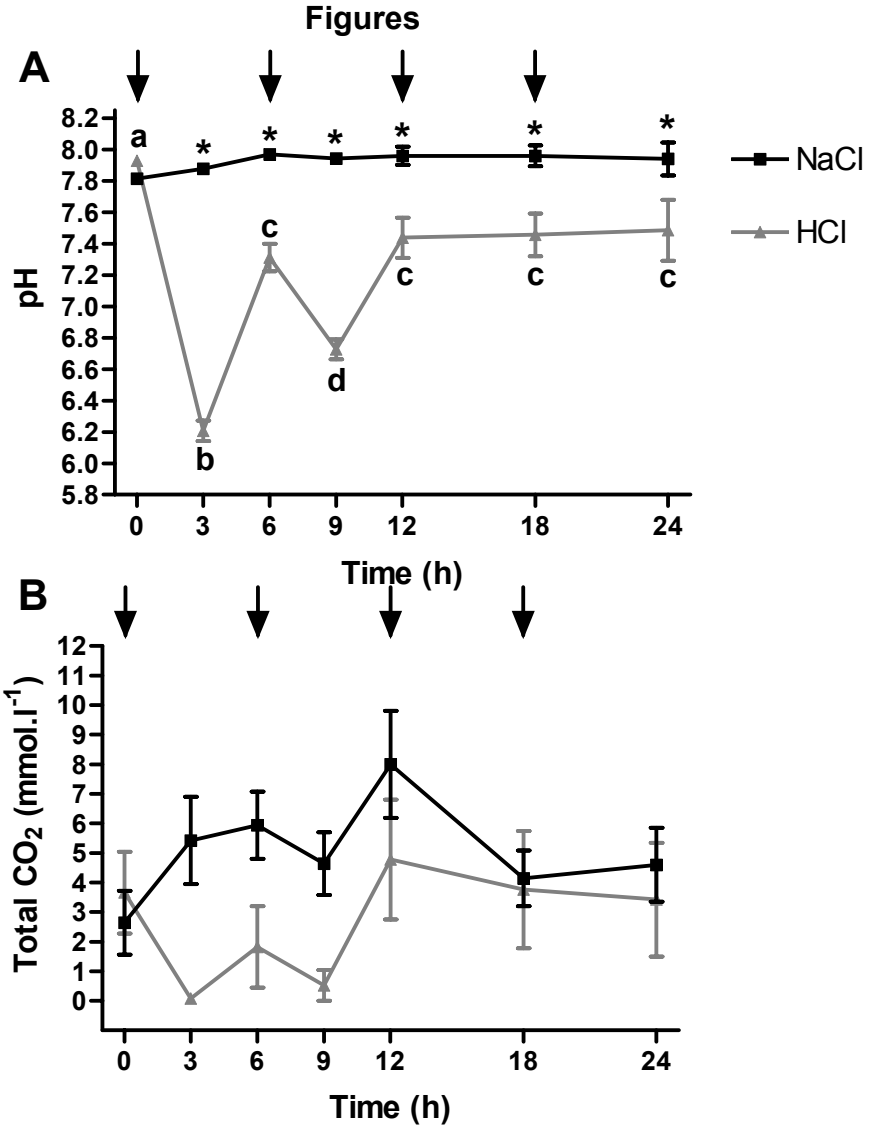

Figure 9. 1 Blood parameters of Pacific hagfish (*Eptatretus stoutii*) injected with either 250 mmol·L^{-1} HCl (6000 µequiv.·kg^{-1}) or an equivalent volume of 500 mmol·L^{-1} NaCl (mean ± SE, *N* = 5).

A Blood pH. Asterisks indicate significant differences between the experimental values (HCl-infused) and control values (NaCl-infused) for the respective time period (two-way RM ANOVA, Bonferroni post hoc test, $p < 0.05$, $N = 5$). Letters indicate significant differences within the HCl-infused group only to analyze the kinetics of the acid-recovery period (one-way RM ANOVA, Bonferroni post hoc test, $p < 0.05$, $N = 5$). ***B*** Plasma total [CO_2].

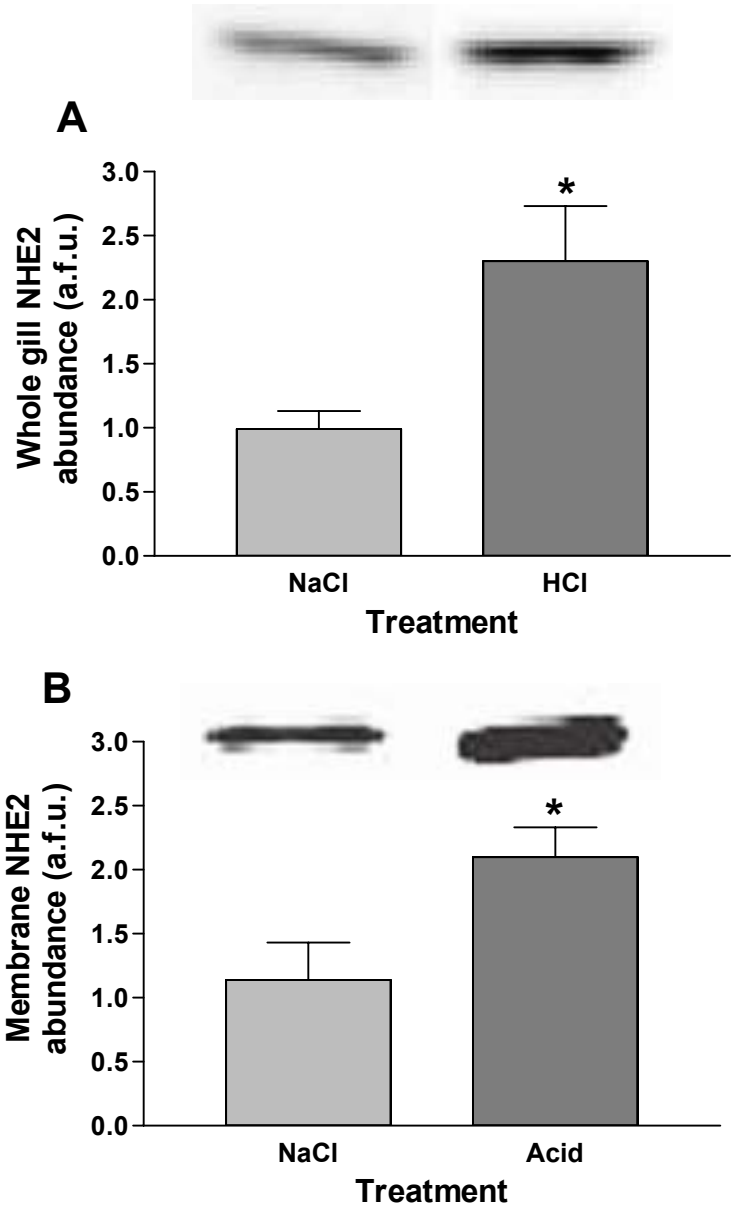

Figure 9. 2 Na^+/H^+ exchanger 2 (NHE2) like abundance

Representative Western blots of whole-gill ***A*** and whole-membrane ***B*** fractions from NaCl- and HCl-infused Pacific hagfish. Asterisks represent significant differences from control (NaCl) values (Student's *t* test, $p < 0.05$, $N = 5$).

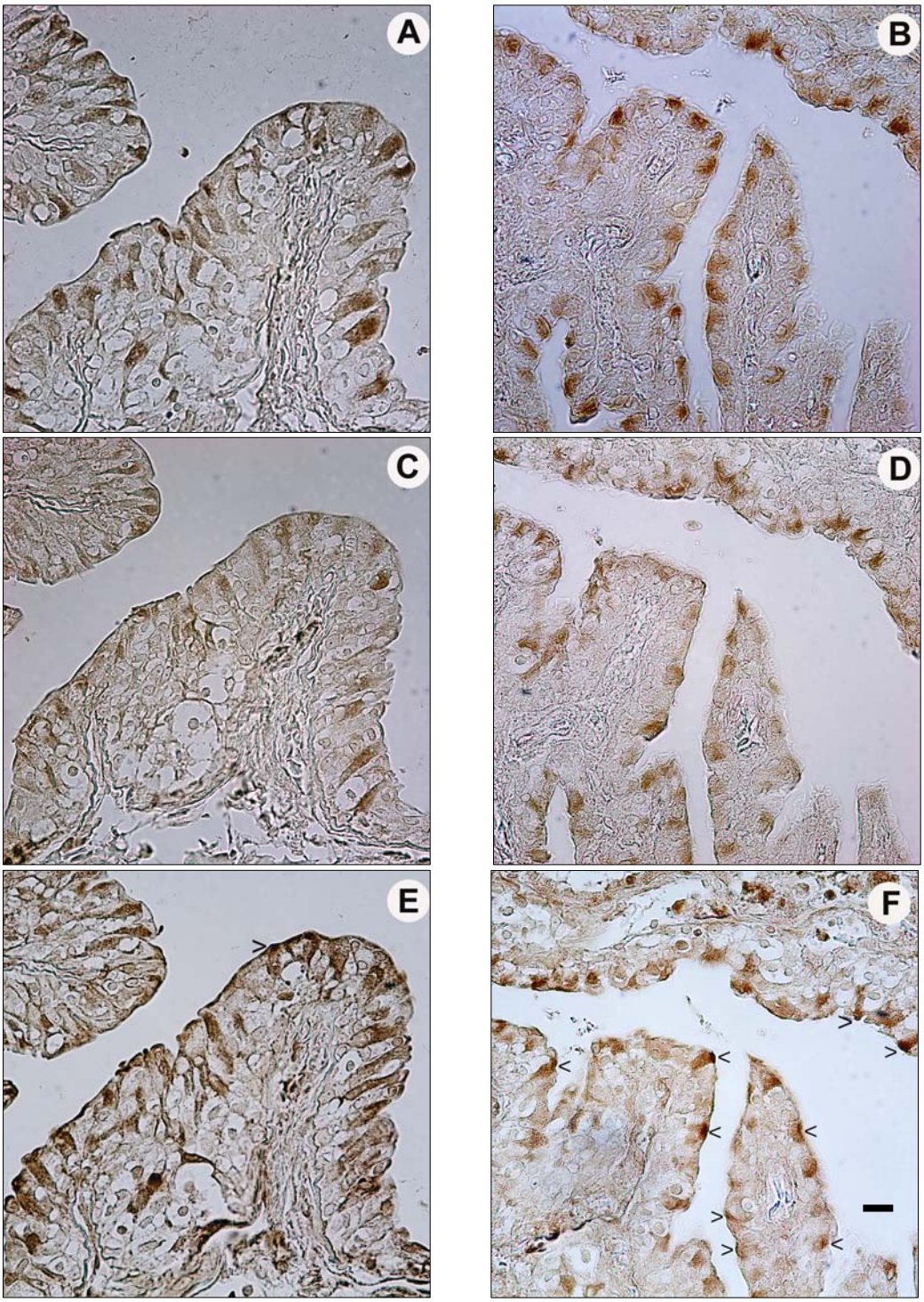

Figure 9. 3 Immunohistochemistry of NKA, VHA, and NHE2 in Pacific hagfish gills.
Na^+/K^+-ATPase (***A***, ***B***), V-H^+-ATPase (***C***, ***D***), and NHE2 L-IR (E, F) in consecutive sections from NaCl- (***A***, ***C***, ***E***) and HCl- (***B***, ***D***, ***F***) infused Pacific hagfish. Labelling patterns remain unaltered for Na^+/K^+-ATPase and V-H^+-ATPase in response to HCl infusions, whereas NHE2 L-IR demonstrates a marked redistribution to the apical region of the cells as indicated by the arrows in ***F***. Scale bar = 10 µm

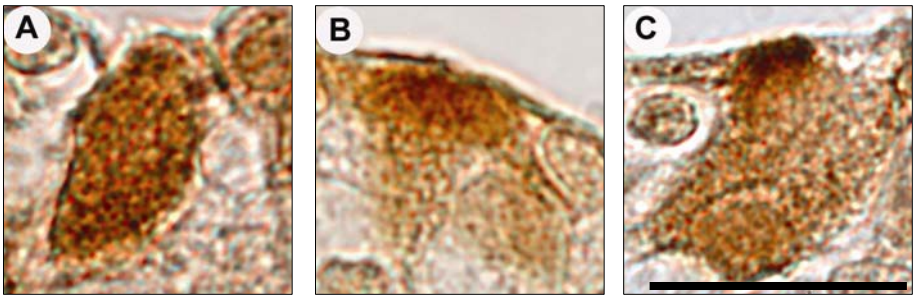

Figure 9. 4 High-magnification (1600×) analysis of NHE2 immunoreactivity Pictures showing the stereotypical NHE2 L-IR pattern for cytoplasmic ***A***, intermediate ***B***, and apical ***C*** localization as quantified in Table 2. Scale bar = 10 µm.

Chapter X: Extremely high pH_i in the anterior midgut of the yellow fever mosquito

[1]A version of this chapter has been accepted for publication

Onken, H., **Parks, S.K.**, Goss, G.G., and Moffett, D.F. Serotonin-induced high intracellular pH aids in alkali secretion in the anterior midgut of larval yellow fever mosquito *Aedes aegypti L.* Accepted for publication on May 21, 2009 by the Journal of Experimental Biology MS ID#: JEXBIO/2009/030221.

Note: This work was carried out in collaboration with Dr. Horst Onken and Dr. David Moffett in our laboratory at the University of Alberta. I contributed to the intracellular pH observations of larval midgut cells as mentioned in this chapter. This included hypothesis development, data analysis, carrying out the actual experiments following sample preparation via Drs. Onken and Moffett, thermodynamic analysis, and manuscript preparation. The other components of the study that were performed elsewhere are referenced in the discussion.

Introduction

The anterior midgut (anterior stomach) of the larval mosquito is responsible for generating a luminal pH that may be greater than 10, as demonstrated first in intact animals by colorimetric methods using ingested pH indicator (Dadd, 1975) and later confirmed by H^+ sensitive microelectrode studies (Onken et al., 2008). The mechanisms of base secretion and/or acid absorption involved have been studied with intact larvae, with semi-intact preparations (Boudko et al., 2001a; Boudko et al., 2001b) and with fully isolated, perfused gut segments (Onken et al., 2008). Immunohistochemical observations (Zhuang et al., 1999) as well as the results of studies with intact and semi-intact larvae have led to the general hypothesis that alkali secretion is energized by a basolateral V-type proton ATPase (Boudko et al., 2001b), in combination with an apical Cl^-/HCO_3^- exchanger (Boudko et al., 2001a). A challenge for the latter part of the hypothesis is presented by the fact that direct HCO_3^- secretion alone can generate only a moderately alkaline pH of about 8.5. Therefore, attaining luminal pH values >10 as reported for the larval mosquito midgut would be impossible by a simple exchange of Cl^- for HCO_3^-. Consequently, it was hypothesized that achieving these high luminal pH values would require a secondary uptake of H^+ from the lumen following HCO_3^- secretion. Another alternative that is as yet unexplored is the possibility that direct secretion of CO_3^{2-}, *per se* could also accomplish a high luminal pH. However, this possibility has always been considered unlikely due to the very low amounts of CO_3^{2-} present at normal intracellular pH (pH_i) values.

In isolated and perfused midgut preparations, the transepithelial potential (V_{te}) declines to a small, usually lumen-negative value within minutes after the onset of perfusion with control saline (Clark et al., 1999; Clark et al., 2000). Luminal alkalinization under these conditions is very slow and hardly detectable (Onken et al., 2008). Application of submicromolar serotonin causes a sustained increase in the V_{te} to values of the order of 10 - 40 mV lumen-negative. This response is maximal in about 20 minutes and is accompanied by a significant stimulation of luminal alkalinization, as measured in stopflow experiments using pH indicator dye or H^+-selective microelectrodes (Onken et al., 2008). Both the electrical and chemical responses are reversible on washout of serotonin. It is probable that serotonin is the major natural exogenous excitatory stimulus for epithelial transport and motility in the midgut, and the gut indeed receives a rich serotonergic innervation (Moffett and Moffett, 2005). On the other hand, roles for other substances, either as intermediators or modulators, are also likely since the gut also has a substantial population of enteroendocrine cells, and modulatory effects of some neuropeptides have been reported (Onken et al., 2004).

The present studies were performed to determine the consequences of stimulation of alkali secretion on the intracellular pH (pH_i) and to evaluate the possibility of passive, conductive uptake of H^+ across the apical membrane as part of this process.

Results

pH_i of anterior and posterior midgut cells under baseline conditions, and the effect of serotonin

In these experiments, the hemolymph-side of the tissue was superfused with standard mosquito saline while the lumen was perfused with 100 mmol l^{-1} NaCl buffered to pH 7.0. . In 71 regions of 10 anterior stomach preparations the average pH_i was found to be 6.89 ± 0.15 (N = 10, ± S.E.M.), whereas the average intracellular pH was 6.87 ± 0.28 (N = 4; ± S.E.M.) in 19 regions of 4 posterior stomach preparations.

Addition of serotonin (0.2 µmol l^{-1}) led to a sustained increase in pH_i in the anterior midgut, from the control mean of 6.89 ± 0.15 to 7.62 ± 0.15 (N = 10, ± S.E.M.; $P < 0.05$). A representative time course of pH_i after serotonin is shown in Fig 10.2. In many cases, pH_i values exceeded 8 – the maximal value recorded was 8.66. The time-course of the pH_i rise was similar to that of the V_{te} response recorded in previous studies (Clark et al., 1999). In contrast, in the four experiments in which measurements were made simultaneously from the posterior midgut, either no significant changes, or modest acidifications of pH_i, were observed (see Fig. 10.2A+B). In the posterior regions pH_i before and after addition of serotonin was 6.87 ± 0.28 and 6.94 ± 0.25 (N = 4, ± S.E.M.; $P > 0.05$).

pH_i response to luminal pH = 10.0 in presence and absence of luminal Zn^{2+}

In these experiments, the lumen was initially perfused with 100 mM NaCl buffered to pH 7.0. After the stability of the preparation was established, serotonin was added to the bath. Following the maximal effect of serotonin, the luminal perfusate was changed to pH 10.0 (buffered with 10 mmol l^{-1} TRIS; 'alkaline luminal perfusate') which would be more typical of physiological conditions in an *in vivo* stimulated gut. A typical experiment is shown in Fig. 10.3A. For 41 areas from 4 tissues the mean pH_i with serotonin was 7.77 ± 0.12 (N = 4, ± S.E.M.) and significantly rose to 8.58 ± 0.14 (N = 4, ± S.E.M.) with alkaline luminal perfusate ($P < 0.05$; see Fig. 10.3B). The highest value recorded was 10.04. It is important to mention here that the pH-dependence of the fluorescence excitation spectrum of BCECF-AM becomes non-linear above a pH of 8.6. Therefore, results above a pH value of 8.6 should be interpreted with cautions as accurate calibrations are not possible. We can only interpret these results as being above a pH of 8.6. Unfortunately, there are no dyes available for accurate ratiometric pH imaging in the high pH range.

To test the potential involvement of inward-directed H^+ conductive channels in the alkalinization of the lumen we performed three additional experiments where the luminal perfusate was pH = 10 and 22 total areas of interest were monitored. $ZnCl_2$ (10 µmol l^{-1}) was included in the alkaline luminal perfusate as a blocker of H^+ channels (DeCoursey, 2003). In these experiments, the mean control value with serotonin was 7.11 ± 0.19 (N = 3, ±

S.E.M.) and after change to alkaline (pH = 10) luminal perfusate in the presence of Zn^{2+}, the mean pH_i attained was 8.18 ± 0.19 (N = 3, ± S.E.M.). The change in pH_i in response to alkaline luminal perfusate in the presence of Zn^{2+} was not significantly different from those recorded in the absence of Zn^{2+} ($P > 0.05$). Furthermore, the rate of increase of pH_i after changing to alkaline luminal perfusate was also not affected ($P > 0.05$) by the presence of Zn^{2+} (see Fig. 10.4A).

Discussion

Methodological aspects

The magnitude of the apparent change in pH_i generated in the serotonin response appears to violate the principle of homeostasis of the intracellular milieu, and a careful consideration of its veracity is in order. In principle, the fluorescence changes reported here could arise as an artifact, in the absence of an actual general cytoplasmic pH change, in two ways. First, the BCECF indicator dye might have become concentrated in an intracellular sub-compartment which then became extremely alkaline as an effect of serotonin, or second, the dye might be secreted or simply leak out of the cells, and accumulate in an extracellular region that became alkaline as a result of the effect of serotonin. However, neither of these possibilities seems tenable. In the first case, the dye compartment giving rise to the artifact would have to represent a significant fraction of the total dye contributing to the optical signal. In preliminary studies conducted at high magnification, no brightly fluorescing intracellular entities were noted in the dye-loaded tissue, although some individual cells appeared to load dye more readily than others. Additionally, the intercellular spaces were not seen to fluoresce brightly in comparison to the cellular interiors, suggesting that alkaline compartments in the cell would not contribute to the observed alkalinization of pH_i. In the second case, accumulation of the dye in the luminal solution would presumably not be a source of optical signal, especially during continuous luminal perfusion. Moreover, experiments where we performed stops and

restarting of perfusion were never accompanied by a change in fluorescence intensity, suggesting that, if dye were transported to the gut lumen, it did not result in any significant signal relative to the cytoplasmic pool of BCECF. The epithelial cells in the anterior midgut do not have a brush border. Only relatively sparse and short microvilli were observed (Clark et al., 2005). Consequently, entrapment of dye in an extracellular space formed by a thick brush border can be excluded.

Another significant aspect that bears consideration is that BCECF fluorescence approaches maximum intensity at pH values above pH 8.6 and extremely alkaline pH_i values should be interpreted with caution. In our experiments, this resulted in a very cautious interpretation of pH_i in the cytoplasm of serotonin stimulated cells, especially during high luminal pH perfusion. Unfortunately, no such dye exists and the development of pH sensitive indicators with an alkaline pK is necessary for accurate assessment of pH_i in this unique tissue.

Extremely alkaline intracellular pH in larval mosquito midgut cells

In the absence of serotonin the pH_i of anterior and posterior midgut cells is neutral to slightly acidic, as has been observed in many other tissues. In the anterior midgut, addition of serotonin results in a significant alkalinization of the intracellular medium, whereas the posterior midgut cells do not respond to serotonin with a pH_i change (see Fig. 10.2A+B). Consequently, the increase of pH_i seems to be a specific response of the cells responsible for luminal alkalinization. Under more *in vivo*-like conditions,

namely in the presence of an alkaline lumen, the pH_i was observed to be between 8 and 9. To our knowledge intracellular pH values of this magnitude have never been observed before. At first sight this observation appears surprising given the dogma of the necessity for pH_i to be highly regulated for proper metabolic function. However, this epithelial tissue is quite unique in that it is responsible for generating an extremely alkaline secretion and an alkaline intracellular medium is likely of mechanistic importance. If the cells have a conventional pH_i of about 7, the whole transepithelial pH gradient of over 3 orders of magnitude would be carried by only the apical membrane that faces the extremely alkaline midgut lumen. By generating (and tolerating) a very alkaline intracellular medium the transepithelial pH gradient is separated into two smaller steps at the basolateral and apical membranes. Knowing that basolateral V-type H^+-ATPases are activated by serotonin and a necessary component of luminal alkalinization (Onken et al., 2008), we can assume that activation of the basolateral V-ATPases is responsible for generating the pH gradient across the basolateral membrane.

Proton-motive forces across the basolateral and apical membranes

From our measurements of intracellular pH (this chapter's data) and transmembrane voltages (Horst Onken and David Moffett data not shown) we can calculate the independent proton-motive forces for the basolateral and apical membranes in the presence of serotonin for two different conditions: i) at a luminal pH of 7, and ii) at a more *in vivo*-like luminal pH of 10. At a neutral pH on both sides of the epithelium, proton-motive forces of above 100

mV dominate both membranes, favoring passive H^+ movements from the extracellular solutions into the cell. In the presence of an alkaline lumen, the transbasal proton-motive force is huge, almost 190 mV, whereas the proton-motive force of the apical membrane is very small. The reversal potential of the V-ATPase, as estimated in various insect systems, is of the order of 120-180 mV (Beyenbach et al., 2000; Moffett, 1980; Moffett and Koch, 1988; Pannabecker et al., 1992). Thus, the proton-motive force across the basolateral membrane can be explained on the basis of H^+-pumping by V-ATPases in this membrane. Of course, it is informative to analyze how the tissue can move from one state to the other, generating an alkaline luminal pH. A controlled opening of a conductive pathway for H^+ in the apical membrane could make use of the transapical proton-motive force at neutral pH for transapical H^+ absorption until H^+ is in equilibrium at a very alkaline midgut lumen. Whereas the present study addressed the conductive pathway in the apical membrane (see below), one question that needs to be addressed in future studies is what determines the transapical voltage under control conditions that is responsible for the high driving force for H^+ at neutral pH in the lumen.

Implications of the results for the mechanism of strong midgut alkalinization

It seems to be well established that basolateral V-ATPase is driving transbasal H^+ absorption and the overall transepithelial acid/base-transport. Boudko and colleagues (Boudko et al., 2001a) analyzed anionic pathways in the apical membrane and proposed that apical Cl^-/HCO_3^- exchange acts to

alkalinize the anterior midgut lumen. However, in the isolated tissue, neither DIDS nor Cl^--free salines affected the capability of the tissue for strong luminal alkalinization (Onken et al., 2008). Based on immunohistochemical observations, Okech and colleagues (Okech et al., 2008) proposed the presence of acid absorption *via* electrogenic cation/2 H^+ exchangers in the apical membrane. Indeed, the present studies (and electrical recordings not shown) show that there would be a driving force of approximately 100 mV which is sufficient for a $2H^+/Na^+$ exchanger (see below). However, in previous experiments (Onken et al., 2008) luminal amiloride did not inhibit luminal alkalinization. Of course, if the transporter mediated $K^+/2H^+$ exchange, the driving forces would be favorable for both ions. However, in the same study, Onken and colleagues (Onken et al., 2008) found that an increased luminal K^+ concentration, reducing the driving force for the exchange, did also not impair luminal alkalinization. Therefore, in the present study we addressed the possibility of transapical absorption of H^+ through H^+ channels. The theory is that the cell would excrete HCO_3^- followed by dissociation in the lumen and apical resorbtion *via* an apical H^+ channel. However, micromolar Zn^{2+}, used at concentrations known to block different H^+ conductances (DeCoursey, 2003) did not significantly affect the pH_i change or the transepithelial voltage (see Fig. 10.4). Moreover, the presence of luminal Zn^{2+} did not prevent luminal alkalinization (Horst Onken and David Moffett data not shown). We recognize that negative results in pharmacological approaches are not necessarily conclusive. However, it could be expected that in the presence of H^+ channels

a membrane would respond with significant voltage changes to alterations of the transmembrane pH gradient. Since no such changes were observed in microelectrode experiments (Horst Onken and David Moffett data not shown), this suggests that apical H^+ channels have no importance for H^+ absorption and strong alkalinization in this tissue.

Carbonic anhydrase is apparently not present in the cells of the anterior midgut of *Aedes aegypti* (Corena et al., 2002) and inhibitors of this enzyme were not effective to impede luminal alkalinization *in vitro* (Onken et al., 2008). After finding the considerably alkaline pH_i the missing cellular carbonic anhydrase is less surprising, because high pH_i values should accelerate the hydration of CO_2 and the dissociation of carbonic acid, reducing the usefulness of cellular CA. Smith and colleagues (Smith et al., 2007) have observed extracellular carbonic anhydrase in the ectoperitrophic space of larval malaria mosquitoes (*Anopheles gambiae*), and this suggests that extracellular conversion of CO_2 to HCO_3^-/CO_3^{2-} and absorption of protons is involved in luminal alkalinization in this species. However, an extracellular carbonic anhydrase has not been found in *Aedes aegypti* and the addition of inhibitors of carbonic anhydrase to the holding water did not prevent the living larvae from alkalinizing their anterior midguts (Horst Onken and David Moffett unpublished observation). If secretion of either HCO_3^- or CO_3^{2-} turns out to be an important component of luminal alkalinization, the source of this HCO_3^-/CO_3^{2-} must be addressed in future studies. Instead of respiratory CO_2 from carbohydrate or lipid catabolism, HCO_3^- from amino acid catabolism is also a

candidate that must be addressed in the absence of measureable CA activity (Fry and Karet, 2007). The latter hypothesis is especially attractive, because amino acid catabolism also produces ammonia which has been found at high concentrations in the mosquito hemolymph (Edwards, 1982a).

Implications of the results for future studies

In a previous study of strong alkalinization in isolated and perfused midgut preparations (Onken et al., 2008) no experimental support was found for the anionic (DIDS-sensitive Cl^-/HCO_3^- exchange) or cationic (amiloride-sensitive cation/H^+ exchange) pathways in the apical membrane that had been proposed on the basis of results obtained with intact or semi-intact larvae (Boudko et al., 2001a; Okech et al., 2008). Future studies with isolated tissues should consider that both pathways may be present, but equally potent to generate strong luminal alkalinization. Thus, experiments that impede both mechanisms at the same time should be conducted.

The results presented herein suggested that perhaps a novel mechanism for alkalinization of the lumen is present in this tissue. In Fig 10.5, two possible models for net alkali secretion are presented that could be present in the anterior midgut of the larval mosquito. The results of this chapter cannot differentiate between these two possibilities and therefore I will discuss each of these potential models separately.

In the first model, the main novel aspect is the proposal for direct CO_3^{2-} secretion via either an apical Na^+/CO_3^{2-} co-transporter (NBC) or via a novel $Na^+/HCO_3^-/CO_3^{2-}$ co-transporter (NBCC) operating in export mode. To our

knowledge, there are no other reports of an NBC functioning in this particular mode (NBCC) simply due to the relative paucity of intracellular [CO_3^{2-}] present in the cells. We have only represented NBCC in the proposed model for clarity (Fig. 10.5A). It is extremely important to consider that fundamental thermodynamic principles support the possibility that our models can operate in the stimulated tissues (see chapter II: (Parks et al., 2008)). It would be highly advantageous for the tissue to directly secrete CO_3^{2-} as this would negate the requirement for potentially deleterious H^+ import mechanisms. The following equation describes the equilibrium point for the net driving forces for a novel electrogenic NBCC as a function of the intra and extracellular concentrations CO_3^{2-}, HCO_3^- and Na^+.

$$\mu_m = FV_m + RT\ln\frac{[Na^+]_i}{[Na^+]_L} + FV_m + RT\ln\frac{[HCO_3^-]_i}{[HCO_3^-]_L} + 2FV_m + 2RT\ln\frac{[CO_3^{2-}]_i}{[CO_3^{2-}]_L}$$

(Equation 10.1)

The total CO_2 in the lumen under stimulated conditions has been measured at 58 mM and the measured intracellular total CO_2 was ~50 mM (Boudko et al., 2001a). Since the pK of the reaction $HCO_3^- \rightarrow CO_3^{2-} + H^+$ is 10.3, we can therefore set the pH of the luminal solution at pH=10.3 and assume that the composition of the luminal fluid to be in equilibrium at 29 mM CO_3^{2-} and 29 mM HCO_3^-. We also know that the measured value for $[Na^+]_i$ is 10 mM (Boudko et al., 2001a) and the luminal [Na^+] in our perfusate is 100 mM Na^+. Additionally, the V_{api} has been measuered to be ~-90 mV (Horst Onken and David Moffett data not shown). Rearranging the above equation

and solving for the required intracellular carbonate levels required to drive the transport yields the following equation:

$$[CO_3^{2-}]_i = [CO_3^{2-}]_L * \sqrt{\frac{[Na^+]_L}{[Na^+]_i}} * \sqrt{\frac{[HCO_3^-]_L}{[HCO_3^-]_i}} * e^{[FV_m/RT]}$$ (Equation 10.2)

At a resting pH_i of 7.0 (measured in this experiment) and a measured intracellular total CO_2 of 50.1 mM (Boudko et al., 2001a), we can calculate the relative amounts of CO_3^{2-} present using the Henderson-Hasselbalch equation. There would only be nominal amounts (~25 μM) of carbonate (CO_3^{2-}) present inside the cells at the resting pH_i. These concentrations would be completely insufficient to allow uphill transport of CO_3^{2-} into the solution present in the lumen. In fact, it would require an apical membrane potential of ~-204 mV to drive this transport. However, at a pH_i of 8.6, the estimated intracellular [CO_3^{2-}] will be ~1 mM, at pH_i = 8.8, it would be 1.6 mM while for pH_i = 9, the estimated intracellular [CO_3^{2-}] will be ~ 2.5 mM. It is important to note that intracellular [CO_3^{2-}] relative to overall measured total CO_2 will rise steeply as pH_i rises closer to its pK of 10.3.

Substituting the measured concentrations of ions into the equation above will yield the required intracellular [CO_3^{2-}] at the known membrane potential (-90 mV) to allow transport of CO_3^{2-} out of the cell. At the measured value of -90 mV, a $[CO_3^{2-}]_i$ of 2.03 mM would be required to drive transport out via a putative NBCC. This value could be achieved at a pH_i of 8.9 which is approximately within the ranges of pH_i in our experiments given the significant limitations placed on us by the dye (see above). At a slightly more

hyperpolarized V_{api} of -100 mV, the required $[CO_3^{2-}]_i$ would fall to 1.45 mM, or the value reached at pH_i = 8.77. Clearly, at these higher pH_i values as measured, the $[CO_3^{2-}]_i$ should become sufficient for direct CO_3^{2-} transport via a NBCC. Moreover, this clearly illuminates the need for an elevation of pH_i to aid in luminal alkalinization.

In the second model of secretion (see Fig. 10.5B), we suggest that the bulk of the base could be secreted as HCO_3^- via an apical Na^+/HCO_3^- co-transporter (NBC) working in export mode followed secondarily by net acid absorption *via* a cation/H^+ exchanger (see Fig. 10.5B). Such a mechanism has been proposed recently (Okech et al., 2008).

Direct evidence for an electrogenic Na^+/H^+ antiporter (NHA) is lacking in our studies; furthermore, a NHA localized in the anterior midgut of *Anopheles gambiae* apparently is not expressed to the plasma membrane (Rheault et al., 2007). We performed a thermodynamic analysis to determine if in fact it could function under the conditions found in the anterior midgut and if the noted intracellular alkalinization would favor the operation of this combined mechanism. The following equation describes the equilibrium point for the net driving forces for an electrogenic NHA as a function of the luminal pH and the membrane potential.

$$H^+_L = H^+_i * \sqrt{\frac{[Na^+]_i}{[Na^+]_L}} * e^{[FV_m/RT]} \quad \text{(Equation 10.3)}$$

Substitution of known parameters allows us to solve for the maximum luminal pH that can be generated to still enable the proper functioning of an NHA with varying pH_i. The results shown in Table 10.1 demonstrate that an

increase in pH_i directly favors higher pH_L values *via* the action of an apical NHA. At a pH_i of 7.0, the maximum luminal pH that can be generated would only be pH 9.0. However, a pH_i of 8.5 would allow for a pH_L of 10.52 which falls within measured values for both *in vivo* and *in vitro* studies of these parameters and demonstrates the necessity for intracellular alkalinization to achieve the high luminal pH values. As mentioned above we are limited in our ability to accurately measure pH_i above 8.6. However, in many traces, the noted fluorescence intensity was far above the highest calibration values suggesting that the pH_i of the anterior midgut does indeed reach levels far greater than 8.6. These extreme pH_i values would allow an even greater alkaline pH_L to exist.

An important task for the future is to identify and characterize those transporters that are responsible for the transapical voltage, because this is a significant component of the transapical proton-motive force (see above). Finally, our finding of an extremely high intracellular pH raises numerous questions about the challenges that this condition would place on other metabolic functions in this unique tissue and these questions will form the basis of future study.

Tables

Table 10. 1 Maximum pH_L attainable as a function of intracellular pH using an apical electrogenic NBC coupled to an NHA

The maximum pH_L attainable refers to the pH in the lumen that could still theoretically allow an electrogenic NHA to function in bringing H^+ into the cell from the lumen. These calculated values assume $[Na^+]_i$ = 10 mM, luminal Na^+ = 100 mM, and V_{api} = -90 mV.

pH_i	**Maximum pH_L attainable**
7.0	9.02
7.5	9.52
8.0	10.02
8.5	10.52
9.0	11.02

Figures

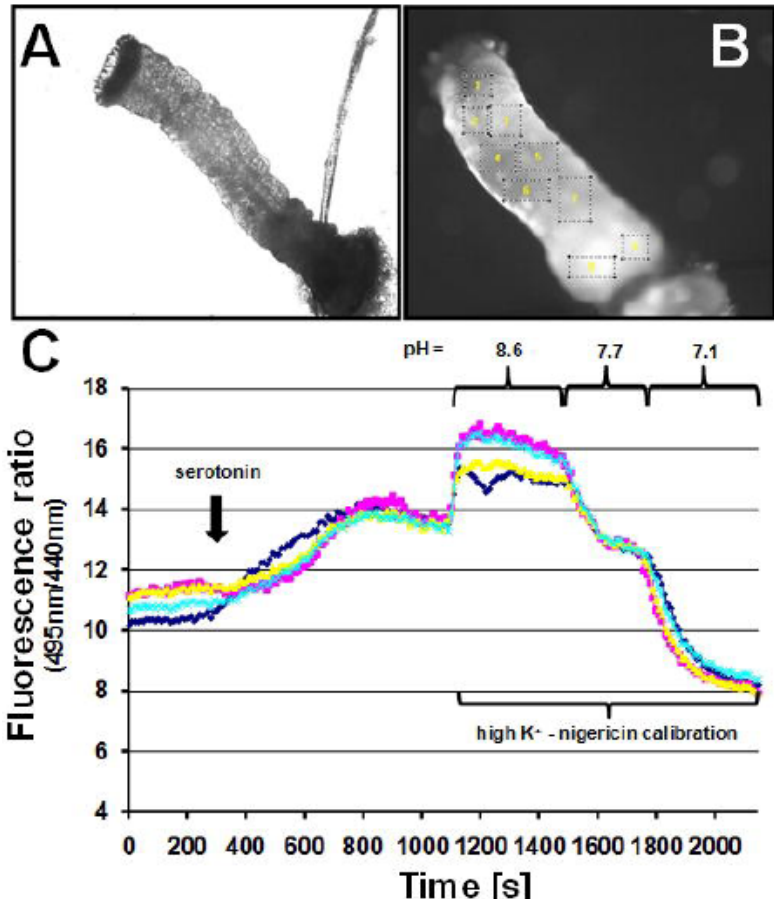

Figure 10. 1 Experimental set-up for pH_i monitoring of regions in the midgut of larval (4^{th} instar) *Aedes aegypti*.

A DIC image of the midgut preparation as observed on the experimental apparatus (scale bar 200 µm). ***B*** Corresponding fluorescence image (f495nm) of the same midgut from figure ***A*** following loading of the pH sensitive dye BCECF-AM. Dotted boxes represent regions of interest that were used to observe ratiometric fluorescence changes (scale bar 200 µm). ***C*** Representative traces of four regions of interest in the midgut and their corresponding fluorescence ratios (f495nm/f440nm) generated from excitation of cells loaded with BCECF-AM. This graph demonstrates the ability to observe changes in fluorescence ratios that can then be converted to pH_i values by using the high K^+-nigericin calibration for each individual cell.

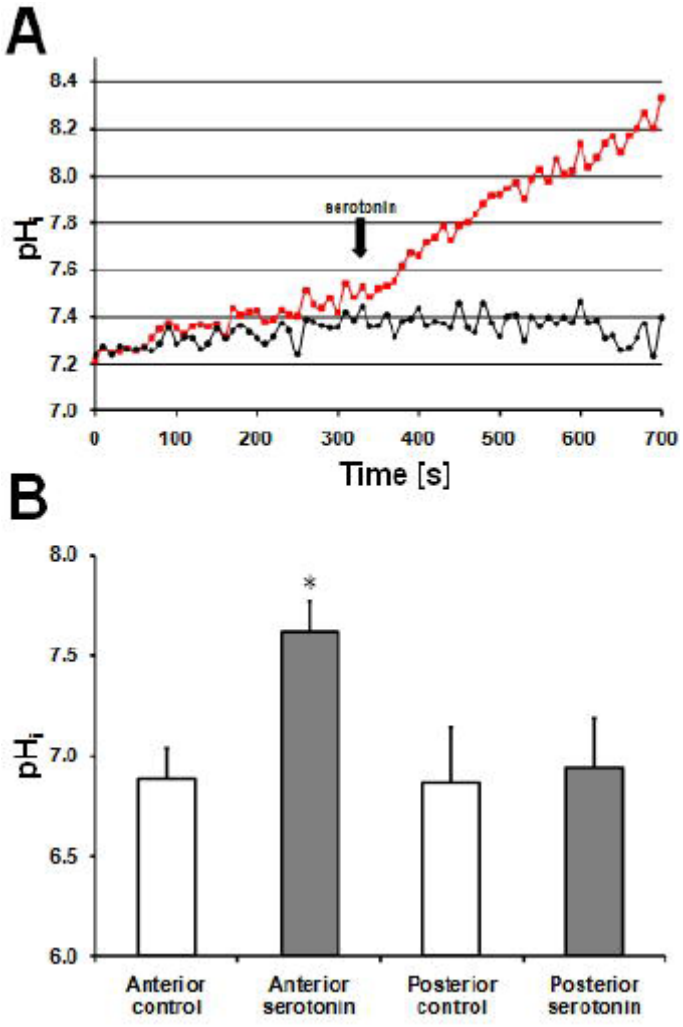

Figure 10. 2 Effects of serotonin on the intracellular pH (pH_i) in isolated and perfused anterior or posterior midguts.

A pH_i time-courses of representative areas of interest from the anterior (red) and posterior (black) midgut of larval (4th instar) *Aedes aegypti*, showing the influence of addition of 0.2 µmol l^{-1} of serotonin (arrow) to the hemolymph-side bath. Hemolymph-side bath: oxygenated mosquito saline (pH = 7). Luminal perfusate: NaCl (100 mmol l^{-1}, pH = 7). ***B*** Average pH_i values for anterior (N = 71 areas of interest of 10 different tissues) and posterior (N = 19 areas of interest of 4 different tissues) midguts before and after addition of serotonin.

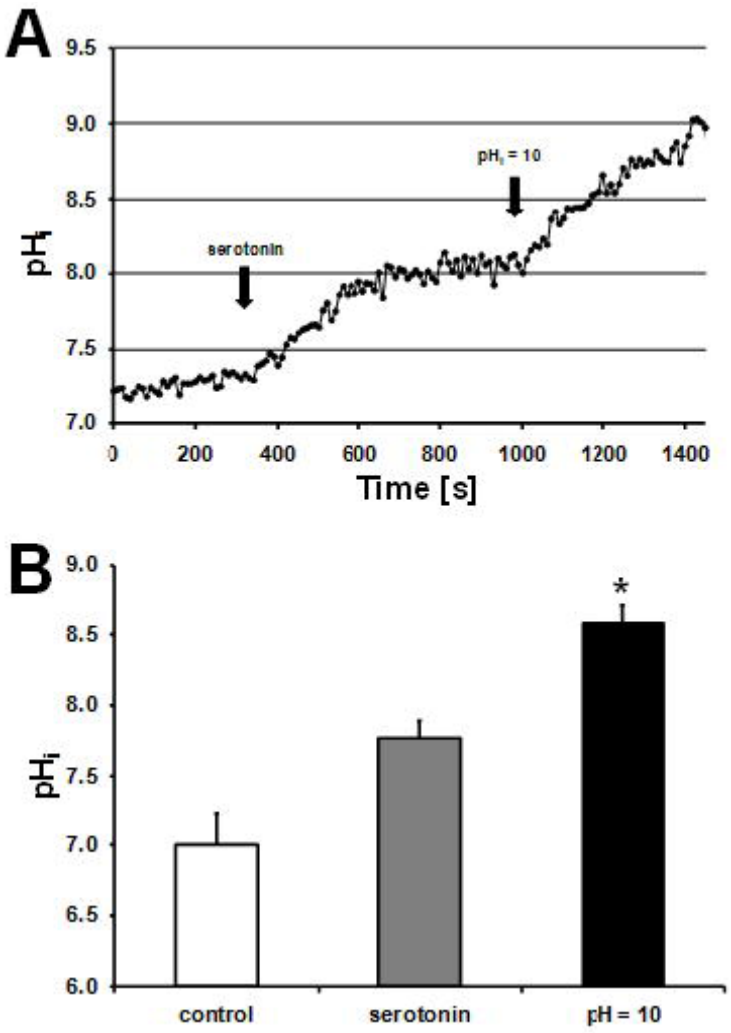

Figure 10. 3 Influence of luminal pH = 10 on pH_i in the anterior midgut.

A pH_i time-course of a representative area of interest from the anterior midgut of larval (4^{th} instar) *Aedes aegypti*, showing the influence of hemolymph-side addition of serotonin (0.2 µmol l^{-1}) in presence of hemolymph-side mosquito saline (pH = 7) and luminal NaCl (100 mmol l^{-1}, pH = 7), and the effect of an increase of the luminal pH (pH_l) to 10. ***B*** Average pH_i for anterior midguts (N = 41 areas of interest of 4 different tissues) under control conditions, after hemolymph-side addition of serotonin, and after switching to a luminal perfusate of pH = 10.

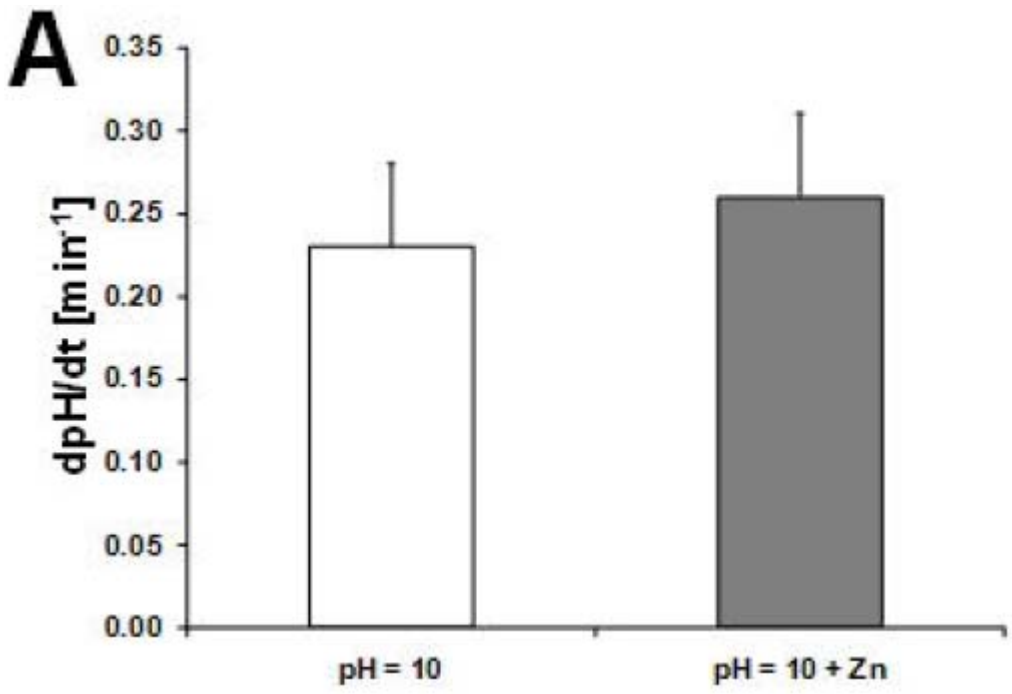

Figure 10. 4 Effect of luminal $ZnCl_2$ (10 µmol l^{-1}) on the rate of pH_i alkalinization after switching to luminal pH = 10 in the presence of serotonin Control: 41 areas of interest of 4 different tissues. In the presence of Zn^{2+}: 22 areas of interest from three different tissues.

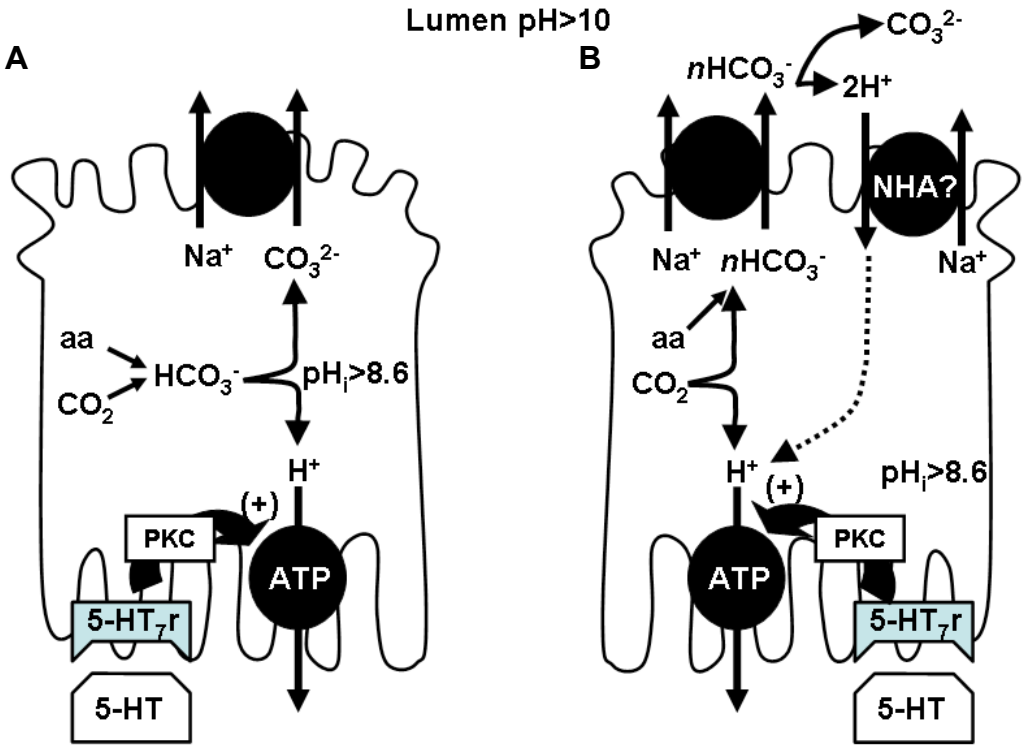

Figure 10. 5 Potential modes of transport in the anterior midgut of the mosquito *Aedes aegypti* used to achieve luminal alkalinization.

A Alkalinization of the lumen is achieved via an apical Na^+/CO_3^{2-} co-transporter of unknown stoichiometry. This process is initiated by 5-HT stimulation of basolateral H^+-ATPase pumping and an unusually high intracellular pH. CO_3^{2-} is proposed to be derived from either amino acid (aa) catabolism or CO_2 hydration and subsequent H^+ removal. ***B*** In this model, luminal alkalinization is achieved by the coordinated action of an apical electrogenic Na^+/HCO_3^- co-transporter of unknown stoichiometry (*n*) and an apical electrogenic Na^+/H^+ antiporter (NHA). Upon secretion into the lumen, HCO_3^- is converted to CO_3^{2-} and H^+ and the H^+ is re-absorbed into the cell via a NHA and then pumped across the basolateral membrane by the action of a basolateral H^+ ATPase. The other components of the model are the same as described for part A of this figure.

Chapter XI: General Discussion

General Summary

My thesis provides a comprehensive analysis of Na^+, H^+, Cl^-, and HCO_3^- transport in a variety of aquatic animals, with a principal focus on the function of gill MR cells. By investigating both the pH_i properties of isolated cells and whole animal responses to blood a/b disturbances my research has resulted in the significant advancement of our knowledge of ion and a/b transport. Although the bulk of my work was performed on rainbow trout, certain conclusions were strengthened using the isolated crab gill preparation, dogfish, or the primitive hagfish illustrating the power of a comparative approach. Finally, my collaborative research into the mechanisms of larval mosquito midgut cells pH_i behaviour has changed our thinking on how we interpret pH_i regulation and challenges long standing dogma in this area. By integrating these studies from a diverse range of animals I have been able to provide novel insights into our understanding of ion and a/b physiology.

Rainbow Trout and Neohelice granulata (South American Rainbow Crab)

Combining chapters II, IV, and VI-VIII I have provided a comprehensive model for both individual cell pH_i regulation and whole animal ion and a/b regulation in rainbow trout gill MR cells. While in chapter II, I laid out a detailed mathematical analysis of the thermodynamic constraints on ion transport in FW. These analyses have provided a framework for my data interpretations throughout the thesis and provide significant strength to the analysis. They also provide important considerations for what type of transporters could function theoretically in FW gill cells and have challenged

other researchers to critically evaluate their own models of transport to fit within these constraints. While we have yet to realize the complete gill ion transport model, new transporters are being added to it as the information becomes available and we are making progress in developing these models. Importantly, my research suggests that we need to use caution in the proposal of function of specific gill ion transporters based on presence or absence of a particular transporter alone.

The main finding of chapter IV was a novel model for transepithelial Na^+ uptake in FW fish. My data indicates that Na^+ moves into the blood across the basolateral membrane primarily *via* an electrogenic NBC as opposed to the exclusive use of NKA as had been originally thought for decades. This was shown in one functionally identified MR cell population only and gave the first distinct proof for two functionally different types of MR cells. I also support the use of an apical Na^+ channel as opposed to NHE in this chapter based on phenamil sensitivity and this led to my further research in chapter VI where I provide some insight into the possible Na^+ channel molecular identity.

In chapter V I presented data from work on the estuarine crab *N. granulata*. Using a properly polarized and intact gill epithelia preparation lead me to report that the crab uses the same Na^+ transport mechanism as described in chapter IV for trout.

In chapter VII, I transitioned into providing functional evidence for the Cl^- and HCO_3^- exchange mechanisms in trout gill cells. I described the first

functional evidence for CBE in isolated gill MR cells and also provided the first ever indication of a Cl^- dependent NHE in any fish species.

I rounded out my work on MR cell membrane transport by focusing specifically on pH_i recovery from acidosis in chapter VIII. These data provided interesting insights into the buffering capacity of these cells. I also proposed a basolateral NHE1-like transporter that requires PKC involvement for activation. These data are the first step in our understanding of cellular signaling mechanisms that control membrane transport in gill MR cells. This chapter also provides a direct linkage of functional behaviours to identified PNA^+ and PNA^- MR cell subtypes confirming my earlier description of functionally distinct MR cell subtypes based on differential pH_i responses to ion manipulation within a mixed population of MR cells.

The following paragraphs will expand on the major conclusions of my thesis and explore future directions that were not addressed in the individual data chapter discussions.

Na^+ transporting mechanisms

In this thesis, I have proposed models for Na^+ transport that involve Na^+ channels, NBCs (coupled to both HCO_3^- and potentially CO_2^{3-}), NHEs, and Cl^- dependent NHEs. Some of these mechanisms are involved in the directional movement of Na^+ across the cell while others appear to be used in pH_i regulation as represented in figure 11.1.

Transepithelial Na^+ uptake model

For years, Na^+ was thought to cross the basolateral membrane *via* the abundant NKA located there (Evans et al., 2005). This was not exclusive to fish however as only the HCO_3^- reabsorbing mechanism in the kidney was shown to transport Na^+ across the basolateral membrane in a way other than the NKA. There were a few studies indicating the role of basolateral NBC (Hirata et al., 2003; Perry et al., 2003a; Scott et al., 2005) leading up to my functional description that helped to interpret what was originally a confusing data set (as discussed in chapter IV). This mechanism of transepithelial Na^+ uptake (at least the basolateral portion) is now cited as the accepted model for the FW fish gill (Evans, 2008; Hwang and Lee, 2007; Katoh et al., 2008; Yan et al., 2007). The only molecular information for NBC in trout gill is from Perry's group (Perry et al., 2003a) and this area holds rich potential for future research. A trout specific NBC antibody needs to be developed to pair with gene expression studies at a whole animal level. These assays would be useful for analyzing various environmental conditions (pH and salinity) that either act to enhance or inhibit ion transport. In addition, a detailed immunogold transmission electron microscopy study of NBC subcellular localization in gill MR cells would help solidify its role in Na^+ transport. Furthermore, direct biochemical characterization of the amino-acid sequence in trout NBC should be performed. In the mammalian literature, there is a proposed metabolon arrangement with a physical linkage of CA to the C-terminal domains (Ct) of both the AEs and NBCs (Gross et al., 2002; Loiselle

et al., 2004; McMurtrie et al., 2004; Pushkin et al., 2004; Sterling et al., 2001; Vince et al., 2000; Vince and Reithmeier, 1998; Vince and Reithmeier, 2000). This association enhances the concentration gradient for HCO_3^- transport with CA providing a "shuttling" of substrate similar to the enzyme metabolons (for review see (McMurtrie et al., 2004)). However, this hypothesis has recently been disputed by Walter Boron's group (Lu et al., 2006; Piermarini et al., 2007b). Direct fusion of CA II to NBCe1-CT did not enhance NBCe1 current which is an index of HCO_3^- transport for this protein (Lu et al., 2006). Theoretical arguments were also presented indicating the unlikelihood of CA II acting to enhance HCO_3^- or CO_3^{2-} transport in a HCO_3^- driven system (Lu et al., 2006). Furthermore, the binding of pure SLC4-Ct (AE1) peptides (rather than GST fusion proteins) to CA II was not found to occur in any of the combinations tested (Piermarini et al., 2007b). These authors do not rule out the possibility of a HCO_3^- transporting metabolon *in vivo* but suggest it must occur in a different fashion than originally proposed. Since then, another CA isoform (CA IX) has been shown to bind to members of the AE family (Morgan et al., 2007) and the HCO_3^- transport metabolon hypothesis is still debatable. As I propose a metabolon-like model for trout (chapter IV), protein analysis of fish NBC will be necessary for the detailed understanding of transepithelial Na^+ uptake at the FW fish gill.

I attempted to look at NBC in hagfish gills using both immunohistochemistry and western blotting (data not shown). Although interesting staining patterns were noticed, particularly around the blood

vessels, the antibody specificity for hagfish was questionable and therefore strong conclusions could not be made. However, assessing NBC function in marine species such as the dogfish and hagfish will be important for understanding the universal nature of this Na^+ transporting mechanism. To my knowledge, the only information for NBC in any marine fish ion transporting mechanisms is from the pufferfish (*Takifugu obscurus*) intestine (Kurita et al., 2008). Nothing is known about its potential role in marine fish gill, kidney, or rectal gland ion transport and this is an area of research waiting to be exploited.

The other half of the proposed apical Na^+ uptake mechanism involves a VHA. Although VHA inhibitors are expensive, it would be useful to conduct specific experiments with isolated MR cells and the inhibition of VHA. These experiments would have to be carefully designed as with ion substitution and isolated cells, you essentially drive transport without the need of endogenous active transport mechanisms. Therefore, ion substitution control experiments would be required using low concentrations of ions to mimic a more realistic FW ion exposure. Following this VHA could be inhibited during the ion substitution to prevent Na^+ uptake from occurring. If this experimental setup requires VHA, inhibitors such as bafilomycin would be as effective in abolishing the Na^+ induced acidification as phenamil and DIDS were shown in chapter IV. PNA^+ and PNA^- MR cell identification will be necessary in these experiments to avoid confusing results as a basolateral and apical localization of VHA have been proposed for each cell type respectively (for review see

chapter II and (Tresguerres et al., 2006a)). VHA inhibitors can also be tested in recovery from acidosis in MR cells in Na^+ free and Cl^- free conditions. Na^+ free recovery was demonstrated to be mostly due to a CBE mechanism in this thesis however the contribution of VHA to pH_i regulation remained unresolved in these cells.

The final piece of the overall transepithelial Na^+ uptake model as proposed in my thesis is in the missing Na^+ channel molecular identity. As this has been discussed at great length in chapters II and VI I will not dwell on this topic here. However, it has recently been shown that ASIC1 and ENaC subunits can form functional heteromeric channels (Meltzer et al., 2007). This phenomenon opens up the possibility of a hybrid-like Na^+ channel existing in fish that has escaped current molecular cloning strategies. As the functional role of ASICs and heteromeric channels remains relatively unknown, there is a distinct possibility of a fish Na^+ conducting channel being realized as further characterizations of Na^+ transport are made in other tissues. Furthermore, it would likely be wise to pursue the full cloning and characterization of ASIC4.2 in rainbow trout following the experiments that I described for zebrafish in chapter VI. This would be useful as the physiological experiments are much easier to perform, control, and measure in trout. This coupled to our cell isolation and characterization procedures would possibly make trout a more attractive model to pursue to molecular characterization of ASIC4.2 than zebrafish.

Na^+/H^+ exchangers

As demonstrated in chapter II, I am not convinced of the use of an NHE in apical Na^+ uptake from low ionic strength FW given the current body of evidence. However, as further information becomes available this view may change. Regardless, there is still a need for understanding NHE function in gill MR cells as they contribute to pH_i regulation and potentially whole animal ion homeostasis. Molecular information for NHE in FW fish gills only became available during the tenure of my PhD research. An original goal of my thesis was to create stable cell lines transfected with the known fish NHE sequences. This can be done in NHE deficient cell cultures (eg. Chinese hamster ovary cell line (AP-1 cells)) that lack endogenous NHE activity. I still feel that this is important work for the field of fish ion transport as it will enable extensive and direct transporter profiling. Pharmacological profiling (amiloride, phenamil, EIPA and others) and substrate requirements (K_m for Na^+ and H^+) would only be provided by this experimental approach and this information is essential to corroborate the data on NHE in FW fish whole animal and molecular studies. This is of particular importance with the controversy over phenamil and amiloride pharmacology for FW Na^+ uptake as discussed in chapter II.

In my thesis I present two unique NHE mechanisms in trout MR cells, an NHE1-like transporter requiring PKC for activation and a Cl^--dependent NHE. Furthering our understanding of these transport mechanisms would also benefit from the cell line expression experiments described above. I

made preliminary attempts to clone the Cl-NHE from trout gill. This is a difficult transporter to clone as only one sequence is available (Sangan et al., 2002). Furthermore, the sequence is highly homologous to NHE1 but is approximately half as long making it difficult to design primers without cloning out the standard NHE1 instead. This challenge is compounded by the lack of trout NHE1 molecular information. A unique 62 amino-acid sequence exists in the C-terminal of the cloned Cl-NHE. I designed various reverse primers in this unique C-terminal region with forward primers designed against homologous regions of Cl-NHE and zebrafish NHE1. Promising sequences were obtained with an exact match of the reverse primer sequence however the open reading frame was insufficient and various other degenerate primers need to be explored. Upon successful cloning of the trout Cl-NHE a long term goal could be the functional characterization in a cell expression system.

Functional characterization of MR cell subtypes

A key goal of my thesis was to provide direct functional evidence that would clarify the presence of distinct MR cells at the FW gill. My data in chapters IV, VII, and VIII provide conclusive functional differences for at least two distinct MR cells at the gill. A nice integration of results occurred with the data from these 3 chapters with regards to individual MR cell function. Na^+ free recovery from acidosis, higher resting pH_i, and increased buffering capacity were found in PNA^+ cells compared to PNA^-.

To further the characterization of MR cell subtypes, further pH_i imaging experiments need to be carried out with identified PNA^+ and PNA^- cells using

the Alexa fluor dyes. This will be of particular importance with future cellular signaling studies (described below) to establish the potential for differential control of ion transport between MR cell subtypes. Molecular gene expression will also be helpful to support the proposed ion transport models in this thesis. A key experiment would be to magnetically isolate populations of MR cells and look for molecular expression of the NBC. According to my data I would predict that expression should be found in PNA^- cells and not PNA^+ cells, or at least be overrepresented in PNA^- cells. Obtaining completely pure populations of PNA^+ and PNA^- MR cells is a potential limiting factor in this analysis. Even a few contaminating cells could result in confounding gene expression results due to the amplification aspect of the molecular techniques. If this is a problem the possibility of performing laser capture and microdisection for obtaining PNA^+ and PNA^- MR cells should be explored. Intact gill epithelia could be stained with PNA-FITC or PNA-TRITC to identify cells of interest and then the tissue obtained could be used for direct molecular comparisons with RT and Q-PCR. The molecular cloning of trout NHE1 and potentially Cl-dependent NHE could also then be assessed in this manner. Finally, immunocytochemistry on isolated MR cell subtypes would be useful following the development of effective antibodies (Abs) for the various transporters implicated in this thesis. (see Ab section below).

Changes in the percentage of kidney intercalated α and β cells (analogous to the trout PNA^- and PNA^+ MR cells) in response to acid-base disturbances remains debatable (Schuster, 1993). However, application of the

CA inhibitor acetazolamide which causes an acute systemic acidification and pH_i alkalinization resulted in a decrease in the percentage of β cells and increase in α cells in the rat cortical collecting duct (Bagnis et al., 2001). Based on this information I would propose that similar changes in gill MR cell subtype expression are possible in relation to systemic a/b disturbances. We know that the relative expression of PNA^+ and PNA^- MR cells can be altered at the gill as it has been shown to occur in response to seawater acclimation (Hawkings et al., 2004). Therefore whole animal blood acidification (hypercarbia) or alkalinization (HCO_3^- infusions) experiments should be performed to look at changes in MR cell subtype density at the gill. I would predict that appropriate changes in gill MR cell subtype expression will be observed matching that found in the mammalian kidney. Therefore increased PNA^- MR cell numbers should occur in response to acidosis compared to PNA^+ MR cells and *vice versa* for alkalosis. These effects at the gill could be even more noticeable than the kidney due to the rapid rate at which gill epithelia are remodeled in response to environmental change. These experiments will be useful in determining the MR cell subtypes *in vivo* role for a/b regulation.

Another area of interest for the further characterization of trout gill MR cell subtypes would be to perform concanavalin A (conA) staining. As discussed in chapter I this marker is utilized for identifying MR cell subtypes in zebrafish skin and gill ionocytes (Lin et al., 2006). It would be useful to assess conA staining in trout to see if there is a commonality with zebrafish. This is of

particular importance as the zebrafish begins to dominate the ion and a/b transport field due to its wealth of genetic information. However, it is still difficult (or near impossible) to perform the physiological measurements of blood chemistry to validate the a/b and ion challenges used in zebrafish. Therefore, elucidating any MR cell markers that are common to both trout and zebrafish will help greatly in our data interpretations. With regards to this point, differential binding of lectins on the surface of one MR cell versus another is still an unknown phenomenon. It would be interesting as a long term goal to investigate possible differences in protein glycosolation that vary between MR cell subtypes. Western blotting analysis of MR cell subtypes with fish specific Abs could be used to explore this question. This would help clarify the MR cell markers binding properties and could provide functional insights for membrane transporting proteins as well.

Genetic tools are not as readily available for trout use as they are for other fish (i.e. zebrafish). RNA interference (RNAi) is a technique used to cause gene knockdown however its use has achieved limited success thus far in fish (Schyth, 2008). As discussed by Schyth, most efforts have focused on embryo studies and fish cell lines. As the use of RNAi improves in fish it will be important to keep the technique in mind as a long term research goal. This would enable knockdown of key components in the ion transport machinery, such as the NBC, and assess the influence on whole animal physiology. A major impediment to RNAi use *in vivo* involves the delivery of the small interference RNA (siRNA) into the cells to initiate the RNAi cascade.

This is because siRNA molecules do not readily cross the membrane of mammalian cells (reviewed by (Dykxhoorn and Lieberman, 2005)). One technique being tested for *in vivo* siRNA delivery is referred to as hydrodynamic delivery. In this technique, large volumes of siRNAs are injected intravenously and effectively taken up into the cells of well vascularized tissues such as the kidney and lung (Dykxhoorn and Lieberman, 2005; Lewis et al., 2002; McCaffrey et al., 2002). It is proposed that this volume load induces high venous pressure and the siRNAs are "hydroporated" into the cells (Dykxhoorn and Lieberman, 2005; Zhang et al., 2004). Therefore, as the gill is extremely well vascularized, this technique could potentially be applied for fish gill functional studies in the future. Obviously this is a more long-term goal but it would be a very promising molecular technique to identify the importance of individual gill membrane transport proteins for overall ion and a/b homeostasis.

A final area of interest to explore would be the effect of feeding status on MR cell subtype expression at the gill. The influence of feeding on gill MR cell transport in zebrafish was discussed at great lengths in chapter VI. This has piqued my curiosity to investigate how the regular feeding status of experimentally reared animals compares to that found in the wild. I would be interested in a more detailed study of the changes in gene expression that are induced by the cessation of feeding alone. Traditionally, all of the experiments performed in fish involve starvation during experimentation or pre-starvation for a given period of time. Does this potentially affect gene expression to a

point where animals are already under an altered gene expression pattern compared to the actual experiment of interest? If so this could have a great impact on our interpretations of molecular data from MR cell subtypes.

Immunohistochemistry

Few fish specific antibodies for the various ion-transporting proteins have been developed. Consequently, other antibodies have been used, generally from mammalian origin, which has generated confusion due to low Ab specificity. Gradually (since the turn of the millennium) Ab's raised against fish specific peptides have been developed and published for killifish VHA (Katoh et al., 2003) Japanese dace VHA, CA II, NHE3, NBC1, and aquaporin 3 (Hirata et al., 2003), eel NKA (Mistry et al., 2001), Atlantic stingray NHE3 (Choe et al., 2005), and NHE2 of sculpin and dogfish to name a few (Catches et al., 2006). In trout, Perry's group have taken the first step in specific transporter localization by performing *in-situ* RNA probe analysis of NHE2 in gill tissue (Ivanis et al., 2008b). This paper suggested NHE2 is located apically in the PNA^+ MR cells which conflicts with previous suggestions for the role of PNA^+ cells in Cl^- uptake (Galvez et al., 2002; Goss et al., 2001a; Tresguerres et al., 2006a). However, *in-situ* analysis cannot demonstrate specific cellular localization and for this reason a trout NHE antibody needs to be developed. This will help to clarify the controversial FW Na^+ uptake mechanism. Microscopic analysis for NHE protein in trout gill can then be performed as suggested for NBC above.

Signaling control of MR cell ion transport

An area that remains unresolved in the fish literature (and other systems for that matter) is the mechanisms of pH and ion sensing and subsequent initiation of ion transport. Early work on the hormone prolactin implicated it as a FW-adapting hormone in fish (Pickford and Phillips, 1959) and cortisol was suggested to act as a SW-adapting hormone with respect to maintaining ion homeostasis (Pickford et al., 1970). Since these early studies the role of prolactin and cortisol has expanded and numerous additional circulating hormones, peptides, and neurotransmitters have all been shown to regulate ion transport at the gill in FW and SW animals (for excellent reviews see: (Evans, 2002; Marshall, 2003; McCormick, 2001). These molecules initiate cellular signaling cascades that ultimately adjust rates of membrane transport in gill MR cells. However, little is known about these signaling mechanisms controlling ion transport and the isolated MR cell preparation used in my thesis is an excellent model system to pursue these questions in the future. I will discuss potential mechanisms to explore below.

PMA stimulation of NHE1-like pH_i recovery in my thesis is the first step in our understanding of direct control over membrane transport in gill MR cells. Currently our lab is following up on this data by investigating the dopamine (DA) signaling pathway. Serotonin (5-HT) pathways will also be explored as discussed below. So far apomorphine (a DA receptor agonist) has been shown to alkalinize gill MR cells potentially *via* an NHE or VHA

mediated mechanism (Ryder, Parks, and Goss unpublished results) and this work will be expanded in the near future.

Protein kinases

A number of protein kinases have been demonstrated to phosphorylate NHE1 and increase its activity. These kinases include the growth factor-mediated p90 ribosomal S6 kinase (RSK) (Takahashi et al., 1999), protein kinase C (PKC) (Fafournoux et al., 1991), calcium calmodulin-dependent protein kinase (Fliegel et al., 1992), p160 Rho-associated kinase (ROCK) (Tominaga and Barber, 1998; Tominaga et al., 1998), and the extracellular signal-regulated kinase (ERK) (Wallert et al., 2005). NHE1 has also been shown to be controlled by members of the mitogen activated protein kinases (MAPK) but in turn also regulate the MAPK pathway (for review see (Pedersen et al., 2007). As there are a large number of kinases associated with NHE1 control in other systems, it will be important to proceed strategically with the analysis of trout NHE signalling interactions. Obviously the most important point is to obtain the NHE1 molecular information for trout and then analyse the sequence for predicted kinase binding domains in relation to other characterised NHE1s. Following these predictions we would be able to pursue individual or combined kinases accordingly. In the immediate future as we have found PKC and dopamine stimulation of an NHE1-like mechanism in trout gill MR cells, pharmacological profiling of these transporters should be pursued.

PKC is a diverse gene family with nine different isoforms (Roffey et al., 2009). Consequently, there are a number of potential pharmacological blocking agents to choose from when designing PKC experiments. These inhibitors range in their specificity and effectiveness (for review see (Roffey et al., 2009)). However, it would be possible using different PKC inhibitors to isolate the isoform responsible for activating ion transport in gill MR cells. These pharmacological results would then enable further detailed molecular characterization (at a gene and protein level) of the PKC signalling pathway with respect to gill ion transport.

Another area of signalling to address is on the potential activation/inactivation of other transporters in MR cells. An alternative explanation for the PMA results in chapter VIII was in the inhibition of a basolateral NBC. Therefore it will be important to asses the cellular signalling mechanisms controlling NBC function in the Na^+ uptake mechanism.

Dopamine and serotonin: influence on ion transport

DA and serotonin (5-hydroxytryptamine, 5-HT) are well established as a control point in ion transport particularly in insect model systems. Both DA and 5-HT stimulate saliva production in the cockroach salivary glands (Just and Walz, 1996; Rietdorf et al., 2003; Walz et al., 2006). However, these amines act via different mechanisms as 5-HT stimulation produced a protein-rich saliva while DA stimulation resulted in a protein free saliva (Just and Walz, 1996). 5-HT was also shown ~40 years ago to cause secretion in the salivary glands of the blowfly *Calliphora vicina* (Berridge, 1970). This salivary

gland secretion is driven by an apical VHA that is activated by elevated cAMP levels following 5-HT stimulation of adenylyl cyclase (Dames et al., 2006; Heslop and Berridge, 1980; Rein et al., 2008; Zimmermann et al., 2003). A universal control has been suggested for VHA activity with respect to the assembly/disassembly of the holoenzyme (for review see (Beyenbach and Wieczorek, 2006)). The VHA consists of two complexes (termed V_1 and V_o) and only the fully assembled VHA will function properly (Beyenbach and Wieczorek, 2006). This assembly of VHA is how salivary production and ion transport is regulated by 5-HT in the blowfly salivary glands. 5-HT stimulates the assembly of the VHA holoenzyme (Zimmermann et al., 2003) that is mediated intracellularly by cAMP (Dames et al., 2006). It has recently been shown that stimulation of VHA by cAMP is mediated by PKA and not cAMP directly (Rein et al., 2008). None of this type of information exists for fish VHA function and regulation. Therefore, any future experiments with 5-HT and gill ion transport should pay close attention to the assembly of the VHA holoenzyme.

5-HT influence on pH_i has been observed in blowfly salivary glands due to its enhancement of H^+ secretion as described above. 5-HT caused an acidification of pH_i at low doses however it also induced multiphasic responses in higher concentrations (Schewe et al., 2008). This was the opposite effect of the expected pH_i alkalinization that would occur as a result of enhanced VHA activity. The authors propose that 5-HT induces an increase in cellular respiration and cytosolic proton accumulation that masks

the pH_i alkalinizing effect of VHA stimulation (Schewe et al., 2008). They also propose that the higher doses of 5-HT that cause multiphasic responses are indeed due to the stimulation of VHA (Schewe et al., 2008). The influence of 5-HT on pH_i characteristics in this study combined with my results from mosquito gut cells in chapter X make 5-HT a prime candidate for future studies on gill MR cell pH_i homeostasis. I predict that 5-HT will result in an alkalinization of pH_i in MR cells by stimulating VHA. This should occur in both MR cell subtypes as they both are proposed to utilise VHA for driving transepithelial ion transport. Following 5-HT experimentation on ion transport in these cells, the intracellular signalling mechanism can be teased out with pharmacological and molecular profiling.

DA induced an acidification of pH_i in salivary ducts of the cockroach *Periplaneta americana* (Hille and Walz, 2007). However, this study focussed on the pH_i recovery from DA induced acidosis and not the mechanism of DA acidification. This contrasts with our preliminary results showing DA induced alkalinization in gill MR cells. Understanding the mechanism behind DA induced pH_i changes in trout MR cells will be the first step in describing any dopamine related signalling pathways that control gill ion transport.

DA binds to different membrane receptors (grouped into D1 and D2 receptor families) and these receptors initiate distinct cellular messaging pathways and have distinct pharmacology (reviewed by (Le Foll et al., 2009)). Preliminary results using Spiperone (an inhibitor of D1 receptors) have blocked the apomorphine induced alkalinization in gill MR cells implicating the

D1 pathway for activation (Ryder, Parks, and Goss unpublished results). Extending the investigation of the receptor binding profile of DA in gill MR cells will be an important step in the future understanding of ion transport control mechanisms at the gill.

Neuronal control of MR cell ion transport

Recently, the neuronal control of gill ion transport has been gaining experimental support (Jonz and Nurse, 2008). 5-HT immunoreactive neurons have been shown in the zebrafish gill filaments and lamellae (Jonz and Nurse, 2003) and appear to be a common feature of gill filaments in teleost fish (Sundin and Nilsson, 2002). The presence of serotonergic neurons at the FW gill strengthens the proposed 5-HT experiments for isolated MR cells suggested above. Recent immunofluorescence confocal analysis has revealed innervation of the zebrafish gill MR cells at the basolateral region of the cell (Jonz and Nurse, 2006). Due to the abundance of NKA present in this region of the cell it was suggested that perhaps the NKA is controlled neuronally and therefore regulates ion transport in MR cells (Jonz and Nurse, 2006; Jonz and Nurse, 2008). This is an interesting concept as neurotransmitters such as dopamine have been shown to inhibit or stimulate NKA activity in a tissue specific manner (for review see (Pedemonte and Bertorello, 2001)). To my knowledge, there are no published reports of DA innervation in the fish gill of any species, however, DA innervation is well established in mussel gills (Carroll and Catapane, 2007), and DA storage and release from the vasculature of the eel has been reported previously

(Kraschinski et al., 1996) indicating that both 5-HT and DA could play a role at the gill. The potential neuronal control of NKA has broad implications for gill ion transport as NKA has been implicated for a long time to act as an energetic step in the overall gill transport mechanism (Evans et al., 2005). Understanding the effects of 5-HT and DA on this transporter and others at the gill holds great promise for future study in the control of acid-base and ion transport in fish. As a series off neurotransmitters and peptides have been shown to mediate ion transport across the *opercular* epithelium including stimulation of Cl^- extrusion via adrenergic receptors (reviewed by (Jonz and Nurse, 2008)) it is reasonable to assume that a similar control of ion transport can occur in the gill MR cells.

Soluble adenylyl cyclase (sAC)

In his PhD thesis, Martin Tresguerres suggested the role of sAC in HCO_3^- sensing and stimulation of base secretion at the dogfish gill. He has followed this up during his postdoctoral position and has now characterized dogfish sAC at a biochemical level (Tresguerres et al. PNAS submitted MS# 2009-04630). This enzyme is now confirmed in HCO_3^- sensing with results from protein, cellular, and whole animal studies (Tresguerres et al. PNAS submitted MS# 2009-04630). This work suggests that HCO_3^- acts as a primitive hormone to regulate ion transport at the gill and is perhaps a universal HCO_3^- sensor. Obviously it will be interesting to extend this hypothesis to MR cell function in FW trout. Experiments on isolated gill MR cells that elevate HCO_3^- concentrations to stimulate ion transport can be

performed while monitoring pH_i changes. Then using sAC inhibitors (KH7, 4CE) a pharmacological role for sAC in HCO_3^- sensing in MR cells could be established. The work proposed above would be combined with molecular cloning of trout sAC from the gill. This molecular information would be vital as sAC is not found in the zebrafish genome database which is an interesting anomaly that will need further explanation. The trout MR cell model provides an excellent means to study this question.

Pacific hagfish

Working on the systemic acid (chapter IX) and base (appendix II) recovery mechanisms in the Pacific hagfish culminated in a description of a single MR cell subtype achieving both functions. The implications for both acid and base secretion within the same cell involve differential insertion of proteins into the apical and basolateral membranes and this is covered extensively in chapter IX and appendix II. Clearly, a co-ordinated cellular signaling pathway controls these protein movements and this can be an area of future research. An obvious first choice would be to look at the sAC pathway and its role in HCO_3^- sensing as the base recovery mechanisms appears to be similar to that described in dogfish. This would help to extend the description of sAC as a universal HCO_3^- sensor. Furthermore, sAC could be involved in the acid secretion mechanism as well by initiating NHE translocation within the cell. Both of these hypotheses can be tested *via* whole animal acid and base infusions coupled with sAC inhibitors and subsequent immunohistochemistry and western blotting.

Another area remaining in the hagfish acid-recovery mechanism is the NHE molecular identity. I performed numerous cloning attempts in this regard ("data" not shown), however, the hagfish NHE remains elusive. The primitive nature of the hagfish and its unique ability to recover from extreme acidosis makes the cloning of hagfish NHE an attractive task for comparative ion transport physiology.

Larval mosquito midgut cells

In chapter X we found that the anterior midgut cells of the larval mosquito (*Aedes aegypti L*) demonstrated an increase in pH_i that reached the alkaline limits of BCECF-AM detection. These data opposed the current dogma of the absolute requirement for pH_i regulation to maintain proper cellular function. It is important to realize that this apparent disruption of pH_i homeostasis could be utilized to achieve the extreme luminal alkalinization of the gut. Therefore, we must consider other unique transport challenges in this light where pH_i manipulations can be used to aid in overcoming unfavourable gradients. This has been proposed in fish MR cells for potential localized regions of high or low pH within the cytoplasm that can help drive particular transporters (see chapter II).

Understanding the use of altered pH_i in overall ion transport requires the development of fluorescent markers that are functional in the more acidic and alkaline ranges. These projects are currently being explored in our lab in collaboration with the lab of Dr. Robert E. Campbell in the department of chemistry. As alluded to in chapter X, it will also be interesting to analyse

various mosquito gut enzyme kinetics to determine how they are affected by these large elevations in pH_i. This unique model system holds promise for uncovering new interpretations of various homeostatic principles.

Conclusion

I am confident that this PhD thesis provides a substantial advance for the understanding of gill ion and a/b homeostasis. My data has resulted in new models for ion transport in gill MR cells while providing the physiological evidence to support previously suggested models as well. I have tried to convey the importance of thermodynamic constraints on ion transport throughout this thesis. When extending the study of these challenging ion gradients, it will remain important to focus on the basic thermodynamic limitations on certain ion transport models.

In my opinion, the most significant advance from this thesis was the functional descriptions of gill MR cell subtypes. The full characterization of these subtypes is required to confirm the overall mechanisms of ion and a/b transport at the freshwater and seawater fish gill. This information will prove to be of environmental relevance for predicting how fish respond to changing conditions in their natural habitat.

Figures

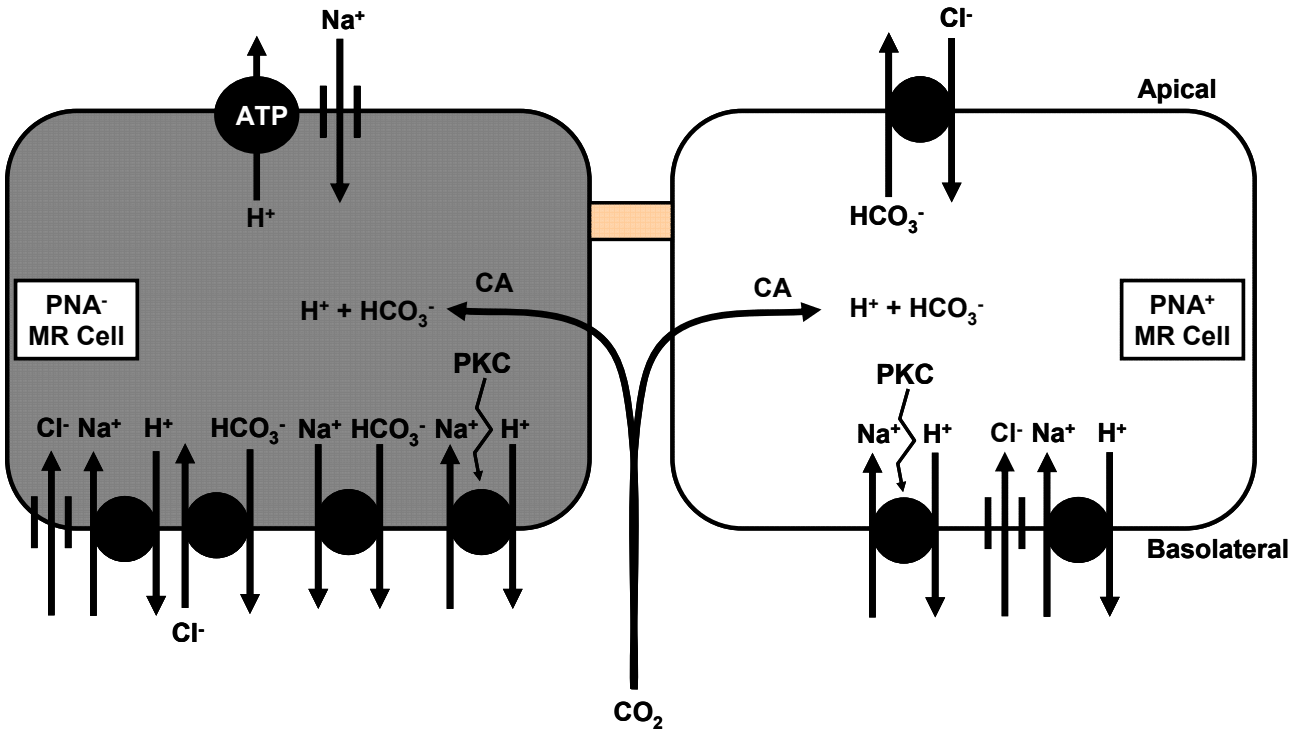

Figure 11. 1 An overall 2 MR cell model for ion and acid-base transport at the FW rainbow trout gill integrating the data described throughout my thesis. Intracellular activation of NHE via PKC is indicated by zig-zag arrow. CA = carbonic anhydrase.

Appendix I: Regulation of ion transport by high HCO_3^- in isolated gills of the crab *Neohelice* (*Chasmagnathus*) *granulata*[1]

[1]A version of this chapter has been published previously.

*****Tresguerres, M., ***Parks, S. K.**, Sabatini, S. E., Goss, G. G. and Luquet, C. Regulation of ion transport by pH and [HCO_3^-] in isolated gills of the crab *Neohelice (Chasmagnathus) granulata*. *American Journal of Physiology-Regulatory Integrative and Comparative Physiology* **294**, R1033-R1043, 2008. *** Both authors contributed equally to all aspects of this work.**

Introduction

Please refer to the introduction for chapter V as it is a common introduction to both this appendix and that chapter.

Results

Elevation of V_{te} and ΔpH by HCO_3^- in isolated perfused gills.

Switching from control [HCO_3^-] saline of 2.50 mmol/l to the "high [HCO_3^-] pH 7.81" (12.50 mmol/l HCO_3^-) saline caused an immediate and significant elevation in V_{te} from 3.02 ± 0.47 to 4.83 ± 0.88 mV (n = 6, P < 0.05). This effect was fully reversible, since V_{te} returned to its basal value after reintroducing the original control saline (3.15 ± 0.49 mV). A subsequent application of a saline with control [HCO_3^-] but with a higher pH of 7.81 did not have any significant effect on V_{te} (2.83 ± 0.45 mV, n = 6, P > 0.05). However, the saline with high [HCO_3^-] and a control pH of 7.75 induced a significant increase on V_{te}, of a similar magnitude to the "high [HCO_3^-] pH 7.81" saline (5.17 ± 0.88 mV, n = 6, P < 0.05). These results indicate that an increase in the saline [HCO_3^-], and not pH, is the stimulus that ultimately causes the elevations on V_{te}. Consequently, only the "high [HCO_3^-] pH 7.75" saline was used for the pharmacological characterization. These results are shown in Fig. 12.1, *A* and *B*.

Gills perfused with the control saline secreted an apparent H^+ flux (J_{H+}) of –43.72 ± 22.5 μequiv·kg^{-1}·h^{-1}. Perfusion with "high [HCO_3^-] pH 7.81" saline

induced the reversion in secretion to an apparent HCO_3^- flux (J_{HCO3}^-) of 84.7 ± 14.4 μequiv·kg^{-1}·h^{-1}. Therefore, the net change ($J_{ctrol} – J_{bicarb}$) in J_{HCO3}^- was of 128.5 ± 31.6 μequiv·kg^{-1}·h^{-1} ($P < 0.05$; $n = 5$, Fig 12.1 *C*). This indicates that the elevations in V_{te} are accompanied by net base efflux across the gill epithelium.

Pharmacological characterization.

To test whether carbonic anhydrase (CA) is involved in the V_{te} response to high [HCO_3^-], we added 200 μmol/l acetazolamide into the high [HCO_3^-] perfusate. Acetazolamide completely and reversibly abolished the increased V_{te} (Fig. 12.2, *A* and *B*). Bafilomycin is a specific inhibitor of V-H^+-ATPases at nanomolar concentrations (Drose and Altendorf, 1997). Basolateral application of bafilomycin (100 nmol/l) did not exert any significant effect on the HCO_3^--stimulated V_{te}, suggesting that V-H^+-ATPase is not important in this process (Fig. 12.2, *A* and *C*). On the other hand, ouabain (5 mmol/l) almost completely blocked V_{te} both during control (not shown) and high [HCO_3^-] conditions (Fig. 12.2*D*), demonstrating that Na^+-K^+-ATPase is the major driving force for the transepithelial transport of ions. To identify the basolateral route of exit of H^+ from the cells into the hemolymph space, we tested the effect of basolateral amiloride (1 mmol/l). This treatment completely and reversibly blocked the HCO_3^--stimulated V_{te}, suggesting that basolateral Na^+/H^+ exchangers (NHE) are critical for the overall transepithelial transport mechanism activated by high [HCO_3^-] (Fig. 12.3, *A* and *B*). Importantly, amiloride did not have any effect on the basal V_{te}, and it completely but

reversibly blocked the HCO_3^-- induced response when added prior to elevating [HCO_3^-] (Fig. 12.3*C*). This indicates that the putative NHE are specifically recruited for the base secreting mechanism. This finding also shows that the concentration of amiloride used does not significantly affect Na^+-K^+-ATPase function.

Our last two experimental series were designed to test for the involvement of apical Cl^-/HCO_3^- exchangers. Introduction of Cl^--free conditions produced a significant decrease in V_{te}, which reflects the importance of Cl^- for the basal ion transport mechanism (see 24, 30, 40). An increase of [HCO_3^-] under Cl^--free conditions did not result in the typical stimulation of V_{te}, indicating that Cl^- ions must be present for the HCO_3^- stimulation to occur (Fig. 12.4, *A* and *B*). Returning to normal Cl^--containing conditions did not restore the original V_{te}, probably because the unnatural Cl^--free saline induced a new basal steady state of ion transport. However, the gill epithelium was able to respond with the typical increase in V_{te} to an elevation in [HCO_3^-], indicating that it was still healthy and functional (Fig. 12.4, *A* and *B*). Finally, we tested the effect of apical DIDS (1 mmol/l) on the V_{te} stimulated by HCO_3^-, but this treatment did not result in any significant changes in V_{te} (Fig. 12.4*C*). Apical SITS (2 mmol/l) was also without any significant effect on V_{te} (not shown).

Discussion

Increasing [HCO_3^-] by 10 mmol/l elevated both V_{te} and base secretion to the apical medium. An equivalent increase in pH alone did not have any effect on V_{te}. This indicates that an electrogenic transepithelial base secretion mechanism is activated directly by [HCO_3^-]. The pharmacology profile suggests that the mechanism activated by high [HCO_3^-] is different from those described in our previous studies (see below).

Carbonic Anhydrase (CA)

As mentioned for the low pH stimulation of V_{te} in chapter 5, CA was imperative in the high HCO_3^- stimulation of V_{te} as well. On the basis of current models for branchial A/B regulation in aquatic animals (Perry and Gilmour, 2006), it is likely that both extracellular and intracellular CA are involved in the response to elevated [HCO_3^-]. In fact, both types of CA are present in the posterior gills of *C. granulatus* (Genovese et al., 2005). Extracellular CA would dehydrate H^+ and HCO_3^- into CO_2, which can diffuse inside the ion-transporting cells. CO2 can then be re-hydrated back into H^+ and HCO_3^- intracellularly (as mentioned in chapter 5) providing the substrate for the HCO_3^- secretion mechanism. As mentioned in chapter 5, additional studies are required to determine the role of both CA types in the HCO_3^- secretion model at the crab gill.

Responses to high [HCO_3^-].

A priori, we were expecting that basolateral V-H^+-ATPases energized the secretion of HCO_3^- as suggested for hagfish (Tresguerres et al., 2006b; Tresguerres et al., 2007a), elasmobranchs (Tresguerres et al., 2005; Tresguerres et al., 2006c; Tresguerres et al., 2007b), and teleost fish (Chang and Hwang, 2004; Perry and Gilmour, 2006; Tresguerres et al., 2006a). However, the [HCO_3^-]-dependent V_{te} was insensitive to 100 nmol/l bafilomycin. Importantly, this was in contrast to the low pH-stimulating mechanism (see chapter 5), indicating that the dose of bafilomycin used is effective in inhibiting V-H^+-ATPase in isolated perfused gills. On the basis of the inhibition of the HCO_3^--induced V_{te} by amiloride, we conclude that the basolateral route of exit for H^+ in crab gills during HCO_3^- stimulation is via a member of the NHE family. Candidate targets for the amiloride sensitivity are some of the NHEs present in the gills of several crustaceans (Kimura et al., 1994; Towle et al., 1997; Towle and Weihrauch, 2001). Importantly, at least some crustacean NHE isoforms are electrogenic and transport two Na^+ for each H^+ (Kimura et al., 1994; Shetlar and Towle, 1989). However, it is not clear whether the electrogenic NHE is located in the basolateral or apical membrane from those studies. Moreover, our study clearly demonstrates that the driving force for HCO_3^- secretion and H^+ reabsorption is Na^+-K^+-ATPase, as seen in the inhibitory effect of ouabain.

Finally, the lack of HCO_3^- stimulation in Cl^--free conditions suggests the involvement of apical Cl^-/HCO_3^- exchangers of some sort (Fig. 12.5).

However, apical application of DIDS and SITS did not have any significant effect in the stimulated V_{te}. It is interesting to note that apical SITS produced a small but significant inhibition of 16% under hypo-osmotic stimulating conditions, and of 45% in similar, but Na^+-free, perfusion saline (Genovese et al., 2005). This was interpreted as indicative of the involvement of a Cl^-/HCO_3^- exchanger in Cl^--uptake. Lack of SITS/DIDS inhibition in our experimental conditions indicates that either a different, DIDS/SITS-insensitive, Cl^-/HCO_3^- exchanger participates in the HCO_3^--induced V_{te} or that these drugs did not cross the cuticle in our experiments.

We have only found one similar study in the literature, performed in isolated perfused gills of the shore crab *Carcinus maenas* (Siebers et al., 1994). This study concluded that the gill could detect an elevated pH of 8.10 in the perfusate (hemolymph space) and reabsorb H^+ to restore a normal pH of 7.70. However, a saline with high pH but without HCO_3^- did not increase H^+ reabsorption significantly, which suggests that the actual stimulus was [HCO_3^-] or at least that HCO_3^- was necessary to the base secretion mechanism. Siebers and colleagues (Siebers et al., 1994) tested a variety of ion-transporting protein inhibitors, but only ouabain affected V_{te} and H^+ reabsorption simultaneously. It is thus possible that *C. maenas*, unlike *C. granulatus*, relies on electroneutral ion transport for gill A/B regulation. Nonetheless, both isolated gill epithelia demonstrated an ability to detect and correct A/B disturbances, a feature that might be common to crustaceans and other aquatic organisms.

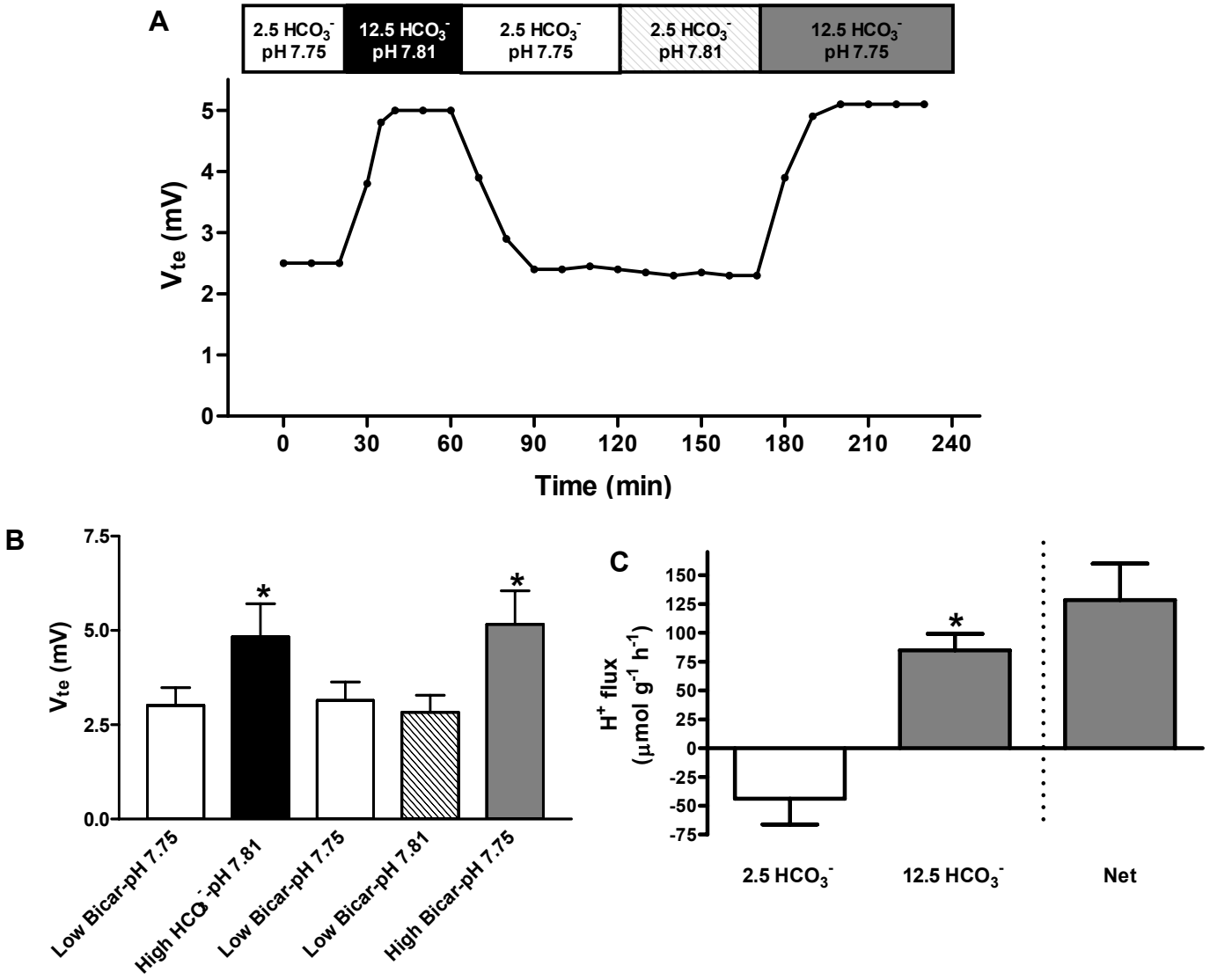

Figure 12. 1 Effect of [HCO_3^-] and pH on V_{te} and base efflux in isolated perfused gills.

A*:** V_{te} representative trace. ***B*:** V_{te} summary statistics. ***C: base secretion. Both solutions had a pH of 7.75. All solutions were symmetrically applied to both perfusate and bath. 2.5 and 12.5 is the [HCO_3^-] in millimoles per liter. The asterisks indicate statistical differences with the control (2.50 mmol/l HCO_3^-, pH 7.75) ($P < 0.05$; $n = 6$; one-way repeated-measures ANOVA and Dunnett's multiple comparison posttest or paired Student's *t*-test).

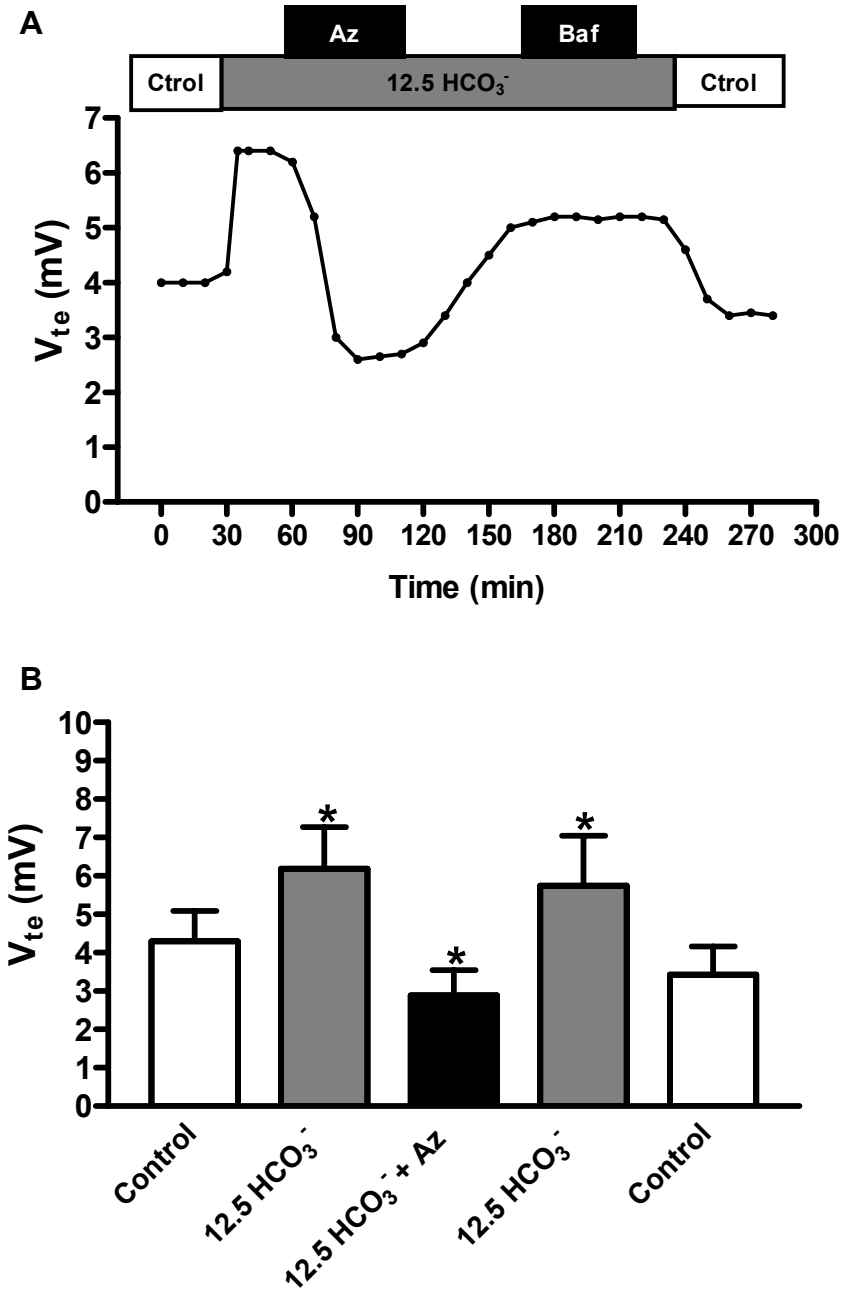

Figure 12. 2 Effects of basolateral acetazolamide, bafilomycin, and ouabain on the HCO_3^--activated V_{te}.

***A*:** representative trace showing a trial experiment in which both drugs were applied to the same preparation, but the data shown in *B* are from independent experiments. ***B*:** acetazolamide (200 µmol/l) summary statistics (*n* = 7).

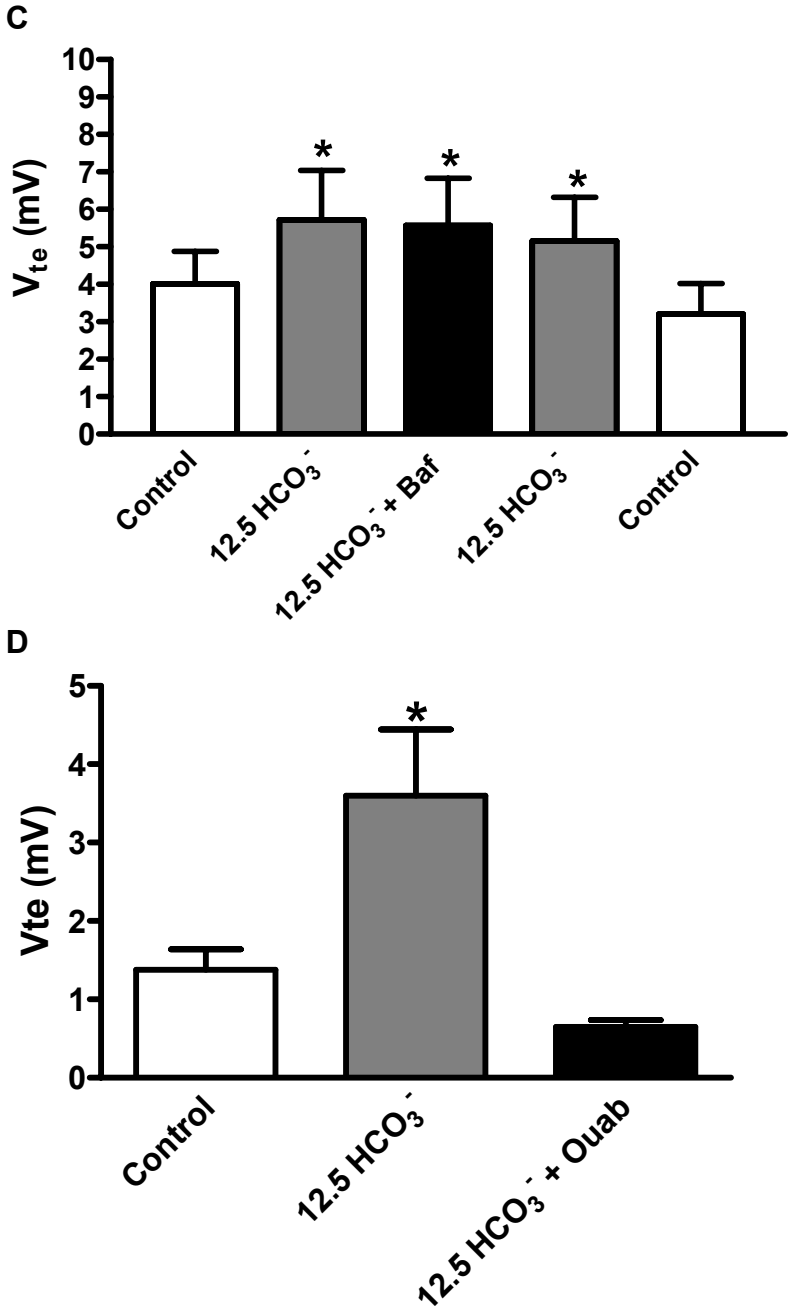

Figure 12.2 Continued. *C*: bafilomycin (100 nmol/l) summary statistics (*n* = 6). ***D*:** ouabain (5.00 mmol/l) summary statistics (*n* = 4). Control saline, 2.50 mmol/l HCO_3^-. 12.5 is the [HCO_3^-] in mmol/l. pH of all saline solutions was adjusted to 7.75. The asterisks indicate statistical differences with the control ($P < 0.05$; one-way repeated-measures ANOVA, Dunnett's multiple comparison posttest).

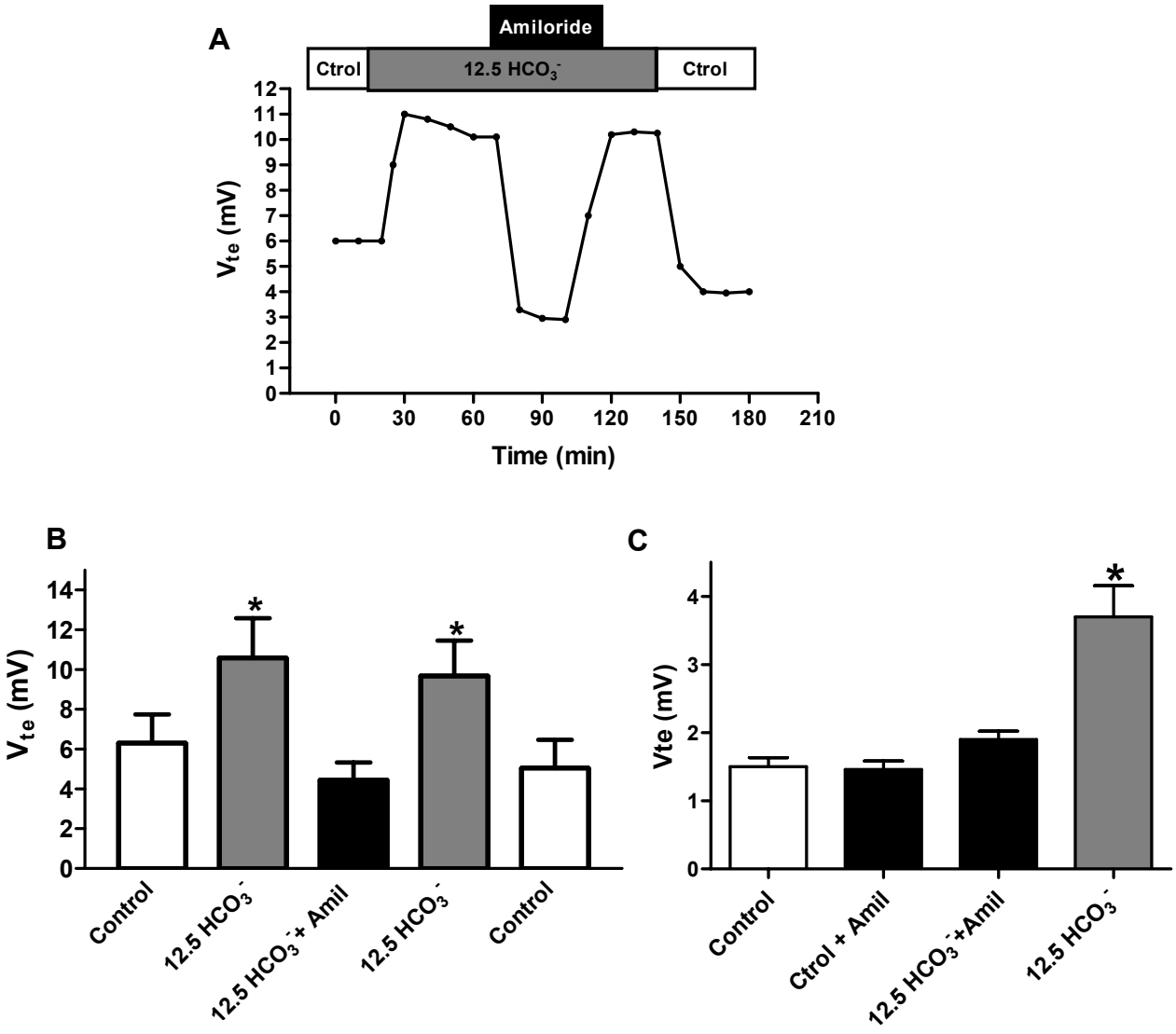

Figure 12. 3 Inhibition of HCO_3^--induced V_{te} activation by basolateral amiloride.

A**:** representative trace. ***B*****:** summary statistics showing amiloride inhibition of the activated V_{te}. ***C*****:** summary statistics showing amiloride during control conditions and prevention of the HCO_3^- stimuation. V_{te}, transepithelial potential difference. Control saline, 2.50 mmol/l HCO_3^-. 12.5 is the [HCO_3^-] in millimoles per liter. Amiloride (1.00 mmol/l) was added in the basolateral perfustate. pH of all salines was adjusted to 7.75 *Statistical differences with the control ($P < 0.05$; $n = 5$; one-way repeated-measures ANOVA, Dunnett's multiple comparison post test).

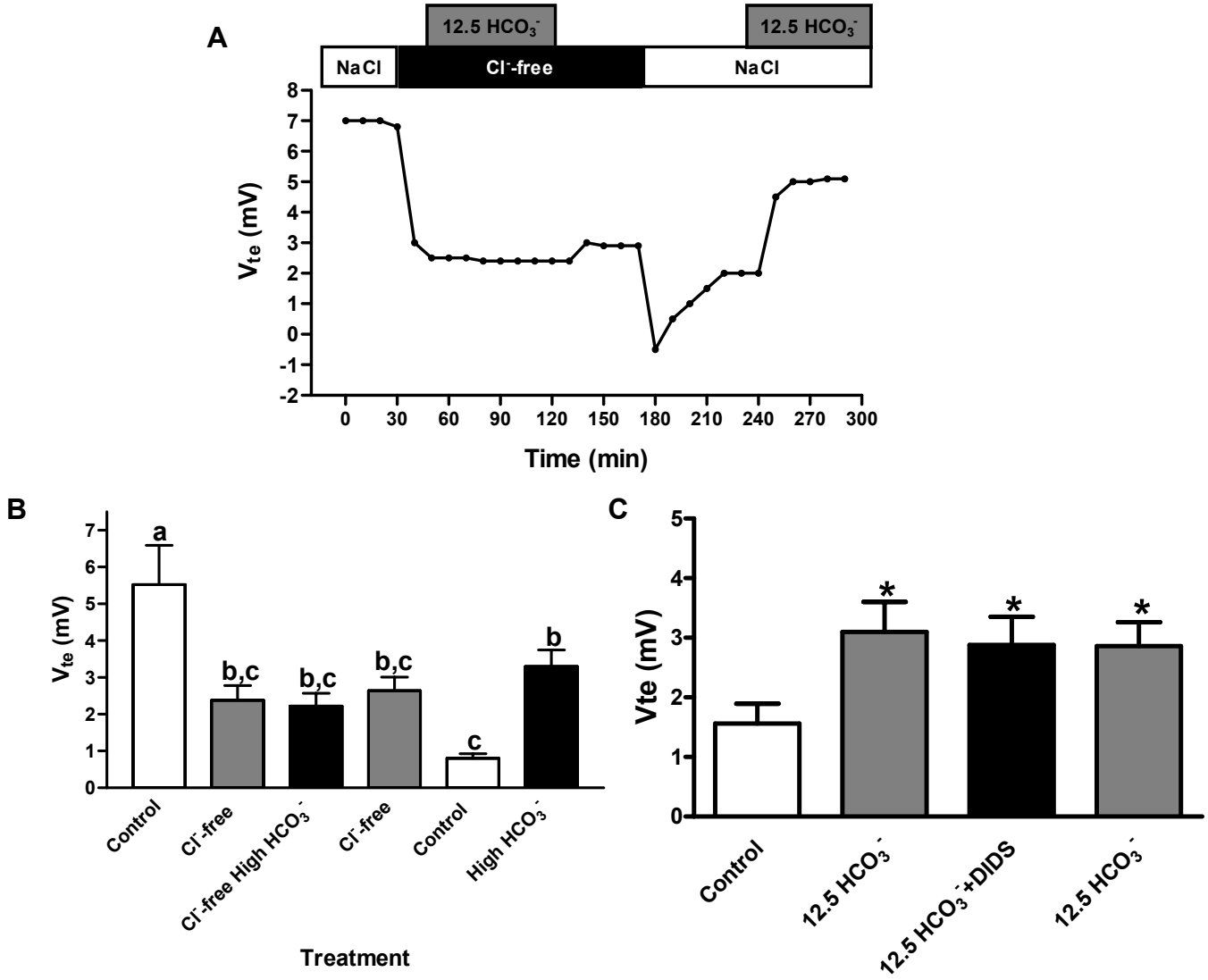

Figure 12. 4 Lack of HCO_3^--induced V_{te} activation in Cl^--free conditions and DIDS and SITS inhibition.

***A*:** representative trace of a Cl^--free experiment. ***B*:** summary statistics of Cl^--free. ***C*:** summary statistics of DIDS. Control saline, 2.50 mmol/l·HCO_3^-·Cl^--free: control saline with all the Cl^- substituted by NO_3^-. 12.5 is the [HCO_3^-] in millimoles per liter. DIDS: 1.00 mmol/l added into the apical bath. SITS (2.00 mmol/l) produced the same results as DIDS (not shown). pH of all salines was adjusted to 7.75. The letters indicate different levels of statistical significance ($P < 0.05$; $n = 5$; one-way repeated-measures ANOVA, Tukey's multiple-comparisons or Dunnett's multiple-comparison posttest).

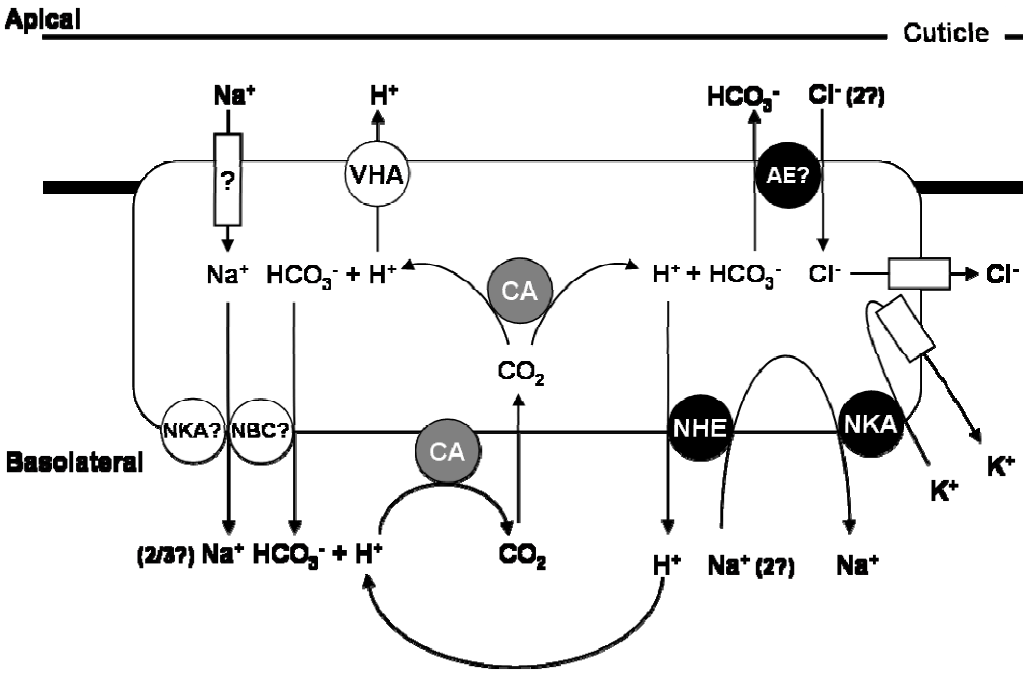

Figure 12. 5 Overall model for HCO_3^- and H^+ secretion in one cell type at the crab gill.

This model combines data for HCO_3^- secretion from this appendix and H^+ secretion from chapter V and is complemented by previous studies in this crab (Luquet and Ansaldo, 1997; Luquet et al., 2002b; Onken et al., 2003; Towle and Weihrauch, 2001) and other aquatic organisms (chapter 4 and (Parks et al., 2007b). The molecular identity and exact stoichiometry of the transporters is unknown, and a question mark (?) indicates that no direct evidence exists for the involvement of the transporter. CA, carbonic anhydrase; NBC, Na^+/HCO_3^- cotransporter; NKA, Na^+-K^+-ATPase; VHA, V-type H^+-ATPase.

Appendix II: Recovery from blood alkalosis in the Pacific hagfish (*Eptatretus stoutii*): Involvement of gill V-H^+-ATPase and Na^+/K^+-ATPase[1]

[1]A version of this chapter has been published previously.

*****Tresguerres, M., ***Parks, S. K**. and Goss, G. G. (2007). Recovery from blood alkalosis in the Pacific hagfish (*Eptatretus stoutii*): Involvement of gill V-H^+-ATPase and Na^+/K^+-ATPase. *Comparative Biochemistry and Physiology a-Molecular & Integrative Physiology* **148**, 133-141**.* Both authors contributed equally to all aspects of this study.**

Introduction

The hagfish gill epithelium has abundant mitochondria-rich (MR) cells (Bartels, 1992; Elger and Hentschel, 1983; Mallatt and Paulsen, 1986), where ion transport-related proteins such as Na^+/K^+–ATPase (NKA), carbonic anhydrase (CA), Na^+/H^+ exchanger (NHE) and vacuolar proton ATPase (VHA) are located (Choe et al., 1999; Choe et al., 2002; Edwards et al., 2001; Mallatt et al., 1987; Tresguerres et al., 2006b). Based on the role of these proteins in fish (see (Evans et al., 2005)), and the fact that hagfish are osmoconformers (Morris, 1965), it is likely that the role of the MR cells is the transport of acid/base relevant ions between the blood and seawater.

To date, the role of hagfish gills in acid/base regulation has mostly been limited to the study of acid secretion. In particular, acid infusions have been used to induce blood acidosis in order to study acid secretion at the whole animal (McDonald et al., 1991) and molecular levels (Edwards et al., 2001). These studies concluded that hagfish have a substantial capacity for overcoming an acidic load, and that a Na^+/H^+ exchanger (NHE) protein is probably involved in the branchial mechanism for acid secretion. Other evidence for NHE presence in hagfish gills have been provided from immunohistochemistry and western blot experiments (Choe et al., 2002; Tresguerres et al., 2006b). I have further strengthened the role for NHE in hagfish gill acid secretion as described in chapter IX (Parks et al., 2007a). On the other hand, we are aware of only one study on base secretion in hagfish (Evans, 1984). This study reported that the Atlantic hagfish *Myxine glutinosa*

was unable to secrete base when placed in Cl^--free seawater, suggesting the existence of a Cl^-/HCO_3^- exchange system. More recently, we found VHA immunoreactivity in the gill epithelium of the Pacific hagfish *Eptatretus stoutii* (Tresguerres et al., 2006b). Based on current models for base secretion in gills of marine elasmobranchs (Piermarini and Evans, 2001; Tresguerres et al., 2005; Tresguerres et al., 2006c), we proposed that VHA is involved in reabsorbing protons to the blood and in energizing HCO_3^- secretion to the water (Tresguerres et al., 2006b).

In order to study the responses to blood alkalosis, hagfish were injected with $NaHCO_3$ (6000 μmol kg^{-1}) into the subcutaneous sinus and blood pH and total CO_2 (TCO_2) were monitored for 6 h. We also induced long-term alkalosis by repeated infusions of $NaHCO_3$ (6000 μmol kg^{-1}) over a 24 h experiment. Our results show that hagfish restore their blood pH by 6 h after each alkaline load, and suggest that basolateral VHA plays a role in the base-secretory mechanism. The methods in this study followed those described in "methods and materials" for hagfish acid recovery experiments.

Results

6 h. Blood and plasma variables

At t = 0, blood pH was 7.78 ± 0.04 and 7.69 ± 0.03 pH units in NaCl-infused (control) and base-infused hagfish (BIH), respectively (P >0.05, n =6). The NaCl injection did not significantly affect blood pH in control hagfish (7.82 ± 0.03 and 7.81 ± 0.05 pH units at t = 1 and 6 h, respectively). In contrast, the 6000 μmol kg^{-1} HCO_3^- injection produced an increase in blood pH at t = 1h (8.05 ± 0.05 pH units), which was significantly higher compared to control, NaCl-injected fish (P < 0.05, n = 6). Blood pH in BIH returned to control values by t = 6 h (7.85 ± 0.08 pH units). These results are shown in Fig. 13.1*A*.

Plasma total CO_2 (TCO_2) essentially followed the same pattern as blood pH (Fig. 13.1*B*). Control hagfish had TCO_2 values of 7.32 ± 0.57, 6.26 ± 0.71 and 5.92 ± 1.19 mmol CO_2 l^{-1} at t = 0, 1 and 6 h, respectively (n = 6). TCO_2 in BIH started at a significantly lower value at t = 0 (5.48 ± 0.52 mmol CO_2 l^{-1}). However, the effect of the HCO_3^- injection was evident at t = 1 h (21.82 ± 2.91 mmol CO_2 l^{-1}), when TCO_2 was significantly higher compared to control hagfish. Similar to blood pH, TCO_2 in BIH had returned to control values by t = 6 h (8.85 ± 1.83 mmol CO_2 l^{-1}) (P > 0.05, n = 6). Plasma [Na^+] and [Cl^-] did not differ between treatments or times.

6 h. Na^+/K^+–ATPase and V–H^+–ATPase gill immunohistochemistry

NKA and VHA gill immunolabeling patterns 6 h after the injections were similar in control and BIH (Fig. 13.2). Most cells that were labelled by one antibody also were labelled by the other antibody, indicating that both transporters exist in the same cells, or at least in a majority of cells. At the cellular level, both NKA and VHA immunolabeling occurred throughout the cell. These results are similar to those obtained for non-injected hagfish (Tresguerres et al., 2006b). Sections incubated with no primary antibody showed no staining as demonstrated in a previous publication that I collaborated on (Tresguerres et al., 2006b) and represented again in Fig 13.2 G.

6 h. Na^+/K^+–ATPase and V–H^+–ATPase gill abundance

The α-NKA antibody recognized a single band of ~105 kDA, while staining with the α-VHA antibody resulted in a single band of ~70 kDa. Both bands were absent in control blots that were incubated without primary antibody (not shown, see (Tresguerres et al., 2006b)). There were no significant differences in NKA or VHA abundance between gills from control and BIH, neither in whole gill homogenates (not shown) nor in the fraction enriched in cell membranes (Fig. 13.3).

24 h. Blood and plasma variables

In this experimental series, four bolus 6000 μmol kg^{-1} HCO_3^- doses were injected into the subcutaneous sinus at t = 0, 6, 12 and 18 h. During the

first 12 h, blood pH showed a pattern similar to the 6 h experiment described in the previous section. There were significant increases in blood pH of BIH compared to control fish 3 h after each injection (8.13 ± 0.06 vs. 7.84 ±0.03 pH units at t = 3 h; 8.16 ± 0.04 vs. 7.94 ± 0.03 pH units at t = 9 h, $P < 0.05$; n = 7 in both cases), but they were fully compensated 3 h later (8.07 ± 0.04 vs. 7.97 ± 0.03 pH units at t = 6 h; 8.01 ± 0.03 vs. 7.98 ± 0.04 pH units at t = 12 h, $P > 0.05$ in both cases). Between 12 and 24 h, blood samples were withdrawn every 6 h instead of every 3 h. While this impaired the temporal resolution of our study, it was done in an effort to prevent anemia. Blood pH did not statistically differ between BIH and controls at t = 18 h (7.99 ± 0.05 vs. 7.97 ± 0.05 pH units) and t = 24 h (8.05 ± 0.05 vs. 7.92 ± 0.08 pH units). Blood pH as a function of time is shown in Fig. 13.4*A*.

TCO_2 in control fish remained between a minimum of 2.80 ±1.10 mmol CO_2 l^{-1} at t = 18 h and a maximum of 7.00 ±1.80 mmol CO_2 l^{-1} at t = 12 h. TCO_2 in BIH was maximum 3 h after the first HCO_3^- infusion, when it reached 13.26 ± 2.90 mmol CO_2 l^{-1} ($P < 0.05$ compared to controls at the same time). In the remaining sampling times TCO_2 from BIH was not significantly different compared to controls (Fig. 13.4*B*). Importantly, this includes t = 9 h (3 h after the second injection) (6.13 ± 0.08 vs. 3.07 ± 1.12 mmol CO_2 l^{-1}, $P > 0.05$).

Plasma [Na^+] and [Cl^-] are shown in Table 13.1. [Na^+] from control and BIH were not different from each other at any sampling time. However, [Na^+] at t = 9 and 12 h were significantly higher compared to t = 0 for both control and BIH, probably due to the higher [Na^+] concentration of the infusion

solutions compared to hagfish plasma. [Cl^-] values were more variable than [Na^+], and did not differ significantly between treatments or times.

24 h. Na^+/K^+–ATPase and V–H^+–ATPase gill immunohistochemistry

NKA and VHA immunoreactivity patterns after the 24 h experiments were similar to those from the 6 h experiments. Both proteins were localized mostly in the same cells, and the immunolabeling occurred throughout the cell (Fig. 13.5).

24 h. Na^+/K^+–ATPase and V–H^+–ATPase gill abundance

Control and BIH had similar NKA levels in whole gill homogenates (1.28 ± 1.19 vs. 1.87 ± 0.34 a.f.u., respectively, n = 7), as estimated from western blots. However, VHA abundance was higher in BIH compared to control hagfish (2.83 ± 0.65 vs. 1.24 ± 0.21 a.f.u., $P < 0.05$, n = 7), indicating that blood alkalosis had induced an upregulation of VHA synthesis (Fig. 13.6).

When samples enriched in gill cell membranes were used for western blotting, we found that membrane-bound NKA had decreased in BIH compared to controls (0.63 ± 0.08 vs. 0.98 ± 0.10 a.f.u.), while membrane-bound VHA abundance had increased in the same group (1.82 ± 0.26 vs. 1.08 ± 0.13 a.f.u.) ($P < 0.05$, n = 7 in both cases) (Fig. 13.7).

Discussion

Our results show that hagfish can readily recover from acute (6 h experiments) and repeated (24 h experiments) blood alkalosis events. Some of the possible routes for reducing blood [HCO_3^-] are production of alkaline urine, accumulation in body tissues or red blood cells (rbc), simple diffusion to seawater, and intestinal or branchial secretion. If we consider the low urinary output of hagfish (Morris, 1965) and their almost non-existent rbc permeability to HCO_3^- (Peters et al., 2000), these two options can be discounted. Although HCO_3^- diffusion to seawater cannot be fully discounted, some characteristics of the blood pH and plasma TCO_2 profiles argue against it. In particular, if diffusion was the main component of the HCO_3^- clearance, we would expect the repeated HCO_3^- injections to exert similar changes in blood pH and plasma HCO_3^-. For example, the first injection elevated blood pH from 7.80 ± 0.07 to 8.13 ± 0.02 pH units at t = 3 h (ΔpH = 0.33 ± 0.07 pH units), while the second injection only elevated blood pH from 8.07 ± 0.04 to 8.16 ± 0.04 pH units (ΔpH = 0.09 ± 0.03 pH units). The effect is most evident in the lack of significant change in TCO_2 3 h after the second HCO_3^- injection (t = 9 h). These results indicate that an active mechanism for HCO_3^- secretion had been upregulated and remained active to prevent greater changes in blood parameters after the subsequent HCO_3^- loads.

We have no data to refute the possible transport of HCO_3^- into the intracellular compartment, for example the muscle. However, this mechanism would likely affect intracellular pH and [HCO_3^-] enormously. Regulation of

blood pH like we observed in our study does not seem to be adaptive if it comes at the expense of dramatic changes in those intracellular parameters.

Given the established role of gills in acid/base regulation in elasmobranch and teleost fishes (Evans et al., 2005), and the changes in branchial NKA and VHA reported in this study, it is likely that branchial HCO_3^- secretion plays a major role in the recovery from blood alkalosis. However, the putative role of intestinal HCO_3^- secretion (Grosell, 2006; Taylor and Grosell, 2006) deserves further investigation.

Current evidence suggest that NKA, VHA (this study) and also an NHE2-like protein (-lp) (Tresguerres et al., 2006b) are located in the same cells. However, there is a minority of cells that are not immunolabeled for all the transporters. This is likely an artifact of using the various antibodies in consecutive sections as explained in detail in (Tresguerres et al., 2005; Tresguerres et al., 2006b). Despite these technical difficulties, the majority of cells that label for one transporter also label for the other two, indicating that the vast majority (if not all) of cells have NKA, VHA and NHE2-lp.

In the short-term (6 h), there were no significant changes in NKA or VHA abundance in whole gill or cell membranes. However, blood pH and TCO_2 fully recovered by the end of the experimentation period. This indicates that the already present base-secretory machinery was sufficient and in place to handle the HCO_3^- load. Possible short term activation of base secretory mechanisms includes direct activation by an increase in substrate concentration ($[HCO_3^-]$) and/or post-translational modification such as

phosphorylation/de-phosphorylation. However, we were unable to accurately measure NKA activity and VHA activity in hagfish gills using the McCormick method (McCormick, 1993). Optimization of the assay for hagfish specific conditions is required to complete this type of analysis.

The long-term (24 h) experiments give more insights into the cellular mechanism for base secretion. The increase in VHA abundance in whole gill homogenates is indicative of upregulation of this enzyme in response to HCO_3^- load. In addition, increased VHA abundance in the gill cell membrane enriched fraction demonstrates that this ATPase inserts into the cell membrane in response to HCO_3^- load. Our centrifugation protocol would not separate the apical from the basolateral membrane. However, the immunolabelled sections suggest that VHA labelling does not occur on the apical membrane. Therefore, it is likely that VHA insertion under our experimental conditions is into the basolateral membrane. At first sight, this seems to be in contradiction with our immunohistochemistry results, which show a cytoplasmic-like VHA immunolabelling. However, hagfish gill MR cell basolateral membrane forms a tubular system that occupies most of the cell cytoplasm (Bartels and Welsch, 1986). Therefore, combining the western blotting, immunohistochemistry and ultrastructure data, we believe that VHA inserts into the basolateral tubular system during blood alkalosis. However, immunogold experiments are required in order to definitely confirm this hypothesis. The function of this insertion would be to reabsorb H^+ to the blood and help with the extrusion of HCO_3^- to seawater via an apical anion

exchanger yet to be identified. This putative anion exchanger could be subjected to additional activation mechanisms in order to increase HCO_3^- secretion.

A complementary explanation for the increased VHA abundance in the membrane-enriched fraction would be that the newly synthesized units of the enzyme (or of the V_o complex) are assembled together in the endoplasmic reticulum (ER) like it has been demonstrated in yeast (Graham et al., 1998). In that case, we predict that the holoenzyme would subsequently migrate and insert into the basolateral membrane. Unfortunately, separation of the plasma membrane from Golgi or ER by differential centrifugation is extremely difficult and hampered by the fact that specific markers (e.g. antibodies) to detect those compartments are not available.

NKA abundance is reduced in the cell membrane enriched fraction of HCO_3^- infused hagfish. Since NKA abundance does not change in whole gill samples, this is likely due to removal of NKA from the basolateral membrane during blood alkalosis. Similar insertion/removal of NKA units has been proposed to regulate Na^+ absorption in the mammalian kidney (Beltowski et al., 2004; Beltowski et al., 2003). In fish gills, NKA is involved in acid secretion (Evans et al., 2005). Therefore, removal of NKA from the basolateral membrane during blood alkalosis is likely related to a concomitant reduction in H^+ secretion to the water, which would help in counteracting alkalosis. Combining all the evidence, it is likely that blood acid–base regulation in the

hagfish is achieved by differential insertion of the relevant ion-transporting proteins into either the apical or the basolateral membrane of the MR cells.

The $NaHCO_3$ loads in our experiments were rather abrupt. For example, in similar experiments in dogfish, the HCO_3^- load was infused gradually and continuously over the experimentation period (Tresguerres et al., 2005; Tresguerres et al., 2006c). It is unclear whether or not hagfish in the wild experience blood alkalosis of this magnitude. However, the robust regulatory mechanism described in our study suggests that hagfish may experience periods of significant blood alkalosis naturally. Some possible sources of alkaline stress include respiratory disturbances related to conditions found in the deep-sea waters or a blood post-feeding alkaline tide as has been reported for elasmobranchs (Wood et al., 2005). Regarding this last possibility, we have recently shown that VHA translocates into the basolateral membrane of dogfish gill cells during a post-feeding alkalosis (Tresguerres et al., 2007b).

Comparisons to the branchial acid/base regulatory mechanisms from fish relatives are almost unavoidable when discussing results obtained from hagfish due to their primitive status. Briefly, a basolateral VHA acting for HCO_3^- secretion and H^+ reabsorption matches the proposed models for acid–base and ionic regulation in freshwater lampreys (Choe et al., 2004), marine (Piermarini and Evans, 2001; Tresguerres et al., 2005; Tresguerres et al., 2006c) and freshwater elasmobranchs (Piermarini and Evans, 2001), and some marine (Catches et al., 2006) and freshwater (Tresguerres et al.,

2006a) teleosts. We conclude that hagfish have gill MR cells for systemic acid–base regulation (see (Mallatt et al., 1987)), and that at least some of the components of the gill Cl^-/HCO_3^- exchange systems present in existing fish (namely, VHA) indeed evolved before the vertebrates entered freshwater (see (Evans, 1984)), since they are present in the primitive hagfish.

Tables

Table 13. 1 Plasma [Na^+] and [Cl^-] of hagfish at the sampling times**.**

Time (h)	[Na^+] (mmol.l^{-1})	[Cl^-] (mmol.l^{-1})
0	440.10 ± 8.17	451.17 ± 27.11
3	429.11 ± 9.95	479.14 ± 53.33
6	436.89 ± 11.34	481.56 ± 36.36
9	488.59 ± 7.93 *	501.52 ± 30.86
12	477.29 ± 9.94 *	491.93 ± 29.30
18	460.07 ± 7.94	439.28 ± 28.60
24	463.66 ± 9.90	452.94 ± 31.20

Note: Values are means ± s.e.m (*n*=14) from the combination of NaCl- and $NaHCO_3$-infused hagfish. The asterisks indicate significant differences compared to *t*=0 (1-way RM-ANOVA, Dunnett's post-test).

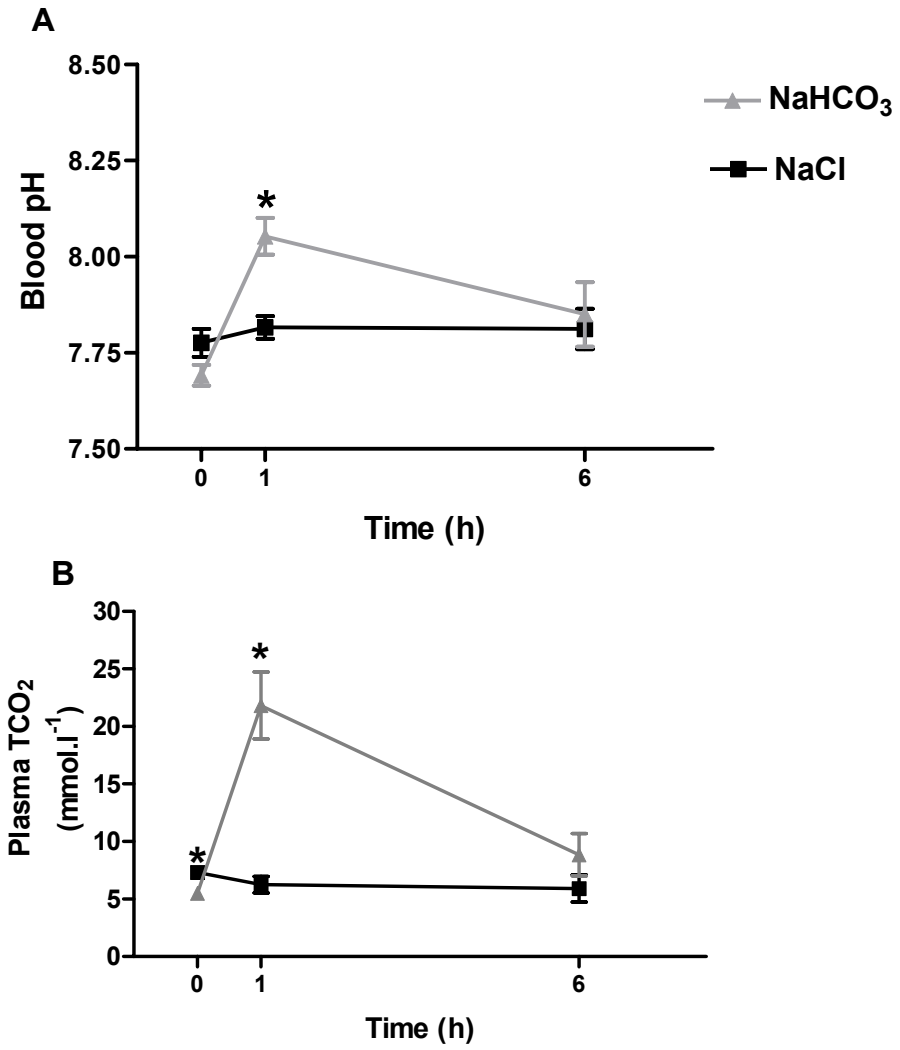

Figure 13. 1 6 h hagfish base infusion experiments.

Blood parameters of hagfish injected with either 250 mmol l^{-1} $NaHCO_3^-$ (6000 µequiv. kg^{-1}) or an equivalent volume of 500 mmol l^{-1} NaCl (Mean ± S.E.M., *n* = 6). ***A*** Blood pH. ***B*** Plasma total [CO_2]. * $P < 0.05$ compared to the control value (NaCl) of the respective time (2-way-RM-ANOVA, Bonferroni's *post* test).

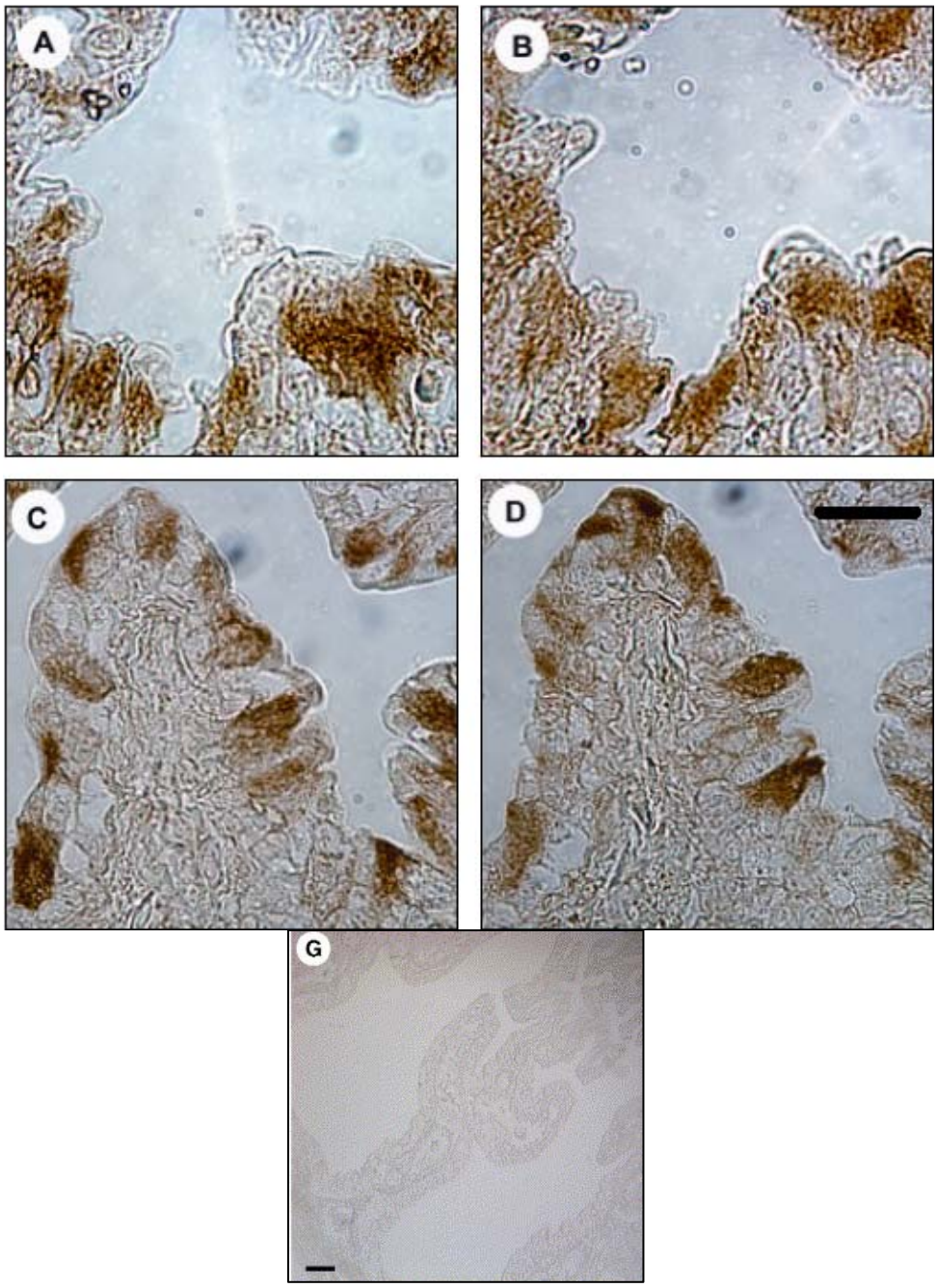

Figure 13. 2 6 h experiments Na^+/K^+–ATPase and V–H^+–ATPase immunoreactivity (IR).

Gill consecutive sections from NaCl-injected (***A***,***B***) and $NaHCO_3$-injected (***C***,***D***) hagfish (6 h experiments). ***A***, ***C*** = Na^+/K^+–ATPase IR. ***B***, ***D*** = V–H^+–ATPase IR. Scale bar = 10 μm. ***G*** Previously published control image of hagfish gill immunohistochemistry (Tresguerres et al., 2006b) lacking primary antibody. Scale bar = 50 μm.

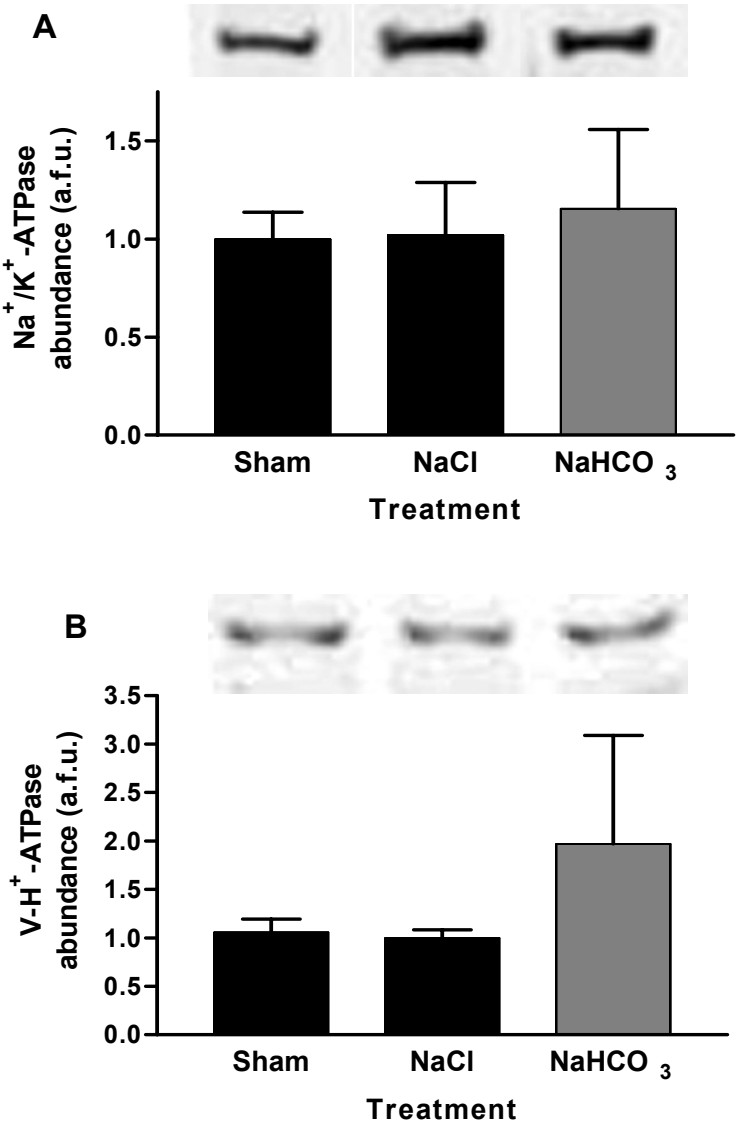

Figure 13. 3 6 h experiments NKA and VHA abundance

Na^+/K^+–ATPase ***A*** and V–H^+–ATPase ***B*** abundance in gills from sham (not-infused), NaCl- and $NaHCO_3$-infused hagfish. These data are from cell membranes, but whole gill homogenates showed the same trend. No significant differences were found between treatments (1-way ANOVA) (*n* = 4–6).

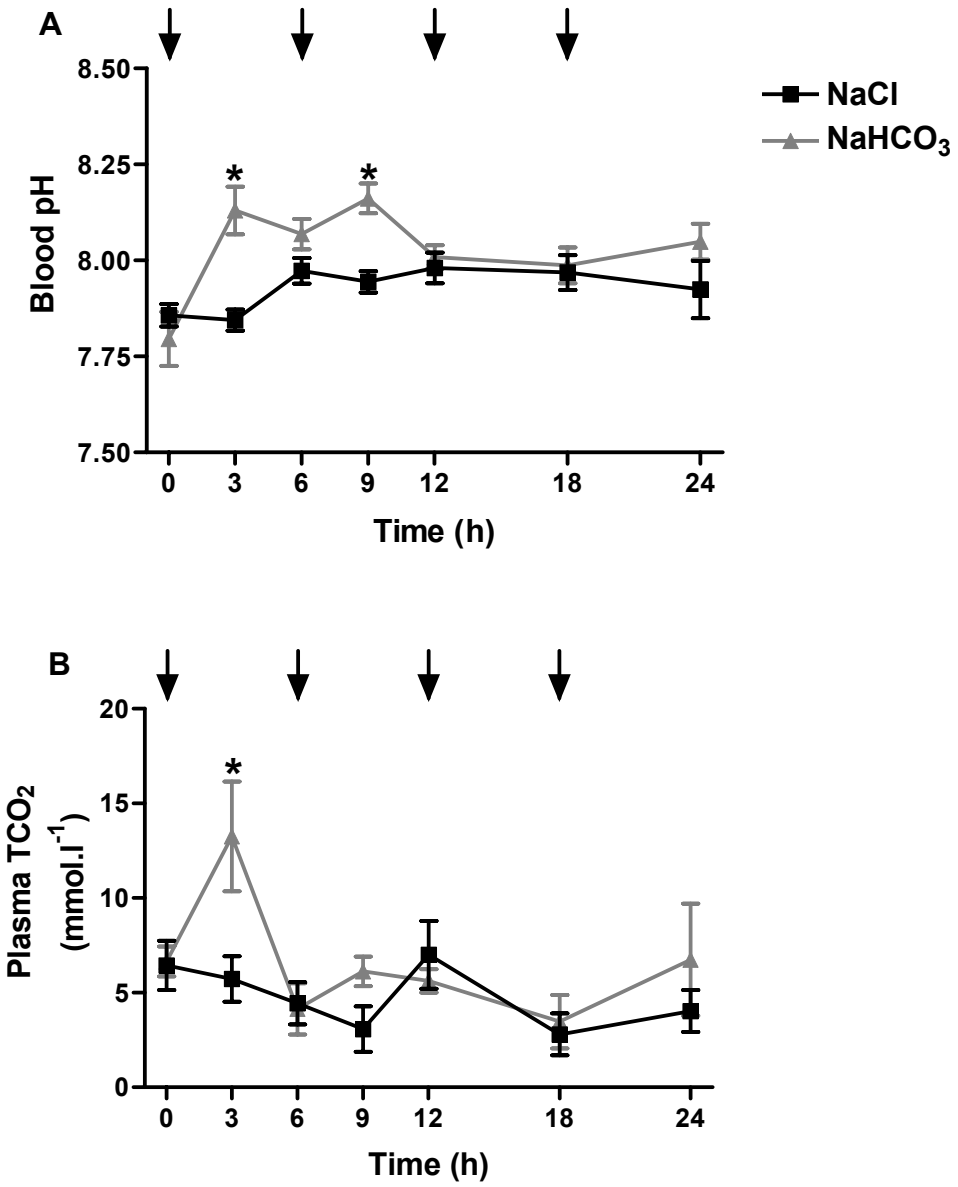

Figure 13. 4 24 h hagfish base infusion experiments.

Blood parameters of hagfish injected with either 250 mmol l^{-1} $NaHCO_3^-$ or 500 mmol l^{-1} NaCl (Mean ± S.E.M., *n* = 6). The arrows indicate 6000 µequiv. kg^{-1} injections of HCO_3^- or equivalent volume or NaCl ***A*** Blood pH. ***B*** Plasma total [CO_2]. * $P < 0.05$ compared to the control value (NaCl) of the respective time (2-way-RM-ANOVA, Bonferroni's *post* test).

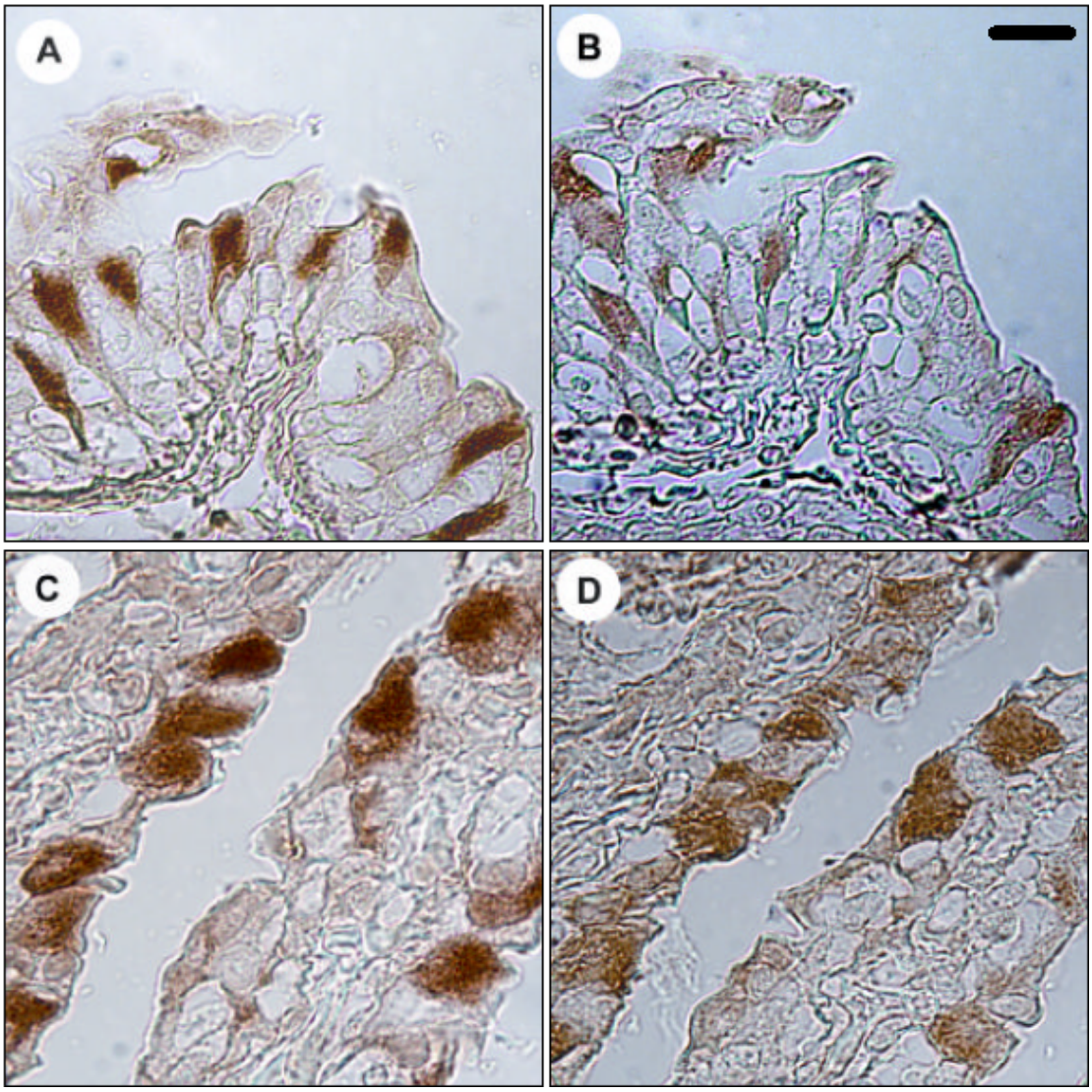

Figure 13. 5 24 h experiments Na^+/K^+–ATPase and V–H^+–ATPase immunoreactivity (IR)

Gill consecutive sections from NaCl-injected (***A***, ***B***) and $NaHCO_3$-injected (***C***,***D***) hagfish (6h experiments). ***A***, ***C*** = Na^+/K^+–ATPase IR. ***B***, ***D*** = V–H^+–ATPase IR. Scale bar = 10 μm.

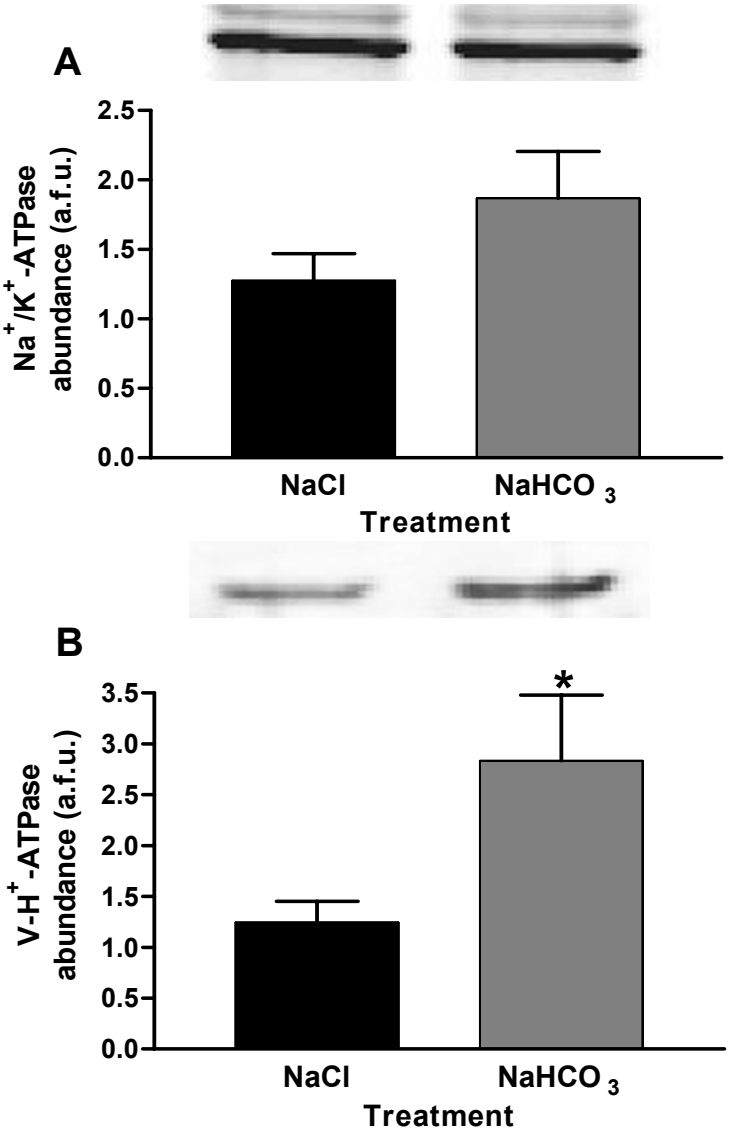

Figure 13. 6 24h NKA and VHA whole gill abundance.

Na^+/K^+–ATPase ***A*** and V–H^+–ATPase ***B*** abundance in whole gill homogenates from NaCl- and $NaHCO_3$-infused hagfish (24h). * $P < 0.05$ compared to the control value (NaCl) (Student's *t*-test) ($n = 7$).

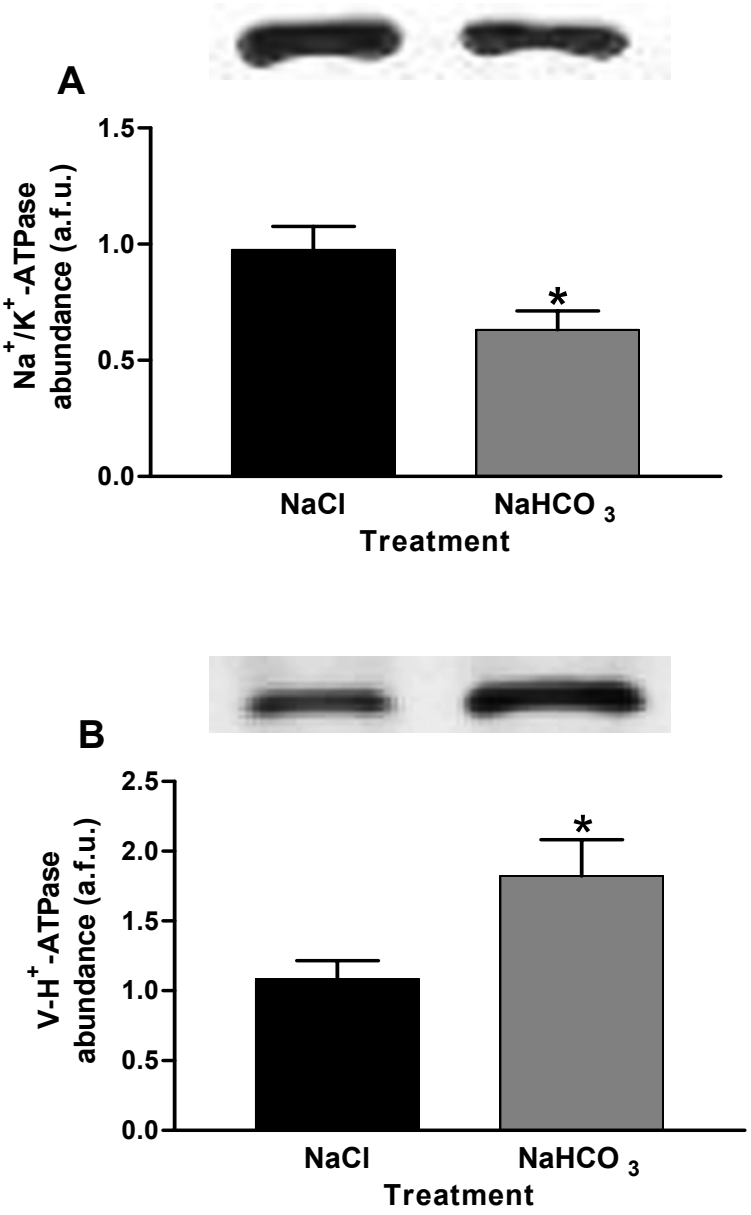

Figure 13. 7 24h NKA and VHA gill cell membranes abundance Na^+/K^+–ATPase ***A*** and V–H^+–ATPase ***B*** abundance in gill cell membranes from NaCl- and $NaHCO_3$-infused (24h) hagfish. * $P < 0.05$ compared to the control value (NaCl) (Student's *t*-test) ($n = 7$).

References

Ahearn, G. A. and Clay, L. P. (1989). Kinetic-Analysis of Electrogenic 2 Na+-1 H+ Antiport in Crustacean Hepatopancreas. *American Journal of Physiology* **257**, R484-R493.

Ahearn, G. A. and Franco, P. (1990). Sodium and Calcium Share the Electrogenic 2 Na+-1 H+ Antiporter in Crustacean Antennal Glands. *American Journal of Physiology* **259**, F758-F767.

Ahearn, G. A. and Franco, P. (1991). Electrogenic 2Na+/H+ Antiport in Echinoderm Gastrointestinal Epithelium. *Journal of Experimental Biology* **158**, 495-507.

Ahearn, G. A., Franco, P. and Clay, L. P. (1990). Electrogenic 2Na+/1H+ Exchange in Crustaceans. *Journal of Membrane Biology* **116**, 215-226.

Alper, S. L. (2006). Molecular physiology of SLC4 anion exchangers. *Experimental Physiology* **91**, 153-161.

Alt, J. M., Stolte, H., Eisenbach, G. M. and Walvig, F. (1981). Renal Electrolyte and Fluid Excretion in the Atlantic Hagfish Myxine-Glutinosa. *Journal of Experimental Biology* **91**, 323-330.

Alvarez de la Rosa, D. A., Canessa, C. M., Fyfe, G. K. and Zhang, P. (2000). Structure and regulation of amiloride-sensitive sodium channels. *Annual Review of Physiology* **62**, 573-594.

Aronson, P. S. (1985). Kinetic-Properties of the Plasma-Membrane Na+-H+ Exchanger. *Annual Review of Physiology* **47**, 545-560.

Aronson, P. S., Nee, J. and Suhm, M. A. (1982). Modifier Role of Internal H+ in Activating the Na+-H+ Exchanger in Renal Microvillus Membrane-Vesicles. *Nature* **299**, 161-163.

Avella, M. and Bornancin, M. (1989). A New Analysis of Ammonia and Sodium-Transport through the Gills of the Fresh-Water Rainbow-Trout (Salmo, Gairdneri). *Journal of Experimental Biology* **142**, 155-175.

Bachmann, O., Reichelt, D., Tuo, B., Manns, M. P. and Seidler, U. (2006). Carbachol increases Na+-HCO3- cotransport activity in murine colonic crypts in a M-3(-), Ca2+/calmodulin-, and PKC-dependent manner. *American Journal of Physiology-Gastrointestinal and Liver Physiology* **291**, G650-G657.

Bagnis, C., Marshansky, V., Breton, S. and Brown, D. (2001). Remodeling the cellular profile of collecting ducts by chronic carbonic

anhydrase inhibition. *American Journal of Physiology-Renal Physiology* **280**, F437-F448.

Bartels, H. (1992). The gills of hagfishes. In *The Biology of Hagfishes*, eds. J. Jorgensen J. Lomholt R. Weber and H. Malte), pp. 205-222. London: Chapman and Hall.

Bartels, H. and Welsch, U. (1986). Mitochondria-rich cells in the gill epithelium of cyclostomes. A thin section and freeze-fracture study. In *Proceedings of the Second International Conference on Indo-Pacific Fishes,* , eds. T. Uyeno T. Taniuchi and K. Matsuura), pp. 58-72. Tokyo: Ichthyological Society of Japan.

Bayaa, M. and Perry, S. F. (2005). Chloride bicarbonate exchange in the zebrafish, Danio rerio. *Comparative Biochemistry and Physiology a-Molecular & Integrative Physiology* **141**, S201-S201.

Beltowski, J., Marciniak, A., Jamroz-Wisniewska, A., Borkowska, E. and Wojcicka, G. (2004). Bidirectional regulation of renal cortical Na+,K+-ATPase by protein kinase C. *Acta Biochimica Polonica* **51**, 757-772.

Beltowski, J., Marciniak, A., Wojcicka, G. and Gorny, D. (2003). Regulation of renal Na+,K+-ATPase and ouabain-sensitive H+,K+-ATPase by the cyclic AMP-protein kinase A signal transduction pathway. *Acta Biochimica Polonica* **50**, 103-114.

Berenbrink, M. (2006). Evolution of vertebrate haemoglobins: Histidine side chains, specific buffer value and Bohr effect. *Respiratory Physiology & Neurobiology* **154**, 165-184.

Bernard, C. (1878). Leçons sur les phénomènes de la vie communs aux animaux et aux végétaux. Paris: J.-B. Baillière et fils.

Berridge, M. J. (1970). Role of 5-Hydroxytryptamine and Cyclic Amp in Control of Fluid Secretion by Isolated Salivary Glands. *Journal of Experimental Biology* **53**, 171-&.

Bevelander, G. (1935). A comparative study of the branchial epithelium in fishes, with special reference to extrarenal excretion. *Journal of Morphology* **56**, 335-351.

Beyenbach, K. W., Pannabecker, T. L. and Nagel, W. (2000). Central role of the apical membrane H+-ATPase in electrogenesis and epithelial transport in Malpighian tubules. *Journal of Experimental Biology* **203**, 1459-1468.

Beyenbach, K. W. and Wieczorek, H. (2006). The V-type H+ ATPase: molecular structure and function, physiological roles and regulation. *Journal of Experimental Biology* **209**, 577-589.

Bezbaruah, R. L., Gogoi, B. K., Pillai, K. R. and Nigam, J. N. (1991). Amylase Production by 3 Bacillus Strains Active at Alkaline Ph. *Journal of Basic Microbiology* **31**, 13-20.

Boisen, A. M. Z., Amstrup, J., Novak, I. and Grosell, M. (2003). Sodium and chloride transport in zebrafish soft water and hard water acclimated (Danio rerio). *Biochimica Et Biophysica Acta-Biomembranes* **1618**, 207-218.

Borgese, F., Sardet, C., Cappadoro, M., Pouyssegur, J. and Motais, R. (1992). Cloning and Expression of a Camp-Activated Na+/H+ Exchanger - Evidence That the Cytoplasmic Domain Mediates Hormonal-Regulation. *Proceedings of the National Academy of Sciences of the United States of America* **89**, 6765-6769.

Boron, W. F. and Boulpaep, E. L. (1983). Intracellular pH Regulation in the Renal Proximal Tubule of the Salamander. *Journal of General Physiology* **81**, 53-94.

Boron, W. F. and Deweer, P. (1976a). Active Proton Transport Stimulated by CO2-HCO3-, Blocked by Cyanide. *Nature* **259**, 240-241.

Boron, W. F. and Deweer, P. (1976b). Intracellular pH Transients in Squid Giant-Axons Caused by CO2, NH3, and Metabolic-Inhibitors. *Journal of General Physiology* **67**, 91-112.

Boron, W. F., Hediger, M. A., Boulpaep, E. L. and Romero, M. F. (1997). The renal electrogenic Na+:HCO3- cotransporter. *Journal of Experimental Biology* **200**, 263-268.

Boron, W. F. and Russell, J. M. (1983). Stoichiometry and Ion Dependencies of the Intracellular-pH-Regulating Mechanism in Squid Giant-Axons. *Journal of General Physiology* **81**, 373-399.

Borzak, S., Reers, M., Arruda, J., Sharma, V. K., Sheu, S. S., Smith, T. W. and Marsh, J. D. (1992). Na+ Efflux Mechanisms in Ventricular Myocytes - Measurement of [Na+]I with Na+-Binding Benzofuran Isophthalate. *American Journal of Physiology* **263**, H866-H874.

Boudko, D. Y., Moroz, L. L., Harvey, W. R. and Linser, P. J. (2001a). Alkalinization by chloride/bicarbonate pathway in larval mosquito midgut. *Proceedings of the National Academy of Sciences of the United States of America* **98**, 15354-15359.

Boudko, D. Y., Moroz, L. L., Linser, P. J., Trimarchi, J. R., Smith, P. J. S. and Harvey, W. R. (2001b). In situ analysis of pH gradients in mosquito larvae using noninvasive, self-referencing, pH-sensitive microelectrodes. *Journal of Experimental Biology* **204**, 691-699.

Boyarsky, G., Ganz, M. B., Sterzel, R. B. and Boron, W. F. (1988). pH Regulation in Single Glomerular Mesangial Cells .1. Acid Extrusion in Absence and Presence of HCO3-. *American Journal of Physiology* **255**, C844-C856.

Brahimi-Horn, M. C., Chiche, J. and Pouyssegur, J. (2007). Hypoxia signalling controls metabolic demand. *Current Opinion in Cell Biology* **19**, 223-229.

Brahimi-Horn, M. C. and Pouyssegur, J. (2007). Oxygen, a source of life and stress. *Febs Letters* **581**, 3582-3591.

Brauner, C. J., Wang, T., Wang, Y., Richards, J. G., Gonzalez, R. J., Bernier, N. J., Xi, W., Patrick, A. and Va, A. L. (2004). Limited extracellular but complete intracellular acid-base regulation during short-term environmental hypercapnia in the armoured catfish, Liposarcus pardalis. *Journal of Experimental Biology* **207**, 3381-3390.

Breton, S. and Brown, D. (2007). New insights into the regulation of V-ATPase-dependent proton secretion. *American Journal of Physiology-Renal Physiology* **292**, F1-F10.

Brett, C. L., Donowitz, M. and Rao, R. (2005). Evolutionary origins of eukaryotic sodium/proton exchangers. *American Journal of Physiology-Cell Physiology* **288**, C223-C239.

Brier, S., Maria, G., Carginale, V., Capasso, A., Wu, Y., Taylor, R. M., Borotto, N. B., Capasso, C. and Engen, J. R. (2007). Purification and characterization of pepsins A1 and A2 from the Antarctic rock cod Trematomus bernacchii. *Febs Journal* **274**, 6152-6166.

Bucking, C. and Wood, C. M. (2006). Gastrointestinal processing of Na+, Cl-, and K+ during digestion: implications for homeostatic balance in freshwater rainbow trout. *American Journal of Physiology-Regulatory Integrative and Comparative Physiology* **291**, R1764-R1772.

Burnett, L. E. and Mcmahon, B. R. (1987). Gas-Exchange, Hemolymph Acid-Base Status, and the Role of Branchial Water Stores during Air Exposure in 3 Littoral Crab Species. *Physiological Zoology* **60**, 27-36.

Bury, N. R. and Wood, C. M. (1999). Mechanism of branchial apical silver uptake by rainbow trout is via the proton-coupled Na+ channel.

American Journal of Physiology-Regulatory Integrative and Comparative Physiology **277**, R1385-R1391.

Cannon, W. B. (1929). Organization for physiological homeostasis. *Physiological Reviews* **9**, 399-433.

Cardone, R. A., Casavola, V. and Reshkin, S. J. (2005). The role of disturbed pH dynamics and the Na+/H+ exchanger in metastasis. *Nature Reviews Cancer* **5**, 786-795.

Carroll, M. A. and Catapane, E. J. (2007). The nervous system control of lateral ciliary activity of the gill of the bivalve mollusc, Crassostrea virginica. *Comparative Biochemistry and Physiology a-Molecular & Integrative Physiology* **148**, 445-450.

Catches, J. S., and Claiborne, J.B. (2004). NHE2 and Na+/K+-ATPase immunoreactivity in Myxocephalus octodecimspinosus. *Bull. Mt. Desert Isl. Biol. Lab* **43**, 22-23.

Catches, J. S., Burns, J. M., Edwards, S. L. and Claiborne, J. B. (2006). Na+/H+ antiporter, V-H+-ATPase and Na+/K+-ATPase immunolocalization in a marine teleost (Myoxocephalus octodecemspinosus). *Journal of Experimental Biology* **209**, 3440-3447.

Chang, I. C. and Hwang, P. P. (2004). Cl- uptake mechanism in freshwater-adapted tilapia (Oreochromis mossambicus). *Physiological and Biochemical Zoology* **77**, 406-414.

Chen, X. M., Polleichtner, G., Kadurin, I. and Grunder, S. (2007). Zebrafish acid-sensing ion channel (ASIC) 4, characterization of homo- and heteromeric channels, and identification of regions important for activation by H+. *Journal of Biological Chemistry* **282**, 30406-30413.

Chiche, J., Ilc, K., Laferriere, J., Trottier, E., Dayan, F., Mazure, N. M., Brahimi-Horn, M. C. and Pouyssegur, J. (2009). Hypoxia-Inducible Carbonic Anhydrase IX and XII Promote Tumor Cell Growth by Counteracting Acidosis through the Regulation of the Intracellular pH. *Cancer Research* **69**, 358-368.

Choe, K. P., Edwards, S., Morrison-Shetlar, A. I., Toop, T. and Claiborne, J. B. (1999). Immunolocalization of Na+/K+-ATPase in mitochondrion-rich cells of the atlantic hagfish (Myxine glutinosa) gill. *Comparative Biochemistry and Physiology a-Molecular & Integrative Physiology* **124**, 161-168.

Choe, K. P., Edwards, S. L., Claiborne, J. B. and Evans, D. H. (2007). The putative mechanism of Na+ absorption in euryhaline elasmobranchs exists in the gills of a stenohaline marine elasmobranch,

Squalus acanthias. *Comparative Biochemistry and Physiology a-Molecular & Integrative Physiology* **146**, 155-162.

Choe, K. P., Kato, A., Hirose, S., Plata, C., Sindic, A., Romero, M. F., Claiborne, J. B. and Evans, D. H. (2005). NHE3 in an ancestral vertebrate: primary sequence, distribution, localization, and function in gills. *American Journal of Physiology-Regulatory Integrative and Comparative Physiology* **289**, R1520-R1534.

Choe, K. P., Morrison-Shetlar, A. I., Wall, B. P. and Claiborne, J. B. (2002). Immunological detection of Na+/H+ exchangers in the gills of a hagfish, Myxine glutinosa, an elasmobranch, Raja erinacea, and a teleost, Fundulus heteroclitus. *Comparative Biochemistry and Physiology a-Molecular and Integrative Physiology* **131**, 375-385.

Choe, K. P., O'Brien, S., Evans, D. H., Toop, T. and Edwards, S. L. (2004). Immunolocalization of Na+/K+-ATPase, carbonic anhydrase II, and vacuolar H+-ATPase in the gills of freshwater adult lampreys, Geotria australis. *Journal of Experimental Zoology Part a-Comparative Experimental Biology* **301A**, 654-665.

Claiborne, J. B., Blackston, C. R., Choe, K. P., Dawson, D. C., Harris, S. P., Mackenzie, L. A. and Morrison-Shetlar, A. I. (1999). A mechanism for branchial acid excretion in marine fish: Identification of multiple Na+/H+ antiporter (NHE) isoforms in gills of two seawater teleosts. *Journal of Experimental Biology* **202**, 315-324.

Claiborne, J. B., Choe, K. P., Morrison-Shetlar, A. I., Weakley, J. C., Havird, J., Freiji, A., Evans, D. H. and Edwards, S. L. (2008). Molecular detection and immunological localization of gill Na+/H+ exchanger in the dogfish (Squalus acanthias). *American Journal of Physiology-Regulatory Integrative and Comparative Physiology* **294**, R1092-R1102.

Claiborne, J. B., Edwards, S. L. and Morrison-Shetlar, A. I. (2002). Acid-base regulation in fishes: Cellular and molecular mechanisms. *Journal of Experimental Zoology* **293**, 302-319.

Claiborne, J. B., Perry, E., Bellows, S. and Campbell, J. (1997). Mechanisms of acid-base excretion across the gills of a marine fish. *Journal of Experimental Zoology* **279**, 509-520.

Clark, T. M., Hutchinson, M. J., Huegel, K. L., Moffett, S. B. and Moffett, D. F. (2005). Additional morphological and physiological heterogeneity within the midgut of larval Aedes aegypti (Diptera : Culicidae) revealed by histology, electrophysiology, and effects of Bacillus thuringiensis endotoxin. *Tissue & Cell* **37**, 457-468.

Clark, T. M., Koch, A. and Moffett, D. F. (1999). The anterior and posterior 'stomach' regions of larval Aedes aegypti midgut: Regional specialization of ion transport and stimulation by 5-hydroxytryptamine. *Journal of Experimental Biology* **202**, 247-252.

Clark, T. M., Koch, A. and Moffett, D. F. (2000). The electrical properties of the anterior stomach of the larval mosquito (Aedes aegypti). *Journal of Experimental Biology* **203**, 1093-1101.

Cohen, R. D. and Iles, R. A. (1975). Intracellular pH: measurement, control and metabolic interrelationships. *Critical Reviews in Clinical Lab Sciences* **6**, 101-143.

Cohen, R. D., Iles, R. A., Barnett, D., Howell, M. E. O. and Strunin, J. (1971). Effect of Changes in Lactate Uptake on Intracellular Ph of Perfused Rat Liver. *Clinical Science* **41**, 159-&.

Copeland, D. E. (1948). The Cytological Basis of Chloride Transfer in the Gills of Fundulus Heteroclitus. *Journal of Morphology* **82**, 201-227.

Corena, M. D., Seron, T. J., Lehman, H. K., Ochrietor, J. D., Kohn, A., Tu, C. and Linser, P. J. (2002). Carbonic anhydrase in the midgut of larval Aedes aegypti: cloning, localization and inhibition. *Journal of Experimental Biology* **205**, 591-602.

Craig, P. M., Wood, C. M. and McClelland, G. B. (2007). Gill membrane remodeling with soft-water acclimation in zebrafish (Danio rerio). *Physiological Genomics* **30**, 53-60.

Crocker, C. E. and Cech, J. J. (1998). Effects of hypercapnia on blood-gas and acid-base status in the white sturgeon, Acipenser transmontanus. *Journal of Comparative Physiology B-Biochemical Systemic and Environmental Physiology* **168**, 50-60.

D'Cruz, L. M., Dockray, J. J., Morgan, I. J. and Wood, C. M. (1998). Physiological effects of sublethal acid exposure in juvenile rainbow trout on a limited or unlimited ration during a simulated global warming scenario. *Physiological Zoology* **71**, 359-376.

D'Cruz, L. M. and Wood, C. M. (1998). The influence of dietary salt and energy on the response to low pH in juvenile rainbow trout. *Physiological Zoology* **71**, 642-657.

Dadd, R. H. (1975). Alkalinity within Midgut of Mosquito Larvae with Alkaline-Active Digestive Enzymes. *Journal of Insect Physiology* **21**, 1847-1853.

Dames, P., Zimmermann, B., Schmidt, R., Rein, J., Voss, M., Schewe, B., Walz, B. and Baumann, O. (2006). cAMP regulates plasma membrane vacuolar-type H+-ATPase assembly and activity in blowfly salivary glands. *Proceedings of the National Academy of Sciences of the United States of America* **103**, 3926-3931.

Davis, B. A., Hogan, E. M. and Boron, W. F. (1994). Shrinkage-induced activation of Na(+)-H+ exchange in barnacle muscle fibers. *Am J Physiol* **266**, C1744-53.

DeCoursey, T. E. (2003). Voltage-gated proton channels and other proton transfer pathways (vol 83, pg 475, 2003). *Physiological Reviews* **83**, 1067-1067.

deHurtado, M. C. C., Alvarez, B. V., Perez, N. G. and Cingolani, H. E. (1996). Role of an electrogenic Na+-HCO3- cotransport in determining myocardial pH(i) after an increase in heart rate. *Circulation Research* **79**, 698-704.

Deitmer, J. W. and Rose, C. R. (1996). pH regulation and proton signalling by glial cells. *Progress in Neurobiology* **48**, 73-103.

Dockray, J. J., Reid, S. D. and Wood, C. M. (1996). Effects of elevated summer temperatures and reduced pH on metabolism and growth of juvenile rainbow trout (Oncorhynchus mykiss) on unlimited ration. *Canadian Journal of Fisheries and Aquatic Sciences* **53**, 2752-2763.

Donowitz, M., Janecki, A., Akhter, S., Cavet, M. E., Sanchez, F., Lamprecht, G., Zizak, M., Kwon, W. L., Khurana, S., Yun, C. H. C. et al. (2000). Short-term regulation of NHE3 by EGF and protein kinase C but not protein kinase A involves vesicle trafficking in epithelial cells and fibroblasts. *Epithelial Transport and Barrier Function* **915**, 30-42.

Doyle, W. H. and Gorecki, D. (1961). The so-called chloride cell of the fish gill. *Physiological Zoology* **34**, 81-85.

Drach, P. and Tchernig.C. (1967). Method for Determining Intermoulting Stages and Its General Application to Crustacea. *Vie Et Milieu Serie a-Biologie Marine* **18**, 595-&.

Drose, S. and Altendorf, K. (1997). Bafilomycins and concanamycins as inhibitors of V-ATPases and P-ATPases. *Journal of Experimental Biology* **200**, 1-8.

Dykxhoorn, D. M. and Lieberman, J. (2005). The silent revolution: RNA interference as basic biology, research tool, and therapeutic. *Annual Review of Medicine* **56**, 401-423.

Eddy, F. B. and Chang, Y. J. (1993). Effects of salinity in relation to migration and development in fish. In *The Vertebrate Gas Transport Cascade; Adaptations to Environment and Mode of Life*, (ed. J. a. B. Eduardo, P.W.), pp. 35-42. Boca Raton CRC Press.

Edwards, H. A. (1982a). Free Amino-Acids as Regulators of Osmotic-Pressure in Aquatic Insect Larvae. *Journal of Experimental Biology* **101**, 153-160.

Edwards, H. A. (1982b). Ion Concentration and Activity in the Hemolymph of Aedes-Aegypti Larvae. *Journal of Experimental Biology* **101**, 143-151.

Edwards, S. L., Claiborne, J. B., Morrison-Shetlar, A. I. and Toop, T. (2001). Expression of Na+/H+ exchanger mRNA in the gills of the Atlantic hagfish (Myxine glutinosa) in response to metabolic acidosis. *Comparative Biochemistry and Physiology a-Molecular and Integrative Physiology* **130**, 81-91.

Edwards, S. L., Donald, J. A., Toop, T., Donowitz, M. and Tse, C. M. (2002). Immunolocalisation of sodium/proton exchanger-like proteins in the gills of elasmobranchs. *Comparative Biochemistry and Physiology a-Molecular and Integrative Physiology* **131**, 257-265.

Edwards, S. L., Tse, C. M. and Toop, T. (1999). Immunolocalisation of NHE3-like immunoreactivity in the gills of the rainbow trout (Oncorhynchus mykiss) and the blue-throated wrasse (Pseudolabrus tetrious). *Journal of Anatomy* **195**, 465-469.

Edwards, S. L., Wall, B. P., Morrison-Shetlar, A., Sligh, S., Weakley, J. C. and Claiborne, J. B. (2005). The effect of environmental hypercapnia and salinity on the expression of NHE-like isoforms in the gills of a euryhaline fish (Fundulus heteroclitus). *Journal of Experimental Zoology Part a-Comparative Experimental Biology* **303A**, 464-475.

Ehrenfeld, J. (1998). Active proton and urea transport by amphibian skin. *Comparative Biochemistry and Physiology a-Molecular & Integrative Physiology* **119**, 35-45.

Ehrenfeld, J. and Garcia-Romeu, F. (1977). Active Hydrogen Excretion and Sodium Absorption through Isolated Frog Skin. *American Journal of Physiology* **233**, F46-F54.

Ehrenfeld, J., Garciaromeu, F. and Harvey, B. J. (1985). Electrogenic Active Proton Pump in Rana-Esculenta Skin and Its Role in Sodium-Ion Transport. *Journal of Physiology-London* **359**, 331-355.

Ehrenfeld, J. and Klein, U. (1997). The key role of the H+ V-ATPase in acid-base balance and Na+ transport processes in frog skin. *Journal of Experimental Biology* **200**, 247-256.

Elger, M. and Hentschel, H. (1983). Morphological evidence for ionocytes in the gill epithelium of the hagfish Myxine glutionosa L. *Bull. Mt. Desert Isl, Biol. Lab* **23**, 4-8.

Esaki, M., Hoshijima, K., Kobayashi, S., Fukuda, H., Kawakami, K. and Hirose, S. (2007). Visualization in zebrafish larvae of Na+ uptake in mitochondria-rich cells whose differentiation is dependent on foxi3a. *American Journal of Physiology-Regulatory Integrative and Comparative Physiology* **292**, R470-R480.

Evans, D. H. (1984). Gill Na+/H+ and Cl–/HCO3– exchange systems evolved before the vertebrates entered freshwater. *Journal of Experimental Biology* **113**, 465-469.

Evans, D. H. (2002). Cell signaling and ion transport across the fish gill epithelium. *J Exp Zool* **293**, 336-47.

Evans, D. H. (2008). Teleost fish osmoregulation: what have we learned since August Krogh, Homer Smith, and Ancel Keys. *Am J Physiol Regul Integr Comp Physiol* **295**, R704-13.

Evans, D. H., Piermarini, P. M. and Choe, K. P. (2005). The multifunctional fish gill: Dominant site of gas exchange, osmoregulation, acid-base regulation, and excretion of nitrogenous waste. *Physiological Reviews* **85**, 97-177.

Fafournoux, P., Ghysdael, J., Sardet, C. and Pouyssegur, J. (1991). Functional Expression of the Human Growth-Factor Activatable Na+/H+ Antiporter (Nhe-1) in Baculovirus-Infected Cells. *Biochemistry* **30**, 9510-9515.

Fenwick, J. C., Bonga, S. E. W. and Flik, G. (1999). In vivo bafilomycin-sensitive Na+ uptake in young freshwater fish. *Journal of Experimental Biology* **202**, 3659-3666.

Fievet, B., Gabillat, N., Borgese, F. and Motais, R. (1995). Expression of Band-3 Anion-Exchanger Induces Chloride Current and Taurine Transport - Structure-Function Analysis. *Embo Journal* **14**, 5158-5169.

Fitz, J. G., Persico, M. and Scharschmidt, B. F. (1989). Electrophysiological Evidence for Na+-Coupled Bicarbonate Transport in Cultured Rat Hepatocytes. *American Journal of Physiology* **256**, G491-G500.

Fliegel, L., Walsh, M. P., Singh, D., Wong, C. and Barr, A. (1992). Phosphorylation of the C-Terminal Domain of the Na+/H+ Exchanger by Ca2+/Calmodulin-Dependent Protein Kinase-Ii. *Biochemical Journal* **282**, 139-145.

Forster, M. E., Davison, W., Satchell, G. H. and Taylor, H. H. (1989). The Subcutaneous Sinus of the Hagfish, Eptatretus-Cirrhatus and Its Relation to the Central Circulating Blood-Volume. *Comparative Biochemistry and Physiology a-Physiology* **93**, 607-612.

Foskett, J. K. and Scheffey, C. (1982). The Chloride Cell - Definitive Identification as the Salt-Secretory Cell in Teleosts. *Science* **215**, 164-166.

Freire, C. A., Onken, H. and McNamara, J. C. (2008). A structure-function analysis of ion transport in crustacean gills and excretory organs. *Comparative Biochemistry and Physiology a-Molecular & Integrative Physiology* **151**, 272-304.

Fry, A. C. and Karet, F. E. (2007). Inherited renal acidoses. *Physiology* **22**, 202-211.

Furimsky, M., Moon, T. W. and Perry, S. F. (2000). Evidence for the role of a Na+/HCO3- cotransporter in trout hepatocyte pHi regulation. *Journal of Experimental Biology* **203**, 2201-2208.

Galvez, F., Reid, S. D., Hawkings, G. and Goss, G. G. (2002). Isolation and characterization of mitochondria-rich cell types from the gill of freshwater rainbow trout. *American Journal of Physiology-Regulatory Integrative and Comparative Physiology* **282**, R658-R668.

Garciadiaz, J. F., Klemperer, G., Baxendale, L. M. and Essig, A. (1986). Cell Sodium Activity and Sodium-Pump Function in Frog-Skin. *Journal of Membrane Biology* **92**, 37-46.

Genovese, G., Ortiz, N., Urcola, M. R. and Luquet, C. M. (2005). Possible role of carbonic anhydrase, V-H+-ATPase, and Cl-/HCO3- exchanger in electrogenic ion transport across the gills of the euryhaline crab Chasmagnathus granulatus. *Comparative Biochemistry and Physiology a-Molecular & Integrative Physiology* **142**, 362-369.

Genovese, G., Senek, M., Ortiz, N., Regueira, M., Towle, D. W., Tresguerres, M. and Luquet, C. M. (2006). Dopaminergic regulation of ion transport in gills of the euryhaline semiterrestrial crab Chasmagnathus granulatus: interaction between D1- and D2-like receptors. *Journal of Experimental Biology* **209**, 2785-2793.

Georgalis, T., Perry, S. F. and Gilmour, K. M. (2006). The role of branchial carbonic anhydrase in acid-base regulation in rainbow trout (Oncorhynchus mykiss). *Journal of Experimental Biology* **209**, 518-530.

Gleeson, D., Smith, N. D. and Boyer, J. L. (1989). Bicarbonate-Dependent and Bicarbonate-Independent Intracellular pH Regulatory Mechanisms in Rat Hepatocytes - Evidence for Na+-HCO3- Cotransport. *Journal of Clinical Investigation* **84**, 312-321.

Goss, G. G., Adamia, S. and Galvez, F. (2001a). Peanut lectin binds to a subpopulation of mitochondria-rich cells in the rainbow trout gill epithelium. *American Journal of Physiology-Regulatory Integrative and Comparative Physiology* **281**, R1718-R1725.

Goss, G. G., Jiang, L. W., Vandorpe, D. H., Kieller, D., Chernova, M. N., Robertson, M. and Alper, S. L. (2001b). Role of JNK in hypertonic activation of Cl--dependent Na+/H+ exchange in Xenopus oocytes. *American Journal of Physiology-Cell Physiology* **281**, C1978-C1990.

Goss, G. G., Laurent, P. and Perry, S. F. (1992). Evidence for a Morphological Component in Acid-Base Regulation during Environmental Hypercapnia in the Brown Bullhead (Ictalurus-Nebulosus). *Cell and Tissue Research* **268**, 539-552.

Goss, G. G., Orr, E. and Katoh, F. (2005). Characterization of SLC26 anion exchangers in rainbow trout. *Comparative Biochemistry and Physiology a-Molecular & Integrative Physiology* **141**, S197-S197.

Goss, G. G., Perry, S. F., Fryer, J. N. and Laurent, P. (1998). Gill morphology and acid-base regulation in freshwater fishes. *Comparative Biochemistry and Physiology a-Molecular & Integrative Physiology* **119**, 107-115.

Goss, G. G., Perry, S.F., Laurent, P. (1995). Ultrastructural and morphometric studies on ion and acid-base transport processes in freshwater fish. In *Cellular and Molecular Approaches to Fish Ionic Regulation*, (ed. C. M. Wood, Shuttleworth, T.J.). San Diego, CA: Academic.

Goss, G. G. and Wood, C. M. (1990a). Na+ and Cl- Uptake Kinetics, Diffusive Effluxes and Acidic Equivalent Fluxes across the Gills of Rainbow-Trout .1. Responses to Environmental Hyperoxia. *Journal of Experimental Biology* **152**, 521-547.

Goss, G. G. and Wood, C. M. (1990b). Na+ and Cl- Uptake Kinetics, Diffusive Effluxes and Acidic Equivalent Fluxes across the Gills of Rainbow-Trout .2. Responses to Bicarbonate Infusion. *Journal of Experimental Biology* **152**, 549-571.

Goss, G. G. and Wood, C. M. (1991). 2-Substrate Kinetic-Analysis - a Novel-Approach Linking Ion and Acid-Base Transport at the Gills of Fresh-Water Trout, Oncorhynchus-Mykiss. *Journal of Comparative Physiology B-Biochemical Systemic and Environmental Physiology* **161**, 635-646.

Graber, M., Dipaola, J., Hsiang, F. L., Barry, C. and Pastoriza, E. (1991). Intracellular pH in the Ok Cell .1. Identification of H+ Conductance and Observations on Buffering Capacity. *American Journal of Physiology* **261**, C1143-C1153.

Graham, L. A., Hill, K. J. and Stevens, T. H. (1998). Assembly of the yeast vacuolar H+-ATPase occurs in the endoplasmic reticulum and requires a Vma12p/Vma22p assembly complex. *Journal of Cell Biology* **142**, 39-49.

Greco, A. M., Fenwick, J. C. and Perry, S. F. (1996). The effects of soft-water acclimation on gill structure in the rainbow trout Oncorhynchus mykiss. *Cell and Tissue Research* **285**, 75-82.

Grichtchenko, I. I., Choi, I. Y., Zhong, X. B., Bray-Ward, P., Russell, J. M. and Boron, W. F. (2001). Cloning, characterization, and chromosomal mapping of a human electroneutral Na+-driven Cl-NCO3 exchanger. *Journal of Biological Chemistry* **276**, 8358-8363.

Grosell, M. (2006). Intestinal anion exchange in marine fish osmoregulation. *Journal of Experimental Biology* **209**, 2813-2827.

Grosell, M. and Wood, C. M. (2002). Copper uptake across rainbow trout gills: mechanisms of apical entry. *Journal of Experimental Biology* **205**, 1179-1188.

Gross, E. and Kurtz, I. (2002). Structural determinants and significance of regulation of electrogenic Na+-HCO3- cotransporter stoichiometry. *American Journal of Physiology-Renal Physiology* **283**, F876-F887.

Gross, E., Pushkin, A., Abuladze, N., Fedotoff, O. and Kurtz, I. (2002). Regulation of the sodium bicarbonate cotransporter kNBC1 function: role of Asp(986), Asp(988) and kNBC1-carbonic anhydrase II binding. *Journal of Physiology-London* **544**, 679-685.

Guizouarn, H. and Motais, R. (1999). Swelling activation of transport pathways in erythrocytes: effects of Cl-, ionic strength, and volume changes. *Am J Physiol* **276**, C210-20.

Halperin, J., Genovese, G., Tresguerres, M. and Luquet, C. M. (2004). Modulation of ion uptake across posterior gills of the crab Chasmagnathus granulatus by dopamine and cAMP. *Comparative*

Biochemistry and Physiology a-Molecular & Integrative Physiology **139**, 103-109.

Hansen, C. A. and Sidell, B. D. (1983). Atlantic Hagfish Cardiac-Muscle - Metabolic Basis of Tolerance to Anoxia. *American Journal of Physiology* **244**, R356-R362.

Harold, F. M. and Papineau, D. (1972). Cation Transport and Electrogenesis by Streptococcus-Faecalis .2. Proton and Sodium Extrusion. *Journal of Membrane Biology* **8**, 45-62.

Harvey, B. J. (1992). Energization of Sodium-Absorption by the H+-Atpase Pump in Mitochondria-Rich Cells of Frog-Skin. *Journal of Experimental Biology* **172**, 289-309.

Harvey, B. J. and Ehrenfeld, J. (1986). Regulation of Intracellular Sodium and pH by the Electrogenic H+ Pump in Frog-Skin. *Pflugers Archiv-European Journal of Physiology* **406**, 362-366.

Harvey, B. J. and Kernan, R. P. (1984). Intracellular Ion Activities in Frog-Skin in Relation to External Sodium and Effects of Amiloride and or Ouabain. *Journal of Physiology-London* **349**, 501-517.

Hawkings, G. S., Galvez, F. and Goss, G. G. (2004). Seawater acclimation causes independent alterations in Na+/K+- and H+-ATPase activity in isolated mitochondria-rich cell subtypes of the rainbow trout gill. *Journal of Experimental Biology* **207**, 905-912.

Hediger, M. A., Romero, M. F., Peng, J. B., Rolfs, A., Takanaga, H. and Bruford, E. A. (2004). The ABCs of solute carriers: physiological, pathological and therapeutic implications of human membrane transport proteins - Introduction. *Pflugers Archiv-European Journal of Physiology* **447**, 465-468.

Heslop, J. P. and Berridge, M. J. (1980). Changes in Cyclic-Amp and Cyclic-Gmp Concentrations during the Action of 5-Hydroxytryptamine on an Insect Salivary-Gland. *Biochemical Journal* **192**, 247-255.

Hille, C. and Walz, B. (2007). A vacuolar-type H+-ATPase and a Na+/H+ exchanger contribute to intracellular pH regulation in cockroach salivary ducts. *Journal of Experimental Biology* **210**, 1463-1471.

Hirata, T., Kaneko, T., Ono, T., Nakazato, T., Furukawa, N., Hasegawa, S., Wakabayashi, S., Shigekawa, M., Chang, M. H., Romero, M. F. et al. (2003). Mechanism of acid adaptation of a fish living in a pH 3.5 lake. *American Journal of Physiology-Regulatory Integrative and Comparative Physiology* **284**, R1199-R1212.

Hiroi, J., Yasumasu, S., McCormick, S. D., Hwang, P. P. and Kaneko, T. (2008). Evidence for an apical Na-Cl cotransporter involved in ion uptake in a teleost fish. *Journal of Experimental Biology* **211**, 2584-2599.

Hirose, S., Kaneko, T., Naito, N. and Takei, Y. (2003). Molecular biology of major components of chloride cells. *Comparative Biochemistry and Physiology B-Biochemistry & Molecular Biology* **136**, 593-620.

Horng, J. L., Lin, L. Y., Huang, C. J., Katoh, F., Kaneko, T. and Hwang, P. P. (2007). Knockdown of V-ATPase subunit A (atp6v1a) impairs acid secretion and ion balance in zebrafish (Danio rerio). *American Journal of Physiology-Regulatory Integrative and Comparative Physiology* **292**, R2068-R2076.

Hummler, E., Merillat, A. M., Rubera, I., Rossier, B. C. and Beermann, F. (2002). Conditional gene targeting of the Scnn1a (alpha ENaC) gene locus. *Genesis* **32**, 169-172.

Hwang, P. P. and Lee, T. H. (2007). New insights into fish ion regulation and mitochondrion-rich cells. *Comparative Biochemistry and Physiology a-Molecular & Integrative Physiology* **148**, 479-497.

Ikuma, M., Geibel, J., Binder, H. J. and Rajendran, V. M. (2003). Characterization of Cl-HCO3 exchange in basolateral membrane of rat distal colon. *American Journal of Physiology-Cell Physiology* **285**, C912-C921.

Ip, Y. K., Peh, B. K., Tam, W. L., Wong, W. P. and Chew, S. F. (2005). Effects of intra-peritoneal injection with NH4Cl, urea, or NH4Cl+urea on nitrogen excretion and metabolism in the African lungfish Protopterus dolloi. *Journal of Experimental Zoology Part a-Comparative Experimental Biology* **303A**, 272-282.

Ivanis, G., Braun, M. and Perry, S. F. (2008a). Renal expression and localization of SLC9A3 sodium/hydrogen exchanger and its possible role in acid-base regulation in freshwater rainbow trout (Oncorhynchus mykiss). *American Journal of Physiology-Regulatory Integrative and Comparative Physiology* **295**, R971-R978.

Ivanis, G., Esbaugh, A. J. and Perry, S. F. (2008b). Branchial expression and localization of SLC9A2 and SLC9A3 sodium/hydrogen exchangers and their possible role in acid-base regulation in freshwater rainbow trout (Oncorhynchus mykiss). *Journal of Experimental Biology* **211**, 2467-2477.

Jensen, L. J., Willumsen, N. J., Amstrup, J. and Larsen, E. H. (2003). Proton pump-driven cutaneous chloride uptake in anuran amphibia. *Biochimica Et Biophysica Acta-Biomembranes* **1618**, 120-132.

Jonz, M. G. and Nurse, C. A. (2003). Neuroepithelial cells and associated innervation of the zebrafish gill: A confocal immunofluorescence study. *Journal of Comparative Neurology* **461**, 1-17.

Jonz, M. G. and Nurse, C. A. (2006). Epithelial mitochondria-rich cells and associated innervation in adult and developing zebrafish. *Journal of Comparative Neurology* **497**, 817-832.

Jonz, M. G. and Nurse, C. A. (2008). New developments on gill innervation: insights from a model vertebrate. *Journal of Experimental Biology* **211**, 2371-2378.

Just, F. and Walz, B. (1996). The effects of serotonin and dopamine on salivary secretion by isolated cockroach salivary glands. *Journal of Experimental Biology* **199**, 407-413.

Katoh, F., Cozzi, R. R., Marshall, W. S. and Goss, G. G. (2008). Distinct Na(+)/K (+)/2Cl (-) cotransporter localization in kidneys and gills of two euryhaline species, rainbow trout and killifish. *Cell Tissue Res*.

Katoh, F., Hyodo, S. and Kaneko, T. (2003). Vacuolar-type proton pump in the basolateral plasma membrane energizes ion uptake in branchial mitochondria-rich cells of killifish Fundulus heteroclitus, adapted to a low ion environment. *Journal of Experimental Biology* **206**, 793-803.

Katoh, F., Shimizu, A., Uchida, K. and Kaneko, T. (2000). Shift of chloride cell distribution during early life stages in seawater-adapted killifish, Fundulus heteroclitus. *Zoological Science* **17**, 11-18.

Katoh, F., Tresguerres, M., Lee, K. M., Kaneko, T., Aida, K. and Goss, G. G. (2006). Cloning of rainbow trout SLC26A1: involvement in renal sulfate secretion. *Am J Physiol Regul Integr Comp Physiol* **290**, R1468-78.

Kern, G., Bosch, S. T., Unterhuber, E. and Pelster, B. (2002). Mechanisms of acid secretion in pseudobranch cells of rainbow trout Oncorhynchus mykiss. *Journal of Experimental Biology* **205**, 2943-2954.

Kerstetter, T. H. and Keeler, M. (1976). Interaction of NH4+ and Na+ Fluxes in Isolated Trout Gill. *Journal of Experimental Biology* **64**, 517-527.

Kerstetter, T. H. and Kirschner, L. B. (1972). Active Chloride Transport by Gills of Rainbow-Trout (Salmo-Gairdnerii). *Journal of Experimental Biology* **56**, 263-272.

Kerstetter, T. H., Kirschner, L. B. and Rafuse, D. D. (1970). On Mechanisms of Sodium Ion Transport by Irrigated Gills of Rainbow Trout (Salmo-Gairdneri). *Journal of General Physiology* **56**, 342-359.

Keys, A. and Willmer, E. N. (1932). "Chloride secreting cells" in the gills of fishes, with special reference to the common eel. *Journal of Physiology-London* **76**, 368-378.

Keys, A. B. (1931a). Chloride and water secretion and absorption by the gills of the eel. *Z. Vergl. Physiol* **15**, 364-389.

Keys, A. B. (1931b). The heart-gill preparation of the eel and its perfusion for the study of a natural membrane in situ. *Z. Vergl. Physiol* **15**, 352-363.

Kimura, C., Ahearn, G. A., Busquetsturner, L., Haley, S. R., Nagao, C. and Decouet, H. G. (1994). Immunolocalization of an Antigen Associated with the Invertebrate Electrogenic 2na(+)/1h(+) Antiporter. *Journal of Experimental Biology* **189**, 85-104.

Kirschner, L. B. (2004). The mechanism of sodium chloride uptake in hyperregulating aquatic animals. *Journal of Experimental Biology* **207**, 1439-1452.

Kirschner, L. B., Greenwald, L. and Kerstetter, T. H. (1973). Effect of Amiloride on Sodium-Transport across Body Surfaces of Freshwater Animals. *American Journal of Physiology* **224**, 832-837.

Kleyman, T. R. and Cragoe, E. J. (1988). Amiloride and Its Analogs as Tools in the Study of Ion-Transport. *Journal of Membrane Biology* **105**, 1-21.

Kopito, R. R. and Lodish, H. F. (1985). Primary Structure and Transmembrane Orientation of the Murine Anion-Exchange Protein. *Nature* **316**, 234-238.

Kraschinski, S., Epple, A. and Nibbio, B. (1996). Macrovascular dopamine release. *American Journal of Physiology-Regulatory Integrative and Comparative Physiology* **39**, R1244-R1249.

Krogh, A. (1937). Osmotic regulation in fresh water fishes by active absorption of chloride ions. *Zeitschrift für Vergleichende Physiologie* **24**, 656-666.

Krogh, A. (1938). The active absorption of ions in some freshwater animals. *Zeitschrift fuï Vergleichende Physiologie* **25**, 335-350.

Krogh, A. (1939). Teleostomi. In *Osmotic Regulation in Aquatic Animals*, pp. 130-153: Cambridge University Press, Cambridge.

Kurita, Y., Nakada, T., Kato, A., Doi, H., Mistry, A. C., Chang, M. H., Romero, M. F. and Hirose, S. (2008). Identification of intestinal bicarbonate

transporters involved in formation of carbonate precipitates to stimulate water absorption in marine teleost fish. *Am J Physiol Regul Integr Comp Physiol* **294**, R1402-12.

Laemmli, U. K. (1970). Cleavage of Structural Proteins during Assembly of Head of Bacteriophage-T4. *Nature* **227**, 680-&.

Lagadic-Gossmann, D., Buckler, K. J. and Vaughan-Jones, R. D. (1992). Role of Bicarbonate in pH Recovery from Intracellular Acidosis in the Guinea-Pig Ventricular Myocyte. *Journal of Physiology-London* **458**, 361-384.

Laurent, P. and Dunel, S. (1980). Morphology of Gill Epithelia in Fish. *American Journal of Physiology* **238**, R147-R159.

Laurent, P. and Perry, S. F. (1990). Effects of Cortisol on Gill Chloride Cell Morphology and Ionic Uptake in the Fresh-Water Trout, Salmo-Gairdneri. *Cell and Tissue Research* **259**, 429-442.

Le Foll, B., Gallo, A., Le Strat, Y., Lu, L. and Gorwood, P. (2009). Genetics of dopamine receptors and drug addiction: a comprehensive review. *Behavioural Pharmacology* **20**, 1-17.

Lehir, M., Kaissling, B., Koeppen, B. M. and Wade, J. B. (1982). Binding of Peanut Lectin to Specific Epithelial-Cell Types in Kidney. *American Journal of Physiology* **242**, C117-C120.

Lewis, D. L., Hagstrom, J. E., Loomis, A. G., Wolff, J. A. and Herweijer, H. (2002). Efficient delivery of siRNA for inhibition of gene expression in postnatal mice. *Nature Genetics* **32**, 107-108.

Lim, C. K., Chew, S. F., Tay, A. S. L. and Ip, Y. K. (2004). Effects of peritoneal injection of NH4HCO3 on nitrogen excretion and metabolism in the swamp eel Monopterus albus - Increased ammonia excretion with an induction of glutamine synthetase activity. *Journal of Experimental Zoology Part a-Ecological Genetics and Physiology* **301A**, 324-333.

Lin, H., Pfeiffer, D. C., Vogl, A. W., Pan, J. and Randall, D. J. (1994). Immunolocalization of H+-Atpase in the Gill Epithelia of Rainbow-Trout. *Journal of Experimental Biology* **195**, 169-183.

Lin, H. and Randall, D. (1991). Evidence for the Presence of an Electrogenic Proton Pump on the Trout Gill Epithelium. *Journal of Experimental Biology* **161**, 119-134.

Lin, H. and Randall, D. J. (1990). The Effect of Varying Water pH on the Acidification of Expired Water in Rainbow-Trout. *Journal of Experimental Biology* **149**, 149-160.

Lin, H. and Randall, D. J. (1993). H+-Atpase Activity in Crude Homogenates of Fish Gill Tissue - Inhibitor Sensitivity and Environmental and Hormonal-Regulation. *Journal of Experimental Biology* **180**, 163-174.

Lin, L. Y., Horng, J. L., Kunkel, J. G. and Hwang, P. P. (2006). Proton pump-rich cell secretes acid in skin of zebrafish larvae. *American Journal of Physiology-Cell Physiology* **290**, C371-C378.

Lin, L. Y. and Hwang, P. P. (2004). Mitochondria-rich cell activity in the yolk-sac membrane of tilapia (Oreochromis mossambicus) larvae acclimatized to different ambient chloride levels. *J Exp Biol* **207**, 1335-44.

Lin, T. Y., Liao, B. K., Horng, J. L., Yan, J. J., Hsiao, C. D. and Hwang, P. P. (2008). Carbonic anhydrase 2-like a and 15a are involved in acid-base regulation and Na+ uptake in zebrafish H+-ATPase-rich cells. *Am J Physiol Cell Physiol* **294**, C1250-60.

Livak, K. J. and Schmittgen, T. D. (2001). Analysis of relative gene expression data using real-time quantitative PCR and the 2(T)(-Delta Delta C) method. *Methods* **25**, 402-408.

Loiselle, F. B., Morgan, P. E., Alvarez, B. V. and Casey, J. R. (2004). Regulation of the human NBC3 Na+/HCO3- cotransporter by carbonic anhydrase II and PKA. *American Journal of Physiology-Cell Physiology* **286**, C1423-C1433.

Lu, J., Daly, C. M., Parker, M. D., Gill, H. S., Piermarini, P. M., Pelletier, M. F. and Boron, W. F. (2006). Effect of human carbonic anhydrase II on the activity of the human electrogenic Na/HCO3 cotransporter NBCe1-A in Xenopus oocytes. *Journal of Biological Chemistry* **281**, 19241-19250.

Lucu, C. and Towle, D. W. (2003). Na+/K+-ATPase in gills of aquatic crustacea. *Comparative Biochemistry and Physiology a-Molecular & Integrative Physiology* **135**, 195-214.

Lukin, J. A. and Ho, C. (2004). The structure-function relationship of hemoglobin in solution at atomic resolution. *Chemical Reviews* **104**, 1219-1230.

Luquet, C. M. and Ansaldo, M. (1997). Acid-base balance and ionic regulation during emersion in the estuarine intertidal crab Chasmagnathus granulata Dana (Decapoda Grapsidae). *Comparative Biochemistry and Physiology a-Physiology* **117**, 407-410.

Luquet, C. M., Genovese, G., Rosa, G. A. and Pellerano, G. N. (2002a). Ultrastructural changes in the gill epithelium of the crab

Chasmagnathys granulatus (Decapoda : Grapsidae) in diluted and concentrated seawater. *Marine Biology* **141**, 753-760.

Luquet, C. M., Postel, U., Halperin, J., Urcola, M. R., Marques, R. and Siebers, D. (2002b). Transepithelial potential differences and Na+ flux in isolated perfused gills of the crab Chasmagnathus granulatus (Grapsidae) acclimated to hyper- and hypo-salinity. *Journal of Experimental Biology* **205**, 71-77.

Luquet, C. M., Rosa, G. A., Ferrari, C. C., Genovese, G. and Pellerano, G. N. (2000). Gill morphology of the intertidal estuarine crab Chasmagnathus granulatus Dana, 1851 (Decapoda, Grapsidae) in relation to habitat and respiratory habits. *Crustaceana* **73**, 53-67.

Luquet, C. M., Weihrauch, D., Senek, M. and Towle, D. W. (2005). Induction of branchial ion transporter mRNA expression during acclimation to salinity change in the euryhaline crab Chasmagnathus granulatus. *Journal of Experimental Biology* **208**, 3627-3636.

Madshus, I. H. (1988). Regulation of Intracellular Ph in Eukaryotic Cells. *Biochemical Journal* **250**, 1-8.

Maetz, J. and Garcia-Romeu, F. (1964). The Mechanism of Sodium and Chloride Uptake by the Gills of a Fresh-Water Fish Carassius Auratus .II. Evidence for NH4+/Na+ and HCO3-/Cl- Exchanges. *Journal of General Physiology* **47**, 1209-1227.

Magro, F., Fraga, S. and Soares-da-Silva, P. (2005). Signaling of short-term and long-term regulation of intestinal epithelial type 1 Na+/H+ exchanger by interferon-gamma. *British Journal of Pharmacology* **145**, 93-103.

Malapert, M., Guizouarn, H., Fievet, B., Jahns, R., GarciaRomeu, F., Motais, R. and Borgese, F. (1997). Regulation of Na+/H+ antiporter in trout red blood cells. *Journal of Experimental Biology* **200**, 353-360.

Mallatt, J., Conley, D. M. and Ridgway, R. L. (1987). Why Do Hagfish Have Gill Chloride Cells When They Need Not Regulate Plasma Nacl Concentration. *Canadian Journal of Zoology-Revue Canadienne De Zoologie* **65**, 1956-1965.

Mallatt, J. and Paulsen, C. (1986). Gill Ultrastructure of the Pacific Hagfish Eptatretus-Stouti. *American Journal of Anatomy* **177**, 243-269.

Marcus, E. A., Moshfegh, A. P., Sachs, G. and Scott, D. R. (2005). The periplasmic alpha-carbonic anhydrase activity of Helicobacter pylori is essential for acid acclimation. *Journal of Bacteriology* **187**, 729-738.

Marshall, W. S. (2003). Rapid regulation of NaCl secretion by estuarine teleost fish: coping strategies for short-duration freshwater exposures. *Biochimica Et Biophysica Acta-Biomembranes* **1618**, 95-105.

Marshall, W. S., Lynch, E. A. and Cozzi, R. R. F. (2002). Redistribution of immunofluorescence of CFTR anion channel and NKCC cotransporter in chloride cells during adaptation of the killifish Fundulus heteroclitus to sea water. *Journal of Experimental Biology* **205**, 1265-1273.

Masereel, B., Pochet, L. and Laeckmann, D. (2003). An overview of inhibitors of Na+/H+ exchanger. *European Journal of Medicinal Chemistry* **38**, 547-554.

Maunsbach, A. B., Vorum, H., Kwon, T. H., Nielsen, S., Simonsen, B., Choi, I., Schmitt, B. M., Boron, W. F. and Aalkjaer, C. (2000). Immunoelectron microscopic localization of the electrogenic Na/HCO2 cotransporter in rat and ambystoma kidney. *Journal of the American Society of Nephrology* **11**, 2179-2189.

McCaffrey, A. P., Meuse, L., Pham, T. T. T., Conklin, D. S., Hannon, G. J. and Kay, M. A. (2002). Gene expression - RNA interference in adult mice. *Nature* **418**, 38-39.

McCormick, S. D. (1993). Methods for Nonlethal Gill Biopsy and Measurement of Na+, K+ -Atpase Activity. *Canadian Journal of Fisheries and Aquatic Sciences* **50**, 656-658.

McCormick, S. D. (1995). Hormonal control of gill Na+, K+-ATPase and chloride cell function. In *Cellular and Molecular Approaches to Fish Ionic Regulation*, (ed. C. M. Wood, Shuttleworth, T.J.). San Diego, CA: Academic.

McCormick, S. D. (2001). Endocrine control of osmoregulation in teleost fish. *American Zoologist* **41**, 781-794.

McDonald, D. G., Cavdek, V., Calvert, L. and Milligan, C. L. (1991). Acid-Base Regulation in the Atlantic Hagfish Myxine-Glutinosa. *Journal of Experimental Biology* **161**, 201-215.

McKenzie, D. J., Taylor, E. W., Dalla Valle, A. Z. and Steffensen, J. F. (2002). Tolerance of acute hypercapnic acidosis by the European eel (Anguilla anguilla). *Journal of Comparative Physiology B-Biochemical Systemic and Environmental Physiology* **172**, 339-346.

McMurtrie, H. L., Cleary, H. J., Alvarez, B. V., Loiselle, F. B., Sterling, D., Morgan, P. E., Johnson, D. E. and Casey, J. R. (2004). The bicarbonate transport metabolon. *Journal of Enzyme Inhibition and Medicinal Chemistry* **19**, 231-236.

Meltzer, R. H., Kapoor, N., Qadri, Y. J., Anderson, S. J., Fuller, C. M. and Benos, D. J. (2007). Heteromeric assembly of acid-sensitive ion channel and epithelial sodium channel subunits. *Journal of Biological Chemistry* **282**, 25548-25559.

Meneton, P., Jeunemaitre, X., De Wardener, H. E. and Macgregor, G. A. (2005). Links between dietary salt intake, renal salt handling, blood pressure, and cardiovascular diseases. *Physiological Reviews* **85**, 679-715.

Mistry, A. C., Honda, S., Hirata, T., Kato, A. and Hirose, S. (2001). Eel urea transporter is localized to chloride cells and is salinity dependent. *American Journal of Physiology-Regulatory Integrative and Comparative Physiology* **281**, R1594-R1604.

Mitchell, P. and Moyle, J. (1969). Translocation of Some Anions Cations and Acids in Rat Liver Mitochondria. *European Journal of Biochemistry* **9**, 149.

Miyata, Y., Muto, S., Yanagiba, S. and Asano, Y. (2000). Extracellular Cl(-) modulates shrinkage-induced activation of Na(+)/H(+) exchanger in rat mesangial cells. *Am J Physiol Cell Physiol* **278**, C1218-29.

Moffett, D. F. (1980). Voltage-Current Relation and K+-Transport in Tobacco Hornworm (Manduca-Sexta) Midgut. *Journal of Membrane Biology* **54**, 213-219.

Moffett, D. F. and Koch, A. R. (1988). Electrophysiology of K+ Transport by Midgut Epithelium of Lepidopteran Insect Larvae .2. The Transapical Electrochemical Gradients. *Journal of Experimental Biology* **135**, 39-49.

Moffett, S. B. and Moffett, D. F. (2005). Comparison of immunoreactivity to serotonin, FMRFamide and SCPb in the gut and visceral nervous system of larvae, pupae and adults of the yellow fever mosquito Aedes aegypti. *Journal of Insect Science* **5**, 20.

Mohr, F. C. and Fewtrell, C. (1987). Ige Receptor-Mediated Depolarization of Rat Basophilic Leukemia-Cells Measured with the Fluorescent-Probe Bis-Oxonol. *Journal of Immunology* **138**, 1564-1570.

Morgan, I. J., Potts, W. T. W. and Oates, K. (1994). Intracellular Ion Concentrations in Branchial Epithelial-Cells of Brown Trout (Salmo-Trutta L) Determined by X-Ray-Microanalysis. *Journal of Experimental Biology* **194**, 139-151.

Morgan, J. D. and Iwama, G. K. (1999). Energy cost of NaCl transport in isolated gills of cutthroat trout. *American Journal of Physiology-Regulatory Integrative and Comparative Physiology* **277**, R631-R639.

Morgan, P. E., Pastorekova, S., Stuart-Tilley, A. K., Alper, S. L. and Casey, J. R. (2007). Interactions of transmembrane carbonic anhydrase, CAIX, with bicarbonate transporters. *American Journal of Physiology-Cell Physiology* **293**, C738-C748.

Morris, R. (1965). Studies on Salt and Water Balance in Myxine Glutinosa (L.). *Journal of Experimental Biology* **42**, 359-&.

Motais, R., Borgese, F., Fievet, B. and Garciaromeu, F. (1992). Regulation of Na+/H+ Exchange and Ph in Erythrocytes of Fish. *Comparative Biochemistry and Physiology a-Physiology* **102**, 597-602.

Mount, D. B. and Romero, M. F. (2004). The SLC26 gene family of multifunctional anion exchangers. *Pflugers Arch* **447**, 710-21.

Nagel, W., Garciadiaz, J. F. and Armstrong, W. M. (1981). Intracellular Ionic Activities in Frog-Skin. *Journal of Membrane Biology* **61**, 127-134.

Natke, E. and Stoner, L. C. (1982). Na+ Transport-Properties of the Peritubular Membrane of Cortical Collecting Tubule. *American Journal of Physiology* **242**, F664-F671.

Nielsen, R. (1982). Effect of Ouabain, Amiloride, and Anti-Diuretic Hormone on the Sodium-Transport Pool in Isolated Epithelia from Frog-Skin (Rana-Temporaria). *Journal of Membrane Biology* **65**, 221-226.

Nikinmaa, M. (1997). Oxygen and carbon dioxide transport in vertebrate erythrocytes: An evolutionary change in the role of membrane transport. *Journal of Experimental Biology* **200**, 369-380.

Nikinmaa, M., Kunnamoojala, T. and Railo, E. (1986). Mechanisms of pH Regulation in Lamprey (Lampetra-Fluviatilis) Red-Blood-Cells. *Journal of Experimental Biology* **122**, 355-367.

O'Donnell, M. J., Kelly, S. P., Nurse, C. A. and Wood, C. M. (2001). A maxi Cl- channel in cultured pavement cells from the gills of the freshwater rainbow trout Oncorhynchus mykiss. *Journal of Experimental Biology* **204**, 1783-1794.

Okech, B. A., Boudko, D. Y., Linser, P. J. and Harvey, W. R. (2008). Cationic pathway of pH regulation in larvae of Anopheles gambiae. *Journal of Experimental Biology* **211**, 957-968.

Onken, H., Graszynski, K. and Zeiske, W. (1991). Na+-Independent, Electrogenic Cl- Uptake across the Posterior Gills of the Chinese Crab (Eriocheir-Sinensis) - Voltage-Clamp and Microelectrode Studies. *Journal of*

Comparative Physiology B-Biochemical Systemic and Environmental Physiology **161**, 293-301.

Onken, H. and McNamara, J. C. (2002). Hyperosmoregulation in the red freshwater crab Dilocarcinus pagei (Brachyura, Trichodactylidae): structural and functional asymmetries of the posterior gills. *Journal of Experimental Biology* **205**, 167-175.

Onken, H., Moffett, S. B. and Moffett, D. E. (2004). The anterior stomach of larval mosquitoes (Aedes aegypti): effects of neuropeptides on transepithelial ion transport and muscular motility. *Journal of Experimental Biology* **207**, 3731-3739.

Onken, H., Moffett, S. B. and Moffett, D. F. (2008). Alkalinization in the isolated and perfused anterior midgut of the larval mosquito, Aedes aegypti. *Journal of Insect Science* **8**, 43.

Onken, H. and Putzenlechner, M. (1995). A V-Atpase Drives Active, Electrogenic and Na+-Independent Cl- Absorption across the Gills of Eriocheir-Sinensis. *Journal of Experimental Biology* **198**, 767-774.

Onken, H. and Riestenpatt, S. (1998). NaCl absorption across split gill lamellae of hyperregulating crabs: Transport mechanisms and their regulation. *Comparative Biochemistry and Physiology a-Molecular and Integrative Physiology* **119**, 883-893.

Onken, H. and Riestenpatt, S. (2002). Ion transport across posterior gills of hyperosmoregulating shore crabs (Carcinus maenas): amiloride blocks the cuticular Na+ conductance and induces current-noise. *Journal of Experimental Biology* **205**, 523-531.

Onken, H., Tresguerres, M. and Luquet, C. M. (2003). Active NaCl absorption across posterior gills of hyperosmoregulating Chasmagnathus granulatus. *Journal of Experimental Biology* **206**, 1017-1023.

Orlowski, J. and Grinstein, S. (2004). Diversity of the mammalian sodium/proton exchanger SLC9 gene family. *Pflugers Archiv-European Journal of Physiology* **447**, 549-565.

Padan, E., Bibi, E., Ito, M. and Krulwich, T. A. (2005). Alkaline pH homeostasis in bacteria: New insights. *Biochimica Et Biophysica Acta-Biomembranes* **1717**, 67-88.

Pannabecker, T. L., Aneshansley, D. J. and Beyenbach, K. W. (1992). Unique Electrophysiological Effects of Dinitrophenol in Malpighian Tubules. *American Journal of Physiology* **263**, R609-R614.

Parker, J. C. (1983). Volume-responsive sodium movements in dog red blood cells. *Am J Physiol* **244**, C324-30.

Parks, S. K., Tresguerres, M. and Goss, G. G. (2007a). Blood and gill responses to HCl infusions in the Pacific hagfish (Eptatretus stoutii). *Canadian Journal of Zoology-Revue Canadienne De Zoologie* **85**, 855-862.

Parks, S. K., Tresguerres, M. and Goss, G. G. (2007b). Interactions between Na+ channels and Na+-HCO3- cotransporters in the freshwater fish gill MR cell: a model for transepithelial Na+ uptake. *American Journal of Physiology-Cell Physiology* **292**, C935-C944.

Parks, S. K., Tresguerres, M. and Goss, G. G. (2008). Theoretical considerations underlying Na+ uptake mechanisms in freshwater fishes. *Comparative Biochemistry and Physiology C-Toxicology & Pharmacology* **148**, 411-418.

Parks, S. K., Tresguerres, M. and Goss, G. G. (2009). Cellular mechanisms of Cl- transport in trout gill mitochondrion-rich cells. *American Journal of Physiology-Regulatory Integrative and Comparative Physiology* **296**, R1161-R1169.

Part, P. and Wood, C. M. (1996). Na/H exchange in cultured epithelial cells from fish gills. *Journal of Comparative Physiology B-Biochemical Systemic and Environmental Physiology* **166**, 37-45.

Pastor-Soler, N., Beaulieu, V., Litvin, T. N., Da Silva, N., Chen, Y. Q., Brown, D., Buck, J., Levin, L. R. and Breton, S. (2003). Bicarbonate-regulated adenylyl cyclase (sAC) is a sensor that regulates pH-dependent V-ATPase recycling. *Journal of Biological Chemistry* **278**, 49523-49529.

Paukert, M., Sidi, S., Russell, C., Siba, M., Wilson, S. W., Nicolson, T. and Grunder, S. (2004). A family of acid-sensing ion channels from the zebrafish - Widespread expression in the central nervous system suggests a conserved role in neuronal communication. *Journal of Biological Chemistry* **279**, 18783-18791.

Pedemonte, C. H. and Bertorello, A. M. (2001). Short-term regulation of the proximal tubule Na+,K+-ATPase: Increased/decreased Na+,K+-ATPase activity mediated by protein kinase C isoforms. *Journal of Bioenergetics and Biomembranes* **33**, 439-447.

Pedersen, S. F., Darborg, B. V., Rentsch, M. L. and Rasmussen, M. (2007). Regulation of mitogen-activated protein kinase pathways by the plasma membrane Na+/H+ exchanger, NHE1. *Archives of Biochemistry and Biophysics* **462**, 195-201.

Perry, S. F. (1997). The chloride cell: Structure and function in the gills of freshwater fishes. *Annual Review of Physiology* **59**, 325-347.

Perry, S. F., Booth, C. E. and Mcdonald, D. G. (1985). Isolated Perfused Head of Rainbow-Trout .2. Ionic Fluxes. *American Journal of Physiology* **249**, R255-R261.

Perry, S. F., Davie, P. S., Daxboeck, C., Ellis, A. G. and Smith, D. G. (1984). PERFUSION METHODS FOR THE STUDY OF GILL PHYSIOLOGY. In *Fish Physiology*, vol. 10 (ed. W. S. Hoar, and Randall, D.J.), pp. 325-388. New York: Academic Press.

Perry, S. F., Furimsky, M., Bayaa, M., Georgalis, T., Shahsavarani, A., Nickerson, J. G. and Moon, T. W. (2003a). Integrated responses of Na+/HCO3- cotransporters and V-type H+-ATPases in the fish gill and kidney during respiratory acidosis. *Biochimica Et Biophysica Acta-Biomembranes* **1618**, 175-184.

Perry, S. F. and Gilmour, K. M. (2006). Acid-base balance and CO2 excretion in fish: Unanswered questions and emerging models. *Respiratory Physiology & Neurobiology* **154**, 199-215.

Perry, S. F., Malone, S. and Ewing, D. (1987). Hypercapnic Acidosis in the Rainbow-Trout (Salmo-Gairdneri) .1. Branchial Ionic Fluxes and Blood Acid-Base Status. *Canadian Journal of Zoology-Revue Canadienne De Zoologie* **65**, 888-895.

Perry, S. F. and McDonald, D. J. (1993). Gas exchange. In *The Physiology of Fishes*, (ed. D. H. Evans), pp. 251-278. Boca Raton, Fl.: CRC.

Perry, S. F. and Randall, D. J. (1981). Effects of amiloride and SITS on branchial ion fluxes in rainbow trout, Salmo gairdneri. *J Exp Zool* **215**, 225-8.

Perry, S. F., Rivero-Lopez, L., McNeill, B. and Wilson, J. (2006). Fooling a freshwater fish: how dietary salt transforms the rainbow trout gill into a seawater gill phenotype. *Journal of Experimental Biology* **209**, 4591-4596.

Perry, S. F., Shahsavarani, A., Georgalis, T., Bayaa, M., Furimsky, M. and Thomas, S. L. Y. (2003b). Channels, pumps, and exchangers in the gill and kidney of freshwater fishes: Their role in ionic and acid-base regulation. *Journal of Experimental Zoology Part a-Comparative Experimental Biology* **300A**, 53-62.

Peters, T., Forster, R. E. and Gros, G. (2000). Hagfish (Myxine glutinosa) red cell membrane exhibits no bicarbonate permeability as detected by O-18 exchange. *Journal of Experimental Biology* **203**, 1551-1560.

Philpott, C. W. (1980). Tubular System Membranes of Teleost Chloride Cells - Osmotic Response and Transport Sites. *American Journal of Physiology* **238**, R171-R184.

Pickford, G. E., Pang, P. K. T., Weinstei.E, Torretti, J., Hendler, E. and Epstein, R. H. (1970). Response of Hypophysectomized Cyprinodont, Fundulus-Heteroclitus, to Replacement Therapy with Cortisol - Effects on Blood Serum and Sodium-Potassium Activated Adenosine Triphosphatase in Gills, Kidney, and Intestinal Mucosa. *General and Comparative Endocrinology* **14**, 524-&.

Pickford, G. E. and Phillips, J. G. (1959). Prolactin, a Factor in Promoting Survival of Hypophysectomized Killifish in Fresh Water. *Science* **130**, 454-455.

Piermarini, P. M., Choi, I. and Boron, W. F. (2007a). Cloning and characterization of an electrogenic Na/HCO3- cotransporter from the squid giant fiber lobe. *American Journal of Physiology-Cell Physiology* **292**, C2032-C2045.

Piermarini, P. M. and Evans, D. H. (2001). Immunochemical analysis of the vacuolar proton-ATPase B-subunit in the gills of a euryhaline stingray (Dasyatis sabina): effects of salinity and relation to Na+/K+-ATPase. *Journal of Experimental Biology* **204**, 3251-3259.

Piermarini, P. M., Kim, E. Y. and Boron, W. F. (2007b). Evidence against a direct interaction between intracellular carbonic anhydrase II and pure C-terminal domains of SLC4 bicarbonate transporters. *Journal of Biological Chemistry* **282**, 1409-1421.

Piermarini, P. M., Verlander, J. W., Royaux, I. E. and Evans, D. H. (2002). Pendrin immunoreactivity in the gill epithelium of a euryhaline elasmobranch. *American Journal of Physiology-Regulatory Integrative and Comparative Physiology* **283**, R983-R992.

Pisam, M., Auperin, B., Prunet, P., Rentierdelrue, F., Martial, J. and Rambourg, A. (1993). Effects of Prolactin on Alpha-Chloride and Beta-Chloride Cells in the Gill Epithelium of the Saltwater Adapted Tilapia Oreochromis-Niloticus. *Anatomical Record* **235**, 275-284.

Pisam, M., Boeuf, G., Prunet, P. and Rambourg, A. (1990). Ultrastructural Features of Mitochondria-Rich Cells in Stenohaline Fresh-Water and Seawater Fishes. *American Journal of Anatomy* **187**, 21-31.

Pisam, M., Caroff, A. and Rambourg, A. (1987). 2 Types of Chloride Cells in the Gill Epithelium of a Fresh-Water-Adapted Euryhaline Fish - Lebistes-Reticulatus - Their Modifications during Adaptation to Saltwater. *American Journal of Anatomy* **179**, 40-50.

Pisam, M., Lemoal, C., Auperin, B., Prunet, P. and Rambourg, A. (1995). Apical Structures of Mitochondria-Rich Alpha and Beta in Euryhaline Fish Gill - Their Behavior in Various Living-Conditions. *Anatomical Record* **241**, 13-24.

Pisam, M. and Rambourg, A. (1991). Mitochondria-Rich Cells in the Gill Epithelium of Teleost Fishes - an Ultrastructural Approach. *International Review of Cytology-a Survey of Cell Biology* **130**, 191-232.

Playle, R. C. and Wood, C. M. (1989). Water Chemistry Changes in the Gill Microenvironment of Rainbow-Trout - Experimental-Observations and Theory. *Journal of Comparative Physiology B-Biochemical Systemic and Environmental Physiology* **159**, 527-537.

Pouyssegur, J., Dayan, F. and Mazure, N. M. (2006). Hypoxia signalling in cancer and approaches to enforce tumour regression. *Nature* **441**, 437-443.

Preest, M. R., Gonzalez, R. J. and Wilson, R. W. (2005). A pharmacological examination of Na+ and Cl+ transport in two species of freshwater fish. *Physiological and Biochemical Zoology* **78**, 259-272.

Prince, V. E., Moens, C. B., Kimmel, C. B. and Ho, R. K. (1998). Zebrafish hox genes: expression in the hindbrain region of wild-type and mutants of the segmentation gene, valentino. *Development* **125**, 393-406.

Pushkin, A., Abuladze, N., Gross, E., Newman, D., Tatishchev, S., Lee, I., Fedotoff, O., Bondar, G., Azimov, R., Ngyuen, M. et al. (2004). Molecular mechanism of kNBC1-carbonic anhydrase II interaction in proximal tubule cells. *Journal of Physiology-London* **559**, 55-65.

Rajendran, V. M., Geibel, J. and Binder, H. J. (1995). Chloride-dependent Na-H exchange. A novel mechanism of sodium transport in colonic crypts. *J Biol Chem* **270**, 11051-4.

Rajendran, V. M., Geibel, J. and Binder, H. J. (1999). Role of Cl channels in Cl-dependent Na/H exchange. *Am J Physiol* **276**, G73-8.

Rajendran, V. M., Geibel, J. and Binder, H. J. (2001). Characterization of apical membrane Cl-dependent Na/H exchange in crypt cells of rat distal colon. *Am J Physiol Gastrointest Liver Physiol* **280**, G400-5.

Randall, D. J., Wood, C. M., Perry, S. F., Bergman, H., Maloiy, G. M. O., Mommsen, T. P. and Wright, P. A. (1989). Urea Excretion as a Strategy for Survival in a Fish Living in a Very Alkaline Environment. *Nature* **337**, 165-166.

Reardon, W., Coffey, R., Chowdhury, T., Grossman, A., Jan, H., Britton, K., Kendall-Taylor, P. and Trembath, R. (1999). Prevalence, age of onset, and natural history of thyroid disease in Pendred syndrome. *Journal of Medical Genetics* **36**, 595-598.

Reid, S. D., Hawkings, G. S., Galvez, F. and Goss, G. G. (2003). Localization and characterization of phenamil-sensitive Na+ influx in isolated rainbow trout gill epithelial cells. *Journal of Experimental Biology* **206**, 551-559.

Rein, J., Voss, M., Blenau, W., Walz, B. and Baumann, O. (2008). Hormone-induced assembly and activation of V-ATPase in blowfly salivary glands is mediated by protein kinase A. *American Journal of Physiology-Cell Physiology* **294**, C56-C65.

Rheault, M. R., Okech, B. A., Keen, S. B. W., Miller, M. M., Meleshkevitch, E. A., Linser, P. J., Boudko, D. Y. and Harvey, W. R. (2007). Molecular cloning, phylogeny and localization of AgNHA1: the first Na+/H+ antiporter (NHA) from a metazoan, Anopheles gambiae. *Journal of Experimental Biology* **210**, 3848-3861.

Rick, R. (1992). Intracellular Ion Concentrations in the Isolated Frog-Skin Epithelium - Evidence for Different Types of Mitochondria-Rich Cells. *Journal of Membrane Biology* **127**, 227-236.

Rick, R., Dorge, A., Vonarnim, E. and Thurau, K. (1978). Electron-Microprobe Analysis of Frog Skin Epithelium - Evidence for a Syncytial Sodium-Transport Compartment. *Journal of Membrane Biology* **39**, 313-331.

Riestenpatt, S., Petrausch, G. and Siebers, D. (1995). Cl- Influx across Posterior Gills of the Chinese Crab (Eriocheir-Sinensis) - Potential Energization by a V-Type H+-Atpase. *Comparative Biochemistry and Physiology a-Physiology* **110**, 235-241.

Rietdorf, K., Lang, I. and Walz, B. (2003). Saliva secretion and ionic composition of saliva in the cockroach Periplaneta americana after serotonin and dopamine stimulation, and effects of ouabain and bumetamide. *Journal of Insect Physiology* **49**, 205-215.

Roffey, J., Rosse, C., Linch, M., Hibbert, A., McDonald, N. Q. and Parker, P. J. (2009). Protein kinase C intervention - the state of play. *Current Opinion in Cell Biology* **21**, 268-279.

Romero, M. F. and Boron, W. F. (1999). Electrogenic Na+/HCO3-cotransporters: Cloning and physiology. *Annual Review of Physiology* **61**, 699-723.

Romero, M. F., Fulton, C. M. and Boron, W. F. (2004). The SLC4 family of HCO3- transporters. *Pflugers Archiv-European Journal of Physiology* **447**, 495-509.

Romero, M. F., Hediger, M. A., Boulpaep, E. L. and Boron, W. F. (1997). Expression cloning and characterization of a renal electrogenic Na+/HCO3- cotransporter. *Nature* **387**, 409-413.

Romero, M. F., Henry, D., Nelson, S., Harte, P. J., Dillon, A. K. and Sciortino, C. M. (2000). Cloning and characterization of a Na+-driven anion exchanger (NDAE1) - A new bicarbonate transporter. *Journal of Biological Chemistry* **275**, 24552-24559.

Roos, A. and Boron, W. F. (1981). Intracellular pH. *Physiological Reviews* **61**, 296-434.

Ruben, J. A. and Bennett, A. F. (1980). Antiquity of the Vertebrate Pattern of Activity Metabolism and Its Possible Relation to Vertebrate Origins. *Nature* **286**, 886-888.

Ruiz, O. S., Qiu, Y. Y., Cardoso, L. R., Arruda, J. A. L. and Wang, L. J. (1997). Regulation of the renal Na-HCO3 cotransporter .7. Mechanism of the cholinergic stimulation. *Kidney International* **51**, 1069-1077.

Russell, J. M. and Boron, W. F. (1976). Role of Chloride Transport in Regulation of Intracellular pH. *Nature* **264**, 73-74.

Salman, N. A. and Eddy, F. B. (1988). Effect of Dietary-Sodium Chloride on Growth, Food-Intake and Conversion Efficiency in Rainbow-Trout (Salmo-Gairdneri Richardson). *Aquaculture* **70**, 131-144.

Sandbichler, A. M. and Pelster, B. (2004). Acid-base regulation in isolated gill cells of the goldfish (Carassius auratus). *Journal of Comparative Physiology B-Biochemical Systemic and Environmental Physiology* **174**, 601-610.

Sangan, P., Rajendran, V. M., Geibel, J. P. and Binder, H. J. (2002). Cloning and expression of a chloride-dependent Na+-H+ exchanger. *J Biol Chem* **277**, 9668-75.

Sardet, C., Franchi, A. and Pouyssegur, J. (1989). Molecular-Cloning, Primary Structure, and Expression of the Human Growth Factor-Activatable Na+/H+ Antiporter. *Cell* **56**, 271-280.

Schafer, J. A., Watkins, M. L., Li, L., Herter, P., Haxelmans, S. and Schlatter, E. (1997). A simplified method for isolation of large numbers of defined nephron segments. *American Journal of Physiology-Renal Physiology* **42**, F650-F657.

Schewe, B., Schmalzlin, E. and Walz, B. (2008). Intracellular pH homeostasis and serotonin-induced pH changes in Calliphora salivary glands: the contribution of V-ATPase and carbonic anhydrase. *Journal of Experimental Biology* **211**, 805-815.

Schmitt, B. M., Biemesderfer, D., Romero, M. F., Boulpaep, E. L. and Boron, W. F. (1999). Immunolocalization of the electrogenic Na+-HCO3- cotransporter in mammalian and amphibian kidney. *American Journal of Physiology-Renal Physiology* **276**, F27-F38.

Schuster, V. L. (1993). Function and Regulation of Collecting Duct Intercalated Cells. *Annual Review of Physiology* **55**, 267-288.

Schyth, B. D. (2008). RNAi-mediated gene silencing in fishes? *Journal of Fish Biology* **72**, 1890-1906.

Scott, D. A., Wang, R., Kreman, T. M., Sheffield, V. C. and Karniski, L. P. (1999). The Pendred syndrome gene encodes a chloride-iodide transport protein. *Nature Genetics* **21**, 440-443.

Scott, G. R., Claiborne, J. B., Edwards, S. L., Schulte, P. M. and Wood, C. M. (2005). Gene expression after freshwater transfer in gills and opercular epithelia of killifish: insight into divergent mechanisms of ion transport. *Journal of Experimental Biology* **208**, 2719-2729.

Shetlar, R. E. and Towle, D. W. (1989). Electrogenic Sodium-Proton Exchange in Membrane-Vesicles from Crab (Carcinus-Maenas) Gill. *American Journal of Physiology* **257**, R924-R931.

Shmukler, B. E., Clark, J. S., Hsu, A., Vandorpe, D. H., Stewart, A. K., Kurschat, C. E., Choe, S. K., Zhou, Y., Amigo, J., Paw, B. H. et al. (2008). Zebrafish ae2.2 encodes a second slc4a2 anion exchanger. *American Journal of Physiology-Regulatory Integrative and Comparative Physiology* **294**, R1081-R1091.

Shmukler, B. E., Kurschat, C. E., Ackermann, G. E., Jiang, L. W., Zhou, Y., Barut, B., Stuart-Tilley, A. K., Zhao, J. H., Zon, L. I., Drummond, I. A. et al. (2005). Zebrafish slc4a2/ae2 anion exchanger: cDNA cloning, mapping, functional characterization, and localization. *American Journal of Physiology-Renal Physiology* **289**, F835-F849.

Siebers, D., Lucu, C., Bottcher, K. and Jurss, K. (1994). Regulation of pH in the Isolated-Perfused Gills of the Shore Crab Carcinus-Maenas. *Journal of Comparative Physiology B-Biochemical Systemic and Environmental Physiology* **164**, 16-22.

Slepkov, E. R., Rainey, J. K., Sykes, B. D. and Fliegel, L. (2007). Structural and functional analysis of the Na+/H+ exchanger. *Biochemical Journal* **401**, 623-633.

Smith, H. W. (1932). Water regulation and its evolution in the fishes. *Quarterly Review of Biology* **7**, 1-26.

Smith, H. W., Farinacci, N. and Breitweiser, A. (1930). The absorption and excretion of water and salts by marine teleosts. *American Journal of Physiology* **93**, 480-505.

Smith, K. E., VanEkeris, L. A. and Linser, P. J. (2007). Cloning and characterization of AgCA9, a novel alpha-carbonic anhydrase from Anopheles gambiae Giles sensu stricto (Diptera : Culicidae) larvae. *Journal of Experimental Biology* **210**, 3919-3930.

Smith, N. F., Eddy, F. B. and Talbot, C. (1995). Effect of Dietary Salt Load on Transepithelial Na+ Exchange in Fresh-Water Rainbow-Trout (Oncorhynchus-Mykiss). *Journal of Experimental Biology* **198**, 2359-2364.

Smith, N. F., Talbot, C. and Eddy, F. B. (1989). Dietary Salt Intake and Its Relevance to Ionic Regulation in Fresh-Water Salmonids. *Journal of Fish Biology* **35**, 749-753.

Soleimani, M. and Burnham, C. E. (2001). Na+: HCO3- cotransporters (NBC): Cloning and characterization. *Journal of Membrane Biology* **183**, 71-84.

Soleimani, M., Grassi, S. M. and Aronson, P. S. (1987). Stoichiometry of Na+-HCO3- Cotransport in Basolateral Membrane-Vesicles Isolated from Rabbit Renal-Cortex. *Journal of Clinical Investigation* **79**, 1276-1280.

Soleimani, M., Greeley, T., Petrovic, S., Wang, Z. H., Amlal, H., Kopp, P. and Burnham, C. E. (2001). Pendrin: an apical Cl-/OH-/HCO3- exchanger in the kidney cortex. *American Journal of Physiology-Renal Physiology* **280**, F356-F364.

Srere, P. A. (1993). 17th Lipmann,Fritz Lecture - Wanderings (Wonderings) in Metabolism. *Biological Chemistry Hoppe-Seyler* **374**, 833-842.

Steinmetz, P. R., Omachi, H. S. and Frazier, H. S. (1987). Independence of hydrogen ion secretion and transport of other electrolytes in turtle bladder. *International Journal of Clinical Investigation* **46**, 1541-1548.

Sterling, D., Reithmeier, R. A. F. and Casey, J. R. (2001). A transport metabolon. Functional interaction of carbonic anhydrase II and

chloride/bicarbonate exchangers. *Journal of Biological Chemistry* **276**, 47886-47894.

Sullivan, G. V., Fryer, J. N. and Perry, S. F. (1995). Immunolocalization of Proton Pumps (H+-Atpase) in Pavement Cells of Rainbow-Trout Gill. *Journal of Experimental Biology* **198**, 2619-2629.

Sullivan, G. V., Fryer, J. N. and Perry, S. F. (1996). Localization of mRNA for the proton pump (H+-ATPase) and Cl-/HCO3- exchanger in the rainbow trout gill. *Canadian Journal of Zoology-Revue Canadienne De Zoologie* **74**, 2095-2103.

Sundin, L. and Nilsson, S. (2002). Branchial innervation. *Journal of Experimental Zoology* **293**, 232-248.

Swenson, E. R. (1998). Carbonic anhydrase inhibitors and ventilation: a complex interplay of stimulation and suppression. *European Respiratory Journal* **12**, 1242-1247.

Takahashi, E., Abe, J., Gallis, B., Aebersold, R., Spring, D. J., Krebs, E. G. and Berk, B. C. (1999). p90(RSK) is a serum-stimulated Na+/H+ exchanger isoform-1 kinase - Regulatory phosphorylation of serine 703 of Na+/H+ exchanger isoform-1. *Journal of Biological Chemistry* **274**, 20206-20214.

Tang, C. H. and Lee, T. H. (2007a). The effect of environmental salinity on the protein expression of Na+/K+-ATPase, Na+/K+/2Cl-cotransporter, cystic fibrosis transmembrane conductance regulator, anion exchanger 1, and chloride channel 3 in gills of a euryhaline teleost, Tetraodon nigroviridis. *Comp Biochem Physiol A Mol Integr Physiol* **147**, 521-8.

Tang, C. H. and Lee, T. H. (2007b). The novel correlation of carbonic anhydrase II and anion exchanger 1 in gills of the spotted green pufferfish, Tetraodon nigrovirids. *J Exp Zool Part A Ecol Genet Physiol* **307**, 411-8.

Taylor, J. R. and Grosell, M. (2006). Evolutionary aspects of intestinal bicarbonate secretion in fish. *Comparative Biochemistry and Physiology a-Molecular & Integrative Physiology* **143**, 523-529.

Thomas, R. C. (1977). Role of Bicarbonate, Chloride and Sodium Ions in Regulation of Intracellular pH in Snail Neurons. *Journal of Physiology-London* **273**, 317-338.

Tominaga, T. and Barber, D. L. (1998). Na-H exchange acts downstream of RhoA to regulate integrin-induced cell adhesion and spreading. *Molecular Biology of the Cell* **9**, 2287-2303.

Tominaga, T., Ishizaki, T., Narumiya, S. and Barber, D. L. (1998). p160ROCK mediates RhoA activation of Na-H exchange. *Embo Journal* **17**, 4712-4722.

Towle, D. W., Rushton, M. E., Heidysch, D., Magnani, J. J., Rose, M. J., Amstutz, A., Jordan, M. K., Shearer, D. W. and Wu, W. S. (1997). Sodium/proton antiporter in the euryhaline crab Carcinus maenas: Molecular cloning, expression and tissue distribution. *Journal of Experimental Biology* **200**, 1003-1014.

Towle, D. W. and Weihrauch, D. (2001). Osmoregulation by gills of euryhaline crabs: Molecular analysis of transporters. *American Zoologist* **41**, 770-780.

Tresguerres, M., Katoh, F., Fenton, H., Jasinska, E. and Goss, G. G. (2005). Regulation of branchial V-H+-ATPase Na+/K+-ATPase and NHE2 in response to acid and base infusions in the Pacific spiny dogfish (Squalus acanthias). *Journal of Experimental Biology* **208**, 345-354.

Tresguerres, M., Katoh, F., Orr, E., Parks, S. K. and Goss, G. G. (2006a). Chloride uptake and base secretion in freshwater fish: A transepithelial ion-transport metabolon? *Physiological and Biochemical Zoology* **79**, 981-996.

Tresguerres, M., Onken, H., Perez, A. F. and Luquet, C. A. (2003). Electrophysiology of posterior, NaCl-absorbing gills of Chasmagnathus granulatus: rapid responses to osmotic variations. *Journal of Experimental Biology* **206**, 619-626.

Tresguerres, M., Parks, S. K. and Goss, G. G. (2006b). V-H+-ATPase, Na+/K+-ATPase and NHE2 immunoreactivity in the gill epithelium of the Pacific hagfish (Epatretus stoutii). *Comparative Biochemistry and Physiology a-Molecular & Integrative Physiology* **145**, 312-321.

Tresguerres, M., Parks, S. K. and Goss, G. G. (2007a). Recovery from blood alkalosis in the Pacific hagfish (Eptatretus stoutii): Involvement of gill V-H+-ATPase and Na+/K+-ATPase. *Comparative Biochemistry and Physiology a-Molecular & Integrative Physiology* **148**, 133-141.

Tresguerres, M., Parks, S. K., Katoh, F. and Goss, G. G. (2006c). Microtubule-dependent relocation of branchial V-H+-ATPase to the basolateral membrane in the Pacific spiny dogfish (Squalus acanthias): a role in base secretion. *Journal of Experimental Biology* **209**, 599-609.

Tresguerres, M., Parks, S. K., Sabatini, S. E., Goss, G. G. and Luquet, C. M. (2008). Regulation of ion transport by pH and [HCO3-] in isolated gills of the crab Neohelice (Chasmagnathus) granulata. *American*

Journal of Physiology-Regulatory Integrative and Comparative Physiology **294**, R1033-R1043.

Tresguerres, M., Parks, S. K., Wood, C. M. and Goss, G. G. (2007b). V-H+-ATPase translocation during blood alkalosis in dogfish gills: interaction with carbonic anhydrase and involvement in the postfeeding alkaline tide. *American Journal of Physiology-Regulatory Integrative and Comparative Physiology* **292**, R2012-R2019.

Tsai, J. R. and Lin, H. C. (2007). V-type H+-ATPase and Na+,K+-ATPase in the gills of 13 euryhaline crabs during salinity acclimation. *Journal of Experimental Biology* **210**, 620-627.

Vince, J. W., Carlsson, U. and Reithmeier, R. A. F. (2000). Localization of the Cl-/HCO3- anion exchanger binding site to the amino-terminal region of carbonic anhydrase II. *Biochemistry* **39**, 13344-13349.

Vince, J. W. and Reithmeier, R. A. F. (1998). Carbonic anhydrase II binds to the carboxyl terminus of human band 3, the erythrocyte Cl-/HCO3-exchanger. *Journal of Biological Chemistry* **273**, 28430-28437.

Vince, J. W. and Reithmeier, R. A. F. (2000). Identification of the carbonic anhydrase II binding site in the Cl-/HCO3- anion exchanger AE1. *Biochemistry* **39**, 5527-5533.

Virkki, L. V., Choi, I., Davis, B. A. and Boron, W. F. (2003). Cloning of a Na+-driven Cl/HCO3 exchanger from squid giant fiber lobe. *American Journal of Physiology-Cell Physiology* **285**, C771-C780.

Wagner, C. A., Finberg, K. E., Breton, S., Marshansky, V., Brown, D. and Geibel, J. P. (2004). Renal vacuolar H+-ATPase. *Physiological Reviews* **84**, 1263-1314.

Wakabayashi, S., Hisamitsu, T., Pang, T. X. and Shigekawa, M. (2003). Kinetic dissection of two distinct proton binding sites in Na+/H+ exchangers by measurement of reverse mode reaction. *Journal of Biological Chemistry* **278**, 43580-43585.

Wakabayashi, S., Shigekawa, M. and Pouyssegur, J. (1997). Molecular physiology of vertebrate Na+/H+ exchangers. *Physiological Reviews* **77**, 51-74.

Wallert, M. A., Thronson, H. L., Korpi, N. L., Olmschenk, S. M., McCoy, A. C., Funfar, M. R. and Provost, J. J. (2005). Two G protein-coupled receptors activate Na+/H+ exchanger isoform 1 in Chinese hamster lung fibroblasts through an ERK-dependent pathway. *Cellular Signalling* **17**, 231-242.

Walz, B., Baumann, O., Krach, C., Baumann, A. and Blenau, W. (2006). The aminergic control of cockroach salivary glands. *Archives of Insect Biochemistry and Physiology* **62**, 141-152.

Wang, T., Busk, H. and Overgaard, J. (2001). The respiratory consequences of feeding in amphibians and reptiles. *Comparative Biochemistry and Physiology a-Molecular & Integrative Physiology* **128**, 535-549.

Weakley, J., Choe, K.P., and Claiborne, J.B. . (2003). Immunological detection of gill NHE2 in the dogfish (Squalus acanthias). *Bull. Mt. Desert Isl. Biol. Lab.* **42**, 81-82.

Weihrauch, D., McNamara, J. C., Towle, D. W. and Onken, H. (2004a). Ion-motive ATPases and active, transbranchial NaCl uptake in the red freshwater crab, Dilocarcinus pagei (Decapoda, Trichodactylidae). *Journal of Experimental Biology* **207**, 4623-4631.

Weihrauch, D., Morris, S. and Towle, D. W. (2004b). Ammonia excretion in aquatic and terrestrial crabs. *Journal of Experimental Biology* **207**, 4491-4504.

Wemmie, J. A., Price, M. P. and Welsh, M. J. (2006). Acid-sensing ion channels: advances, questions and therapeutic opportunities. *Trends in Neurosciences* **29**, 578-586.

Wheatly, M. G. and Henry, R. P. (1992). Extracellular and Intracellular Acid-Base Regulation in Crustaceans. *Journal of Experimental Zoology* **263**, 127-142.

Wills, N. K. and Lewis, S. A. (1980). Intracellular Na+ Activity as a Function of Na+ Transport Rate across a Tight Epithelium. *Biophysical Journal* **30**, 181-186.

Wilson, J. M., Laurent, P., Tufts, B. L., Benos, D. J., Donowitz, M., Vogl, A. W. and Randall, D. J. (2000). NaCl uptake by the branchial epithelium in freshwater teleost fish: An immunological approach to ion-transport protein localization. *Journal of Experimental Biology* **203**, 2279-2296.

Wilson, R. W., Wood, C. M., Gonzalez, R. J., Patrick, M. L., Bergman, H. L., Narahara, A. and Val, A. L. (1999). Ion and acid-base balance in three species of Amazonian fish during gradual acidification of extremely soft water. *Physiological and Biochemical Zoology* **72**, 277-285.

Wong, C. K. C. and Chan, D. K. O. (1999a). Chloride cell subtypes in the gill epithelium of Japanese eel Anguilla japonica. *American Journal of*

Physiology-Regulatory Integrative and Comparative Physiology **277**, R517-R522.

Wong, C. K. C. and Chan, D. K. O. (1999b). Isolation of viable cell types from the gill epithelium of Japanese eel Anguilla japonica. *American Journal of Physiology-Regulatory Integrative and Comparative Physiology* **276**, R363-R372.

Wood, C. M., Kajimura, M., Mommsen, T. P. and Walsh, P. J. (2005). Alkaline tide and nitrogen conservation after feeding in an elasmobranch (Squalus acanthias). *Journal of Experimental Biology* **208**, 2693-2705.

Wood, C. M. and Lemoigne, J. (1991). Intracellular Acid-Base Responses to Environmental Hyperoxia and Normoxic Recovery in Rainbow-Trout. *Respiration Physiology* **86**, 91-113.

Wood, C. M. and Part, P. (2000). Intracellular pH regulation and buffer capacity in CO2/HCO3--buffered media in cultured epithelial cells from rainbow trout gills. *Journal of Comparative Physiology B-Biochemical Systemic and Environmental Physiology* **170**, 175-184.

Wood, C. M., Wheatly, M. G. and Hobe, H. (1984). The Mechanisms of Acid-Base and Ionoregulation in the Fresh-Water Rainbow-Trout during Environmental Hyperoxia and Subsequent Normoxia .3. Branchial Exchanges. *Respiration Physiology* **55**, 175-192.

Wood, C. M., Wilson, R. W., Gonzalez, R. J., Patrick, M. L., Bergman, H. L., Narahara, A. and Val, A. L. (1998). Responses of an Amazonian teleost, the tambaqui (Colossoma macropomum), to low pH in extremely soft water. *Physiological Zoology* **71**, 658-670.

Wright, P. A., Heming, T. and Randall, D. J. (1986). Downstream pH Changes in Water Flowing over the Gills of Rainbow-Trout. *Journal of Experimental Biology* **126**, 499-512.

Yan, J. J., Chou, M. Y., Kaneko, T. and Hwang, P. P. (2007). Gene expression of Na+/H+ exchanger in zebrafish H+-ATPase-rich cells during acclimation to low-Na+ and acidic environments. *American Journal of Physiology-Cell Physiology* **293**, C1814-C1823.

Yoshitomi, K. and Fromter, E. (1985). How Big Is the Electrochemical Potential Difference of Na+ across Rat Renal Proximal Tubular Cell-Membranes Invivo. *Pflugers Archiv-European Journal of Physiology* **405**, S121-S126.

Zhang, Y., Zhang, Y. F., Bryant, J., Charles, A., Boado, R. J. and Pardridge, W. M. (2004). Intravenous RNA interference gene therapy

targeting the human epidermal growth factor receptor prolongs survival in intracranial brain cancer. *Clinical Cancer Research* **10**, 3667-3677.

Zhuang, Z. P., Linser, P. J. and Harvey, W. R. (1999). Antibody to H+V-ATPase subunit E colocalizes with portasomes in alkaline larval midgut of a freshwater mosquito (Aedes aegypti L.). *Journal of Experimental Biology* **202**, 2449-2460.

Zimmermann, B., Dames, P., Walz, B. and Baumann, O. (2003). Distribution and serotonin-induced activation of vacuolar-type H+-ATPase in the salivary glands of the blowfly Calliphora vicina. *Journal of Experimental Biology* **206**, 1867-1876.